MAPPING CONFORMATIONAL CHANGES ALONG THE ACTIVATION PATHWAY OF THE HETEROTRIMERIC G PROTEIN α SUBUNIT WITH SITE-DIRECTED SPIN-LABELING

By

William Michael Oldham

Dissertation

Submitted to the Faculty of the

Graduate School of Vanderbilt University

in partial fulfillment of the requirements

for the degree of

DOCTOR OF PHILOSOPHY

in

Pharmacology

August, 2006

Nashville, Tennessee

Approved:

Heidi E. Hamm, Ph.D.

Vsevolod Gurevich, Ph.D.

P. Jeffrey Conn, Ph.D.

Hassane Mchaourab, Ph.D.

To Mom and Dad, who seem to keep getting smarter as I get older, and

To my beautiful wife, Julie, for her love, support, and infinite understanding

Scientists are a friendly, atheistic, hard-working, beer-drinking lot whose minds are preoccupied with sex, chess, and baseball when they are not preoccupied with science.

Yann Martel, *Life of Pi*

ACKNOWLEDGEMENTS

Over the course of my graduate training, I have been incredibly fortunate to work with a number of very talented scientists. Foremost among these is Dr. Heidi Hamm, who has been an excellent research advisor and mentor. Heidi's enthusiasm for science is contagious, and I am grateful that, despite having many other responsibilities as Chair of Pharmacology, her door has always been open for even the most random of scientific discussions. I am also very grateful for the many opportunities to speak at meetings, to work on grants, to write review articles, to mentor rotation students, and to interact with other scientists. Heidi has generously shared these experiences with me, and they have been an invaluable component of my training.

The Hamm lab has been an exciting place to work, and I certainly benefited from the scientific experiences of the other students and fellows who have spent time there over the past few years. In particular, Dr. Anita Preininger taught me all about G protein expression and purification when I joined the lab and Mrs. Guihua Liao has been a valuable and talented assistant who has always kept my work moving forward. All members of the lab deserve my thanks for bearing with many a group meeting filled with squiggly lines, and I appreciate their role as the primary reviewers of this work.

I would also like to thank the members of my dissertation committee, Drs. Seva Gurevich (chair), Jeff Conn, Terry Lybrand, and Hassane Mchaourab. Their support and enthusiasm for this work was unwavering, and I have learned much from each of them. Seva has been an excellent role model for this young scientist, and I have benefited from his sensible perspective. Jeff always reminded me to think broadly about the impact of my research beyond our simple experimental system. Terry offered a deep knowledge of structural biology and computational approaches. I am especially grateful to Hassane as the resident expert on EPR and fluorescence spectroscopy for teaching me about these techniques and lending his insight to our data. Each of these scientists is a leader in their respective fields and I was very fortunate that they took time out of their busy schedules to serve on my dissertation committee.

Most of my research has been conducted in close collaboration with Drs. Wayne Hubbell and Ned Van Eps at the Jules Stein Eye Institute at the University of California in Los Angeles. Wayne is the foremost expert on the application of SDSL in the study of protein dynamics, and I have been very fortunate to learn EPR from him. In addition, I have also enjoyed working with Dr. Tina Iverson and Mr. Michael Funk at Vanderbilt University and Drs. Martin Caffrey and Vadim Cherezov at Ohio State University in attempts to crystallize receptors and G proteins. Drs. Eric Dawson and Jarrod Smith in the Center for Structural Biology at Vanderbilt have been an invaluable resource for all of the computational aspects of my graduate work.

The Department of Pharmacology has provided an excellent training environment thanks, in part, to a great Director of Graduate Studies, Dr. Joey Barnett, and Educational Coordinator, Karen Gieg. Joey and Karen always had time to answer questions or listen to concerns, and I appreciated all of their help and advice. Certainly all of the faculty and administrators in the Department contributed to my education, but I would particularly like to thank my fellow graduate students in Pharmacology from whom I learned the most.

Since I have chosen to pursue this graduate degree by way of medical school (or a medical degree by way of graduate school), the Medical Scientist Training Program has been a critical component of my education. I am especially indebted to Dr. Terry Dermody, the MSTP Director, for his guidance and support, as well as my colleagues in the MSTP who have been a constant reminder that I was not alone in and foolish for pursuing a Ph.D.

Funding for my training and research has been provided by the Medical Scientist Training Program, the National Eye Institute, and a Pre-doctoral Fellowship in Pharmacology and Toxicology from the PhRMA Foundation.

Nobody has been more important in this pursuit than the members of my family. I would like to thank them for their support, even when they were still trying to understand the mess I had gotten myself into by joining the MSTP. My parents have been a constant source of encouragement, particularly in the stressful days leading to the completion of my graduate work. I have been lucky to have them for role

models. Finally, I owe an immeasurable debt of gratitude to my beautiful and loving wife, Julie. She has shared every moment of this experience with me, and nothing has been more supportive than her encouragement to scribble upon yet another napkin so that she could better understand my life in the lab.

TABLE OF CONTENTS

Page

DEDICATION iii

ACKNOWLEDGEMENTS v

LIST OF TABLES xii

LIST OF FIGURES xiii

LIST OF ABBREVIATIONS xiii

INTRODUCTION xxiii

Chapter

I. HETEROTRIMERIC G PROTEINS 1

Introduction 1
Heterotrimeric G Protein Structure 3
G protein α subunit 3
G protein βγ dimer 10
Unique role of $G\beta_5$ in complexes with RGS proteins 12
Heterotrimeric G protein structure 14
Lipid modifications direct membrane association 15
Receptor-G Protein Complexes 16
Low affinity interactions between inactive receptors and G proteins 16
Receptor activation exposes the high-affinity G protein binding site 17
Receptor-G protein interaction surface 18
Structural determinants of receptor-G protein specificity 23
Models of the receptor-G protein complex 26
Sequential interactions may form the receptor-G protein complex 30
Molecular Basis for G Protein Activation 31
Potential mechanisms of receptor-catalyzed GDP release 31
GTP-mediated alteration of the receptor-G protein complex 38
Activation of Downstream Effector Proteins 40
Gα interactions with effectors 40
Gβγ interactions with effectors and regulatory proteins 44
G Protein Inactivation 49
Intrinsic GTPase activity of Gα 49
GTPase activating proteins 53
Novel Regulation of G Protein Signaling 55
Novel Approaches to Study G Protein Structure and Function 56
Nuclear magnetic resonance spectroscopy 56
Studies of G protein function in living cells 58
Summary 60

II. APPROACH TO THE STUDY OF G PROTEIN DYNAMICS 61

Research Goals 61
Experimental Strategy 63
Electron paramagnetic resonance spectroscopy 63
Site-directed spin-labeling in the G protein α subunit 67
Materials and Methods 71
Materials 71
Construction, expression and purification of Gα subunits 71
Preparation of ROS membranes, $G\alpha_t$, and $G\beta_1\gamma_1$ from bovine retina 72
Intrinsic fluorescence activity assay 73
Nucleotide exchange assay 74
Rhodopsin binding assay 74
Electron paramagnetic resonance spectroscopy 75
Four-pulse DEER distance measurements 76

III. MECHANISM OF RECEPTOR-CATALYZED GDP RELEASE 78

Introduction 78
Results 80
Characterization of spin-labeled mutants 80
Conformational changes distant from receptor contacts 82
Conformational changes couple R* binding to GDP release 86
Modeling the structural change 87
Discussion 90

IV. STRUCTURE AND DYNAMICS OF SWITCH II IN G PROTEIN ACTIVATION 95

Introduction 95
Results 96
Gα(GDP) 98
Heterotrimer formation 98
Receptor activation-dependent conformational changes 104
Activated Gα(GTPγS) 104
Discussion 107
Solution structure and dynamics in Gα(GDP) 107
Sites in Switch II and the α4 helix sense heterotrimer formation 110
Absence of R*-mediated structural changes in Switch II 111
Switch II structure and dynamics in Gα(GDP), Gαβγ, and Gα(GTPγS) 112
Summary 113

V. DYNAMICS OF SWITCH I IN G PROTEIN ACTIVATION 115

Introduction 115
Results 117
Characterization of spin-labeled mutants 117
Gα(GDP) 119
Heterotrimer formation 119
Receptor activation-dependent conformational changes 121
Activated Gα(GTPγS) 123

Discussion 123
Switch I structure and dynamics in Gα(GDP), Gαβγ, and Gα(GTPγS) 125
Receptor activation-dependent conformational changes near Switch I 126
Summary 128

VI. ADDITIONAL SDSL STUDIES OF G PROTEIN STRUCTURAL CHANGES 129

Introduction 129
Results and Discussion 129
Comparison of Gα(GDP) and Gα(GDP)βγ 132
Structural changes upon formation of the R*-G protein complex 136
Structural changes upon activation with GTPγS 138

VII. COMPLEMENTARY APPROACHES TO STUDY G PROTEIN STRUCTURE 142

Mutagenesis of Evolutionarily Conserved Residues in the α5 Helix 142
Introduction 142
Results and Discussion 143
Double Cysteine Mutagenesis in $G\alpha_{i1}$ 150
Preliminary cross-linking experiments 150
Crystallographic study of a fast exchanging mutant $G\alpha_{i1}$ 154
In Meso Crystallization Trials of Rhodopsin Complexes 161
Introduction 161
Materials 161
Rhodopsin solubilization 162
Addition of all-trans-retinal to MAG 162
Crystallization screens 163
Results 164
Discussion 164
BEST Analysis of G Protein Structures 166
Introduction 166
Theory 167
Results 169
Discussion 171

VIII. FUTURE DIRECTIONS 174

Assembling the Receptor-G Protein Complex 174
Additional targets for SDSL in Gα 174
Modeling the R*-bound, nucleotide-free conformation of Gα 176
Improving models of the R*-G protein complex 177
Mapping Conformational Changes Along the Inactivation Pathway 180
Alternate Approaches to Study G Protein Dynamics 181
Site-directed labeling 181
Hydrogen-deuterium exchange mass spectrometry 182
Mapping allosteric connectivity with computational approaches 184

IX. PERSPECTIVE AND CONCLUSIONS 189

Appendix

A. $G\alpha_{i1}$ MUTANT CONSTRUCTS 191

B. BIOCHEMICAL CHARACTERIZATION OF SPIN-LABELED MUTANTS 197

C. COMPARISON OF SALT BRIDGE MUTANT EXCHANGE RATES 201

REFERENCES 202

LIST OF TABLES

Table		Page
1.	Heterotrimeric G protein structures	5
2.	Effector proteins of heterotrimeric G protein subunits	41
3.	Data collection and refinement statistics for 56-333(GDP·AlF_4^-) crystals	160
4.	Summary of double cysteine mutants for distance measurements	178
5.	Single-site mutant constructs for SDSL studies of $G\alpha_{i1}$	192
6.	Miscellaneous constructs	194

LIST OF FIGURES

Figure		Page
1.	Introduction to signal transduction	xxiv
2.	Discovery of heterotrimeric G proteins	xxix
3.	Heterotrimeric G protein cycle	2
4.	Primary sequence identity of G protein subunit genes	4
5.	Structural features of heterotrimeric G proteins	8
6.	GTP-dependent myristoyl switch	11
7.	Heptahelical receptor structure	19
8.	Receptor contact sites on the G protein	21
9.	Models of the receptor-G protein complex	29
10.	Structural elements connecting receptor contacts to the GDP-binding pocket	34
11.	Two hypotheses on the role of Gβγ in GDP release	36
12.	Subunit interactions with effector proteins	46
13.	Mechanisms of GTP hydrolysis by Gα	51
14.	Site-directed spin-labeling and EPR spectroscopy	64
15.	EPR spectra are sensitive to protein structure	66
16.	Summary of site-directed cysteine mutants	69
17.	Typical EPR experiment	70
18.	Biochemical characterization of mutants	77
19.	Summary of mobility changes observed for sites near the α5 helix	79
20.	Biochemical characterization of mutants near the α5 helix	81
21.	Receptor activation-dependent conformational changes in the α5 helix	83
22.	Models of the R1 side chain at sites near the α5 helix	85

23. Movement of the α5 helix is necessary for GDP release 89
24. Distance measurements support the proposed rotation-translation of the α5 helix 91
25. Location of spin-labeled sites in Switch II 97
26. Biochemical characterization of spin-labeled mutants in Switch II 99
27. EPR spectra of GDP-bound Switch II mutants 100
28. Switch II mutants report two spectral components in Gα(GDP) 101
29. Structural changes in Switch II upon heterotrimer formation 102
30. Spin-labeled sites within Gα are sensors of heterotrimer formation 105
31. Probing the structure of Switch II in the R*-G protein complex 106
32. Sites in Switch II sense the identity of the bound nucleotide 108
33. S- and Q-band spectra of Switch II mutants 109
34. Location of spin-labeled sites in the Switch I region 116
35. Biochemical characterization of spin-labeled mutants near Switch I 118
36. Structural changes in Switch I upon heterotrimer formation 120
37. Receptor activation-dependent conformational changes in Switch I 122
38. Comparison of Switch I dynamics in GTPγS- and GDP-bound Gα 124
39. Location of spin-labeled mutants 130
40. Biochemical characterization of spin-labeled mutants 131
41. Conformational changes upon heterotrimer formation 133
42. Gradient of backbone mobility within the α5 helix 135
43. Receptor activation-dependent conformational changes 137
44. Comparison between the GTPγS- and GDP-bound conformations 140
45. Alignments of evolutionarily conserved residues in Gα subunits 144
46. Basal exchange rates of salt bridge mutants 148
47. Locations of double cysteine mutations in $G\alpha_{i1}$ 151

48. SDS-PAGE analysis of CuPh-treated double cysteine mutants 153

49. Basal exchange rates of BMOE-treated double cysteine mutants 155

50. Basal nucleotide exchange rate of the double cysteine mutant 56-333 157

51. Crystallographic data from the 56-333($GDP \cdot AlF_4^-$) double cysteine mutant 159

52. Hits from an in meso crystallization trial 165

53. Enumeration of the protein ensemble 168

54. Residue-specific stability constants for $G\alpha_{i1}$ structures 170

55. Residue-specific stability constants for $G\alpha_t$ structures 172

56. Optimal docking areas in $G\alpha_{i1}$ 188

57. Nucleotide exchange rates for spin-labeled mutants 198

58. Rhodopsin binding data for spin-labeled mutants 199

59. Mapping biochemical data onto the $G\alpha_{i1}$ crystal structure 200

60. Summary of salt bridge mutant exchange rates 201

LIST OF ABBREVIATIONS

°C	degrees Celsius
3°	tertiary
5G	five-glycine
Å	angstroms (1×10^{-10} meters)
aa	amino acid
Ac	acetyl
AC	adenylyl cyclase; 9 membrane-bound isoforms and 1 soluble (S) isoform
ADP	adenosine 5'-diphosphate
AFM	atomic force microscopy
AGS	activator of G protein signaling
$AlCl_3$	aluminum chloride
AlF_4^-	aluminum tetrafluoride
AMP	adenosine 5'-monophosphate
APS	Advanced Photon Source, Argonne National Laboratory
ARF	ADP-ribosylation factor; monomeric G protein in the Ras family
ATD	anisotropic thermal diffusion
β-APP	β-amyloid protein; accumulates in the brains of Alzheimer's patients
βARK	β-adrenergic receptor kinase (GRK2); role in GPCR desensitization
βME	β-mercaptoethanol
BEST	Biology through Ensemble-based Structural Thermodynamics
Bis-Tris	2-bis(2-hydroxyethyl)amino-2-(hydroxymethyl)-1,3-propanediol
BMOE	bis-maleimidoethane
C-terminus	carboxyl terminus

cAMP	adenosine 3', 5'-cyclic monophosphate
Cdc42Hs	cell division control protein 42 homologue precursor
cDNA	complementary DNA
cGMP	guanosine 3'-5'-cyclic monophosphate
CuPh	copper phenanthroline
$CuSO_4$	copper sulfate
DEER	double electron-electron resonance EPR spectroscopy
DNA	deoxyribonucleic acid
DTT	dithiothreitol; reducing agent
E. coli	*Escherichia coli*
EC_{50}	concentration that produces a half-maximal effect
EDTA	ethylenediaminetetraacetic acid; chelates divalent cations
EPR	electron paramagnetic resonance spectroscopy
g	gram
g	gravity (9.8 m/s^2)
G	gauss
G protein	heterotrimeric GTP-binding protein; any GTP-binding protein
Gα	α subunit of heterotrimeric G proteins
Gβ	β subunit of heterotrimeric G proteins
$G\beta_{5S/L}$	the short or long isoform of $G\beta_5$, respectively
Gβγ	constitutive dimer of Gβ and Gγ
Gγ	γ subunit of heterotrimeric G proteins
G_{gust}	gustatory heterotrimeric G protein
G_i	heterotrimeric G protein that inhibits adenylyl cyclase
G_{olf}	olfactory heterotrimeric G protein

G_s	heterotrimeric G protein that stimulates adenylyl cyclase
G_t	transducin
GAP	GTPase activating protein
GAP-43	growth associated protein 43
GDI	guanine nucleotide dissociation inhibitor; GDP dissociation inhibitor
GDP	guanosine 5'-diphosphate
GEF	guanine nucleotide exchange factor
GGL	Gγ-like domain
GIRK	G protein-coupled inward rectifying K^+ channel
GMP	guanosine 5'-monophosphate
GPCR	G protein-coupled receptor; heptahelical receptor
Gpp(NH)p	guanosine 5′-[β, γ-imido]triphosphate; non-hydrolysable GTP analogue
GRIN	G protein-regulated inducer of neurite outgrowth
GRK	G protein-coupled receptor kinase; role in GPCR desensitization
GTP	guanosine 5'-triphosphate
GTPγS	guanosine 5'-[γ-thio]triphosphate; non-hydrolysable GTP analogue
GTPase	enzyme that catalyzes the hydrolysis of GTP to GDP
h	hour
HCl	hydrochloric acid
HDAC	histone deacetylase
HEPES	N-2-hydroxyethylpiperazine-N'-2-ethanesulfonic acid
HPLC	high performance liquid chromatography
HTG	heptylthioglucoside
HXMS	hydrogen exchange mass spectrometry
IC	intracellular loops of heptahelical receptors

IMCA-CAT	Industrial Macromolecular Crystallography Association Collaborative Access Team
IPTG	isopropyl β-D-1-thiogalactopyranoside
K	Kelvin
KCl	potassium chloride
K_d	dissociation constant; varies inversely with the affinity
kDa	kilodalton (1,000 g/mol)
λ	wavelength (nm)
L	liter
LARG	leukemia-associated RhoGEF
$Li(CH_3COO)$	lithium acetate
Li_2SO_4	lithium sulfate
μg	microgram
μL	microliter
μm	micron
μM	micromolar
μs	microsecond
M	molar
MAG	monoacylglycerol
MBP	maltose-binding protein
MES	2-morpholinoethanesulfonic acid
Meta II	metarhodopsin II; signaling conformation of rhodopsin
Mg^{2+}	magnesium ion
$MgCl_2$	magnesium chloride
min	minute

mL	milliliter
mM	millimolar
mol	mole (6.02×10^{23} atoms)
MOMD	microscopic order macroscopic disorder
MOPS	3-(N-morpholino)propanesulfonic acid
ms	millisecond
MTSSL	methanethiosulfonate spin label; *S*-(1-oxy-2,2,5,5-tetramethylpyrrolinyl-3-methyl) methanethiosulfonate
mW	milliwatt
N.D.	not determined
N-terminus	amino terminus
NaCl	sodium chloride
NaF	sodium fluoride
nL	nanoliter
nm	nanometer
nM	nanomolar
NMR	nuclear magnetic resonance spectroscopy
ns	nanosecond
OD_{600}	optical density at 600 nm
ODA	optimal docking area
P_i	inorganic phosphate (HPO_4^{2-})
PAGE	polyacrylamide gel electrophoresis
PAR1	protease-activated receptor 1
PCR	polymerase chain reaction
PDE	phosphodiesterase; hydrolyses cNMP to NMP
PEG	polyethylene glycol

PI3K	phosphoinositide 3-kinase
PKD	protein kinase D
PLC	phospholipase C
PLD	phospholipase D
PMSF	phenylmethylsulfonyl fluoride
psi	pounds per square inch
PWR	plasmon-waveguide resonance spectroscopy
R	inactive G protein-coupled receptor
R*	activated G protein-coupled receptor
R1	nitroxide side chain formed by cysteine modification with MTSSL
RACK	receptor for activated protein kinase C
Res.	resolution
RGS	regulator of G protein signaling
RKIP	Raf kinase inhibitor protein
Ric-8A	resistance to inhibitors of cholinesterase 8A protein
RMS	root mean square
ROS	rod outer segment
rpm	rotations per minute
s	second
S	order parameter
SCA	statistical coupling analysis
SDS	sodium dodecyl sulfate
SDSL	site-directed spin-labeling
SNAP-25	synaptosome-associated protein of 25 kDa
SPR	surface plasmon resonance spectroscopy
$SrCl_2$	strontium chloride

τ_c	correlation time
Tris	tris(hydroxymethyl)aminomethane
UV	ultraviolet
v/v	percentage by volume by volume
W	Watt
WD40	40 aa motifs terminating in WD that make up the blades of Gβ
w/w	percentage weight by weight
$Zn(CH_3COO)_2$	zinc acetate
$Zn_3(PO_4)_2$	zinc phosphate

Amino Acid Abbreviations:

A	alanine	C	cysteine	D	aspartic acid
E	glutamic acid	F	phenylalanine	G	glycine
H	histidine	I	isoleucine	K	lysine
L	leucine	M	methionine	N	asparagine
P	proline	Q	glutamine	R	arginine
S	serine	T	threonine	V	valine
W	tryptophan	Y	tyrosine	R1	nitroxide probe

INTRODUCTION

Everything we do relies on the close cooperation of the nearly 100 trillion individual cells that make up the human body. This cooperation is achieved through a complex network of chemical signals that allows cells to communicate with each other. Each cell is wired into the network by an extensive repertoire of proteins in the cell membrane that sense the extracellular environment. These receptor proteins recognize a specific chemical signal, or ligand, and transduce that information across the cell membrane to initiate the appropriate cellular response. The responses to extracellular stimuli can include changes in cell growth, mobility, or metabolism, as well as changes in gene expression, the release of additional chemical signals, and even cell death (Fig. 1). Disruptions in this signaling network play a role in every human disease, from the common cold to cancer to Parkinson's disease, and the general question of how extracellular signals are converted into cellular responses is of fundamental importance in our efforts to understand human physiology. My dissertation research has focused on the function of one key player in this process, the heterotrimeric G protein, whose history dates to the beginning of the signal transduction field.

In 1955, Earl W. Sutherland, Jr., wrote that "the precise mechanism of action of any hormone has not yet been clearly established" (Beavo & Brunton, 2002). At the time, Sutherland was studying how the hormone epinephrine (adrenaline) activates the enzyme phosphorylase, which leads to the formation of glucose from the breakdown of glycogen stored in the liver. This reaction releases additional energy into the bloodstream in the form of glucose in preparation for a "fight or flight" response. The following year, Sutherland and colleagues demonstrated that the activity of the phosphorylase enzyme was regulated by the incorporation of phosphate (Wosilait & Sutherland, 1956; Rall*, et al.*, 1956). When studying this phenomenon in broken cell systems, they noted that the effects of epinephrine were lost after centrifugation separated the cell membranes from the cytoplasm. In an exciting series of experiments, they were able to show that the membrane fraction was producing a small molecule in response to

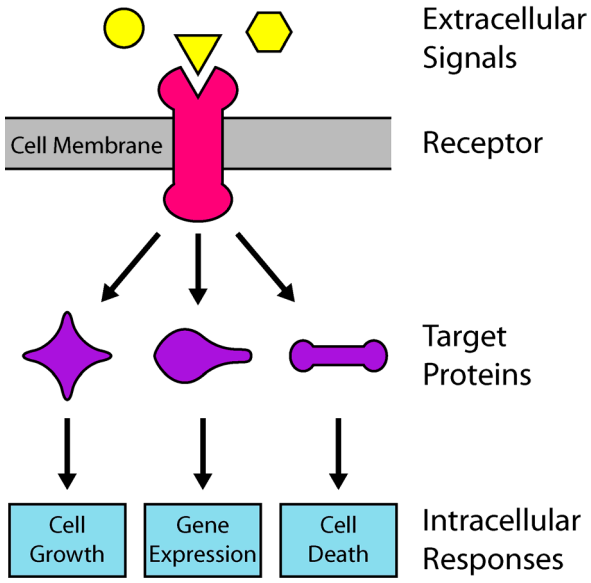

Figure 1 | Introduction to signal transduction When a receptor protein embedded in the cell membrane is activated by a specific extracellular signal, it initiates an intracellular signaling cascade that leads to a cellular response. Each cell has thousands of different receptors that activate dozens of different intracellular signaling pathways, all of which are interconnected. The cell is like a sophisticated computer processor that integrates a variety of inputs (extracellular signals) to produce a measured response to its environment.

epinephrine, later identified as cyclic AMP, which led to the phosphorylation and activation of the phosphorylase enzyme in the cytoplasm (Berthet*, et al.*, 1957). Based on these experiments, Sutherland developed a model whereby epinephrine binds to the β-adrenergic receptor outside of the cell, causing activation of the membrane-bound enzyme, adenylyl cyclase, that makes cAMP. The cAMP acts as the "second messenger" (epinephrine is the first messenger) leading to phosphorylase activation in the cytoplasm. Since these early studies, the role of receptors in converting extracellular signals into cellular responses through intracellular second messengers has proven to be a common mechanism of signal transduction (Fig. 2a) and, in 1971, Sutherland was awarded the Nobel Prize in Medicine or Physiology for his discoveries concerning "the mechanisms of the action of hormones."

In 1967, Sutherland proposed the simplest molecular explanation for the production of cAMP at the membrane when he wrote, "It seems likely that in most and perhaps all tissues the β receptor and adenylyl cyclase are the same." (Fig. 2a) (Robison*, et al.*, 1967). However, in 1969, Martin Rodbell and Lutz Birnbaumer demonstrated that a variety of hormones could stimulate adenylyl cyclase in adipocytes. If each adenylyl cyclase was a distinct receptor for these various hormones, then stimulation with the maximal effective concentrations of multiple hormones should result in additive production of cAMP, yet it did not, suggesting that each receptor was activating a common pool of adenylyl cyclase (Birnbaumer & Rodbell, 1969). Once radioactive ligands were developed, the interaction between receptors and their activators could be studied directly without relying on an indirect functional readout, like cAMP production. When cell membranes were solubilized with detergent, the β-adrenergic receptor ligand binding activity and the cAMP production activity of adenylyl cyclase could be separated by size exclusion chromatography (Limbird & Lefkowitz, 1977). This experiment definitively showed that the receptor and adenylyl cyclase were distinct molecular entities, begging the question, how was the receptor coupled to activation of adenylyl cyclase?

Although the next simplest model was that the receptor and adenylyl cyclase are separate proteins that directly interact with each other, Rodbell and colleagues demonstrated that GTP reduced the affinity

of glucagon for its receptor, and that GTP was required for the activation of adenylyl cyclase in addition to the hormone itself (Rodbell*, et al.*, 1971b; Rodbell*, et al.*, 1971a). Based on these studies, Rodbell suggested that the signal transduction machinery consisted of the hormone-binding receptor, an effector protein like adenylyl cyclase, and also a GTP-binding transducer protein connecting the two (Fig. 2b).

Interestingly, the addition of non-hydrolysable analogs of GTP, such as Gpp(NH)p, resulted in the persistent stimulation of adenylyl cyclase (Londos*, et al.*, 1974). Based on this result, Rodbell also proposed that the transducer protein was a GTP hydrolase, an enzyme that could convert GTP to GDP. Receptor-stimulated GTPase activity was subsequently demonstrated in red blood cell membranes by Cassel and Selinger (Cassel & Selinger, 1976). Additional studies showed that GTP hydrolysis does turn off adenylyl cyclase and that GDP can maintain adenylyl cyclase in an inactive state (Cassel & Selinger, 1978), although at this time, Cassel and Selinger thought that the adenylyl cyclase itself was regulated by guanine nucleotides. However, this work eventually provided the evidence that receptors activated signaling pathways by exchanging GTP for GDP bound to the transducer protein proposed by Rodbell (Fig. 2b).

Proof of the three-component signaling model was provided by Al Gilman and colleagues who were interested in the cytocidal effects of cAMP on clonal S49 murine lymphoma cells (Daniel*, et al.*, 1973). One variant of these cells, *cyc*$^{-}$, lacked adenylyl cyclase activity despite a normal abundance of adrenergic receptors on the cell surface (Bourne*, et al.*, 1975; Insel*, et al.*, 1976). As a first step toward overcoming the effects of the *cyc*$^{-}$ mutation, Gilman and Elliott Ross extracted adenylyl cyclase from cells lacking adrenergic receptors and reconstituted the adenylyl cyclase extract with membranes from the *cyc*$^{-}$ cells. As expected, they observed hormone-induced stimulation of cAMP in the reconstituted system (Ross & Gilman, 1977b), however, not for the anticipated reasons. When the adenylyl cyclase in the extract was heat-inactivated, they still observed undiminished hormone-sensitive cAMP production! (Ross & Gilman, 1977a). Clearly, at least two proteins in the extract were necessary to couple receptor activation to cAMP production in the *cyc*$^{-}$ membranes, adenylyl cyclase and a novel stimulatory protein (Fig. 2c). Additional experiments showed that this transducer protein was likely the hormone-sensitive

GTPase suggested by Rodbell (Ross*, et al.*, 1978). In 1980, Gilman and colleagues reported the purification of a 45 kDa polypeptide, which co-purified with a 35 kDa protein and an 7-8 kDa protein, corresponding to the α, β, and γ subunits of a heterotrimeric guanine nucleotide-binding protein, now known as the stimulatory G protein, G_s, which was sufficient for activation of adenylyl cyclase in *cyc*$^-$ membrane preparations (Northup*, et al.*, 1980; Hildebrandt*, et al.*, 1984). For their discovery of "G proteins and the role of these proteins in signal transduction in cells," Rodbell and Gilman were awarded the Nobel Prize in Medicine or Physiology in 1994.

While Gilman and associates were working to purify G_s, several interesting similarities between the adenylyl cyclase system and the retinal phototransduction system were noted. In the retina, light activates cyclic GMP phosphodiesterase, which breaks down cGMP into GMP. In 1977, the activation of cGMP phosphodiesterase was shown to require GTP and, moreover, light-responsive GTPase activity was identified in the retina, which was necessary to shut off cGMP phosphodiesterase (Wheeler & Bitensky, 1977). These observations led to the purification of transducin, or G_t, a soluble, multimeric protein composed of α, β, and γ subunits (Godchaux & Zimmerman, 1979; Kuhn, 1980; Fung*, et al.*, 1981). Shortly thereafter, the molecular target of islet activating protein, a toxin from *Bordetella pertussis* that blocks hormone-mediated inhibition of adenylyl cyclase, was shown to be an inhibitory GTP-binding protein, G_i (Katada & Ui, 1982; Bokoch*, et al.*, 1984). At this time, it was clear that G_s, G_t, and G_i represented a family of structurally homologous guanine nucleotide-binding proteins with similar α and β subunits (Manning & Gilman, 1983).

Today, we recognize that the family of heterotrimeric G proteins plays a critical role as molecular switch proteins that couple the activation of nearly 1,000 different cell surface receptors to a vast array of intracellular effector proteins. These signaling systems underlie the physiological responses to hormones, neurotransmitters, chemokines, odorants, tastants, and light. The receptors that activate G proteins are also the molecular targets of nearly 50% of all drugs currently on the market. Tremendous progress has been made in the fifty years since Sutherland noted that nothing was known about the mechanism of

action of any hormone, however, many important questions still remain regarding the structure and function of heterotrimeric G proteins.

Figure 2 | Discovery of heterotrimeric G proteins (**a**) Sutherland was the first to propose a model of signal transduction whereby activation of a cell surface receptor (the β receptor in Sutherland's work) by a first messenger leads to the intracellular production of a second messenger (cAMP) leading to protein activation (phosphorylase phosphorylation). However, the simple model proposed by Sutherland suggested that the receptor and adenylyl cyclase (AC) were the same protein. (**b**) Based on several lines of experimental evidence, Rodbell proposed the existence of a transducing protein (G) that coupled receptor (R) activation to adenylyl cyclase stimulation. This protein could be activated by GTP binding and could hydrolyze GTP to turn off the signal. (**c**) When a detergent extract of membrane proteins was added to so-called *cyc*$^-$ membranes, which were thought to lack adenylyl cyclase, epinephrine was able to stimulate cAMP production. This suggested to Gilman and Ross that adenylyl cyclase had been added back to the deficient membranes to reconstitute the signaling pathway (*left*). In the control experiment, where adenylyl cyclase in the protein extract had been heat-inactivated, cAMP was still produced when the protein extract was added to the *cyc*$^-$ membranes! (*center*). This led to the discovery that the *cyc*$^-$ membranes did contain adenylyl cyclase, but did not contain a third component, the G protein, that was necessary to activate it (*right*) (adapted from Linder & Gilman, 1992).

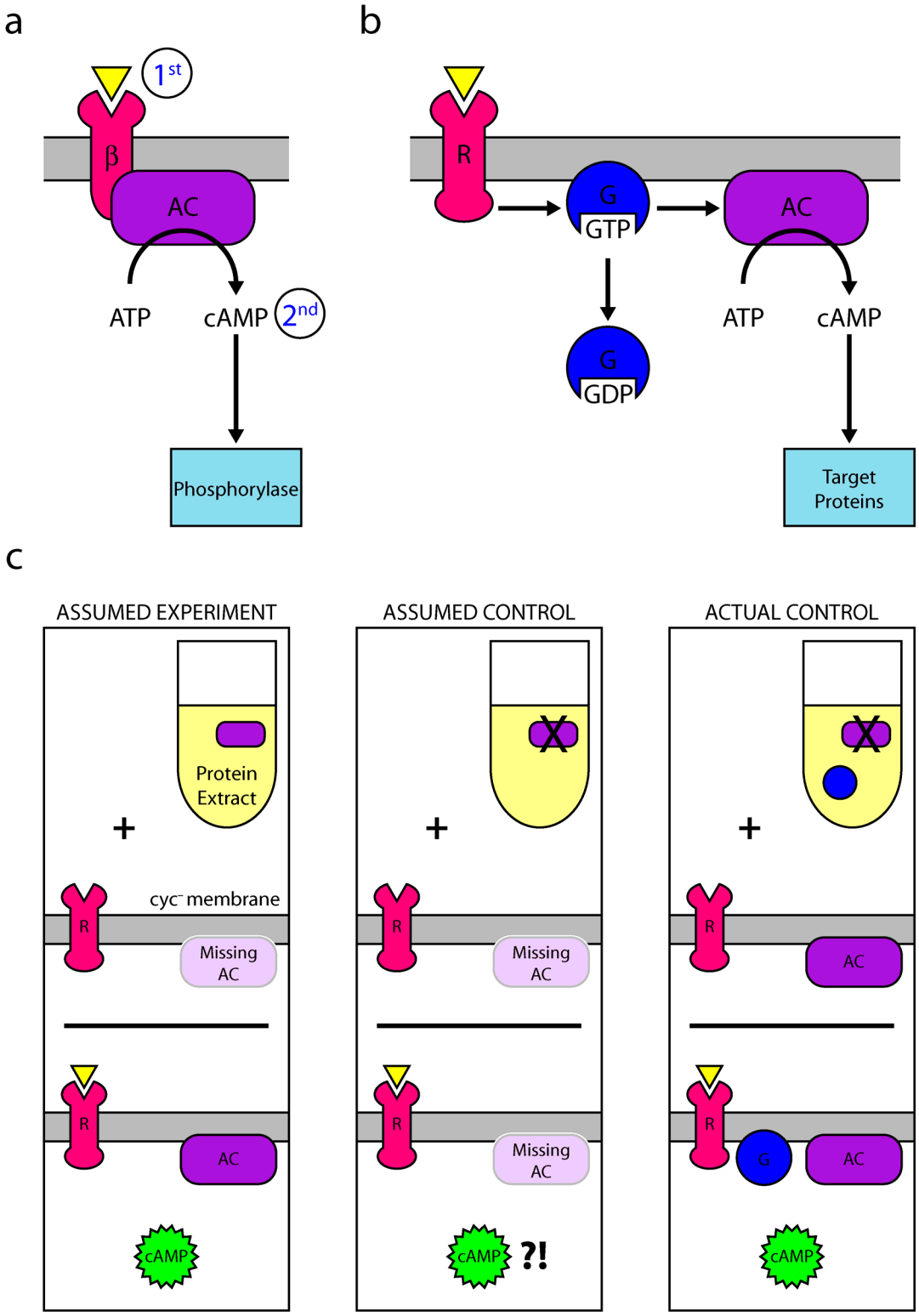
a
1st
β
AC
ATP
cAMP
2nd
Phosphorylase
b
R
G
GTP
AC
G
GDP
ATP
cAMP
Target
Proteins
c
ASSUMED EXPERIMENT
ASSUMED CONTROL
ACTUAL CONTROL
Protein
Extract
+
cyc⁻ membrane
R
Missing
AC
AC
G
cAMP
?!

CHAPTER I

HETEROTRIMERIC G PROTEINS

Introduction

Heterotrimeric guanine-nucleotide-binding proteins act as molecular switches in signaling pathways by coupling the activation of heptahelical receptors at the cell surface to intracellular responses. This role depends on the ability of G protein α subunits to cycle between a resting conformation primed for interaction with an activated receptor and a signaling conformation capable of modulating the activity of downstream effector proteins, including a variety of enzymes and ion channels. As the primary intermediary between receptors and effectors, G proteins play a critical role in determining the specificity and temporal characteristics of the cellular responses to a diverse array of extracellular stimuli.

G proteins are inactive in the heterotrimeric conformation where Gα binds GDP and the constitutive Gβγ dimer. Extracellular stimuli, such as hormones, neurotransmitters, chemokines, light, odorants, and tastants, activate receptors by inducing a conformational change that permits G protein binding and catalyzes GDP release from Gα, thereby resulting in the formation of a stable, high-affinity complex between the activated receptor and the G protein. Binding of GTP to Gα destabilizes this complex, leading to a structural rearrangement of Gα(GTP), Gβγ, and the receptor. Both subunits, Gα(GTP) and Gβγ, go on to interact with downstream effector proteins. The cellular response is terminated when Gα hydrolyzes GTP to GDP and re-associates with Gβγ, thus completing the cycle (Fig. 3). This chapter will serve as a review of our current understanding of the structural determinants of the function, specificity and regulation of heterotrimeric G proteins.

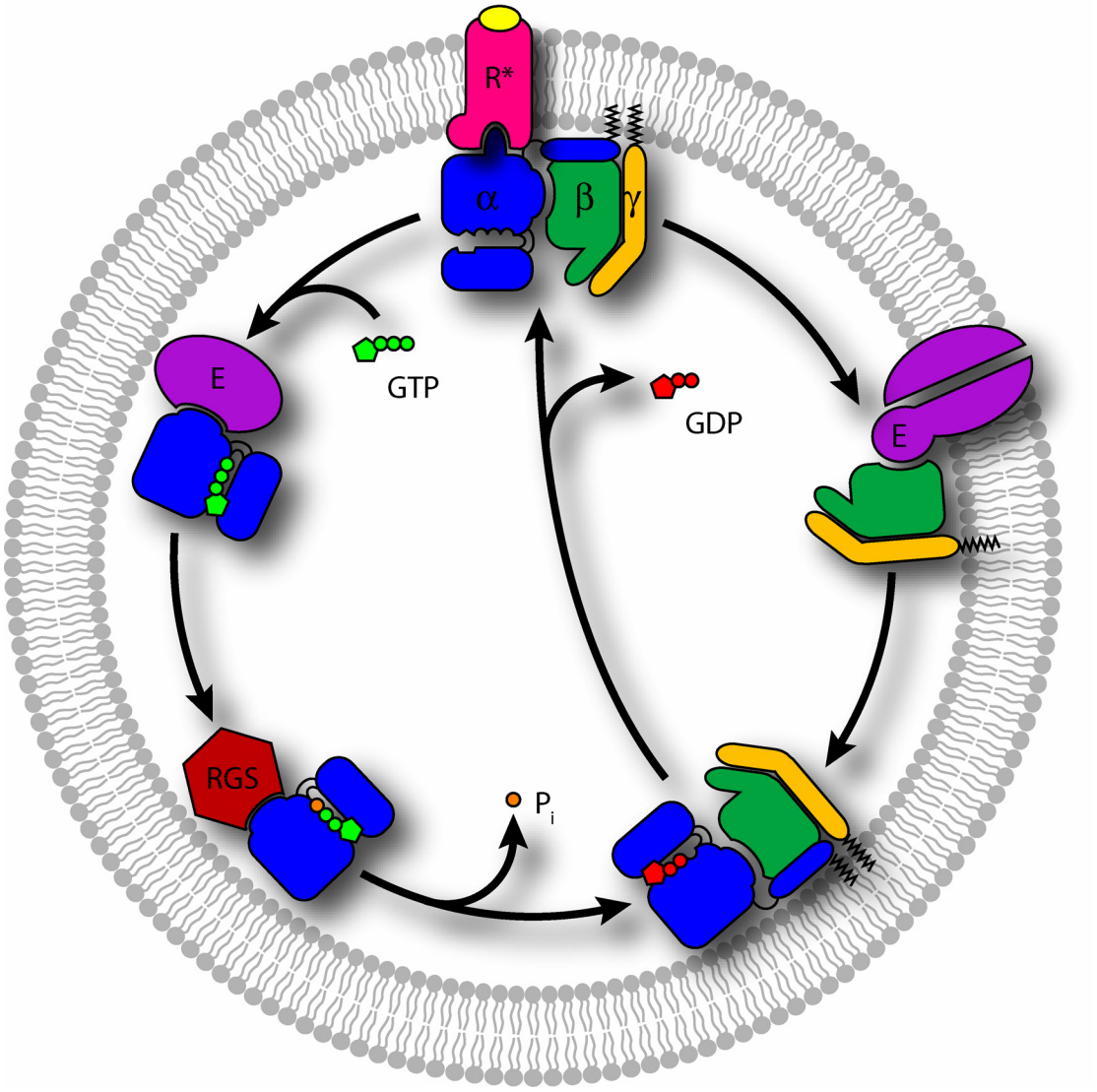

Figure 3 | Heterotrimeric G protein cycle In the resting state, G proteins are heterotrimers of GDP-bound α (*blue*), β (*green*), and γ (*gold*) subunits. Agonist (*yellow*) binding to heptahelical receptors (*pink*) in the cell membrane results in a conformational change leading to G protein binding and, subsequently, GDP release from Gα. The high-affinity, nucleotide-free complex is stable until GTP binding causes a structural rearrangement in R*, Gα(GTP), and Gβγ, allowing the G protein subunits to go on to activate a variety of downstream effector proteins (*purple*). The signal is terminated upon the hydrolysis of GTP to GDP by Gα, which may be catalyzed by RGS proteins (*red*).

Heterotrimeric G Protein Structure

Although nearly nine hundred different heptahelical receptors are known (Fredriksson & Schiöth, 2005), they interact with a relatively small number of G proteins composed of α, β, and γ subunits. At last count, there are 21 Gα subunits encoded by 16 genes, 6 Gβ subunits encoded by 5 genes, and 12 Gγ subunits in humans (Fig. 4) (Downes & Gautam, 1999).

G protein α subunit

Heterotrimeric G proteins are typically divided into four main classes based on the primary sequence similarity of the Gα subunits: $G\alpha_s$, $G\alpha_i$, $G\alpha_q$, and $G\alpha_{12}$ (Simon*, et al.*, 1991). Members of this family range in size from 39-52 kDa and share between 35-95% sequence identity (Fig. 3) (Downes & Gautam, 1999). Many crystal structures of these proteins in a variety of conformations have been resolved, and these structures provide the framework for our understanding of the biomechanics of G protein signaling (Table 1).

All of the Gα structures reveal a conserved protein fold composed of two domains, a GTPase domain and a helical domain (Fig. 5a). The GTPase domain is structurally homologous to the family of monomeric G proteins, and is composed of a six-stranded β-sheet surrounded by five α-helices. The most highly conserved sequences in this domain are the five loops that contain the consensus sequences for guanine nucleotide binding, the diphosphate-binding loop (GxGESGKS), the Mg^{2+}-binding domain (RxxTxGI and DxxG), and the guanine ring-binding motifs (NKxD and TCAT). This domain also contains three flexible loops near the γ-phosphate binding site, named Switches I, II, and III, where significant structural differences between the GDP-bound (Lambright*, et al.*, 1994; Mixon*, et al.*, 1995) and GTPγS-bound (Noel*, et al.*, 1993; Coleman*, et al.*, 1994a) conformations of Gα are found (Fig. 5c). The GTPase domain hydrolyzes GTP and contains sites for binding to the Gβγ dimer, heptahelical receptors and downstream effector proteins. The helical domain is composed of six α-helices that form a

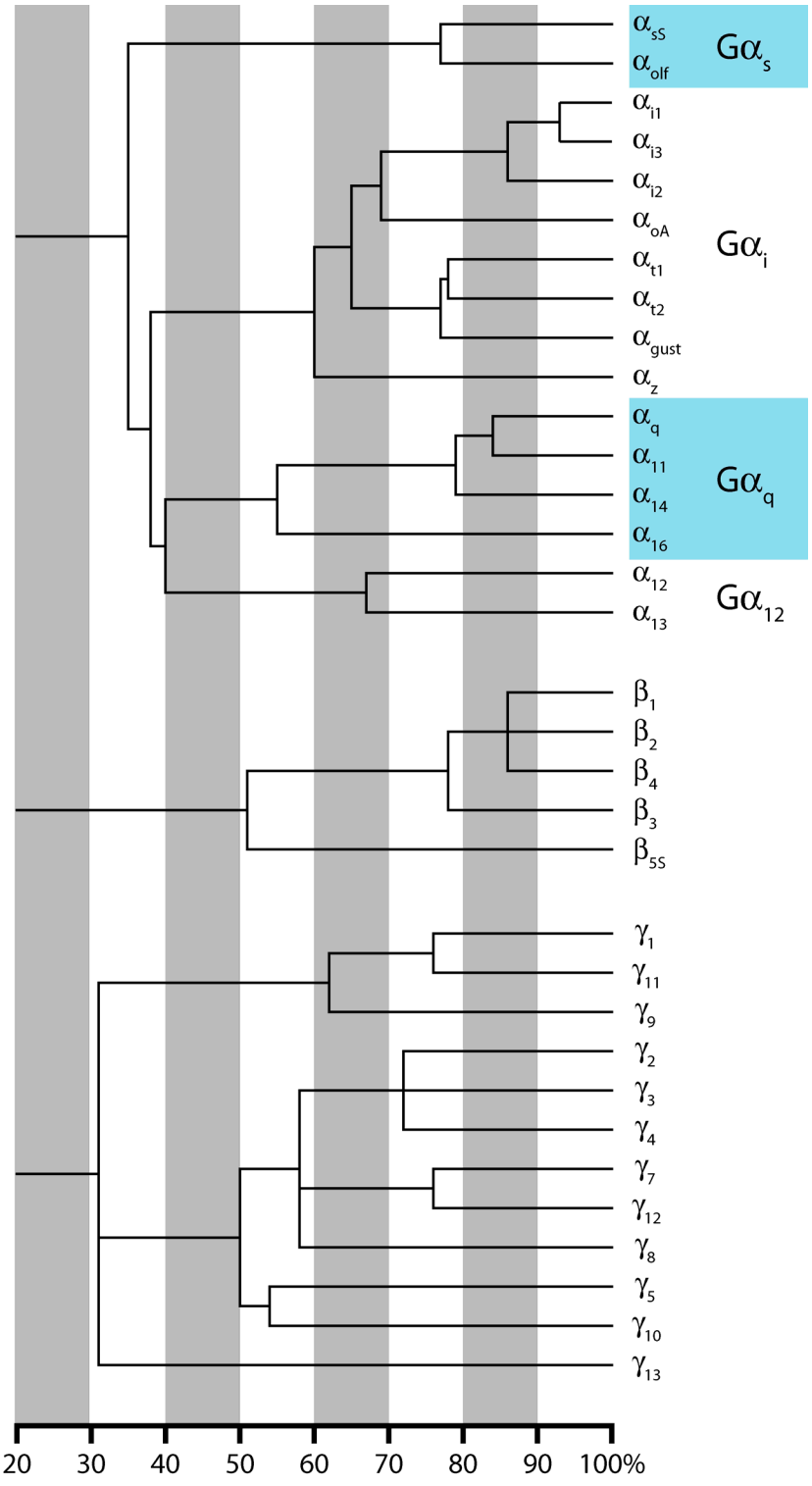

Figure 4 | Primary sequence identity of G protein subunit genes Not shown are the other splice variants of $G\alpha_s$ (3), $G\alpha_o$ (1) and $G\beta_5$ (1).

Table 1 | Heterotrimeric G protein structures

PDB[a]	Complex	Missing Regions (# aa) & Notes	Res. (Å)	Reference
G protein subunits				
1TAG	$G\alpha_t$(GDP)	N[b] (27), C (10)	1.8	(Lambright, *et al.*, 1994)
1GDD	$G\alpha_{i1}$(GDP)	N (8), Switches II (16) & III (6)	2.2	(Mixon, *et al.*, 1995)
1BOF	$G\alpha_{i1}$(GDP)[c]	N (9), Switches II (14) & III (7)	2.2	(Coleman & Sprang, 1998)
1AS3	G42V-$G\alpha_{i1}$(GDP)	N (8), Switches II (10) & III (6)	2.4	(Raw, *et al.*, 1997)
1ZCB	$G\alpha_{i/13}$(GDP)	N (27), Switch II (7), α4/β6 (2), C (5); N from $G\alpha_{i1}$	2.0	(Kreutz, *et al.*, 2006)
1TBG	$G\beta_1\gamma_1$	Cγ (3, F)	2.1	(Sondek, *et al.*, 1996)
Gα complexes with GDIs				
1GOT	$G\alpha_{t/i}\beta_1\gamma_1$ Heterotrimer	Nα (5), Cα (7), Nγ (8), Cγ (5, F); 216-294 from $G\alpha_{i1}$	2.0	(Lambright, *et al.*, 1996)
1GP2	$G\alpha_{i1}\beta_1\gamma_2$ Heterotrimer	Nα (4), Cα (6), Nγ (7), Cγ (7, G)	2.3	(Wall, *et al.*, 1995)
1GG2	G203A-$G\alpha_{i1}\beta_1\gamma_2$ Heterotrimer	Nα (4), Cα (6), Nγ (7), Cγ (7, G)	2.4	(Wall, *et al.*, 1995)
1KJY	$G\alpha_{i1}$(GDP)·RGS14 GoLoco	Nα (29), Cα (5)	2.7	(Kimple, *et al.*, 2002)
Elements that undergo R-mediated conformational changes*				
1AQG	$G\alpha_t$ C-terminus	aa 340-350	NMR	(Kisselev, *et al.*, 1998)
1LVZ	$G\alpha_t$ C-terminus	aa 340-350 with K340R, C346S	NMR	(Koenig, *et al.*, 2002)
1MF6	Gγ C-terminus	aa 60-71, no F	NMR	(Kisselev & Downs, 2003)
Activated Gα subunits				
1TND	$G\alpha_t$(GTPγS)	N (26), C (1)	2.2	(Noel, *et al.*, 1993)
1GIA	$G\alpha_{i1}$(GTPγS)	N (33), C (11)	2.0	(Coleman, *et al.*, 1994a)
1CIP	$G\alpha_{i1}$(GppNHp)	N (31), C (7)	1.5	(Coleman & Sprang, 1999)
1AS0	G42V-$G\alpha_{i1}$(GTPγS)	N (31), C (10)	2.0	(Raw, *et al.*, 1997)
1GIL	Q204L- $G\alpha_{i1}$(GTPγS)	N (33), C (11)	2.3	(Coleman, *et al.*, 1994b)
1BH2	A326S-$G\alpha_{i1}$(GTPγS)	N (31), C (8)	2.1	(Posner, *et al.*, 1998)
1SVS	K180P-$G\alpha_{i1}$(GppNHp)	N (31), C (7)	1.5	(Thomas, *et al.*, 2004)
1AZT	$G\alpha_s$(GTPγS)	N (34), C (3)	2.3	(Sunahara, *et al.*, 1997b)

Table 1 | Continued

PDB	Complex	Missing Regions (# aa) & Notes	Res. (Å)	Reference
Complexes with effectors and other binding proteins				
1FQJ	$G\alpha_{t/i}(GDP{\cdot}AlF_4^-){\cdot}RGS9{\cdot}PDE\gamma$	Nα (27), Cα (6); 216-294 from $G\alpha_{i1}$; RGS box only	2.0	(Slep*, et al.*, 2001)
1AZS	$G\alpha_s(GTP\gamma S){\cdot}ACV/II$[d]	Nα (35), Cα (1); AC VC1 & IIC2 catalytic domains	2.3	(Tesmer*, et al.*, 1997b)
2BCJ	$G\alpha_{i/q}(GDP{\cdot}AlF_4^-){\cdot}GRK2{\cdot}G\beta_1\gamma_2$	Nα (29), Cα (5), Nγ (3), Cγ (1, G); N from $G\alpha_{i1}$	3.1	(Tesmer*, et al.*, 2005)
1SHZ	$G\alpha_{13/i}(GDP{\cdot}AlF_4^-){\cdot}$p115RhoGEF	Nα (30), Cα (5); $G\alpha_{13}$ HD, Switches I-III; RGS only	2.9	(Chen*, et al.*, 2005b)
2TRC	$G\beta_1\gamma_1{\cdot}$Phosducin	Cγ (3, F)	2.4	(Gaudet*, et al.*, 1996)
1A0R	$G\beta_1\gamma_1{\cdot}$Phosducin	Nγ (1), Cγ (5); F is present	2.8	(Loew*, et al.*, 1998)
1B9X	$G\beta_1\gamma_1{\cdot}$S73E-Phosducin	Cγ (3, F)	3.0	(Gaudet*, et al.*, 1999)
1B9Y	$G\beta_1\gamma_1{\cdot}$Phosducin	Cγ (3, F)	3.0	(Gaudet*, et al.*, 1999)
1OMW	$G\beta_1\gamma_2{\cdot}$GRK2	Nγ (7), Cγ (G)	2.5	(Lodowski*, et al.*, 2003)
1XHM	$G\beta_1\gamma_2{\cdot}$SIGK peptide	Nγ (6), Cγ (17, G)	2.7	(Davis*, et al.*, 2005)
Transition-state structures in GTP hydrolysis				
1TAD	$G\alpha_t(GDP{\cdot}AlF_4^-)$	N (26), C (6)	1.7	(Sondek*, et al.*, 1994)
1GFI	$G\alpha_{i1}(GDP{\cdot}AlF_4^-)$	N (32), C (9)	2.2	(Coleman*, et al.*, 1994a)
1SVK	K180P-$G\alpha_{i1}(GDP{\cdot}AlF_4^-)$	N (32), C (9)	2.0	(Thomas*, et al.*, 2004)
1ZCA	$G\alpha_{i/12}(GDP{\cdot}AlF_4^-)$	N (34), C (9); N from $G\alpha_{i1}$	2.9	(Kreutz*, et al.*, 2006)
1AS2	G42V-$G\alpha_{i1}(GDP{\cdot}P_i)$	N (31), C (8)	2.8	(Raw*, et al.*, 1997)
1GIT	G203A-$G\alpha_{i1}(GDP{\cdot}P_i)$	N (31), C (6)	2.6	(Berghuis*, et al.*, 1996)
1FQK	$G\alpha_{t/i}(GDP{\cdot}AlF_4^-){\cdot}RGS9$	Nα (27), Cα (5); 216-294 from $G\alpha_{i1}$	2.3	(Slep*, et al.*, 2001)
1AGR	$G\alpha_{i1}(GDP{\cdot}AlF_4^-){\cdot}RGS4$	Nα (4)	2.8	(Tesmer*, et al.*, 1997a)

[a] The Protein Data Bank at www.pdb.org.

[b] Abbreviations: (N) residues missing from the amino terminal methionine; (C) residues missing from the C-terminus or isoprenylation site (Gγ); (F) farnesyl; (G) geranylgeranyl; (HD) helical domain.

[c] This structure was solved in the presence of Mg^{2+}, distinguishing it from 1GDD.

[d] Additional structures of this complex have been solved with different ligands for AC: 1CJK, 1CJT, 1CJU, 1CJV (Tesmer*, et al.*, 1999), 1CS4 and 1CUL (Tesmer*, et al.*, 2000).

lid over the nucleotide-binding site, burying bound nucleotides in the core of the protein. Functions of the helical domain include increasing the affinity of Gα for guanine nucleotides (Remmers, *et al.*, 1999; Warner, *et al.*, 1998) and increasing the GTP hydrolysis activity of the protein (Markby, *et al.*, 1993). As this domain is the most divergent among Gα subunits, it may also play a significant role in coupling specific G proteins to specific effectors (Liu, *et al.*, 1998).

Less is known about the structure of two other important regions of Gα, the amino and carboxyl termini, because they were either removed from the protein or disordered in the crystals. In the two structures of G protein heterotrimers, the N-terminus forms an α-helix that is ordered by its interaction with Gβ (Fig. 5a) (Lambright, *et al.*, 1996; Wall, *et al.*, 1995), however, its structure and location in most of the other conformations of the protein remain unknown. Both termini are key determinants of receptor binding specificity and play a critical role in G protein activation.

The N-terminus is also the site of the fatty acid modifications on Gα subunits that regulate G protein localization and protein-protein interactions. All of these proteins, except $G\alpha_t$, are modified post-translationally with the saturated 16-carbon fatty acid palmitate, and some ($G\alpha_q$, $G\alpha_{11}$, $G\alpha_{13}$, and $G\alpha_{15}$) are palmitoylated at multiple sites. Palmitate is attached by a reversible thioester bond to cysteines near the N-terminus of Gα, which is subject to regulation by protein acyltransferases and thioesterases (reviewed in Chen & Manning, 2001; Smotrys & Linder, 2004). Members of the $G\alpha_i$ family are also myristoylated, which results from the co-translational addition of the saturated 14-carbon fatty acid myristate to an N-terminal glycine following removal of the initiating methionine residue. Since a stable amide bond links the myristate to the protein, myristoylation is an irreversible modification (reviewed in Chen & Manning, 2001).

Recently, we have shown that myristoylation also plays an important role in the structure of the N-terminal helix of Gα. In the non-myristoylated protein, this region is dynamically disordered, and upon binding to Gβγ, the N-terminus becomes ordered (Medkova, *et al.*, 2002), consistent with its conformation as an ordered α-helix in the crystal structures of G protein heterotrimers

Figure 5 | Structural features of heterotrimeric G proteins (**a**) Ribbon model of the $G\alpha_{t/i}(GDP)\beta_1\gamma_1$ heterotrimer (1GOT), where α is *blue*, β is *green*, and γ is *gold*. The three Switch regions in Gα are highlighted in *yellow*. GDP (*red*) is buried between the GTPase and helical domains of Gα. (**b**) The subunits have been rotated to show the intersubunit interface, which is primarily composed of the αN helix (truncated in this view) and Switch II on Gα and blades 1-3 on Gβ. (**c**) When the GDP-bound (1TAG), GTPγS-bound (1TND), and heterotrimer (1GOT) structures of $G\alpha_t$ are aligned, significant conformational differences are found in the three Switch regions (compare *gray* and *colored* backbone). The crystal structures indicate that, upon GTP binding (*green backbone*), these regions collapse toward the γ-phosphate of GTP. The Gα(GDP) conformation (*blue backbone*) is likely a short-lived transition state *in vivo* due to the large hydrophobic surface presented by this conformation of the Switch regions.

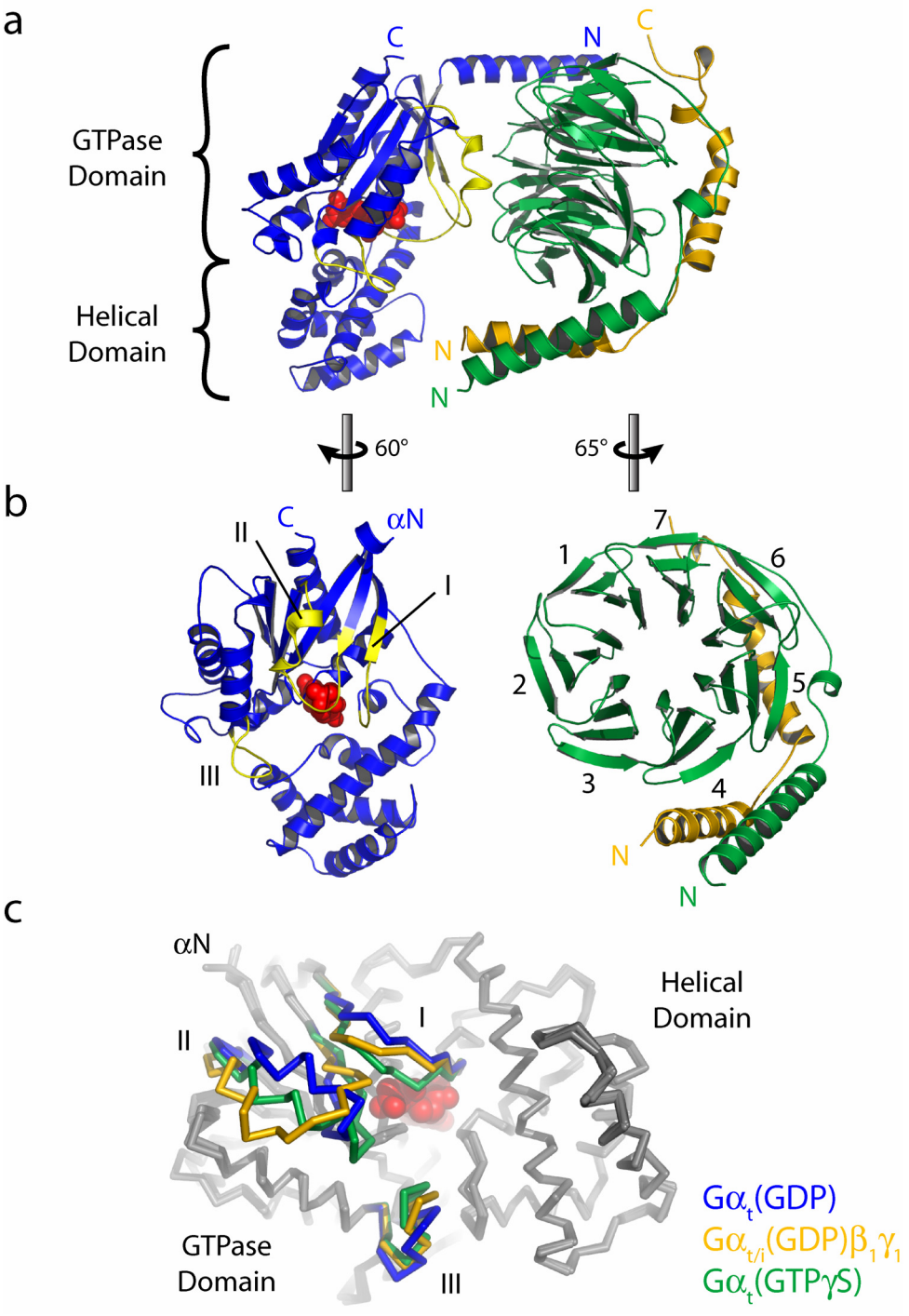
a
GTPase Domain
Helical Domain
C
N
C
N
N
60°
65°
b
C
αN
II
I
III
7
1
6
2
5
3
4
N
N
c
αN
II
I
Helical Domain
GTPase Domain
III
Gα$_t$(GDP)
Gα$_{t/i}$(GDP)β$_1$γ$_1$
Gα$_t$(GTPγS)

(Wall, *et al.*, 1995; Lambright, *et al.*, 1996). However, the myristoylated N-terminus is highly ordered in Gα(GDP), and no further conformational changes are observed upon binding to Gβγ (Preininger, *et al.*, 2003). Thus, myristoylation plays a structural role in ordering the αN helix, even in the absence of Gβγ. Furthermore, steady-state fluorescence and fluorescence anisotropy indicate that the myristoylated N-terminus is less solvent exposed and less mobile than the non-myristoylated N-terminus, pointing to a putative intramolecular binding site in Gα(GDP) for the myristoylated N-terminus (Fig. 6) (Preininger, *et al.*, 2003). Myristoylation also affects the interactions between Gα and effectors (Gallego, *et al.*, 1992; Taussig, *et al.*, 1993; Dessauer, *et al.*, 1998) and the soluble guanine nucleotide exchange factor, Resistance to inhibitors of cholinesterase 8A (Tall & Gilman, 2005).

G protein βγ dimer

All six Gβ subunits are approximately 36 kDa, and share 50-90% sequence identity, with the long and short splice variants of $G\beta_5$ being the least similar to the other four members of the family (Fig. 4) (Downes & Gautam, 1999). Although not as dynamic a protein as Gα, Gβ is certainly more attractive with its seven-bladed β-propeller structure formed from seven WD40 sequence repeats (Fig. 5b). Each blade is composed of four antiparallel β-strands, where one WD40 sequence contributes the last three strands in one blade and the first strand in the next blade. Consequently, the final blade requires the N-terminus of Gβ to contribute the fourth β-strand, and thereby close the ring. The remaining N-terminal residues adopt an α-helical conformation that forms a coiled coil that is essential for interaction with Gγ or Gγ-like motifs and six (Fig. 5) (Sondek, *et al.*, 1996). All of the Gγ subunits undergo post-translational isoprenylation at their C-termini with a 15-carbon farnesyl ($G\gamma_1$, $G\gamma_8$, and $G\gamma_{11}$) or 20-carbon geranylgeranyl (all others) moiety. These isoprenoids are first attached by a stable thioether bond to a cysteine residue located in the C-terminal CaaX sequence of Gγ. Then the three C-terminal amino acids are removed, and the new prenylated C-terminus is carboxylmethylated (reviewed in Zhang & Casey, 1996). If the X residue in the CaaX motif is serine, methionine, glutamine, or alanine, then Gγ is

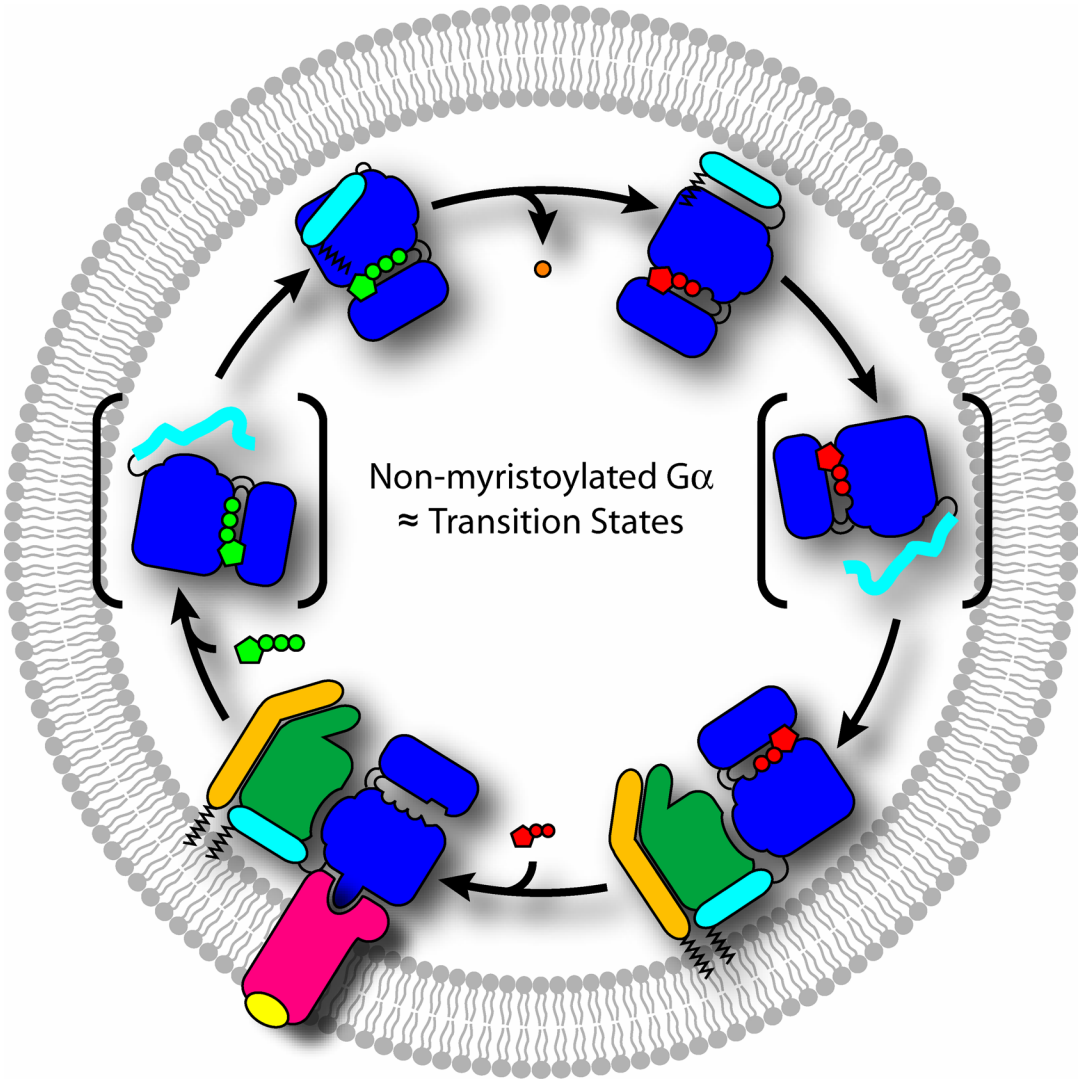

Figure 6 | GTP-dependent myristoyl switch Biophysical studies using fluorescence and EPR spectroscopy have shown that myristoylation plays a critical role in the structure of the N-terminus (*cyan*) of Gα subunits. In the non-myristoylated proteins, the N-terminus is disordered in both the GDP-bound and GTP-bound conformations. By contrast, this helix is ordered in the myristoylated proteins. Upon GTP binding to the myristoylated Gα, the N-terminus enters into a more hydrophobic environment than in either the Gα(GDP) or heterotrimeric conformations, suggesting that G protein activation exposes an intramolecular binding site for the N-terminus. The disordered structures observed in non-myristoylated G proteins may reflect the transition states following activation and prior to heterotrimer formation.

farnesylated, while leucine at this position directs geranylgeranylation (reviewed in Higgins & Casey, 1996). Carboxylmethylation increases the affinity of Gβγ for the membrane by neutralizing the negatively charged C-terminus (Fukada, *et al.*, 1994).

The G protein β and γ subunits form a functional unit that is not dissociable except by denaturation (Schmidt, *et al.*, 1992). Although most β subunits can interact with most γ subunits, not all of the sixty possible combinations of dimers form (Clapham & Neer, 1997). For example, $G\gamma_1$ interacts with $G\beta_1$, but not $G\beta_2$ despite its high (87%) sequence identity to $G\beta_1$, and $G\beta_2$ does bind to $G\gamma_2$ despite its similarity to $G\gamma_1$ (38% identity) (Garritsen & Simonds, 1994; Downes & Gautam, 1999; Schmidt, *et al.*, 1992; Pronin & Gautam, 1992). Substituting three consecutive residues in the middle of $G\gamma_1$ with homologous residues from $G\gamma_2$, including a leucine that is conserved in all Gγ subunits except for $G\gamma_1$, enables $G\gamma_1$ binding to $G\beta_2$, however the reverse substitution does not allow $G\gamma_2$ to bind to $G\beta_2$, suggesting that additional regions are also important for the specificity of dimer formation (Lee, *et al.*, 1995a). Several different Gβγ dimers can interact with the same Gα isoform (Graf, *et al.*, 1992), suggesting that differential expression or subcellular localization may be an important determinant of signaling specificity.

Unique role of $G\beta_5$ in complexes with RGS proteins

$G\beta_5$ is unique among Gβ isoforms. While $G\beta_{1\text{-}4}$ share 80-90% sequence identity and are ubiquitously expressed, $G\beta_5$ shares only 50% identity and is preferentially expressed in the nervous system (Fig. 4) (Downes & Gautam, 1999). Additionally, $G\beta_{1\text{-}4}$ are entirely particulate proteins while $G\beta_5$ is found in both the particulate and soluble fractions. The N-terminus of $G\beta_5$ is also significantly longer than the other subunits (Watson, *et al.*, 1994). Although this region is important for binding Gγ (Garritsen, *et al.*, 1993), $G\beta_5$ can still form dimers and functional heterotrimers, as well as interact with a number of effectors following receptor activation (Zhang, *et al.*, 1996; Bayewitch, *et al.*, 1998b; Fletcher,

et al., 1998; Watson*, et al.*, 1994; Watson*, et al.*, 1996). Unlike the other Gβ subunits, $G\beta_5$ can be easily dissociated from Gγ and is stable in solution as a monomer (Cabrera*, et al.*, 1998; Yoshikawa*, et al.*, 2000). Interestingly, free $G\beta_5$ has been shown to form complexes with regulators of G protein signaling proteins, a family of GTPase activating proteins, that contain a Gγ-like domain (Levay*, et al.*, 1999; Makino*, et al.*, 1999). The GGL domain is a 64-amino acid sequence that is found in RGS6, 7, 9, 11, and the *C. elegans* RGS protein, EGL-10 (Snow*, et al.*, 1998). The interaction between these RGS proteins and $G\beta_5$ enhances their ability to accelerate the GTPase activity of Gα subunits (Kovoor*, et al.*, 2000). In addition, this interaction allows RGS6, 7, and 11 to selectively GAP $G\alpha_o$ (Snow*, et al.*, 1998).

These unique associations beg the question as to whether $G\beta_5$ interacts with RGS proteins, Gγ, or both *in vivo*. Despite the extensive *in vitro* biochemical evidence, there is little data to support a $G\beta_5\gamma$ complex *in vivo*, although this may be due to the technical difficulties resulting from the somewhat weaker interactions between these proteins than in other dimers (Jones*, et al.*, 2004). By contrast, in native preparations of vertebrate photoreceptors, the long isoform of $G\beta_5$ is in a tight complex with RGS9 (Makino*, et al.*, 1999). When RGS9 is knocked out, $G\beta_{5L}$ cannot be found in the retinal tissue of these animals, despite the presence of normal $G\beta_5$ mRNA levels (Chen*, et al.*, 2000). The protein levels for the short isoform were normal in these animals, suggesting that RGS9 may be required for the stability of $G\beta_{5L}$, while $G\beta_{5S}$ is stabilized by interactions with Gγ or other RGS proteins (Chen*, et al.*, 2000). Similarly, the protein expression of all GGL-containing RGS proteins is eliminated or substantially reduced in $G\beta_5$ knockout mice (Chen*, et al.*, 2003). Several other provocative questions are posed by these complexes, including why $G\beta_5$ is specifically enriched in the brain, whether they can form functional heterotrimers *in vivo* and what the physiological roles of the various complexes in signal transduction are. Clearly they are important for the fast inactivation of the photoreceptor response (Chen*, et al.*, 2000), and roles in opioid and dopaminergic signaling pathways are emerging (reviewed in Jones*, et al.*, 2004), yet we are only beginning to understand the functional consequences of these interactions.

Heterotrimeric G protein structure

Two crystal structures of G protein heterotrimers, $G\alpha_{t/i}\beta_1\gamma_1$ and $G\alpha_{i1}\beta_1\gamma_2$, show two sites of interaction between Gα and Gβγ (Fig. 5a) (Lambright*, et al.*, 1996; Wall*, et al.*, 1995). The primary interaction surface is between Switches I and II of Gα and residues from five of seven blades on Gβ. This switch interface buries approximately 1,800 $Å^2$ of solvent-accessible surface area, and is composed of hydrophobic residues stabilized by hydrogen bonds and two ion pairs. A second interaction between the N-terminus of Gα and blade one of Gβ buries 900 $Å^2$ of solvent-accessible surface area.

Neither crystal structure provides evidence for Gα-Gγ contacts, although the acylated amino and carboxyl termini of Gα and Gγ, respectively, would likely be in close proximity to each other, suggesting that their lipids insert cooperatively into the plasma membrane (Bigay*, et al.*, 1994; Seitz*, et al.*, 1999). In addition to their membrane anchoring role, the lipid modifications have been shown to increase the affinity of Gα for Gβγ, and *vice versa*, and this effect may be independent of the presence of the membrane (Linder*, et al.*, 1991; Iniguez-Lluhi*, et al.*, 1992; Iiri*, et al.*, 1996). Since these modifications are absent from the two G protein heterotrimer crystals, additional studies are needed to understand the structural features of these hydrophobic moieties and their effect on Gα-Gβγ interactions.

Comparing the structures of Gα(GDP) (Lambright*, et al.*, 1994; Mixon*, et al.*, 1995) and the G protein heterotrimers shows that Gβγ binding significantly alters the conformation of Switches I and II, while the rest of Gα remains relatively unperturbed (Fig. 4c). By stabilizing these two flexible loops and, in the G_{i1} heterotrimer, forming a new salt bridge between the P-loop and Switch I, Gβγ locks GDP into the nucleotide-binding pocket (Wall*, et al.*, 1995). This reorganization also appears to disassemble the binding sites for Mg^{2+} and the GTP γ-phosphate (Fig. 14a), explaining the observation that GTP and Gβγ binding to Gα are negatively cooperative (Higashijima*, et al.*, 1987b). In contrast to the rearrangements observed in Gα upon heterotrimer formation, significant structural changes are not observed in Gβγ.

Lipid modifications direct membrane association

One clear function of the fatty acid modifications on Gα and Gγ is to direct the association of the heterotrimer with the membrane. For $G\alpha_i$ family members, both fatty acid modifications, myristoylation and palmitoylation, contribute to membrane localization. Mutations that prevent palmitoylation shift the localization of myristoylated proteins from the membrane to the cytoplasm (Degtyarev*, et al.*, 1994; Morales*, et al.*, 1998; Mumby*, et al.*, 1994; Wise*, et al.*, 1997a). Similarly, mutating the N-terminal glycine to block myristoylation not only increases the amount of soluble protein, but also inhibits palmitoylation of these proteins (Mumby*, et al.*, 1990; Galbiati*, et al.*, 1994; Hallak*, et al.*, 1994; Wilson & Bourne, 1995). These observations support a two-signal membrane trapping model for anchoring Gα to the plasma membrane (Shahinian & Silvius, 1995). In this model, myristoylation is the first signal that leads to a transient interaction of Gα with the membrane. Palmitoylation is the second signal that serves to securely attach the protein to the membrane. Consistent with the requirement of two hydrophobic moieties for membrane localization, non-myristoylated $G\alpha_i$ and $G\alpha_o$ can be trafficked to the membrane by isoprenylated Gβγ, where they are subsequently palmitoylated. Since only membranes with the capacity for palmitoylation can trap G proteins in this model, this modification may specifically concentrate the G proteins at the plasma membrane rather than at intracellular organelle membranes that have less palmitoyl acyltransferase activity (Chen & Manning, 2001; Morales*, et al.*, 1998; McCabe & Berthiaume, 1999). Alternatively, Gβγ may be the primary determinant of Gα localization, as a mutant Gβγ that targets to mitochondrial membranes will recruit $G\alpha_z$ to the mitochondria independent of palmitoylation (Fishburn*, et al.*, 2000).

In the remaining Gα family members that are not myristoylated, mutations that prevent palmitoylation can markedly impair membrane association (Wedegaertner*, et al.*, 1993; Degtyarev*, et al.*, 1993; Wise*, et al.*, 1997b; Bhattacharyya & Wedegaertner, 2000). For these proteins, the hydrophobic isoprenyl group on Gγ may act as the first signal, leading to membrane binding and palmitoylation. Mutants of $G\alpha_s$ and $G\alpha_q$ that could not interact with Gβγ were localized in the cytosol and were not

palmitoylated. When the $G\alpha_q$ mutant was myristoylated, its membrane localization and palmitoylation were restored (Evanko*, et al.*, 2000). Additionally, the over-expression of $G\beta\gamma$ was able to rescue the membrane localization of $G\beta\gamma$-binding deficient mutants of $G\alpha_s$ and $G\alpha_q$ in a subtype-specific manner (Evanko*, et al.*, 2001). The two signal model may also apply to the targeting of $G\beta\gamma$ to the plasma membrane as heterotrimer formation and isoprenylation appear to be required for this process (Takida & Wedegaertner, 2003; Evanko*, et al.*, 2001). Indeed, the addition of a palmitoylation site to $G\gamma_2$ as a putative second membrane targeting signal can recover the appropriate plasma membrane localization of $G\beta_1\gamma_2$ in the absence of $G\alpha$ (Takida & Wedegaertner, 2003).

Receptor-G Protein Complexes

Low affinity interactions between inactive receptors and G proteins

Early studies of receptor-G protein interactions in the visual transduction field demonstrated that transducin can bind to dark rhodopsin, albeit at a much lower affinity (Hamm*, et al.*, 1987). Pure phospholipid vesicles could not bind G_t, while vesicles containing rhodopsin could bind the G protein in both the dark and the light (Fung, 1983). The dark membrane binding site saturated at 25% of the rhodopsin concentration (Liebman & Sitaramayya, 1984), and the only protein present at that concentration in washed rod outer segment membranes is rhodopsin (Hamm & Bownds, 1986). Interestingly, sulfhydryl modification with N-ethylmaleimide of what is now known to be the C-terminal cysteine in $G\alpha_t$ does not disturb the interaction between dark rhodopsin and G_t, while it completely blocks binding to the photoactivated receptor (Hofmann & Reichert, 1985). More recently, surface plasmon-waveguide resonance spectroscopy has been used to study the interaction between rhodopsin and G_t. These studies indicate that G_t binds to dark rhodopsin with an apparent K_d of 64 nM (Alves*, et al.*, 2005). Although this is consistent with an earlier result obtained by surface plasmon resonance spectroscopy, a similar method (Salamon*, et al.*, 1996), it is beyond the lower limit of the previously published values for

this interaction, ranging from 10-0.1 μM (Schleicher & Hofmann, 1987; Liebman & Sitaramayya, 1984). The affinity of G_t for light activated rhodopsin is approximately 1 nM (Bennett & Dupont, 1985; Alves*, et al.*, 2005). A high affinity interaction between rhodopsin and transducin in the dark suggests that all of the G_t-binding sites in ROS are constitutively saturated, which is a surprising conclusion. Clearly transducin is able to interact with dark rhodopsin, however, much more work is required to explore the structural features and physiological consequences of this interaction.

Similar complexes between the inactive receptor and G protein have been observed in other receptor systems. For example, G_i co-purified through several steps with the α_2-adrenergic receptor (Cerione*, et al.*, 1986). The antagonist-bound δ-opioid receptor has approximately 50-fold lower affinity for G proteins than the agonist-bound receptor, as shown by PWR. Interestingly, GTPγS did not cause dissociation of the antagonist- or inverse agonist-bound δ-opioid receptor-G protein complexes, suggesting that these are complexes with the GDP-bound heterotrimer (Alves*, et al.*, 2003). Additional support for the formation of these complexes is also provided by kinetic studies of rhodopsin-catalyzed nucleotide exchange in $G\alpha_t$, where a distinct $R{\cdot}G\alpha(GDP)\beta\gamma$ complex is required to fit the double displacement (ping-pong) mechanism described (Heck & Hofmann, 2001). In hormone-sensitive cells that contain only a few thousand receptors, preformed receptor-G protein complexes could have a major impact on the kinetics of intracellular events (Hamm*, et al.*, 1987).

Receptor activation exposes the high-affinity G protein binding site

G protein-coupled receptors have a common body plan with seven transmembrane-spanning α-helices with an extracellular N-terminus, intracellular C-terminus and three interhelical loops on each side of the membrane (Fig. 7). The C-terminal tail contains an eighth α-helix and palmitoylation sites that create a fourth intracellular loop (Palczewski*, et al.*, 2000). Although the overall sequence homology between receptors is low, there are several highly conserved microdomains including helix VIII and the palmitoylation sites, as well as the D(E)RY and $NPxxYx_5F$ motifs, which are near the intracellular face of

the receptors and play an important role in receptor and G protein activation (Fig. 7) (reviewed in Kristiansen, 2004). Despite extensive effort, the dark (inactive) conformation of rhodopsin remains the only receptor for which crystal structures have been solved (Palczewski, *et al.*, 2000; Teller, *et al.*, 2001; Okada, *et al.*, 2002; Okada, *et al.*, 2004; Li, *et al.*, 2004). Although these structures shed little light on the G protein coupling mechanism, they have provided a useful framework for the interpretation of numerous biophysical studies on the conformational changes associated with receptor activation (reviewed in Hubbell, *et al.*, 2003). Extensive site-directed spin-labeling studies of rhodopsin have shown that photoactivation primarily results in an outward movement of helix VI, thereby opening a crevice in the intracellular face of the receptor (Fig. 7) (Farrens, *et al.*, 1996). This outward movement appears to be essential for G protein activation as disulfide and metal-ion cross-links between helices III and VI prevent light-stimulated nucleotide exchange in G_t (Farrens, *et al.*, 1996; Sheikh, *et al.*, 1996). A similar movement has also been observed in other receptors, suggesting that it is an important component of the conformational change leading to G protein binding (reviewed in Gether, 2000; Gether, *et al.*, 2002).

Receptor-G protein interaction surface

The newly formed pocket in the cytoplasmic face of the receptor forms the binding site for the C-terminus of Gα (Janz & Farrens, 2004), which is the best characterized receptor contact site in G proteins. Structural information for this region is lacking from G protein crystal structures, however, as these residues are either absent or disordered in most of them (Table 1). Upon binding light-activated rhodopsin, eleven amino acid C-terminal peptides from $G\alpha_t$ form an α_L-type C-cap motif (Fig. 9) (Dratz, *et al.*, 1993; Kisselev, *et al.*, 1998; Koenig, *et al.*, 2002). Interestingly, the structure of the activated rhodopsin-bound peptide was similar to that observed in the $G\alpha_{i1}(GDP{\cdot}AlF_4^-){\cdot}$RGS4 structure (Tesmer, *et al.*, 1997a; Kisselev, *et al.*, 1998). The angle between the axis of the helix with respect to the membrane normal was determined to be approximately 40° based on the combination of transfer nuclear Overhauser effect and residual dipolar coupling nuclear magnetic resonance data (Koenig, *et al.*, 2002). This same

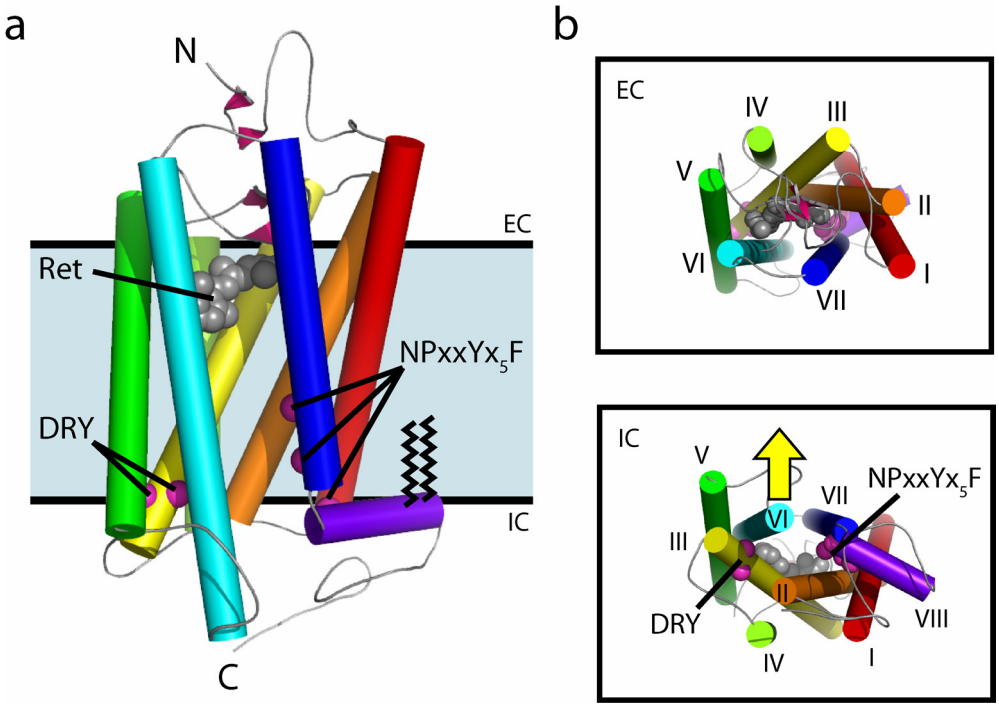

Figure 7 | Heptahelical receptor structure (**a**) Cartoon model of dark (inactive) bovine rhodopsin (1U19), showing the seven transmembrane-spanning α-helices (*red* to *blue*) and 11-*cis*-retinal (*gray spheres*). Conserved residues important for receptor and G protein activation are shown (*magenta spheres*), including the DRY motif on helix III (*yellow*) and NpxxYx$_5$F motif on helices VII and VIII (*blue* and *purple*). (**b**) The extracellular and intracellular faces of rhodopsin are shown. Receptor activation results in an outward movement of helix VI (*yellow arrow*), which opens a gap in the cytoplasmic face of the receptor, exposing residues critical for G protein activation, such as the DRY motif on helix III (*yellow*).

peptide stabilizes the metarhodopsin II signaling conformation of rhodopsin, and will compete with the G_t heterotrimer for binding to the receptor (Hamm, *et al.*, 1988; Aris, *et al.*, 2001). Screening a combinatorial library for peptides that could stabilize Meta II demonstrated that the C-terminal seven amino acids of $G\alpha_t$ are the most important for this interaction (Martin, *et al.*, 1996). Several mutations in this region have been shown to uncouple G proteins from their receptors, including an arginine-to-proline mutation in $G\alpha_s$, first identified in the *unc* clone of S49 murine lymphoma cells, that has since been associated with Albright's hereditary osteodystrophy (Sullivan, *et al.*, 1987; Schwindinger, *et al.*, 1994; Osawa & Weiss, 1995). Similarly, the pertussis toxin-catalyzed ADP-ribosylation of the C-terminal cysteine in $G\alpha_i$ family members also uncouples signaling through G_i-coupled receptors (West, *et al.*, 1985). This cysteine can only be substituted with other hydrophobic residues (Aris, *et al.*, 2001), evidence that it is binding to a hydrophobic pocket in the activated receptor.

A number of residues in the $\alpha4/\beta6$ loop at the C-terminus of $G\alpha$ have also been implicated in receptor contact by alanine-scanning mutagenesis (Fig. 8) (Onrust, *et al.*, 1997), chimeric studies (Bae, *et al.*, 1997; Bae, *et al.*, 1999), sequence analysis of conserved residues in $G\alpha$ subclasses (Lichtarge, *et al.*, 1996a), chemical cross-linking (Cai, *et al.*, 2001), and tryptic proteolysis (Mazzoni & Hamm, 1996). Five residues in the $\alpha3/\beta5$ loop of $G\alpha_s$, when replaced with the homologous amino acids in $G\alpha_{i2}$, decrease receptor-mediated GTP binding while increasing receptor affinity (Fig. 8) (Grishina & Berlot, 2000). The αN helix also interacts with the receptor, as shown by peptide competition (Hamm, *et al.*, 1988), mutagenesis (Onrust, *et al.*, 1997), chemical cross-linking (Taylor, *et al.*, 1994; Itoh, *et al.*, 2001), and $G\alpha$ chimeras (Ho & Wong, 2000) (Fig. 8).

The $G\beta\gamma$ subunit also binds receptors and is required to stabilize the receptor-$G\alpha$ interface. The C-terminal sixty amino acids of $G\beta$ can be cross-linked to a peptide corresponding to the third intracellular loop of the α_2-adrenergic receptor (Fig. 8) (Taylor, *et al.*, 1994; Taylor, *et al.*, 1996). Alanine-scanning mutagenesis in $G\beta$ identified several mutants with normal heterotrimer formation, but defective receptor-mediated GTPγS uptake, indicating a role for $G\beta\gamma$ in this process, either directly or

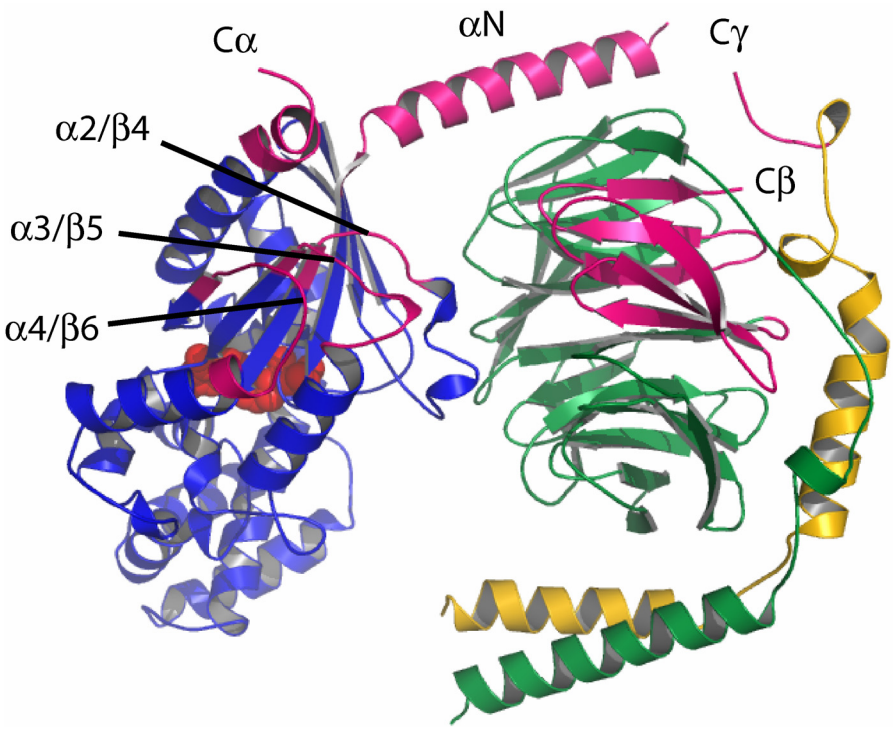

Figure 8 | Receptor contact sites on the G protein Ribbon diagram of the heterotrimeric G protein (1GOT) with the C-terminal tail of $G\alpha_t$ attached (1AQG). The G protein has been rotated toward the viewer from the putative receptor-binding orientation to visualize the receptor contact sites (*magenta*).

indirectly through stabilization of the Gα subunit (Ford, *et al.*, 1998). A farnesylated C-terminal twelve amino acid peptide of $G\gamma_1$ will stabilize Meta II (Kisselev, *et al.*, 1995). This Gγ peptide forms an amphipathic helix upon interaction with activated rhodopsin (Kisselev & Downs, 2003). Other mutational, peptide mapping, and biophysical studies have also demonstrated regions of Gβγ that interact with receptors (Kisselev, *et al.*, 1999; Phillips, *et al.*, 1992; Kisselev & Gautam, 1993; Kisselev, *et al.*, 1994; Azpiazu, *et al.*, 1999).

Although there is extensive data describing the receptor-binding surface on G proteins, somewhat less is known about the specific point-to-point interactions between these proteins. Generally, the membrane-proximal sections of intracellular loops 2, 3, and 4 form the primary interaction surface on the receptor. Additional contact sites in the transmembrane helices may also be formed as the Gα C-terminus enters deeply into its binding pocket in the activated receptor (Janz & Farrens, 2004). Peptides corresponding to IC loops 2, 3, and 4 block the stabilization of Meta II by $G\alpha_t$ (Konig, *et al.*, 1989; Marin, *et al.*, 2000). A reverse substitution approach, where each intracellular loop was first substituted with polyalanine sequences and then individual alanine residues were mutated back to the native amino acid, demonstrated that residues adjacent to the transmembrane helices in these loops were the most important for G protein activation (Natochin, *et al.*, 2003). Chemical cross-linking experiments between rhodopsin and $G\alpha_t$ indicate that residue 240 in IC 3 of rhodopsin is near the amino and carboxyl termini of Gα, as well as the α4/β6 loop (Fig. 8a) (Cai, *et al.*, 2001; Itoh, *et al.*, 2001). Five residues at the C-terminus of Gα were shown to specifically interact with four noncontiguous residues in IC 3 (Liu, *et al.*, 1995). Peptides corresponding to IC 3 also cross-link to the N-terminus of Gα and the C-terminus of Gβ (Taylor, *et al.*, 1996; Taylor, *et al.*, 1994). Recently, the binding site for the C-terminal peptide of Gα was mapped to a hydrophobic patch on the inner face of helix VI in Meta II based on the ability of the tryptophan-labeled peptide to quench the fluorescence of bimane labels on the receptor (Janz & Farrens, 2004), and both the Gα and Gγ C-termini of G_t interact with IC 4 of rhodopsin (Ernst, *et al.*, 2000).

These data provide important information about specific contacts between receptors and G proteins, however, more constraints are needed to improve our current model of the receptor-G protein interface.

Structural determinants of receptor-G protein specificity

Relatively few types of G proteins transduce signals from a vast number of heptahelical receptors, thus each member of the G protein family must be capable of interacting with many different receptors. Furthermore, many receptors are capable of activating multiple G protein signaling pathways. Regulating the specificity of these interactions is important for proper signal transduction. Therefore, the receptor-G protein interface must also encode important information that determines which G proteins can interact with a particular receptor. Even after identifying many of the contact sites that comprise this interface, the connections that define the coupling between receptors and specific G protein family members remain unclear.

Each of the contact sites described in the previous section has been shown to contribute to coupling specificity. Carboxyl terminal chimeras of Gα subunits have been frequently used to switch receptor-effector coupling. For example, replacing the C-terminus of $G\alpha_q$ with that of $G\alpha_i$ results in a G protein that is activated by G_i-coupled receptors, but stimulates phospholipase C, a $G\alpha_q$ effector (Conklin*, et al.*, 1993). Many mutations in this region have also been shown to alter receptor-G protein coupling (Blahos*, et al.*, 1998; Kostenis*, et al.*, 1997c; Conklin*, et al.*, 1996; Natochin*, et al.*, 2000), including single point mutations (Kostenis*, et al.*, 1997a). The C-terminal eleven amino acids in $G\alpha_t$ and $G\alpha_i$ are nearly identical, yet the $5HT_{1B}$-serotonin receptor activates only G_i through a specific interaction with two amino acids in the α4 helix of this protein (Bae*, et al.*, 1999). Other key specificity determinants in Gα are the N-terminus (Kostenis*, et al.*, 1997b; Kostenis*, et al.*, 1998), αN/β1 loop (Blahos*, et al.*, 2001), α2/β4 loop (Lee*, et al.*, 1995b), and the α3/β5 loop (Grishina & Berlot, 2000), and studies suggest that coupling selectivity involves subtle and cooperative interactions among all of these various domains (Slessareva*, et al.*, 2003). Interestingly, mutations in the α2/β4 and α4/β6 loops in $G\alpha_s$ do not affect

binding to the β_2-adrenergic receptor, while mutations in the $\alpha 3/\beta 5$ loop increase receptor binding affinity (Grishina & Berlot, 2000). This may suggest differential determinants of G protein coupling in different G protein families. Recently, a mutation in a highly conserved glycine in Linker 1 of $G\alpha$ was shown to increase the activation of $G\alpha_q$ by G_i- and G_s-coupled receptors, demonstrating that sites distant from the receptor-G protein interface may also be important for controlling coupling (Heydorn, *et al.*, 2004). Further, coupling specificity may involve cooperative interactions between Linker 1 and the C-terminus (Kostenis, *et al.*, 2005).

In addition to the structural determinants on $G\alpha$, specific isoforms of $G\beta$ and $G\gamma$ have been shown to preferentially interact with specific receptors. For example, both $G\beta_1\gamma_2$ and $G\beta_5\gamma_2$ can couple $G\alpha_q$ to endothelin B and M_1-muscarinic receptors, however only $G\beta_1\gamma_2$ promotes $G\alpha_i$ binding to the endothelin B receptor (Lindorfer, *et al.*, 1998). Additional work showed that $G\beta_5\gamma_2$ specifically couples $G\alpha_q$ to receptors (Fletcher, *et al.*, 1998). Similarly, the M_2-muscarinic receptor interacts with $G\alpha_o$ heterotrimers with $G\beta_4\gamma_2$, but not $G\beta_1\gamma_2$ (Hou, *et al.*, 2001). The A_1-adenosine receptor couples equally well to $G\alpha_{i1}$ heterotrimers containing $G\beta_1\gamma_2$, $G\beta_1\gamma_3$, $G\beta_2\gamma_2$, and $G\beta_2\gamma_3$ (Figler, *et al.*, 1996), however, $G\beta_1$ dimers with $G\gamma_2$ and $G\gamma_3$ had a much faster receptor-catalyzed nucleotide exchange rate as compared to dimers with $G\gamma_1$ (Figler, *et al.*, 1997). A similar study measuring the ability of each of the five $G\beta\gamma_2$ dimers to couple to the β_1-adrenergic and A_{2a}-adenosine receptors found that $G\beta_4$ coupled the best while $G\beta_5$ coupled the worst. Interestingly, although $G\beta_1$ had a similar potency to $G\beta_4$ in coupling to the β_1-adrenergic receptor, its potency was 20-fold lower when coupling to the adenosine receptor (McIntire, *et al.*, 2001).

The $G\gamma$ subunit also plays an important role as a determinant of receptor-G protein coupling specificity. Coupling of $G\alpha_{i1}$ to the α_{2a}-adrenergic receptor was significantly affected depending on which of the eight different $G\gamma$ subunits studied was used to form the heterotrimer (Richardson & Robishaw, 1999). Similarly, the M_2-muscarinic receptor does not interact with $G\alpha_o$ heterotrimers

containing $G\beta_1\gamma_2$, although $G\beta_1\gamma_5$ and $G\beta_1\gamma_7$ could mediate binding to this receptor (Hou*, et al.*, 2000), and several other studies offer additional examples of Gγ-directed coupling specificity in other receptor systems (Lim*, et al.*, 2001; Jian*, et al.*, 1999; Butkerait*, et al.*, 1995). The principal determinant of this specificity is likely the primary sequence of the C-terminal third of Gγ, independent of the type of lipid modification, as shown by studies with chimeric Gγ subunits (Jian*, et al.*, 2001; Myung*, et al.*, 2005). However, the type of lipid modification also has an effect on receptor coupling, as a geranylgeranyl moiety on $G\gamma_1$ or $G\gamma_2$ increases the affinity of the G protein for rhodopsin (Jian*, et al.*, 2001) and the A_1-adenosine receptor (Yasuda*, et al.*, 1996), respectively.

Much of the difficulty in understanding coupling specificity between receptors and G proteins arises from the poor sequence homology of the intracellular loops that comprise the G protein binding site (reviewed in Wess, 1998). Even closely related receptors that activate the same G protein can have dissimilar intracellular loops, making coupling determinations based on primary structure impossible (Hedin*, et al.*, 1993), although a recently described statistical approach may help to overcome this difficulty (Muramatsu & Suwa, 2006). Extensive studies have shown that IC 2 and 3 are the most common selectivity determinants in receptors, while occasionally, IC 1 and 4 modulate receptor-G protein interactions (reviewed in Wess, 1997). Frequently, mutations in other regions of the receptor distant from the G protein binding site can affect coupling, suggesting that the global conformation of the receptor or changes in its dynamics may be just as important as specific side chain interactions in determining receptor-G protein selectivity (Gilchrist*, et al.*, 1996; Perez*, et al.*, 1996).

Indeed, the observation that different agonists can affect which G proteins are activated by a given receptor supports a model where specific receptor conformations may be more or less favorable for coupling to specific G proteins (reviewed in Kenakin, 2003; Perez & Karnik, 2005). In one recent example of ligand-directed signaling, structurally different ligands of the CB_1-cannabinoid receptor differentially regulated the binding of the three homologous $G\alpha_i$ proteins to the receptor. Interestingly, while one ligand was shown to behave as an agonist for G_{i1} and G_{i2} and as an inverse agonist for G_{i3},

another ligand was shown to behave exactly opposite, as an inverse agonist of G_{i1} and G_{i2} and as an agonist for G_{i3} (Mukhopadhyay & Howlett, 2005). Similarly, the functional responses of protease-activated receptor 1 activation differ whether the receptor is activated by thrombin or an agonist peptide. Mathematical modeling of the downstream signaling pathways indicates that the peptide may favor $G\alpha_q$ activation over $G\alpha_{12/13}$ activation by 800-fold, while thrombin-mediated activation of PAR1 does not discriminate between the G proteins (McLaughlin*, et al.*, 2005). Clearly, specific receptor-G protein coupling results from a complex relationship between specific side chain interactions as well as the agonist-induced tertiary structure of the G protein binding site.

Models of the receptor-G protein complex

Recently, computational techniques have enabled investigators to apply this extensive amount of biochemical and biophysical information to the high resolution structures of rhodopsin and G_t to develop a molecular model of the receptor-G protein complex (Fig. 9) (Slusarz & Ciarkowski, 2004; Fotiadis*, et al.*, 2004; Ciarkowski*, et al.*, 2005). Currently, the building blocks available for this complex are the inactive structure of rhodopsin (Teller*, et al.*, 2001), the GDP-bound transducin heterotrimer (Lambright*, et al.*, 1994), and the NMR structures of the C-termini of $G\alpha_t$ and $G\gamma_1$ (Kisselev*, et al.*, 1998; Kisselev & Downs, 2003). The first step in the modeling process is to "activate" the receptor to provide a binding site for G_t. Two different techniques have been used to develop models of activated rhodopsin. In the first, simplified energy calculations were used to find sterically and energetically reasonable arrangements of the transmembrane helices around all-*trans* retinal. Of these, the arrangement that agreed most well with the conformation suggested by SDSL studies of rhodopsin was selected and the non-transmembrane structural elements were reconstructed (Nikiforovich & Marshall, 2003). The second technique used target-driven molecular dynamics simulations to forcefully modify the cytoplasmic side of rhodopsin to meet the experimentally derived distances from SDSL (Slusarz & Ciarkowski, 2004). Both of these

methods resulted in reasonable working models for activated rhodopsin that are consistent with experimental evidence.

Since a critical receptor-binding site, the C-terminus of Gα, is absent in both structures of the heterotrimer (Lambright, *et al.*, 1996; Wall, *et al.*, 1995), it must be attached using the NMR structure of the C-terminal peptide bound to activated rhodopsin (Kisselev, *et al.*, 1998). Next, the G protein was visually docked onto a model of the activated receptor. The topology and electrostatic potential of the binding site significantly limit the possible orientations between the receptor and G protein. This particular model highlights three clusters of conserved interactions between the Gα C-terminus and the receptor, suggesting that the conserved residues in these proteins form a core interaction surface that may be shared among different receptor-G protein complexes (Slusarz & Ciarkowski, 2004).

According to this model, the cytoplasmic surface of the receptor is not large enough to accommodate both the Gα C-terminus in its binding pocket and the Gγ C-terminus (Fig. 9a) (Slusarz & Ciarkowski, 2004). One possible resolution is that receptors function as dimers, and increasing experimental evidence suggests that this is the case (reviewed in Javitch, 2004; Milligan, 2004), including the demonstration by neutron scattering of an $R_2 \cdot G\alpha\beta\gamma$ assembly between a leukotriene B_4 receptor, BLT1, dimer and G_i (Baneres & Parello, 2003). Rhodopsin also seems to be arranged in paracrystalline rows of dimers in native disk membranes as shown by atomic force microscopy (Fotiadis, *et al.*, 2003; Fotiadis, *et al.*, 2004; Liang, *et al.*, 2003). A model of the rhodopsin dimer was constructed by packing the rhodopsin crystal structure into the unit cell constraints determined by AFM (Liang, *et al.*, 2003; Fotiadis, *et al.*, 2004). The interface between the two rhodopsin monomers is between helices IV and V in this model, as other orientations were excluded due to geometrical or energetic limitations. The outward movement of helix VI during receptor activation was modeled as a 90° rotation of the helix about its long axis perpendicular to the membrane, which swings the intracellular half of this kinked helix away from the transmembrane bundle. After adding the missing termini onto the G protein, the G protein was docked on a rhodopsin dimer where one monomer had been "activated". In the resulting structure, the

Gα C-terminus is inserted into the pocket formed upon receptor activation, the N-terminal helix of Gα occupies a groove that runs between the two monomers and the farnesyl group at the C-terminus of Gγ interacts with the inactive receptor in the dimer (Fig. 9b) (Fotiadis*, et al.*, 2004). An alternative model based on a different orientation of rhodopsin monomers within the rows of dimers was also proposed (Ciarkowski*, et al.*, 2005). However, the issue of the dimerization of rhodopsin-like heptahelical receptors remains a contentious one, where some maintain that receptor monomers are the functional unit in G protein coupling (Chabre & le Maire, 2005).

The structural complementarity between the cytoplasmic face of dark rhodopsin and G_t was also recently explored using computational techniques to sample the rotational and translational space of several models of G_t with respect to rhodopsin (Fanelli & Dell'Orco, 2005). The best 4000 solutions were winnowed down based on broad distance constraints from experimental data and then the remaining solutions were subjected to cluster analysis followed by energy minimization of the representative models in each cluster. All of the parameters converge on the same rhodopsin-G_t complex, placing the $G\alpha_t$ C-terminus in a shallow pocket at the center of the transmembrane helices where it is almost accessible to the conserved arginine in the D(E)RY motif that is important for G protein activation. Interestingly, the architecture of the best complex between monomeric rhodopsin and G_t was also one of the best-scored solutions when G_t was docked to models of rhodopsin dimers or oligomers (Liang*, et al.*, 2003). The authors go on to propose that G_t may catalyze the structural changes from metarhodopsin I to Meta II, and that activation of both of these proteins may be concurrent processes in a supramolecular complex (Fanelli & Dell'Orco, 2005).

Although a provocative model, the physiological implications of this supramolecular complex in phototransduction are less clear. In the typical operating range of rhodopsin, with approximately one photoactivated receptor per disc membrane, the probability of hitting a preformed complex would be only 10%, and stimulation of a preformed complex would only seem to activate one G protein. In order to achieve the tremendous amplification of the visual signal, a sufficiently fast exchange

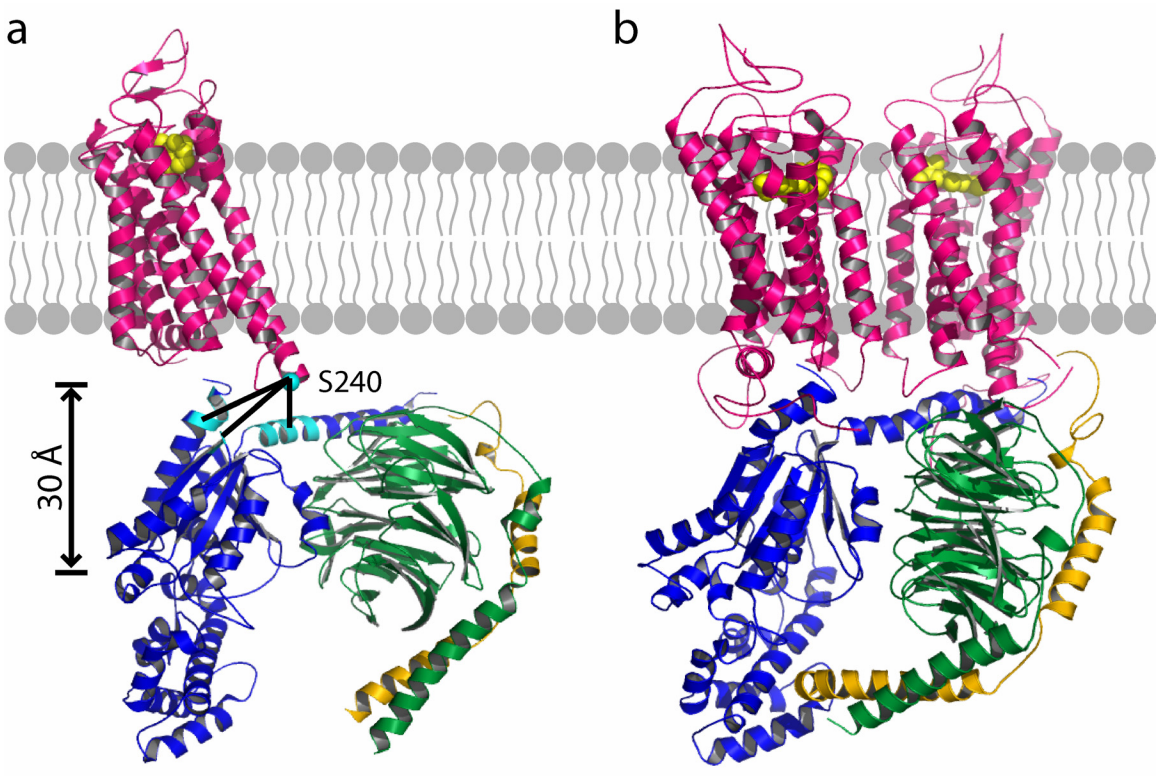

Figure 9 | Models of the receptor-G protein complex Two representations of receptor-G protein complexes are shown. (**a**) The R*·Gα(O)βγ complex was created by manually docking the G protein onto an activated receptor model based on the rhodopsin crystal structure (1GZM). Sites on Gα that cross-link to residue S240 (*cyan sphere*) on the receptor are highlighted (*cyan*). This type of data will be critical for improving models of the receptor-G protein complex, as it provides constraints for the location of IC 3 relatively to Gα. In this model, the nucleotide-binding pocket is some 30 Å away from the receptor-binding surface. (**b**) The model of an R_2·Gα(O)βγ complex is based on coordinates generously provided by K. Palczewski (published in Fotiadis*, et al.*, 2004).

G proteins on rhodopsin seems necessary for the efficient excitation of the photoresponse (Hamm*, et al.*, 1987).

Current molecular models of the receptor-G protein complex meet most of the important experimental constraints cited above, and therefore provide a reasonable framework for the design and interpretation of future studies. Particularly important information will come from additional distance constraints between the receptor and G protein, such as novel cross-links or interprobe measurements from fluorescence or electron paramagnetic resonance spectroscopy. Also, models of the complex were first assembled from models of the components, the inactive receptor and C-termini of Gα and Gγ, and any improvement in the determination of these structures will enhance our ability to model the complex. Finally, the modeling process does not yet take into account conformational changes in the G protein, which are necessary to cause GDP release from Gα, because little is known about specific receptor-mediated structural rearrangements in this protein.

Sequential interactions may form the receptor-G protein complex

An alternative hypothesis to account for the widely separated receptor binding sites on the C-termini of Gα and Gγ is that these regions interact sequentially with the activated receptor (Herrmann*, et al.*, 2004). Kinetic light scattering was used to follow the association of maltose-binding protein-tagged peptides to photolyzed rhodopsin. The peptide sequences used corresponded to the wild type $G\alpha_t$ C-terminus, two high-affinity homologues of this peptide, and the farnesylated $G\gamma_1$ C-terminus. The binding of the $G\alpha_t$ and $G\gamma_1$ constructs was mutually exclusive, and free Gα peptide could compete off MBP-Gγ and *vice versa*. In the holo G protein, at least one lipid modification was necessary for rhodopsin binding and no binding was observed in the absence of lipid modifications, despite binding of the MBP-Gα C-terminal peptide. When the C-terminus of Gα was replaced with a high-affinity sequence, the authors noted the same kinetics of complex formation. Combined with the previous observation that the C-terminus of Gα cannot confer binding to the non-acylated heterotrimer, the authors conclude that the Gα

C-terminus is not involved in the initial encounter between the receptor and G protein. They propose a model where Gβγ shields the Gα C-terminus until the farnesylated C-terminus of Gγ interacts with the receptor. Once the C-terminus of Gα is exposed, it interacts with the receptor, leading to GDP release. This sequential fit mechanism is compatible with receptor dimers, but it does not require dimerization in order to explain previous observations about receptor contact sites on the G protein.

Molecular Basis for G Protein Activation

Activated receptors catalyze GDP release from G protein heterotrimers. This is the rate-limiting step in G protein activation and, consequently, the activation of all downstream signaling proteins (Higashijima*, et al.*, 1987b). Until GTP binds, a high-affinity complex between the receptor and G protein is formed (Rodbell*, et al.*, 1971b; Emeis*, et al.*, 1982; Bornancin*, et al.*, 1989). Based on the current models of this interaction, the nucleotide-binding pocket is some 30 Å away from the nearest receptor contact site (Fig. 9a) (Bourne, 1997; Hamm, 1998; Slusarz & Ciarkowski, 2004; Fotiadis*, et al.*, 2004; Ciarkowski*, et al.*, 2005). Thus, the receptor must induce a conformational change in the G protein to cause GDP release over this distance. Several potential mechanisms for receptor-catalyzed GDP release have been proposed, mainly based on the effects of various mutations on the basal and receptor-catalyzed nucleotide exchange rates of the G protein. To date, there is little direct evidence of specific receptor-mediated conformational changes in G proteins, and the molecular mechanism of receptor-catalyzed nucleotide exchange remains one of the most important unanswered questions in the field of G protein signaling.

Potential mechanisms of receptor-catalyzed GDP release

Tracing structural elements from known receptor contact sites to the nucleotide-binding pocket highlights several potential routes that may transmit the conformational changes causing GDP release

(Fig. 10). Perhaps the most obvious connection is the α5 helix, which links the C-terminus of Gα to the β6/α5 loop containing the guanine ring-binding TCAT motif. Mutations in this motif greatly enhance spontaneous GDP release (Iiri*, et al.*, 1994; Posner*, et al.*, 1998; Thomas*, et al.*, 1993), including the activating mutation in $G\alpha_s$, A366S, that causes pseudohypoparathyroidism and gonadotropin-independent precocious puberty in male patients (Iiri*, et al.*, 1994). A homologous mutation in $G\alpha_{i1}$ also greatly enhances GDP release (Posner*, et al.*, 1998). No significant structural differences were observed in the crystal structure of the $G\alpha_{i1}$-A326S heterotrimer compared to the wild type protein, but the GDP-binding site was only partially occupied. The authors suggest that GDP release can occur without large conformational changes in Gα (Posner*, et al.*, 1998). However, inspection of the crystal structures seems to require a significant structural rearrangement to free the GDP buried between the GTPase and helical domains. Unfortunately, crystallography cannot elucidate the structural transition that occurred to release GDP from ~70% of heterotrimers in this crystal. The crystal lattice could be working to reinforce the more stable, GDP-bound conformation in the nucleotide-free heterotrimers, which is why no significant structural differences were observed.

Several mutagenesis studies have implicated the α5 helix in receptor-catalyzed nucleotide exchange. Alanine-scanning mutagenesis of $G\alpha_t$ identified three residues on the inward face of the helix with substantially increased rates of basal and receptor-catalyzed exchange, and several residues on the outward face of this helix that decreased catalyzed exchange (Marin*, et al.*, 2001b). A similar study based on proline-scanning mutagenesis of the α5 helix generally resulted in mutants with increased rates of basal exchange and decreased rates of catalyzed exchange (Marin*, et al.*, 2002). A flexible five-glycine linker inserted between the extreme C-terminus and the α5 helix only modestly decreased binding to the receptor, but severely reduced receptor-mediated nucleotide exchange, possibly due to disruption of the connection between the receptor contact site and GDP-binding pocket. Doubling the length of the α5 helix by repeating its sequence generated a mutant whose receptor coupling was only modestly reduced. This mutant argues that preserving the rigid connection between the C-terminus and GDP-binding pocket

is important for exchange, and further, that the α5 helix may be sufficient for coupling, as extending the helix increases the distance between the receptor and the protein core of Gα, thereby disrupting other potential receptor contacts (Natochin*, et al.*, 2001). Recently, an isoleucine-to-proline mutation at the C-terminus of the α5 helix has been shown to reduce the stimulatory activity of a D_2-dopamine receptor mimetic peptide on nucleotide exchange in G_i (Nanoff*, et al.*, 2006). In addition to providing a direct connection between the Gα C-terminus and the β6/α5 loop, receptor-induced perturbations in the α5 helix may be transmitted to the GDP-binding pocket *via* the α1 helix and β2 and β3 strands, as suggested by mutagenesis and computational studies (Marin*, et al.*, 2001b; Ceruso*, et al.*, 2004). Using SDSL, we have been able to observe receptor activation-dependent conformational changes in the α5 helix at sites distant from the receptor contact surface. The five-glycine linker uncouples these conformational changes from receptor binding (Chapter III).

Similar to the α5 helix, the β6 strand may connect receptor binding of the α4/β6 loop to the binding pocket at the β6/α5 loop (Fig. 10). Several alanine mutations in this region demonstrated reduced receptor-catalyzed activation, despite normal receptor binding (Onrust*, et al.*, 1997). The α3/β5 loop in $G\alpha_s$ appears to be a receptor contact site (Grishina & Berlot, 2000) that may transmit a conformational change along the α3 helix to Switch III. Interactions between Switch III and the αD/αE loop at the domain interface have been implicated in receptor-mediated activation of $G\alpha_s$ (Grishina & Berlot, 1998). Disruption of these interactions may open the gap between the helical and GTPase domains to release GDP. Interestingly, an arginine-to-glutamate mutation in Switch III has recently been shown to stabilize the nucleotide-free conformation of $G\alpha_t$ and, excitingly, this mutant blocks the rhodopsin-catalyzed activation of wild type G_t (Pereira & Cerione, 2005). If applicable in other systems, this dominant negative mutant will be extremely valuable for the investigation of G protein coupling.

Several intramolecular contacts with the N-terminal region have also been implicated in nucleotide exchange (Fig. 10). Carboxyl terminal truncations in $G\alpha_o$ and $G\alpha_{i2}$ resulted in reduced affinity for GDP because of impaired interactions with the β1 and β3 strands

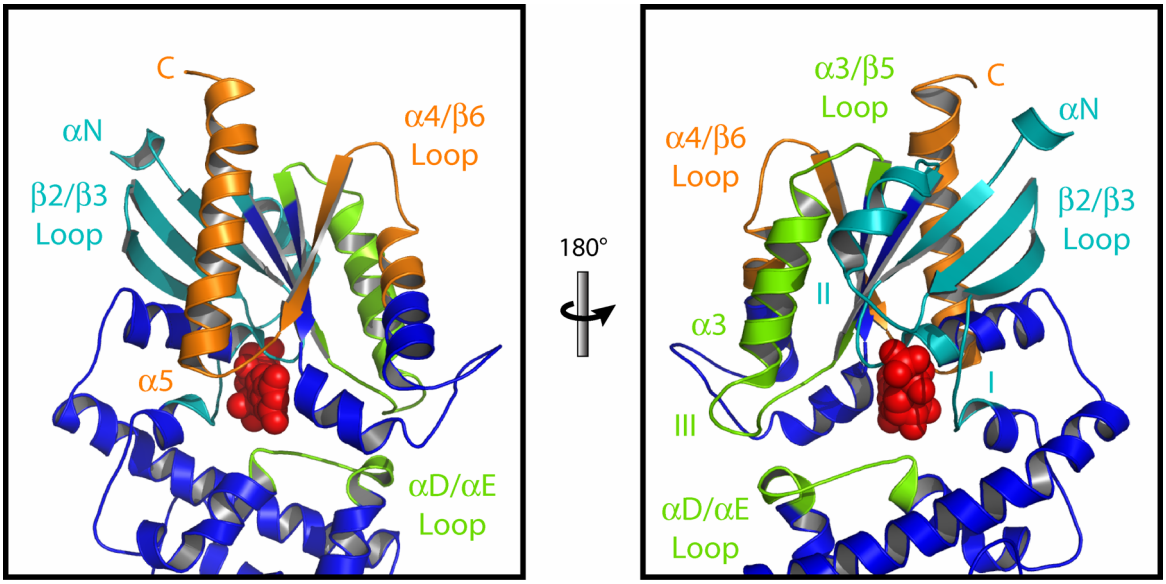

Figure 10 | Structural elements connecting receptor contacts to the GDP-binding pocket The α5 helix and β6 strand connect the C-terminus and α4/β6 loop to the nucleotide binding pocket at the β6/α5 loop (*orange*). The α3/β5 loop is connect to Switch III by the α3 helix (*lime*). Perturbations in Switch III may be communicated across the interdomain interface through its interactions with the αD/αE loop (*lime*). The αN helix is connected to the P-loop and Switches I and II through its interactions with β strands 1-3 (*teal*). Additionally, these β strands also interact with the α5 helix (*orange*) and may participate in front-to-back communication between these elements.

(Denker, *et al.*, 1995; Denker, *et al.*, 1992). A hydrophobic interaction between the β1 strand and α5 helix in $G\alpha_t$ stabilizes the GDP-bound conformation (Natochin, *et al.*, 2000). The mutations described in these studies perturb the hydrophobic core of the Gα subunit, which may account for their effects on nucleotide exchange more than any specific side chain interactions. However, through its interactions with the αN helix and αN/β1 loop, the activated receptor may similarly disturb these key stabilizing interactions, reducing the protein's affinity for GDP. Conformational changes in these regions could also affect β strands 1-3, and thereby alter Switches I, II and the P-loop, all of which form important interactions with GDP.

Two models for receptor-mediated GDP release require that the receptor change the relative orientation of the Gα and Gβγ subunits (Fig. 11). In the first model, the receptor uses the N-terminal helix of Gα as a lever-arm to pull Gβγ away from Gα. This would pry Switches I and II away from the nucleotide-binding pocket, resulting in GDP release (Iiri, *et al.*, 1998). In support of this hypothesis, shortening the αN helix by f four amino acids at its C-terminus to mimic the putative orientation induced by the receptor allows Gβγ to act as an exchange factor for $G\alpha_s$ (Rondard, *et al.*, 2001). The second, gear-shift, model proposes that the receptor uses the αN helix to force Gβγ into Gα, allowing the N-terminus of Gγ to engage the helical domain of Gα. This interaction may cause the interdomain gap between the helical and GTPase domains of Gα to open, leading to GDP release (Cherfils & Chabre, 2003).

These models propose that Gβγ plays a homologous role to the guanine nucleotide exchange factors for monomeric G proteins, and that the interaction between Gα and Gβγ plays a critical role in G protein activation. Indeed, several alanine mutations at the switch interface of Gβ are defective in receptor-catalyzed nucleotide exchange despite normal heterotrimer formation (Ford, *et al.*, 1998). Furthermore, mutations in the C-terminus of Gγ have been shown to increase receptor-catalyzed nucleotide exchange (Azpiazu & Gautam, 2001). A small peptide has also recently been shown to increase spontaneous nucleotide exchange in $G\alpha_{i1}$. Structural studies indicate that this peptide dramatically displaces Switch II away from the nucleotide- binding pocket, presumably leading to GDP

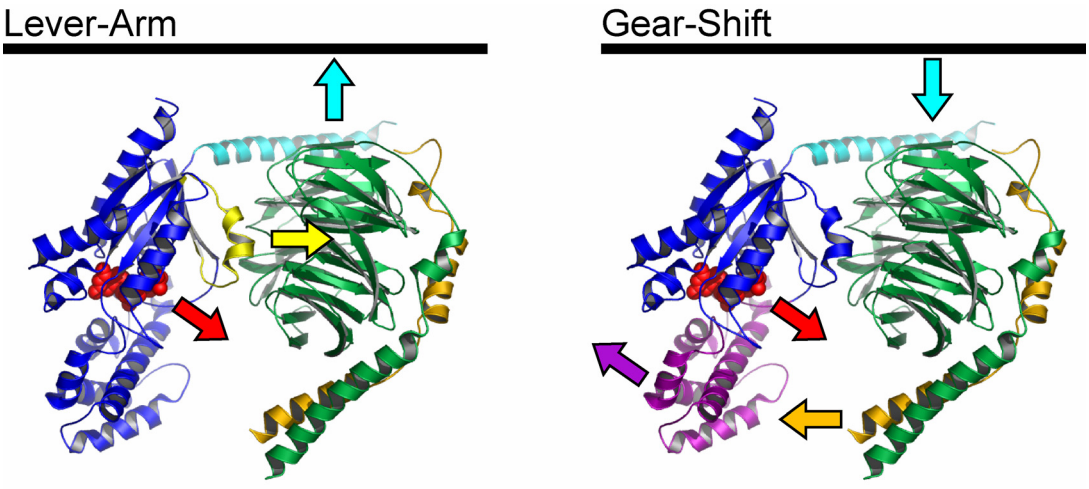

Figure 11 | Two hypotheses on the role of Gβγ in GDP release In the lever-arm model, the receptor uses the αN helix (*cyan*) as a lever to pull Gβγ away from Gα, thereby prying Switch II (*yellow*) away from the nucleotide binding pocket and causing GDP release (*red arrow*). The alternative, gear-shift, model requires that the receptor push Gβγ closer to Gα. This allows the N-terminus of Gγ (*gold*) to engage the helical domain (*purple*), thus forcing the binding pocket due to the reorientation of the two domains.

release, although the nucleotide remains bound in the crystal structure of the complex (Johnston, *et al.*, 2005). This study supports the lever-arm mechanism of nucleotide exchange. With direct examination of the Gα-Gβ interface using SDSL, we observe only subtle R*-mediated conformational changes in Switch II, but significant decreases in the mobility of labeled side chains in Switch I (Chapters IV and V). Additional studies are necessary to test the catalytic role of Gβγ in receptor-catalyzed GDP release.

Bound GDP is buried between the GTPase and helical domains of Gα (Fig. 5), although the direct interactions are formed by the GTPase domain. In order for GDP to be released, some of the contacts between these two domains may likely be broken. Several mutagenesis studies have implicated these contacts in nucleotide exchange, however, the results seem to differ depending on the Gα subunit involved. In $G\alpha_s$ and $G\alpha_{i1}$, disrupting these interactions resulted in increased rates of basal or decreased rates of receptor-catalyzed exchange (Marsh, *et al.*, 1998; Warner, *et al.*, 1998; Grishina & Berlot, 1998; Warner & Weinstein, 1999). The former indicating that an opening of the interdomain cleft reduces GDP affinity, and the latter indicating that the receptor may induce conformational changes across the domain interface through these interactions. However, these connections do not seem to be important for regulating the basal and catalyzed exchange rates in $G\alpha_t$ (Marin, *et al.*, 2001a). Thus, the role of interdomain interactions in G protein activation remains unclear, but inspection of the crystal structure seems to require a movement of these two domains relative to each other in order to release GDP. Indeed, an interdomain reorientation has been suggested by molecular dynamics simulations of $G\alpha_t$ (Ceruso, *et al.*, 2004) and glycine-to-proline mutations in each of the interdomain linkers enhances the basal nucleotide exchange rate of Gα (Majumdar, *et al.*, 2004).

Although each of the conformational changes described above is supported by mutagenesis and biochemical data, additional information is needed to understand the structural basis of receptor-mediated G protein activation. Certainly, a high resolution crystal structure would answer many questions about the orientation of these two proteins, the sites of interaction between them and the activating

conformational changes that lead to complex formation and trigger GDP release. Unfortunately, this complex has proven exceedingly difficult to crystallize, and its structure may not be solved in the near future. In the meantime, different experimental approaches must be employed to refine current molecular models of the receptor-G protein complex and characterize the conformational changes leading to GDP release.

Some knowledge about the nature of conformational changes in the G protein also enables speculation about the molecular trigger causing a particular type of change. Site-directed mutagenesis of residues on the side of the α5 helix opposite the β6 strand significantly increase the basal nucleotide exchange rate of Gα (Marin*, et al.*, 2001b). Perhaps the receptor disrupts these interactions in a similar manner. Assuming the general mechanism of receptor-catalyzed GDP release is conserved among receptor-G protein couplings, sequence analysis of conserved residues in these proteins may further serve to illustrate the important interactions for this process. One model suggests that there is a conserved binding site between the α5 helix and the adjacent β2/β3 loop for the conserved arginine in the D(E)RY motif of receptors, and that this interaction may underlie the mechanism for R*-mediated conformational changes in Gα (Oliveira*, et al.*, 1999). Much work remains to be done, however, to identify the structural basis of G protein activation, characterize the nucleotide-free conformation of the G protein and incorporate these data into improved models of the receptor-G protein complex.

GTP-mediated alteration of the receptor-G protein complex

Physiologically, the receptor-G protein complex is transient due to rapid binding of GTP, the concentration of which exceeds that of GDP by several-fold in cells. Binding of GTP to the Gα subunit causes a structural rearrangement of Gα(GTP), Gβγ and the receptor that permits effector interactions. A comparison between the Gα(GDP) (Lambright*, et al.*, 1994; Mixon*, et al.*, 1995) and Gα(GTPγS) (Noel*, et al.*, 1993; Coleman*, et al.*, 1994a) crystal structures reveals conformational changes in the three Switch regions (Fig. 5c). This structural rearrangement eliminates the Gβγ binding surface, mediating subunit

separation. The overall similarity of these crystal structures suggests that separation from the receptor is likely due to a reversal of the conformational changes that led to GDP release. GDP can also cause complex dissociation (Birnbaumer, *et al.*, 1972), and shares a similar affinity as GTP for the receptor-bound nucleotide-free Gα (Heck & Hofmann, 2001). Thus, irreversible G protein activation relies on the greater concentration of GTP within the cell and a structural rearrangement of Gα and Gβγ following its binding. However, there is little direct experimental evidence describing the GTP-induced conformational changes in the receptor-G protein complex.

Studies of G protein activation in cells suggest that the receptor and G protein subunits may remain closely associated following receptor activation *in vivo* (Bunemann, *et al.*, 2003), so questions as to the structural consequences of GTP binding to this complex remain unanswered. Recent evidence suggests that Gβγ may be necessary to cause the dissociation of Gα from the receptor (Herrmann, *et al.*, 2004). A mutant $G\alpha_t$ that has a C-terminal sequence with an increased affinity for Meta II can bind independently of its GDP- or GTP-bound conformational state, but dissociates like the native protein only in the presence of Gβγ. One explanation for this observation is that the G protein may proceed through a reversed sequence of interactions from those described above, leading to complex dissociation, which would require Gβγ (Herrmann, *et al.*, 2004).

In addition to the conformational changes observed in the Switch regions, GTP binding also causes a conformational change in the myristoylated N-terminus of Gα. Site-directed fluorescence labeling indicates that, while the non-myristoylated N-terminus returns to its dynamically disordered conformation, the myristoylated N-terminus moves into an even more hydrophobic environment in the Gα(GTP) state than in either the Gα(GDP) or heterotrimeric conformations (Fig. 6). These data suggest that the conformational changes associated with GTP binding expose an intramolecular binding site for the N-terminus (Preininger, *et al.*, 2003). Heterotrimeric G proteins may undergo a GTP-dependent myristoyl switch causing subunit dissociation similar to that described for the small GTPase ARF, where nucleotide exchange is coupled to a conformational change that leads to dissociation from the membrane

(Goldberg, 1998). The disordered state of the non-myristoylated N-terminus of Gα(GTP) may reflect the transition state leading to intramolecular binding (Fig. 6) (Preininger*, et al.*, 2003). Additional studies are necessary to identify the binding site for the N-terminus, such as crystallization of myristoylated Gα or biophysical distance measurements. Also, the structural consequences for the N-terminus of non-myristoylated Gα subunits remain unexplored.

Activation of Downstream Effector Proteins

Following subunit dissociation, Gα(GTP) and Gβγ each go on to activate specific downstream effector proteins (Table 2). Several crystallographic studies provide significant insight into the structural basis of G protein-effector interactions (Fig. 12).

Gα interactions with effectors

The first structural information concerning the mechanism of effector activation came from a comparison of the Gα(GTPγS) (Noel*, et al.*, 1993; Coleman*, et al.*, 1994a) and Gα(GDP) (Lambright*, et al.*, 1994; Mixon*, et al.*, 1995) structures. Significant structural differences were identified in three flexible loops, Switches I-III, near the γ-phosphate binding site. Upon GTP binding, these flexible loops become ordered in a structural rearrangement that disrupts the Gβγ-binding site to form a new surface for effector interactions. Although the crystal structures suggest that GTP binding orders the Switch regions, SDSL studies of Switch II indicate that this region is flexible in both conformations and that GTP binding actually increases its dynamics (see Chapter IV).

Each Gα family member interacts with effector proteins in a highly specific manner. Classical Gα effectors include photoreceptor cGMP phosphodiesterase ($G\alpha_t$ sequesters the inhibitory PDEγ subunit), adenylyl cyclase ($G\alpha_s$ activates, $G\alpha_i$ inhibits), phospholipase C β ($G\alpha_q$), and p115RhoGEF

Table 2 | Effector proteins of heterotrimeric G protein subunits (Adapted from Kristiansen, 2004)

Family	Subunit	Effector	Regulation	Reference
G_s	α_s	AC1-9	Stimulates	(Pierce, *et al.*, 2002)
		c-Src	Stimulates	(Cabrera-Vera, *et al.*, 2003)
		RGS-PX1	Stimulates	
		Tubulin	Stimulates GTPase activity	
	α_{olf}	ACS	Stimulates	
G_i	α_{t1}	PDE6	Stimulates	(Mochizuki, *et al.*, 1999)
	α_{t2}	PDE6	Stimulates	(Pierce, *et al.*, 2002)
	α_{gust}	PDE	Stimulates	(Cabrera-Vera, *et al.*, 2003)
	$\alpha_{i1\text{-}3,o}$	AC5, 6	Inhibits	
		c-Src	Stimulates	
		Rap1GAP	Sequesters	
		Ca^{2+} channels	Inhibits (α_o)	
		GIRK channels	Stimulates (α_i)	
		Tubulin	Stimulates GTPase activity	
		GRIN1, 2	Unknown	
	$\beta\gamma$	PI3Kβ, γ	Stimulates	(Pierce, *et al.*, 2002)
		AC2[a], 4[a], 7	Stimulates	(Cabrera-Vera, *et al.*, 2003)
		AC1	Inhibits	(Willets, *et al.*, 2003)
		PLC$\beta_{1\text{-}3}$	Stimulates	(Preininger, *et al.*, 2006)
		PLD	Inhibits	(Spiegelberg & Hamm, 2005)
		GRK2, 3	Recruits to membrane	(Gerachshenko, *et al.*, 2005)
		GIRK1, 2, 4	Stimulates	
		ATP-sensitive K^+ channels	Stimulates	
		Rho, Rac	Recruits to membrane	
		Bruton's tyrosine kinase	Stimulates	
		Tsk tyrosine kinase	Stimulates	

Table 2 | Continued

Family	Subunit	Effector	Regulation	Reference
G_i	$\beta\gamma$	PKD	Stimulates	
		Calmodulin	Inhibits calmodulin kinase	
		Tubulin	Stimulates GTPase activity	
		Dynamin I	Stimulates GTPase activity	
		Shc	Stimulates (MAPK)	
		HDAC5	Inhibits	
		SNAP-25	Inhibits exocytosis	
		Ras GEF CDC25Mm	Stimulates (Ras)	
G_q	$\alpha_{q,11,14,16}$	$PLC\beta_{1-4}$	Stimulates	(Pierce, *et al.*, 2002)
		LARG	Stimulates (Rho)	(Cabrera-Vera, *et al.*, 2003)
		GRK2, 3	Stimulates	(Willets, *et al.*, 2003)
		Bruton's tyrosine kinase	Stimulates (p38 MAPK)	
G_{12}	$\alpha_{12,13}$	p115-, PDZ-, LA-RhoGEF	Stimulates (Rho; stress fibers)	(Jiang, *et al.*, 1998)
		Ras GAP GAP1m	Stimulates (Ras)	(Pierce, *et al.*, 2002)
		E-cadherin	Stimulates (β-catenin release)	

[a] AC2 and AC4 are activated synergistically by $G\alpha_s$ and $G\beta\gamma$.

($G\alpha_{13}$). Structures of representative effector complexes from each Gα subfamily have been solved, $G\alpha_s$·AC (Tesmer, *et al.*, 1997b), $G\alpha_t$·PDEγ·RGS9 (Slep, *et al.*, 2001), $G\alpha_{13}$·p115RhoGEF (Chen, *et al.*, 2005b), and $G\alpha_q$·GRK2·Gβγ (Tesmer, *et al.*, 2005), demonstrating a localized effector binding surface on Gα (Fig. 12). In each complex, hydrophobic side chains from the effector insert into a pocket formed between the N-termini of the α2 (Switch II) and α3 helices (Fig. 12a). Additional contacts are made between the C-termini of these helices and the α2/β4 and α3/β5 loops that determine effector specificity. The tertiary structures of these interacting regions are well conserved, with the exception of the α3/β5 loop in $G\alpha_s$, suggesting that in most subfamilies effector specificity is determined by the primary sequence of the Gα subunit (Tesmer, *et al.*, 2005). The specificity of $G\alpha_s$ is regulated by backbone conformation as well as primary sequence (Sunahara, *et al.*, 1997b). The recently solved structure of the $G\alpha_q$·GRK2·Gβγ complex also reveals an interesting 105° rotation of $G\alpha_q$ that brings Switch I, Switch II, Linker 1, and the αB/αC loop in closest proximity to the membrane surface 30 Å away (Fig. 12c) (Tesmer, *et al.*, 2005). Both the $G\alpha_t$·PDEγ·RGS9 and $G\alpha_{13}$·p115RhoGEF structures would allow a similar reorientation of Gα, but the $G\alpha_s$·AC structure would not.

Unfortunately, the N-terminal helix of $G\alpha_q$ is disordered in this structure, and its role in complex formation is unclear. Myristoylation of the N-terminus of $G\alpha_{i1}$ is important for the inhibition of AC (Gallego, *et al.*, 1992; Taussig, *et al.*, 1993; Dessauer, *et al.*, 1998) and at least one N-terminal cysteine in $G\alpha_q$ is necessary for normal activation of $PLC\beta_1$ (Wedegaertner, *et al.*, 1993) regardless of its palmitoylation state (Hepler, *et al.*, 1996). Additional studies are needed to dissect the role of the N-terminus and its fatty acid modifications in the modulation of effector interactions. In addition to the effector binding site illustrated by the crystal structures, several studies indicate that the α4/β6 loop of Gα is important for PDEγ binding to $G\alpha_t$ (Rarick, *et al.*, 1992; Liu, *et al.*, 1999) and the activation of AC by $G\alpha_s$ (Berlot & Bourne, 1992).

The structural features of these interactions also underlie several other observations regarding effector activation. First, the GDP-bound Gα subunit has some ability to interact with effectors, although with 20-100-fold reduced potency than the GTP-bound protein (Skiba, *et al.*, 1996; Sunahara, *et al.*, 1997a). These data suggest that reassociation of Gα with Gβγ is required for the complete termination of G protein signaling. Second, even closely related Gα subunits activate unique complements of effector proteins. For example, $G\alpha_{i2}$ and $G\alpha_{i3}$ specifically inhibit only the forskolin- or $G\alpha_s$-stimulated activation of AC, respectively (Ghahremani, *et al.*, 1999). Similarly, the α_1-adrenergic receptor elevates intracellular Ca^{2+} through two distinct mechanisms by coupling to $G\alpha_q$ and $G\alpha_{11}$ (Macrez-Lepretre, *et al.*, 1997). Finally, some Gα subunits have only one identified effector, like $G\alpha_t$ (PDEγ), while some couple to several effector proteins, like $G\alpha_{12}$ [several RhoGEFs, PLCε, and protein phosphatase 5, among others (reviewed in Riobo & Manning, 2005)]. Certainly not all Gα effectors have been identified, and the search for novel proteins that interact with Gα subunits is an active area of research.

Gβγ interactions with effectors and regulatory proteins

Initially, Gβγ was thought to facilitate the termination of the G protein signal by passively binding to Gα and hastening the return of the heterotrimer to the plasma membrane, thereby reducing spontaneous activation of Gα in the absence of receptor stimulation (Neer, 1995). This perspective changed when Gβγ was shown to activate a K^+-selective ion channel in cardiac atrial cells (Logothetis, *et al.*, 1987). Since that time, many other effectors of Gβγ have been identified (Table 2), including $PLC\beta_2$ and β_3 (Katz, *et al.*, 1992; Li, *et al.*, 1998), AC (Tang & Gilman, 1991), β-adrenergic receptor kinase (Pitcher, *et al.*, 1992), phosphoinositide-3-kinase (Stephens, *et al.*, 1994), mitogen-activated protein kinase pathway components (Inglese, *et al.*, 1995), and K^+ and Ca^{2+} ion channels (Logothetis, *et al.*, 1987; Reuveny, *et al.*, 1994; Ikeda, 1996; Herlitze, *et al.*, 1996). More novel effectors are being discovered all the time (Dell, *et al.*, 2002; Spiegelberg & Hamm, 2005; Blackmer, *et al.*, 2001; Blackmer, *et al.*, 2005; Gerachshenko, *et al.*, 2005).

Many mutational and structural studies demonstrate that effector proteins share unique, but overlapping binding sites on Gβγ (Fig. 12b). Alanine-scanning mutagenesis in Gβ identified several residues that mediate interactions with $PLC\beta_2$, ACII, βARK, and ion channels (Ford, *et al.*, 1998; Panchenko, *et al.*, 1998; Li, *et al.*, 1998). For example, the ACII interaction surface maps roughly to blades 2, 3, and 5, while the N-terminal interface of Gβ interacts with G protein-activated inwardly rectifying K^+ (GIRK) channels 1 and 4 (Ford, *et al.*, 1998). Point mutations in blades 1-4 or the outer loops of blades 2, 6, and 7 inhibit $PLC\beta_2$ binding (Ford, *et al.*, 1998; Panchenko, *et al.*, 1998), whereas the interaction between $PLC\beta_3$ and Gβγ is blocked by point mutations within blades 2 and 5 (Li, *et al.*, 1998). Crystal structures of Gβγ in complex with the regulatory protein phosducin (Gaudet, *et al.*, 1996; Loew, *et al.*, 1998), the effector, GRK2, (Lodowski, *et al.*, 2003; Tesmer, *et al.*, 2005) and a small peptide that blocks these interactions (Davis, *et al.*, 2005), as well as competition studies using Gβ peptides that block the interaction between Gβγ and the receptor for activated C kinase 1 (Chen, *et al.*, 2005a), further demonstrate that Gβγ-binding proteins use a unique complement of residues within a common binding surface to mediate binding (Davis, *et al.*, 2005). Moreover, this surface is also the binding site for the Switch II region in Gα subunits, and thus, Gα subunits are effective inhibitors of Gβγ-effector interactions.

The overall structure of Gβγ is preserved in all of the crystal structures solved thus far, although the interstrand loops move significantly upon complex formation to form an appropriate binding site for specific interacting proteins. The dynamics of these loops probably enable Gβ to bind to such a variety of structurally diverse targets. An additional structural change is observed in $G\beta_1\gamma_1$·phosducin structures (Gaudet, *et al.*, 1996; Loew, *et al.*, 1998; Gaudet, *et al.*, 1999), where a cavity is introduced between blades 6 and 7 that may represent a putative farnesyl-binding pocket for Gγ C-terminus (Loew, *et al.*, 1998). Phosducin sequesters $G\beta_1\gamma_1$ away from the membrane in photoreceptor cells to attenuate G protein signaling, and this phosducin-induced switch in the Gγ farnesyl moiety provides the structural basis for membrane dissociation. This structural change in Gβγ may be a general mechanism by which Gβγ-

Figure 12 | Subunit interactions with effector proteins (**a**) Surface rendering of $G\alpha_t(GTP\gamma S)$ with the PDEγ binding site highlighted (*purple*). In all of the effector-Gα crystals that have been solved to date, the effector proteins interact with a hydrophobic pocket (*yellow asterisk*) lined by the α2 (Switch II) and α3 helices (adapted from Tesmer*, et al.*, 2005). (**b**) Surface renderings of $G\beta_1\gamma_1$ (1GOT) highlighting the unique, but overlapping binding sites of several interacting proteins. The surfaces in the top row were determined by crystallography, and the surfaces in the bottom row were determined by alanine-scanning mutagenesis in $G\beta_1$ as well as peptide competition studies (RACK1). (**c**) The recently solved structure of the $G\alpha_{i/q}$·GRK2·$G\beta_1\gamma_2$ complex (2BCJ) clearly demonstrates illustrates the structure of subunit-effector interactions. Moreover, this complex suggests the importance of macromolecular complexes for organizing signal transduction pathways *in vivo*.

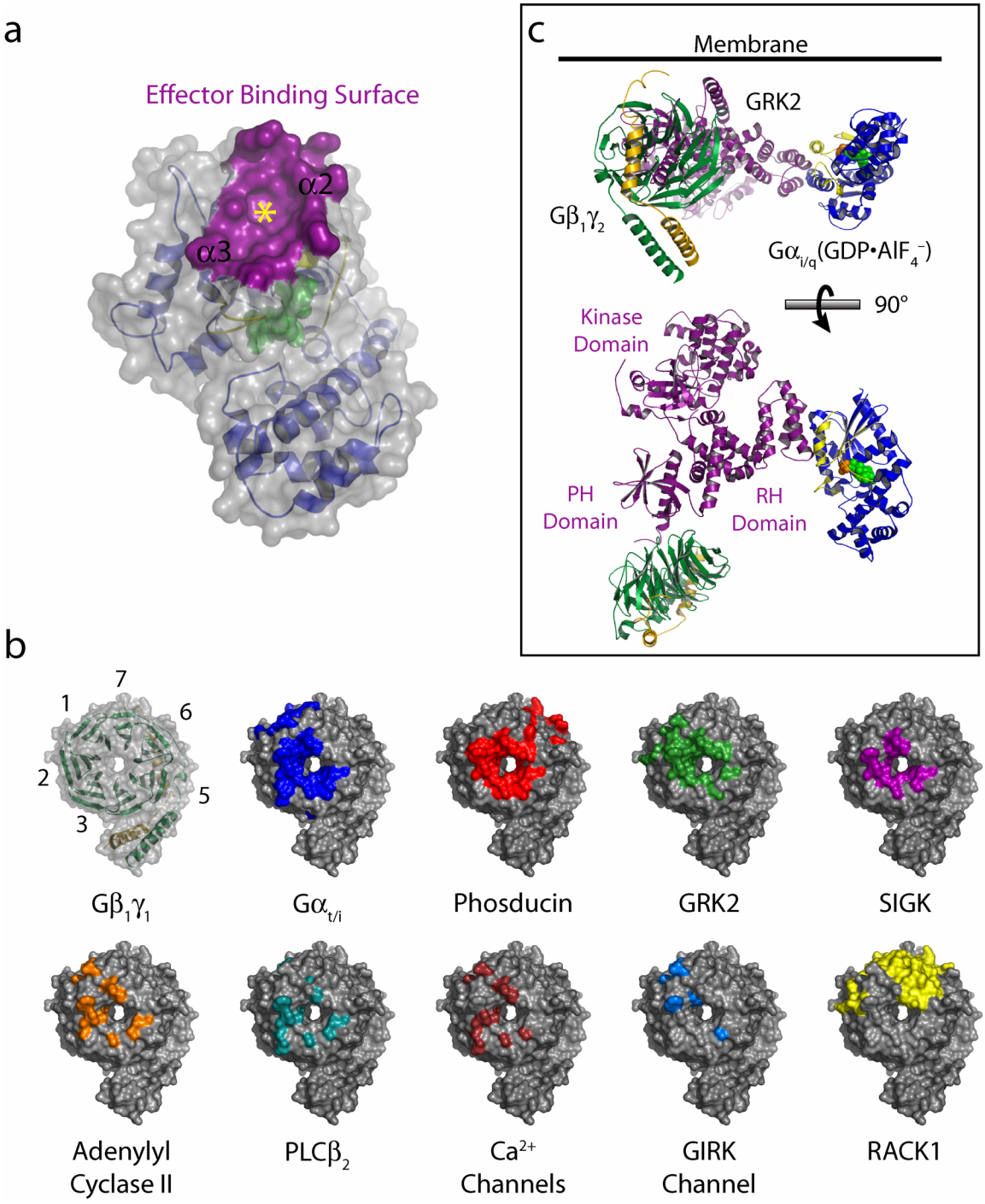
a
Effector Binding Surface
α2
α3
c
Membrane
GRK2
Gβ1γ2
Gαi/q(GDP•AlF4−)
90°
Kinase Domain
PH Domain
RH Domain
b
7
1
6
2
5
3
Gβ1γ1
Gαt/i
Phosducin
GRK2
SIGK
Adenylyl Cyclase II
PLCβ2
Ca2+ Channels
GIRK Channel
RACK1

binding proteins regulate the localization of Gβγ and attenuate signaling through Gα subunits, however, it has not been observed in other complexes.

Downstream signaling through Gβγ may also be regulated through the specific composition of the dimer. All of the possible dimers formed from combinations of $G\beta_1$ or $G\beta_2$ with $G\gamma_1$, $G\gamma_2$, $G\gamma_3$, $G\gamma_5$, or $G\gamma_7$ could activate PLCβ isoforms except the retinal-specific dimer, $G\beta_1\gamma_1$ (Iniguez-Lluhi, *et al.*, 1992; Ueda, *et al.*, 1994). Similarly, $G\beta_1\gamma_1$ was less effective at stimulating ACII and inhibiting ACI than other dimer combinations (Iniguez-Lluhi, *et al.*, 1992; Ueda, *et al.*, 1994). Comparing $G\beta_1\gamma_2$ with $G\beta_5\gamma_2$ demonstrates that $G\beta_5\gamma_2$ is a much weaker inhibitor of ACI, ACV, and ACVI, and $G\beta_1\gamma_2$ stimulates ACII while $G\beta_5\gamma_2$ inhibits it (Bayewitch, *et al.*, 1998b; Bayewitch, *et al.*, 1998a). Later studies showed that the remaining Gβ subunits activate ACII with a potency similar to $G\beta_1$, and $G\beta_2$ and $G\beta_4$ inhibited ACI as well as $G\beta_1$, while $G\beta_3$ was 10-fold less potent (McIntire, *et al.*, 2001). Interestingly, the specificity of these subtype interactions differ among effectors, as both $G\beta_1\gamma_2$ and $G\beta_5\gamma_2$ activate $PLC\beta_2$ with similar potency and efficacy (Zhang, *et al.*, 1996). Additionally, the potency of Gβγ inhibition of voltage-dependent N-type Ca^{2+} currents differs depending on the identity of the Gβ subunit in the dimer (Ruiz-Velasco & Ikeda, 2000). Similarly, GRK2 can be recruited to the plasma membrane by $G\beta_1$ and $G\beta_2$, but not $G\beta_3$, to initiate receptor desensitization (Daaka, *et al.*, 1997). Together, these data indicate that the Gβ isoform is a major determinant of effector coupling specificity.

In addition, the Gγ isoform and, in particular, its lipid modification has been shown to affect effector coupling. The native geranylgeranylated $G\beta_1\gamma_2$ is more effective in activating PLCβ than farnesylated $G\beta_1\gamma_1$ and $G\beta_1\gamma_{11}$ (Myung, *et al.*, 1999). If the prenyl groups are reversed on these proteins, farnesylated $G\beta_1\gamma_2$ becomes less able to activate PLCβ, while the activity of the geranylgeranylated $G\beta_1\gamma_1$ and $G\beta_1\gamma_{11}$ increases (Myung, *et al.*, 1999). Similarly, farnesylation of $G\beta_1\gamma_2$ decreased its ability to activate ACII, but geranylgeranylation of $G\beta_1\gamma_1$ and $G\beta_1\gamma_{11}$ was unable to restore their activity, suggesting that the primary sequence as well as the prenyl modification are important determinants of effector

activation (Myung, *et al.*, 1999). Altering the position of the geranylgeranyl by insertions, deletions, or mutations in the C-terminus of $G\gamma_5$ also disrupted its interactions with PLCβ (Akgoz, *et al.*, 2002). Most recently, studies with Gγ chimeras have shown that the N-terminus of $G\gamma_2$ is a better activator of ACII than the N-terminus of $G\gamma_1$. Also, the geranylgeranylated C-terminus of $G\gamma_2$ is a more potent activator of $PLC\beta_2$ and a more potent inhibitor of ACI than the geranylgeranylated C-terminus of $G\gamma_1$ or farnesylated C-terminus of $G\gamma_2$ (Myung, *et al.*, 2005). Clearly, the composition of the Gβγ dimer plays an important role in coupling to specific effectors. Areas of future research include identifying the structural features responsible for this specificity and characterizing many of these interactions in systems *in vivo*.

G Protein Inactivation

Intrinsic GTPase activity of Gα

Termination of the G protein signal is achieved upon the intrinsic hydrolysis of GTP to GDP by the Gα subunit and reassociation of the heterotrimer (Fig. 13). Structural insight into the mechanism of GTP hydrolysis in Gα subunits was provided by crystal structures of Gα(GDP) bound to aluminum fluoride (Sondek, *et al.*, 1994; Coleman, *et al.*, 1994a). Aluminum fluoride is a strong activator of Gα and binds with GDP in the active site as a tetracoordinate AlF_4^- ion (Sondek, *et al.*, 1994; Coleman, *et al.*, 1994a). In the crystal structures of $G\alpha(GDP{\cdot}AlF_4^-)$, the fluoroaluminate is in a square planar configuration, with the oxygen of the β-phosphate and a water molecule as transaxial ligands, forming a tetragonal bipyramid (Sondek, *et al.*, 1994; Coleman, *et al.*, 1994a; Sprang, 1997). Inspection of this transition state active site reveals the functional roles of several residues important for GTPase activity, including a conserved glutamine that polarizes and orients the nucleophilic water molecule and a conserved arginine that stabilizes the developing negative charge on the leaving group to facilitate its release (Fig. 13a) (Noel, *et al.*, 1993; Coleman, *et al.*, 1994a). Due to its important role in GTP hydrolysis, ADP-ribosylation of this arginine by cholera toxin abolishes the GTPase activity of $G\alpha_s$ and

$G\alpha_t$ (Freissmuth & Gilman, 1989; Van Dop*, et al.*, 1984), as do mutations of this residue (Coleman*, et al.*, 1994a; Landis*, et al.*, 1989; Sprang, 1997). Mutations that slow GTP hydrolysis lead to constitutive activation of Gα, which has been shown to cause sporadic endocrine tumors (Lyons*, et al.*, 1990) and McCune-Albright syndrome (Weinstein*, et al.*, 1991). Two mutations in the nucleotide-binding pocket, a glycine-to-valine substitution in the P-loop and a glycine-to-alanine mutation in Switch II, stabilize a $G\alpha_{i1}(GDP{\cdot}P_i)$ complex that is associated with a substantial conformational change in Switch II (Fig. 13a) (Berghuis*, et al.*, 1996; Raw*, et al.*, 1997). An additional lysine-to-proline mutation in Switch I accelerates a conformational change in the Switch regions, but decreases the rate of GTP hydrolysis, suggesting that this transition is an obligatory step leading to bond breakage (Thomas*, et al.*, 2004). Thus, the dynamics of the Switch regions may be critical for GTP hydrolysis.

Recently, structures of $G\alpha_{12}(GDP{\cdot}AlF_4^-)$ and $G\alpha_{13}(GDP)$ highlight a novel conformational change that is likely coupled to GTP hydrolysis in this family of Gα subunits (Fig. 13c) (Kreutz*, et al.*, 2006). A comparison of these two structures indicates that the αD/αE1 loop puckers upon binding AlF_4^-, and that a glutamate residue in this loop acts as a spring to rotate the helical domain away from the GTPase domain upon GTP hydrolysis. This conformational change may facilitate dissociation of these Gα subunits from effector proteins or influence the rates of nucleotide exchange or hydrolysis, however, additional studies are needed to appreciate the consequences of this unique structural feature of the $G\alpha_{12}$ family.

The intrinsic GTP hydrolysis activity varies among Gα family members, where the $G\alpha_s$ (3.5 min^{-1} at 20 °C) and $G\alpha_i$ (1.8-2.4 min^{-1} at 20 °C) family members have higher GTPase activity than members of the $G\alpha_q$ (0.8 min^{-1} at 30 °C) or $G\alpha_{12}$ (0.2 min^{-1} at 30 °C) families (except $G\alpha_z$, 0.05 min^{-1} at 30 °C). The structural reasons for this difference are not clear, but may include differences in the helical domains, N- and C-termini, or subtle fluctuations in backbone dynamics (Cabrera-Vera*, et al.*, 2003; Fields & Casey, 1997). The mechanisms responsible for the variations have not been studied in detail, but rather,

Figure 13 | Mechanisms of GTP hydrolysis by Gα (**a**) Crystallographic snapshots of GTP hydrolysis. Four important residues for stabilizing the transition state are shown (*yellow side chains*), including the highly conserved arginine (Arg) and glutamine (Gln) residues. In the Gα(GTP) conformation (1GIA), serine (Ser) and threonine (Thr) coordinate Mg^{2+}, and the nucleophilic water molecule is observed approaching the γ-phosphate (loop between Arg and Thr is removed in subsequent panels for clarity). Prior to bond breakage, a conformational change occurs in Switches I and II that orients Gln and Arg toward the γ-phosphate (based on $G\alpha_t$(GDP); 1TAG) in a pre-transition state complex. The transition state is stabilized by Gln and Arg (1GFI), and a conformational change in Switch II is observed in Gα(GDP·P_i) following bond breakage (1AS2). The switch regions are disordered in $G\alpha_{i1}$(GDP) (1GDD), and Gβγ binding significantly remodels the nucleotide binding pocket (1GP2). (This series of snapshots was based on the discussion presented in Thomas*, et al.*, 2004). (**b**) Structure of the RGS9 RGS domain binding to $G\alpha_t$(GTP·AlF_4^-) (1FQK). The RGS proteins enhance the basal GTP hydrolysis rate of Gα subunits by stabilizing the transition state. Structures of these complexes indicate that the RGS domain itself does not directly interact with the nucleotide, unlike the GAPs of monomeric G proteins. (**c**) The recently solved structures of $G\alpha_{i/12}$(GTP·AlF_4^-) (1ZCA) and $G\alpha_{i/13}$(GDP) (1ZCB) suggest that GTP hydrolysis leads to an 8.5° rotation of the helical domain away from the GTPase domain in this family of Gα subunits (*arrow*). This rotation is apparently due to an activation dependent "spring" in the αD/αE loop mediated by a glutamate residue (*stick side chains*) unique to the $G\alpha_{12}$ family. In the active conformation, this glutamate (*green*) puckers the αD/αE loop. Following GTP hydrolysis, this residue forms a salt bridge with an adjacent lysine across the binding pocket (*yellow*).

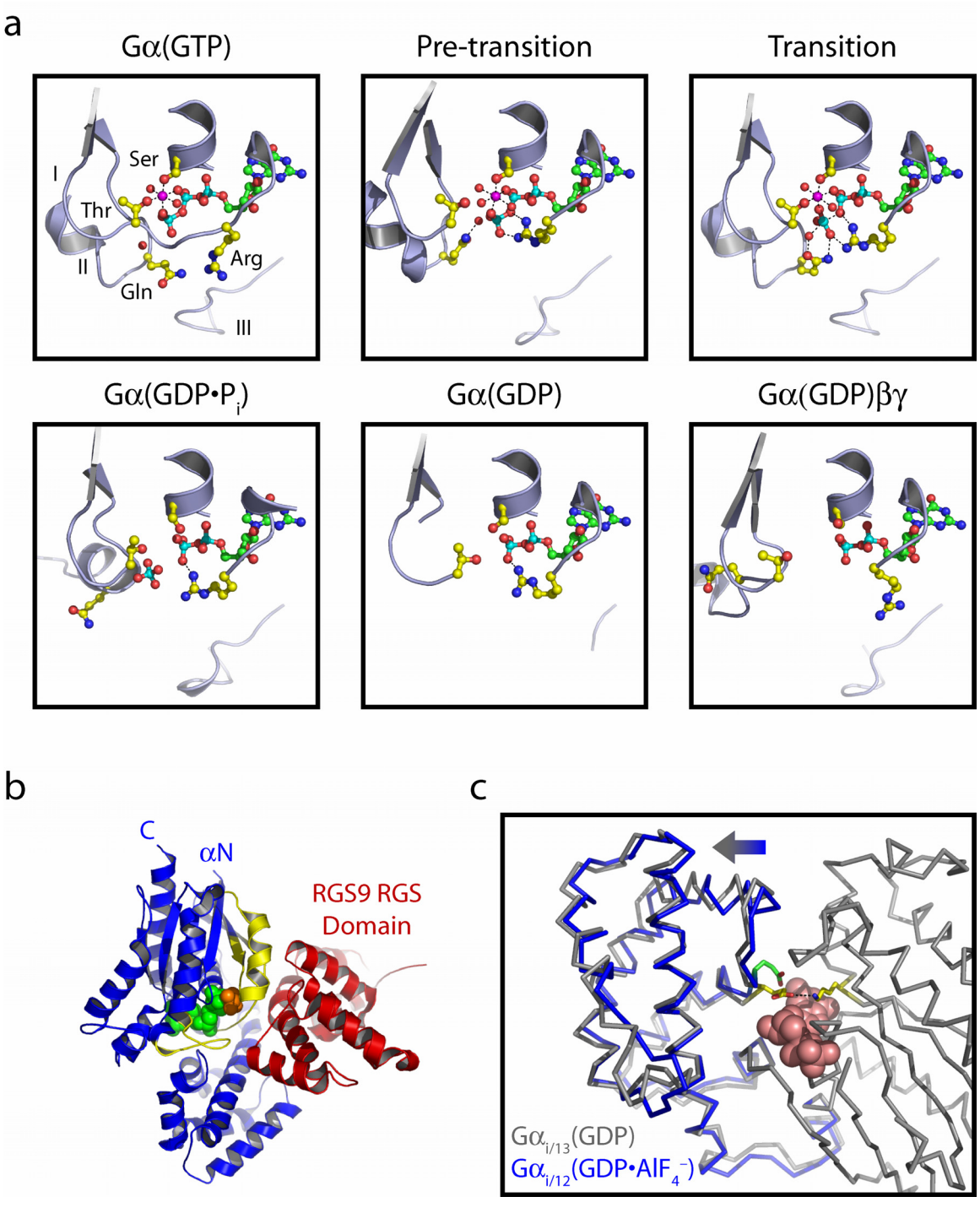
a
Gα(GTP)
Pre-transition
Transition
Ser
I
Thr
II
Gln
Arg
III
Gα(GDP•P$_i$)
Gα(GDP)
Gα(GDP)βγ
b
C
αN
RGS9 RGS
Domain
c
Gα$_{i/13}$(GDP)
Gα$_{i/12}$(GDP•AlF$_4^-$)

research in this area has focused on the identification and characterization of the increasing number of proteins that regulate the intrinsic GTPase activity of Gα subunits.

GTPase activating proteins

Initially, the hydrolysis of GTP was thought to be an unregulated function of Gα subunits that offered intrinsic control of the duration of the G protein signal. However, it was soon noted that the intrinsic GTPase activity of many purified Gα subunits *in vitro* was much slower than the deactivation rates of G protein signaling processes *in vivo*, suggesting that some GTPase accelerating factor was lost during purification (reviewed in Ross & Wilkie, 2000). The first two GAPs identified were the Gα effectors PLCβ_1 ($G\alpha_q$) and PDEγ ($G\alpha_t$) (Berstein, *et al.*, 1992; Arshavsky & Bownds, 1992). More recently, it has been demonstrated that ACV is a GAP for $G\alpha_s$ (Scholich, *et al.*, 1999). Thus, there is a common paradigm that effectors, after activation by Gα, can negatively regulate the amplitude and duration of the G protein signal.

In addition to effector-mediated feedback inhibition, another class of GAPs has been identified, the RGS proteins. These proteins share a common 120-amino acid RGS domain that forms a bundle of nine α-helices that binds to the Switch regions on Gα. This domain enhances the GTPase activity of Gα by stabilizing the transition state conformation and orienting the Gα backbone to stabilize the nucleophilic water molecule (Fig. 13b) (Slep, *et al.*, 2001; Tesmer, *et al.*, 1997a). However, the RGS domain itself does not directly take part in the chemistry of hydrolysis, unlike the GAPs for small G proteins that contribute an extrinsic catalytic arginine residue to the active site (reviewed in Sprang, 1997). The molecular mechanism for effector-mediated GAP activity has not been clearly determined. These proteins may also stabilize the transition state, but differences in activity between effector GAPs and RGS GAPs have been observed. For example, RGS4 produces a two-fold greater activation of GTP hydrolysis in $G\alpha_q$ over PLCβ, but PLCβ is 100 times more potent than RGS4 (Mukhopadhyay & Ross, 1999). However, Gβγ can inhibit the GAP activity of both of these proteins (Chidiac & Ross, 1999),

consistent with the idea that Gβγ, effectors and RGS proteins all compete for binding to Gα. This effect may also be due to Gβγ-mediated stabilization of Gα(GDP), which binds poorly to effectors and RGS proteins. Regardless, RGS proteins could inhibit effector activation in addition to accelerating GTP hydrolysis. Alternatively, the $G\alpha_t$ effector, PDEγ, enhances the GAP activity of RGS9 on $G\alpha_t$ by increasing its affinity for the protein (Skiba, *et al.*, 1999; Skiba, *et al.*, 2000), and structural studies indicate that the effectors and GAPs may have evolved to interact with non-overlapping binding sites (Tesmer, *et al.*, 2005).

Again, the N-terminal domain of Gα is an important, but uncharacterized, regulator of Gα-GAP interactions (Ross & Wilkie, 2000). Proteolysis, phosphorylation, and palmitoylation (Wang, *et al.*, 1998; Tu, *et al.*, 1997; Glick, *et al.*, 1998) have all been shown to decrease the affinity of Gα for GAPs by 100-fold, while myristoylation increases the affinity of this interaction (Tu, *et al.*, 1997). Mutations in the αN helix reduce the basal GTP hydrolysis rate of $G\alpha_z$, suggesting that its role may be to maintain the structure of the active site (Wang, *et al.*, 1999). The helix may also contribute to the binding site for the GAP, although this type of interaction is not observed in either crystal structure (Slep, *et al.*, 2001; Tesmer, *et al.*, 1997a). Other regions in both proteins outside of the known molecular interface have also been shown to influence Gα-GAP interactions. For example, the helical domain of $G\alpha_t$ is a key molecular determinant of RGS9 selectivity of $G\alpha_t$ over $G\alpha_i$ (Skiba, *et al.*, 1999), and flanking regions of RGS4 are important for binding to $G\alpha_q$, but not $G\alpha_i$. Along with their role as key desensitizers of heterotrimeric G protein signaling, RGS proteins are recognized as important scaffolds that facilitate the rapid and specific activation and termination of signal transduction pathways mediated by heptahelical receptors (reviewed in McCudden, *et al.*, 2005; Ross & Wilkie, 2000).

Novel Regulation of G Protein Signaling

The basic model of G protein signaling can be expanded to include two additional regulatory mechanisms, non-receptor GEFs and guanine nucleotide dissociation inhibitors (GDIs). Several proteins have been identified that increase GTPγS binding to Gα subunits, including GAP-43, β-APP, presenilin 1, RKIP, Ric-8A, and AGS1 (reviewed in Sato*, et al.*, 2006). These proteins appear to be selective for the $G\alpha_i$ family, although Ric-8A can also activate $G\alpha_q$ *in vitro* (Tall*, et al.*, 2003). Additional work remains to be done before the regulation of the GEF activity of these proteins and its functional consequences are completely understood, although Ric-8A has been shown to play a critical role in asymmetric cell division during embryogenesis in *C. elegans* (reviewed in McCudden*, et al.*, 2005) and AGS1 is important for processing signals in the suprachiasmatic nucleus during the circadian cycle (reviewed in Sato*, et al.*, 2006).

By contrast to the soluble GEFs, which cause GDP release, the class of GDI proteins inhibit GDP dissociation from $G\alpha_i$ family members, which can dampen signaling through Gα or prolong signaling through Gβγ (reviewed in McCudden*, et al.*, 2005; Sato*, et al.*, 2006). The GDI proteins have been implicated as crucial players in asymmetric cell division during embryogenesis (reviewed in McCudden*, et al.*, 2005; Willard*, et al.*, 2004; Sato*, et al.*, 2006). Most of these proteins contain one or more GoLoco motifs (reviewed in Willard*, et al.*, 2004). The GoLoco domain is a 19-amino acid sequence that slows spontaneous GDP release from Gα(GDP) and prevents its interaction with Gβγ. A crystal structure shows that the N-terminus of the GoLoco domain of RGS14 forms an α-helix that is sandwiched between Switch II and the α3 helix of $G\alpha_i$(GDP) (Kimple*, et al.*, 2002). The GoLoco peptide extends to the helical domain, and contacts Switch I and GDP. Perturbation of Switch II would preclude coincident binding of Gβγ to this complex. The arginine in the highly conserved DNR sequence in GoLoco motifs, inserts into the nucleotide binding pocket and interacts with the α- and β-phosphates of GDP and the bridging oxygen atom between them. GoLoco binding also results in the formation of a salt bridge

between the P-loop and Switch I that is also observed in the structure of the G_i heterotrimer (Wall*, et al.*, 1995), which locks GDP into the binding pocket. These two new stabilizing interactions provide the structural basis for the GDI activity of GoLoco-containing proteins (Kimple*, et al.*, 2002).

Novel Approaches to Study G Protein Structure and Function

Nuclear magnetic resonance spectroscopy

Recently, the high yield expression and purification of an isotopically-labeled $G\alpha_t$ chimera has been reported, thereby greatly facilitating the study of this protein with NMR (Abdulaev*, et al.*, 2005b). The two-dimensional ^{1}H-^{15}N heteronuclear single-quantum correlation (^{15}N-HSQC) spectrum of $G\alpha$(GDP) is relatively well dispersed and 340 of 397 cross-peaks are readily identifiable. Upon the addition of AlF_4^-, many of the amide resonances in the spectrum shift, particularly the indole ^{1}HN and ^{15}N resonances of two tryptophan residues in Switch II and the adjacent $\alpha 3$ helix, consistent with the crystal structures of the protein in these conformations (Sondek*, et al.*, 1994; Lambright*, et al.*, 1994). After this initial study, the authors measured the ^{15}N-HSQC spectrum of a reconstituted heterotrimer (Abdulaev*, et al.*, 2005a). Interestingly, the chemical shifts observed upon $G\beta\gamma$ binding are generally similar to those observed in the spectra for the AlF_4^-- and GTPγS-bound $G\alpha$ subunit, specifically for the three tryptophan residues and C-terminal phenylalanine for which definitive assignments were made, suggesting that these two protein conformations are also similar. A model is proposed whereby $G\beta\gamma$ organizes the C-terminus of $G\alpha$ and the nucleotide-binding pocket for binding to R* and GTP, respectively. In order to reconcile the NMR results with the crystal structures of these conformations, the authors point out that the conformation of $G\alpha(GDP{\cdot}AlF_4^-)$ can be modeled into the structure of the heterotrimer with minimal changes in the interfacial contacts between the proteins. This model rotates the helical domain of $G\alpha$ closer to the N-terminus of $G\gamma$, similar to the gear-shift model described above, and it is not inconsistent with the structural heterogeneity observed between the crystal structures of G protein heterotrimers (Wall,

et al., 1995; Lambright*, et al.*, 1996). However, it seems extremely unlikely that AlF_4^- can bind in the presence of Gβγ as this event is highly dependent on a structural rearrangement of Switch II.

This approach has also been used to monitor conformational changes associated with receptor-catalyzed GTPγS binding (Ridge*, et al.*, 2006). In this study, the authors found that R*-generated Gα(GTPγS) was more conformationally dynamic than that generated independently of R*, suggesting that the increase in protein dynamics may be due to interactions with R* and Gβγ. Changes in the NMR spectra during R*-catalyzed exchange continued several hours after GTPγS binding appeared to be complete, which the authors suggest is due to slow dissociation of Gα(GTPγS) and Gβγ. Support for this hypothesis comes from the observation that a soluble receptor mimic that does not catalytically activate the G protein (Abdulaev*, et al.*, 2000) is found to form a stable complex with a GTPγS-bound heterotrimer (Ridge*, et al.*, 2006). The C-terminus, which displays two conformational states in the heterotrimer (Abdulaev*, et al.*, 2005a), is found exclusively in an "activated" conformation in the putative R*·Gα(GTP)βγ complex and the Gα(GTPγS) conformation (Ridge*, et al.*, 2006).

Although complete assignment of the cross-peaks and analysis of the solution structures will be necessary before the differences between the crystal structures and the NMR data are completely understood, the current analysis raises some questions. For example, it seems unlikely that the dynamics of a tryptophan residue in Switch II, a region that contributes significantly to the Gβγ-binding surface (Lambright*, et al.*, 1996; Wall*, et al.*, 1995), would increase upon heterotrimer formation. Indeed, these flexible loops are absent in the structure of $G\alpha_{i1}$ that lacks either crystal contacts or Gβγ to stabilize this region (Mixon*, et al.*, 1995). Our own SDSL studies indicate that Gβγ dampens the backbone dynamics of Switch II (Chapter IV). Also, the authors suggest that Gβγ pre-organizes the nucleotide-binding site for GTP, but this role is difficult to reconcile with the well-established negative cooperativity between heterotrimer formation and GTP binding (Higashijima*, et al.*, 1987b), as is the observation that the heterotrimer dissociates slowly following GTP binding. Certainly this effort is in the initial stages, but it has already raised some provocative issues concerning the dynamics of G protein signaling. Moreover, it

is on a trajectory to provide the first high resolution structural information for the nucleotide-free Gα, which would hopefully lend further insight into the molecular mechanism of GDP release.

Studies of G protein function in living cells

Much of our understanding of G protein structure and function is the result of a vast number of biochemical experiments conducted *in vitro* where the constituents of an assay can be carefully controlled and manipulated. Although this reductionist approach is often the only way to dissect a particular experimental question, it does set aside the basic fact that the G protein cycle runs inside of cells in the presence of a variety of regulatory and scaffolding proteins that almost certainly influence every one of the reactions and interactions that have been carefully described *in vitro*. Recently, several groups have adopted fluorescence-based approaches to study G proteins in living cells (reviewed in Hebert*, et al.*, 2006). One method is based on the nonradiative energy transfer from *Renilla reniformis* luciferase attached to the C-terminus of the receptor to a blue-shifted variant of *Aequorea victoria* green fluorescent protein attached to one of the three G protein subunits (Gales*, et al.*, 2005). Upon degradation of its substrate, luciferase emits light at a wavelength that will excite GFP when the two molecules are within 100 Å of each other. This bioluminescence resonance energy transfer approach detected basal coupling of receptors and G proteins, rapid ligand-induced increases in the association of receptors and G proteins, as well as a slow decrease in BRET reflecting receptor desensitization. Interestingly, the agonist-promoted increase in BRET was highly dependent on the Gα isoform present in the complex, suggesting that this assay provides a new tool to assess the specificity of receptor-G protein interactions *in vivo*.

Fluorescence resonance energy transfer is similar to BRET, where the energy donor is a fluorescent protein that is excited by an external light source rather than a chemical reaction. Receptor activation increases FRET between fluorescent proteins attached to the $G\alpha_i$ helical domain and the N-terminus of Gγ, reaching maximum in 1-2 s, which is five times slower than the rate of receptor activation (Bunemann*, et al.*, 2003). Somewhat surprisingly, the increase in FRET indicates that the fluorescent

proteins are coming closer together following receptor activation, not moving farther apart as would be expected if the subunits dissociated following activation. Energy transfer between Gα and a Gγ subunit tagged at the C-terminus decreased after receptor stimulation, further supporting a conformational rearrangement in the heterotrimer rather than subunit dissociation. This observation runs contrary to biochemical experience, as well as an earlier study using this technique to study G protein activation in yeast (Janetopoulos*, et al.*, 2001), which support the subunit dissociation hypothesis. Recent evidence suggests that the discrepancy may be due to the identity of the Gα subunit. Upon extending the FRET studies to include all members of the $G\alpha_i$ family, $G\alpha_o$ was the only member to exhibit a receptor activation-dependent decrease in FRET, suggesting subunit dissociation. When a region of the helical domain containing αB/αC loop in $G\alpha_i$ was replaced with the homologous sequence from $G\alpha_o$, the mutant $G\alpha_i$ demonstrated a decrease in FRET, suggesting that this region was critical for preventing subunit dissociation following activation (Frank*, et al.*, 2005).

These fluorescence-based techniques have raised some provocative questions regarding G protein activation in intact cells. Unfortunately, the fluorescent protein tags are relatively large, and may have a substantial impact on the structure and dynamics of the system under study. Fortunately, new technologies are being developed that allow the use of a small molecule as an energy donor, rather than a bulky fluorescent protein, and this approach has been used to explore conformational changes in receptors while preserving downstream signaling (Hoffmann*, et al.*, 2005). Additional studies seem to be necessary before the structural changes responsible for the differences in energy transfer are truly understood. Perhaps these *in vivo* systems might benefit from a brief return to the test tube, where much more detailed biochemical analyses may be carried out to assess the impact of the intracellular milieu and the fluorescent tags on G protein activation and subunit dissociation.

Summary

Many of the unanswered questions about the structural basis for function in heterotrimeric G proteins can be framed in terms of what is not known from the many crystal structures of these proteins in a variety of conformations and complexes. For example, the amino and carboxyl termini of Gα play key functional roles in mediating its interaction with regulatory proteins, yet limited structural information for these regions is available from crystallographic studies. Furthermore, answers to some of the most important questions in G protein signaling await a better understanding of the structure of the receptor-G protein complex, including agonist-mediated conformational changes in receptors, point-to-point interactions between the receptor and G protein, the transition leading to GDP release, the structural determinants of R*-G protein specificity, and the functional role of receptor dimerization in G protein activation. Unfortunately, this complex has been exceedingly difficult to crystallize despite the extensive efforts of a number of investigators. In the interim, alternative biophysical approaches can be combined with the currently available structural information to develop increasingly better models for the structural basis of receptor-catalyzed G protein activation. Additionally, these biophysical approaches can provide important information on the dynamics of proteins that is unavailable from crystal structures. The dynamic nature of proteins is critical for normal enzymatic function, interaction with effector proteins, and binding of chemical ligands. Thus, studies of G protein dynamics, such as those described here, will complement the extensive structural data to improve our understanding of the biomechanics of heterotrimeric G protein signaling.

CHAPTER II

APPROACH TO THE STUDY OF G PROTEIN DYNAMICS

Research Goals

As described in Chapter I, a great deal is known about the structure of heterotrimeric G proteins from x-ray crystallography, providing insight into GTP-induced conformational changes, how these conformational changes allow interaction with effector proteins, and the mechanism of GTP hydrolysis. However, despite the fundamental importance of receptor-catalyzed G protein activation in cellular signaling, relatively little is known about this process as compared to the other regulatory events in the G protein cycle.

When heptahelical receptors embedded in the cell membrane are activated by an extracellular agonist, they undergo a conformational change that allows G protein binding (Farrens*, et al.*, 1996). This interaction leads to GDP release from the Gα subunit, which is the rate-limiting step in the activation of all downstream signaling pathways (Higashijima*, et al.*, 1987b). Subsequently, a high-affinity complex between the activated receptor and nucleotide-free conformation of the G protein is formed, which is stable in the absence of guanine nucleotides (Rodbell*, et al.*, 1971b; Emeis*, et al.*, 1982; Bornancin*, et al.*, 1989). Biochemical studies described in the previous chapter suggest that GDP is bound nearly 30 Å distant from the nearest receptor-contact site on the G protein (Bourne, 1997; Hamm, 1998), suggesting the hypothesis that **the receptor must induce some sort of conformational change in the G protein to cause GDP release** over this distance. The primary goal of my dissertation research has been to determine the structural mechanism by which an activated receptor causes GDP release through the approach described by the following specific aims:

Specific Aim 1: Identify regions of Gα that undergo receptor activation-dependent conformational changes.

Specific Aim 2: Specifically define the nature of the conformational changes in these regions.

Specific Aim 3: Determine the functional role of these conformational changes in mediating GDP release.

Each of these specific aims relies on site-directed spin-labeling and EPR spectroscopy, which allow us to directly monitor the dynamics of specific regions within the G protein. As discussed in Chapter I, many biochemical studies provide indirect evidence for a variety of routes from receptor contact sites to the nucleotide binding pocket. In Specific Aim 1, several of these regions were tested for receptor activation-dependent conformational changes using EPR, including the α5 helix and Switches I and II (Chapters III-V), among others (Chapter VI). The activation-dependent conformational changes observed in the α5 helix were chosen for additional studies comprising Specific Aims 2 and 3. With this work, we were able to show that a specific rigid-body movement of the α5 helix couples receptor binding to GDP release (Chapter III).

In addition to receptor activation-dependent conformational changes, our experimental approach enables the examination of each structural transition throughout the G protein activation pathway from heterotrimer formation to GTP binding. As a result, a secondary goal of my research has been to characterize these transitions in terms of changes in protein dynamics with respect to the differences observed in the crystal structures of G proteins in various conformations. While EPR is very useful for exploring protein conformations for which structural data is limited, such as the receptor-bound G protein, it also provides valuable information about how the protein behaves in solution, which may be different than predictions based on crystallized proteins. For example, in the GTP-bound conformation, Switch II adopts a highly flexible backbone conformation, a result that is the opposite of previous predictions based on the crystal structures of these two conformations (Chapter IV). Essentially, the overall goal of this

work was to animate the crystallographic snapshots of heterotrimeric G proteins at all points of the G protein cycle to learn more about how these proteins function in solution.

Experimental Strategy

Our lab has adopted a site-directed spin-labeling approach to study G protein dynamics with EPR spectroscopy. This approach relies on the incorporation of a thiol-reactive paramagnetic probe at a specific site in the protein to serve as a reporter of local structure and dynamics. Structural changes can be identified as differences in the EPR spectra recorded for different conformations of the G protein (Fig. 14a).

Electron paramagnetic resonance spectroscopy

Electron paramagnetic resonance spectroscopy measures the absorption of microwave radiation by an unpaired electron oriented in a magnetic field. This is very similar to nuclear magnetic resonance spectroscopy, which measures the absorption of radiofrequency radiation by spin-active nuclei. In either method, the electron or nucleus is extremely sensitive to its local environment, enabling the spectrum to provide detailed structural information. Indeed, a continuous-wave EPR spectrum provides information about mobility, solvent accessibility, and distances between paramagnetic centers (reviewed in Hubbell*, et al.*, 2000).

The thiol-reactive methanethiosulfonate spin label is the most commonly used paramagnetic probe in biophysical studies of proteins (Fig. 14b). This label reacts with cysteine residues in proteins to generate the nitroxide side chain R1, and the dynamics of the nitroxide on the nanosecond time scale can be determined by spectral lineshape analysis (Budil*, et al.*, 1996). In helices and loops, at sites where the nitroxide does not contact other residues, the internal motion of R1 is dominated by torsional oscillations of dihedrals χ_4 and χ_5 (Mchaourab*, et al.*, 1996; Langen*, et al.*, 2000; Columbus*, et al.*, 2001), giving rise to a characteristic anisotropic motion of the nitroxide (Columbus*, et al.*, 2001). This inherent motion is

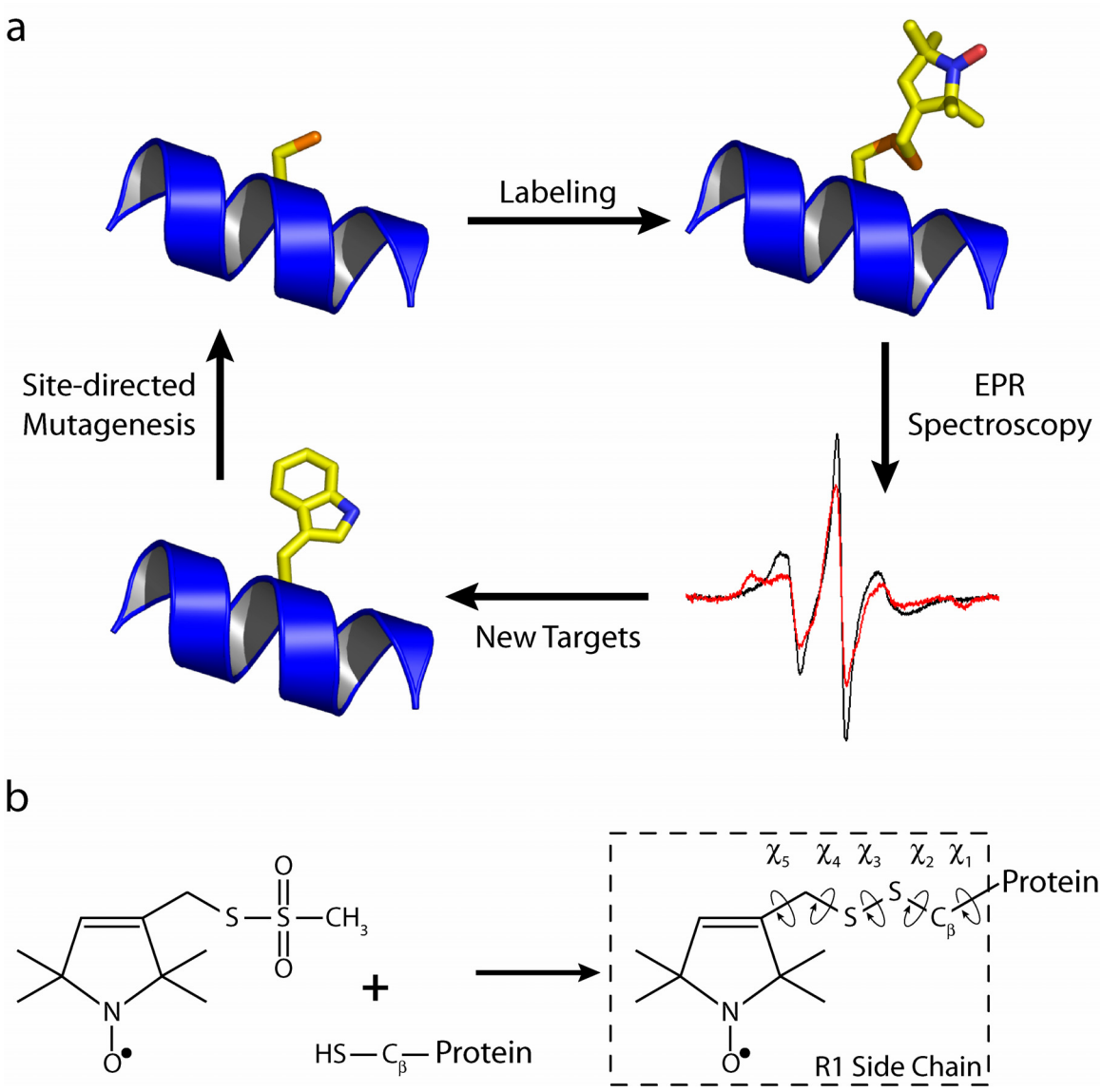

Figure 14 | Site-directed spin-labeling and EPR spectroscopy (**a**) Site-directed cysteine mutagenesis provides a reactive thiol group for the specific incorporation of the paramagnetic nitroxide probe. Local structural changes in the labeled region can be identified by comparing the EPR spectra recorded for different conformations of the protein (*red* and *black* traces). (**b**) The methanethiosulfonate spin label reacts with a cysteine residue in the protein to generate the paramagnetic side chain, R1.

modulated by backbone motion on the nanosecond time scale, and variations in motion of R1 at different sites within helices reflect variations in local backbone motions (Columbus & Hubbell, 2004; Columbus & Hubbell, 2002). The internal motion of R1 is also modulated by weak interactions of the nitroxide, a situation readily recognized in the lineshape by the appearance of features corresponding to reduced amplitudes and/or rates of motion. This property confers spectral sensitivity to the local structure of the protein (Fig. 15) (Mchaourab*, et al.*, 1996; Hubbell*, et al.*, 2000). Thus, the EPR spectra of R1 at a selected set of sites can be used to gain information on both local backbone dynamics and conformation. Additionally, conformational exchange on the micro- to millisecond time scale is slow on the X-band EPR time scale and, in principle, the presence of multiple protein conformations in exchange can be recognized by multiple components in the spectrum.

Although spectral lineshape analysis is the predominant means of analysis in our studies, EPR can also be used to determine the distance between the R1 side chain and another paramagnetic center, such as a metal ion or second spin label. Conventional, continuous-wave EPR can accurately measure distances between 8-20 Å (Rabenstein & Shin, 1995), while pulsed techniques, such double electron-electron resonance EPR, can potentially extend that distance to approximately 70 Å (Pannier*, et al.*, 2000). This latter method uses the dipolar coupling between the paramagnetic centers to measure the distance, similar to two-dimensional NMR experiments that measure the dipolar coupling between adjacent nuclei.

Site-directed spin-labeling has become a powerful tool in the study of protein structure and function because it offers several advantages over traditional approaches. In contrast to NMR, EPR is not restricted by the size of the protein because only the paramagnetic centers are spectroscopically visible. Additionally, membrane proteins and large protein complexes have proven difficult to crystallize, however, these systems are amenable to study with SDSL. Indeed, extensive spin-labeling studies of rhodopsin were the first to reveal the conformational changes that accompany receptor activation (Farrens*, et al.*, 1996). However, EPR is unable to provide the structural resolution attainable by NMR

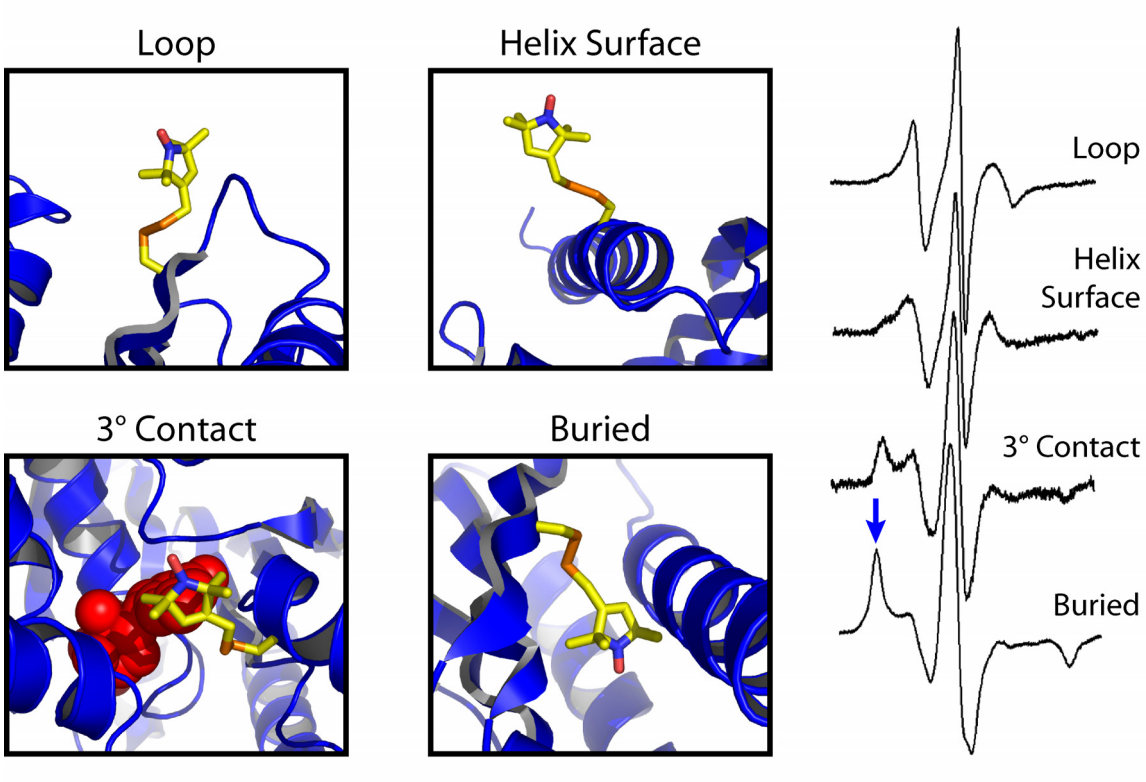

Figure 15 | EPR spectra are sensitive to protein structure Models of the R1 side chain at several sites in the α subunit of the G_{i1} heterotrimer (1GP2) are shown together with the corresponding EPR spectra. Each spectrum is a fingerprint of the local environment of the spin label, and these four spectra are characteristic of R1 side chains in loops, α-helices, sites of tertiary contact, and buried sites. As the mobility of the side chain decreases, the spectra become broader and the intensity of the low-field peak increase (*blue arrow*). If a conformational change in the protein decreases the mobility of the spin label at one site, similar changes are observed in its EPR spectrum. In this way, changes in the EPR spectrum can be interpreted in terms of changes in the mobility of the spin-labeled side chain.

and x-ray crystallography, and perturbations in the structure due to incorporation of the probe, although small, are also a concern (Langen*, et al.*, 2000). Fortunately, we have been able to interpret the results of our SDSL studies in terms of the numerous G protein crystal structures. By combining static, high resolution structural data with dynamic, low resolution EPR data, we can enhance our understanding of G protein function beyond the information provided by either method alone.

Site-directed spin-labeling in the G protein α subunit

In order to begin these studies, a cysteine-depleted $G\alpha_{i1}$ base mutant was constructed so that cysteines could be introduced at specific locations for labeling with a fluorophore or paramagnetic probe. The $G\alpha_{i1}$ protein was selected as the template for the base mutant since it is more easily expressed in bacteria than transducin, and can interact with rhodopsin nearly as well (Medkova*, et al.*, 2002). Since these two Gα subunit family members share 80% sequence similarity (Gilman, 1987), and both interact with rhodopsin, the conformational changes observed in the $G\alpha_{i1}$ background are likely to be a good approximation of those in $G\alpha_{t}$. Rhodopsin will be used as the receptor in this system because it can be easily purified in large quantities from bovine retina. Moreover, much of what is known about GPCR structure and function comes originally from studies on rhodopsin that have since been extended to other receptors.

The base mutant was generated by substituting six solvent-accessible cysteines (of ten total cysteines) with conservative amino acids. These mutations were C3S, C66A, C214S, C305S, C325A, and C351I. The substituted amino acid was chosen based on the specific environment of the native cysteine, where serine was placed at more polar sites and alanine was chosen for less polar sites. The isoleucine substitution at C351 at the extreme C-terminus of Gα was critical for maintaining normal interactions with the receptor as serine and alanine substitutions prevented receptor-catalyzed GTPγS binding. The base mutant expresses well, is folded properly, and has rates of receptor-catalyzed [^{35}S]GTPγS binding and GTP hydrolysis similar to wild type $G\alpha_{i1}$ (Medkova*, et al.*, 2002).

Once the endogenous reactive cysteines were removed, site-directed cysteine mutagenesis in the base mutant allowed us to specifically incorporate paramagnetic labels to monitor local conformational changes virtually anywhere in the protein. To date, the lab has generated nearly sixty single (Fig. 16) and twenty double cysteine mutants of the base mutant, most of which express functional protein for labeling and study with EPR spectroscopy (Appendix A).

A typical EPR experiment begins by recording an EPR spectrum for the purified, labeled Gα subunit, which can be compared to the location of the labeled side chain in the G protein structure. Next, each limit conformation of Gα is examined by recording EPR spectra after the addition $G\beta_1\gamma_1$, dark (inactive) rhodopsin in urea-washed rod outer segment membranes, light, and finally, GTPγS (Fig. 17). Conformational changes are identified by comparing the EPR spectra recorded for any two states of the G protein. For example, the receptor activation-dependent conformational changes in Gα leading to GDP release can be observed by comparing the EPR spectra recorded before and after photoactivation of the receptor (Fig. 17). In this way, we have mapped the dynamics of each structural transition along the activation pathway of Gα for numerous sites in the protein.

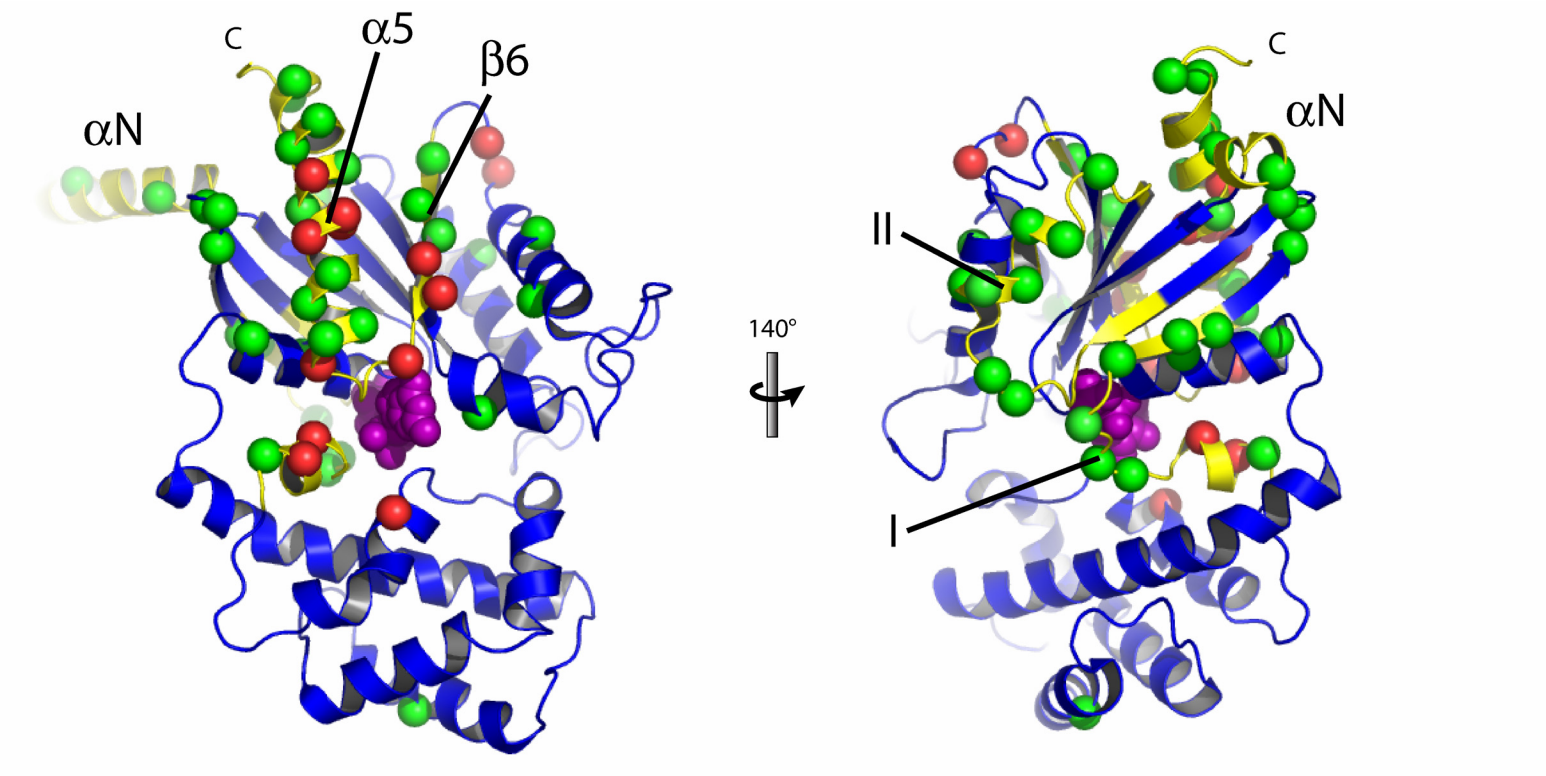

Figure 16 | Summary of site-directed cysteine mutants Many single cysteine mutations have been engineered into the base mutant background. Most of the mutants have been successfully labeled for study with EPR spectroscopy (*green spheres*), although some did not express (*red spheres*). So far, the lab has focused on the αN helix (Medkova*, et al.*, 2002; Preininger*, et al.*, 2003), the α5 helix and β6 strand (Chapter III) and Switches I and II (Chapters IV and V). Certainly other interesting regions of the molecule remain to be explored.

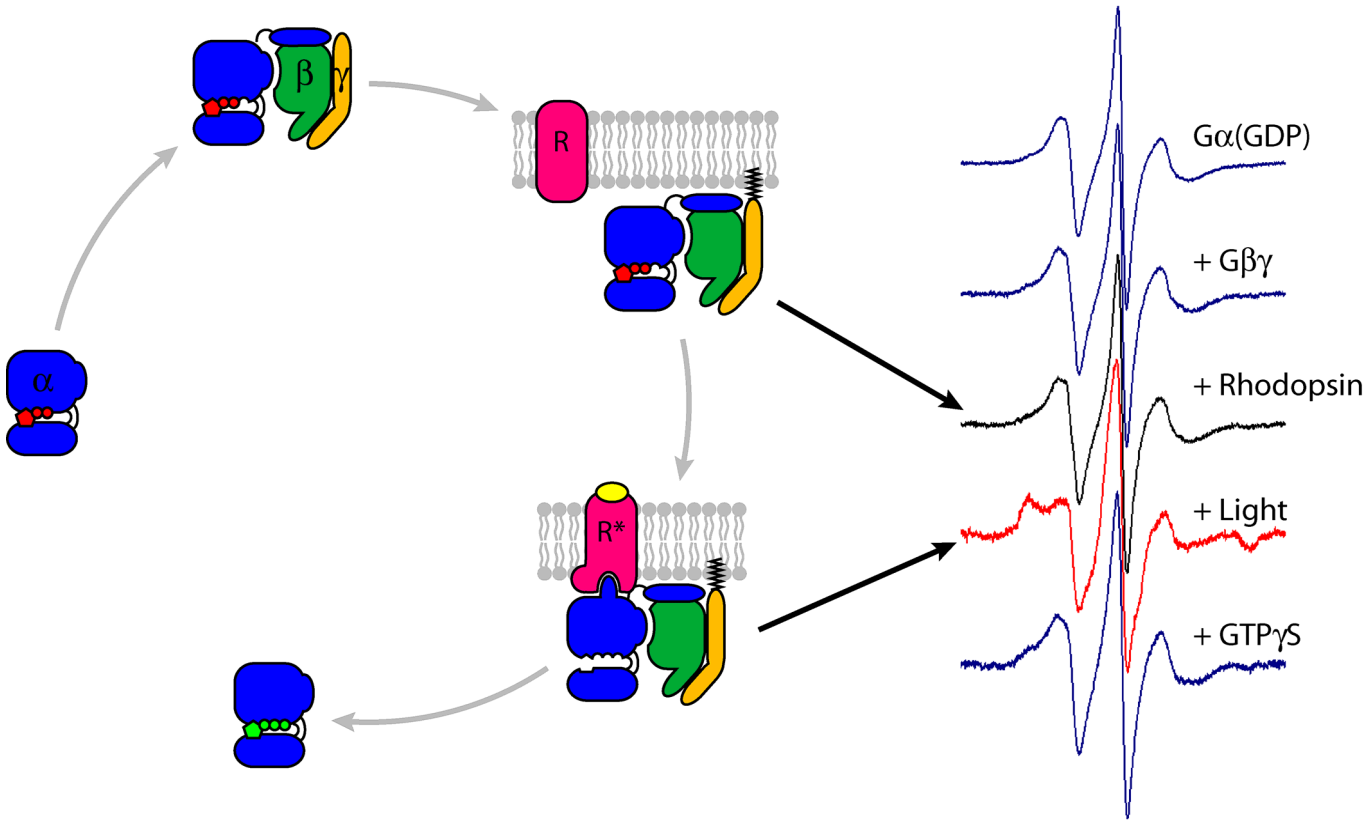

Figure 17 | Typical EPR experiment Beginning with the purified, labeled GDP-bound Gα subunit, each limit conformation of Gα is explored by EPR. Conformational changes are identified by comparing the EPR spectra recorded for any two conformations. In this example, there is a receptor activation-dependent decrease in the mobility of the spin-labeled side chain (compare *black* and *red* traces).

Materials and Methods

Since most of the methods used to obtain the data presented in the subsequent chapters are the same (Fig. 18), I will include a description of the common methods used in this work here, and address unique approaches in the appropriate sections.

Materials

GDP, GTP, and GTPγS were purchased from Sigma-Aldrich, Inc. (St. Louis, MO). The methanethiosulfonate spin label reagent, *S*-(1-oxy-2,2,5,5-tetramethylpyrrolinyl-3-methyl) methanethiosulfonate, was purchased from Toronto Research Chemicals, Inc. (North York, Ontario, Canada). All other reagents and chemicals were of the highest purity available.

Construction, expression and purification of Gα subunits

An expression vector containing the $G\alpha_{i1}$ cDNA sequence with a hexahistidine tag between amino acid residues M119 and T120 in the helical domain was generously provided by Dr. Maureen Linder (Washington University, St. Louis, MO). All mutations were made in this construct using the Quickchange® Site-directed Mutagenesis kit (Stratagene, La Jolla, CA), where the $G\alpha_{i1}$ expression vector is PCR-amplified with two antiparallel primers (Integrated DNA Technologies, Inc., Coralville, IA) containing the mutant codon sequence with *Pfu* DNA polymerase according to the manufacturer's protocol. The parent plasmids are degraded by *Dpn*I endonuclease, and the mutant plasmid is transformed into *Epicurian coli* XL1-Blue supercompetent cells (Stratagene, La Jolla, CA). The plasmid is isolated using the Wizard® *Plus* SV Minipreps DNA Purification System (Promega Corp., Madison, WI) and sequenced to verify the mutation (Vanderbilt DNA Sequencing Core, Nashville, TN).

Expression and purification were conducted essentially as previously described (Medkova*, et al.*, 2002). Mutant plasmid DNA is transformed into BL21-Gold (DE3) *Escherichia coli* (Stratagene, La

Jolla, CA) for protein expression. These cells are grown at room temperature to an OD_{600} of 0.3-0.6 units and then induced with 100 μM IPTG for 12-16 h. Post-induction cell pellets from a 1 L culture are resuspended in 40 mL of Buffer A (50 mM NaH_2PO_4, pH 8.0, 300 mM NaCl) containing 20 μM GDP, 10 mM β-mercaptoethanol, 5 mM imidazole, 100 mM PMSF and 1 μg/mL each of the protease inhibitors pepstatin A, leupeptin, and aprotinin. Cells are disrupted by sonication, and then high-speed centrifugation separates the soluble and particulate fractions. The recombinant proteins are then purified on a HIS-Select™ column (Sigma-Aldrich, Inc., St. Louis, MO) according to the manufacturer's instructions with minor variations. The cytosolic fraction is incubated with 5 mL of a 50% slurry of nickel affinity resin for 1 h at 4 °C and poured into a column. The unbound proteins are removed by washing with 20 mL of Buffer A containing 5 mM imidazole. Mutant Gα is eluted with 8 mL of Buffer A containing 40 mM imidazole and dialyzed against Buffer B (50 mM Tris, pH 8.0, 50 mM NaCl, 2 mM $MgCl_2$) with 20% glycerol, 20 μM GDP, 10 mM βME, 100 μM PMSF and 1 μg/mL each of pepstatin A, leupeptin, and aprotinin overnight at 4 °C. The dialysate is then loaded onto a 5 mL Source™ 15Q column (Amersham Biosciences, Piscataway, NJ). The sample is chromatographed at 150 psi on a Beckman System Gold® HPLC system (Beckman Coulter, Fullerton, CA) with a linear gradient from 50 to 200 mM NaCl in buffer B, and the $G\alpha_{i1}$ mutant subunit elutes at approximately 150 mM NaCl. The protein is concentrated and exchanged into Buffer B with 100 μM GDP and 10% glycerol. After anion exchange, purification typically results in 1-5 mg of greater than 85% pure protein as estimated by Coomassie blue staining of SDS-polyacrylamide gels. Protein concentrations are determined by the Coomassie blue method using bovine serum albumin as a standard (Pierce Biotechnology, Inc., Rockford, IL).

Preparation of ROS membranes, $G\alpha_t$, and $G\beta_1\gamma_1$ from bovine retina

ROS membranes were prepared from bovine retinas as previously described and stored at -80 ºC in buffer containing 10 mM MOPS, pH 8.0, 90 mM KCl, 30 mM NaCl, 2 mM $MgCl_2$, 0.1 mM EDTA, 1

mM DTT, and 50 μM PMSF (Mazzoni*, et al.*, 1991). Urea-washed ROS membranes were stripped with 4 mM urea as previously described (Yamanaka*, et al.*, 1985). Rhodopsin concentration was determined by measuring the absorbance of solubilized ROS membrane suspensions at 500 nm before and after bleaching.

Bovine $G\alpha_t$ and $G\beta_1\gamma_1$ were extracted from unwashed ROS membranes as described (Mazzoni*, et al.*, 1991). Briefly, ROS membranes were washed four times with isotonic buffer (5 mM Tris, pH 8.0, 120 mM KCl, 0.6 mM $MgCl_2$, 1 mM DTT, 0.1 mM EDTA, and 0.1 mM PMSF) and twice with hypotonic buffer (0 mM KCl). Transducin was eluted from the membranes by washing twice with hypotonic buffer containing 0.1 mM GTP. The two subunits were then resolved with a HiTrap™ Blue HP blue sepharose column (Amersham Biosciences, Piscataway, NJ) on a Biologic LP system (Bio-Rad Laboratories, Inc., Hercules, CA) at 4 ºC after the addition of 40 mM $MgSO_4$ to encourage subunit dissociation. $G\beta\gamma$ does not bind to the blue sepharose and elutes in the flow-through in Buffer C (10 mM Tris, pH 7.5, 20 mM $MgSO_4$, 1 mM EDTA, 10% glycerol, and 14.3 mM βME) containing 150 mM NaCl. The $G\beta\gamma$ subunit is concentrated and exchanged into storage buffer (10 mM Tris, pH 7.5, 100 mM NaCl, 5 mM βME, and 10% glycerol) and placed at -80 ºC. $G\alpha_t$ begins to elute at approximately 500 mM NaCl in Buffer C. The $G\alpha_t$ subunit is concentrated and exchanged into storage buffer containing 10 μM GDP. All urea-washed ROS and $G\beta_1\gamma_1$ samples were buffer exchanged into Buffer D (20 mM MES, pH 6.8, 100 mM NaCl, 2 mM $MgCl_2$, and 10% glycerol) prior to EPR experiments.

Intrinsic fluorescence activity assay

In order to ensure that the mutant proteins are folded properly, have GDP bound and can undergo a GTP-dependent conformational change, a minimum 40% increase in the intrinsic fluorescence of W211 must be measured following the addition of AlF_4^-. The fluorescence of 100 nM of the $G\alpha$ subunit is monitored in Buffer B by excitation at 300 nm and emission at 345 nm before and after the addition of

AlF_4^- (10 mM NaF and 50 μM $AlCl_3$) using a Varian Cary Eclipse fluorescence spectrophotometer (Varian, Inc., Mulgrave, Victoria, Australia).

Nucleotide exchange assay

The basal rate of GTPγS binding is determined by monitoring the relative increase in the intrinsic fluorescence (λ_{ex} 300 nm, λ_{em} 345 nm) of Gα (500 nM) in Buffer G (10 mM MOPS, pH 7.2, 130 mM NaCl, 2 mM $MgCl_2$) for 40 min at 15 ºC following the addition of 10 μM GTPγS. Similarly, the receptor-catalyzed rate is measured by monitoring the increase in the intrinsic fluorescence of Gα reconstituted with $G\beta_1\gamma_1$ (500 nM) in the presence of 100 nM rhodopsin at 15 ºC for 40 min following the addition of GTPγS. The data are normalized to the baseline (0%) and the fluorescence maximum (100%). The exchange rate is determined by fitting the data to the exponential association equation,

$$Fl = Fl_{max} (1\text{-}e^{-kt}) \quad \text{(Eq. 1)}$$

where Fl is the percent of the maximum fluorescence (Fl_{max}) at time t seconds and k is the catalytic activation rate constant of GTPγS binding in s^{-1}. These data are typically presented as bar graphs of the GTPγS binding rate (k) (Fig. 18).

Rhodopsin binding assay

The ability of the mutant Gα subunits to bind to rhodopsin in urea-washed ROS membranes was determined by incubating spin-labeled Gα mutants (10 μM) with $G\beta_1\gamma_1$ (10 μM) and rhodopsin (100 μM) in Buffer B in the light ± GTPγS (100 μM). Following a 30 min incubation at 20 °C, the membranes were pelleted by centrifugation at 20,000 × *g* for 1 hour, and the supernatants were resolved by SDS-PAGE, visualized with Coomassie blue and quantified by densitometry (Molecular Imager ChemiDoc™ XRS System, Biorad, Hercules, CA). The percent bound is calculated form the equation,

$$\text{Percent Bound} = 1 - \frac{G\alpha\ L}{G\alpha\ G} \qquad \text{(Eq. 2)}$$

where Gα L and Gα G are the amount of Gα in the light and GTPγS supernatants, respectively (Fig. 18).

Electron paramagnetic resonance spectroscopy

All EPR measurements were performed in collaboration with Wayne L. Hubbell, Ph.D. and Ned Van Eps, Ph.D. in the Departments of Chemistry & Biochemistry and Ophthalmology at the Jules Stein Eye Institute, the University of California, Los Angeles.

For the labeling reaction, MTSSL was added at a 1:1 molar ratio to the cysteine mutants (50 μM) in Buffer D containing 50 μM GDP, and incubated at room temperature for 5 min. Non-covalently bound probe was removed by extensive washing with Buffer D. Gβγ and rhodopsin are exchanged into the same buffer prior to the EPR measurements.

For EPR spectroscopy, a series of spectra were recorded for each spin-labeled mutant. First, cysteine mutants (30 μM) were loaded into a sealed quartz flat cell and spectra were recorded at room temperature on a Bruker E580 spectrometer using a high-sensitivity resonator (HS0118) at X-band microwave frequencies (Bruker BioSpin Corp., Billerica, MA). Each spectrum was collected using a 100 G field scan at a microwave power of 19.92 mW. Optimal field modulation amplitudes were selected to give maximal signal intensity without lineshape distortion. The data were typically averages of 20-50 scans. After collecting each Gα spectrum, Gβγ was added in a 1:1 molar ratio to form heterotrimers. The diluted samples were concentrated to the same concentration as the initial Gα mutants. The EPR spectra of each heterotrimer was recorded both alone in solution and upon addition of urea-washed ROS in the dark (150 μM). For each mutant, a dark spectrum was recorded and the sample was subsequently irradiated for 30 s using a tungsten lamp (cutoff filter; $\lambda > 500$ nm). The EPR spectra were collected immediately after bleaching. Finally, GTPγS (200 μM) was added to the samples to form activated Gα.

Fitting of spectra to the MOMD model of Freed and coworkers followed previously published methods (Columbus*, et al.*, 2001) using principle values for the A and g tensors of $A_{xx} = A_{yy} = 6$ G, $A_{zz} = 37$ G, $g_{xx} = 2.0078$, $g_{yy} = 2.0058$ and $g_{zz} = 2.0023$. Qualitative analysis of spectra in terms of nitroxide mobility is as described in the literature (20, 28). The fitting procedure gives values for the order parameter and the diffusion tensor of the nitroxide, D_{xx}, D_{yy}, D_{zz}. The correlation time is defined as,

$$\tau_c = \frac{\sqrt[3]{D_{xx} D_{yy} D_{zz}}}{6} \qquad \text{(Eq. 3)}$$

Four-pulse DEER distance measurements

The spin-labeled heterotrimeric proteins were mixed with dark-adapted ROS (both in 10% glycerol) and flash frozen in the dark in quartz capillaries in a liquid-solid slush of Freon-22 at 127 K. DEER measurements were performed at 50 K on a Bruker Elexsys 580 spectrometer with a 2 mm split-ring resonator (Bruker BioSpin Corp., Billerica, MA). Four-pulse DEER was carried out as previously described (Pannier*, et al.*, 2000) with the π pump pulse (16 ns) positioned at the absorption maximum of the center line and the observer π (16 ns) and $\pi/2$ (8 ns) pulses at the absorption maximum of the low-field line. After acquiring dark state data, the samples were thawed, illuminated with light (cutoff filter; $\lambda > 500$ nm), and refrozen for a second DEER measurement. Distance distributions were obtained from the raw dipolar time evolution data by the program Deer Analysis 2004 (Jeschke*, et al.*, 2002; Weese, 1992).

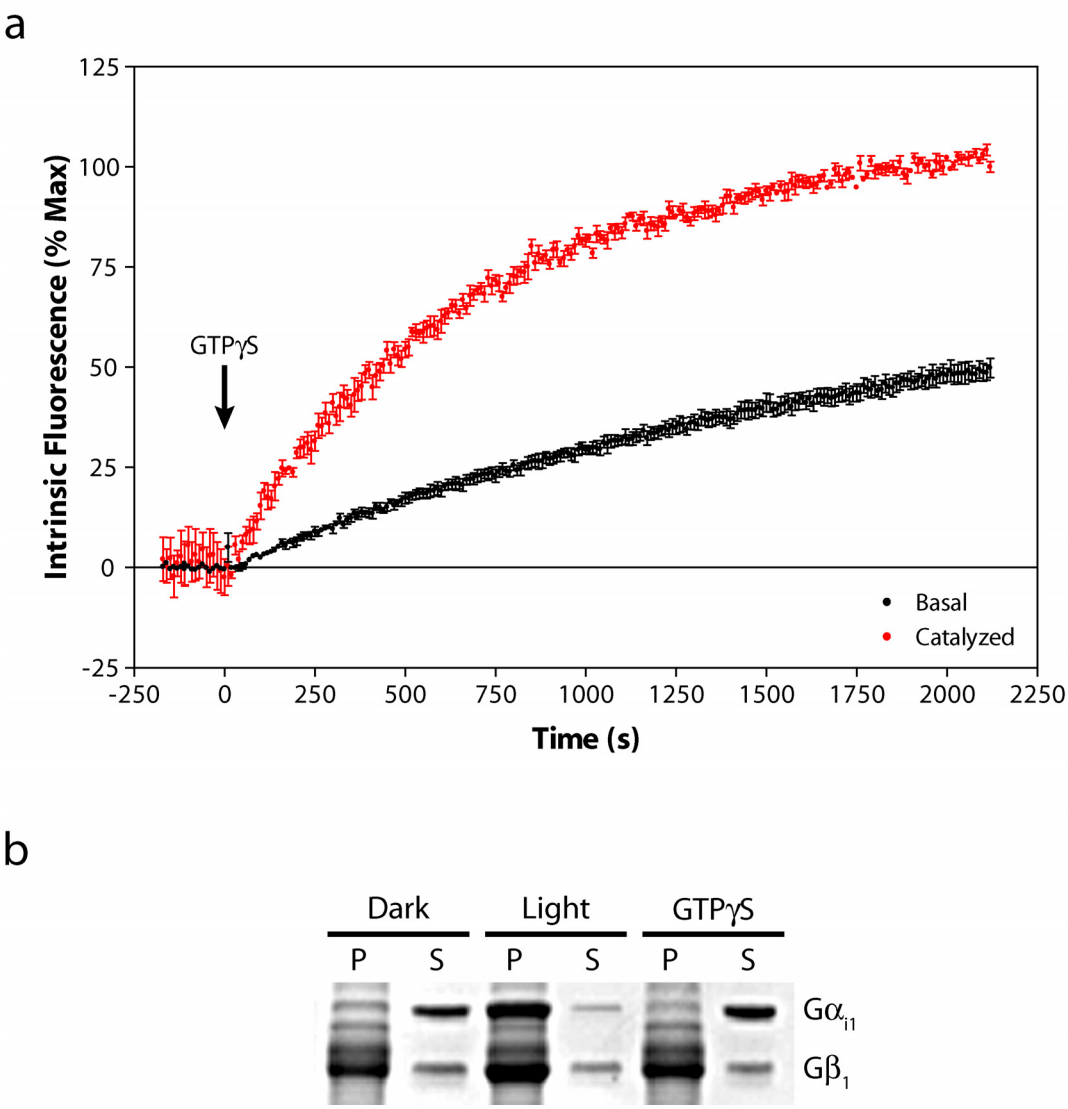

Figure 18 | Biochemical characterization of mutants (**a**) Nucleotide exchange rates for $G\alpha_{i1}$. The increase in the intrinsic fluorescence of Gα alone (●) or in the presence of $G\beta_1\gamma_1$ and photolyzed rhodopsin (●) is monitored following the addition of GTPγS. These traces are fit to an exponential association curve to determine the exchange rate. (**b**) In the rhodopsin binding assay, Gα is incubated with $G\beta_1\gamma_1$ and rhodopsin under three conditions: dark, light, and light with GTPγS. The samples are centrifuged and the membrane fraction (*P*) and supernatant fraction (*S*) are analyzed by SDS-PAGE. Upon light activation, the G protein moves from the supernatant to the membrane, and it is released upon the addition of GTPγS. (See Appendix B for summary of biochemical data.)

CHAPTER III

MECHANISM OF RECEPTOR-CATALYZED GDP RELEASE

Introduction

A variety of extracellular signals activate G protein-coupled receptors, which initiate intracellular signaling by catalyzing GDP release from the α subunit of heterotrimeric G proteins (Cabrera-Vera*, et al.*, 2003). GDP release is the rate-limiting step in G protein activation (Higashijima*, et al.*, 1987a), and results in the formation of a high-affinity complex between the activated receptor and a nucleotide-free conformation of the G protein (Rodbell*, et al.*, 1971b; Emeis*, et al.*, 1982; Bornancin*, et al.*, 1989). Despite its crucial role in cell signaling, this complex is the only major G protein conformation for which structural information is lacking, and much remains to be discovered about the mechanism of receptor-mediated GDP release.

Previous research has identified several important receptor contact sites on the G protein, including the N- and C-termini of Gα (Hamm*, et al.*, 1988; Itoh*, et al.*, 2001; Onrust*, et al.*, 1997; Cai*, et al.*, 2001; Dratz*, et al.*, 1993; Kisselev*, et al.*, 1998), the α4/β6 loop of Gα (Cai*, et al.*, 2001; Mazzoni & Hamm, 1996; Onrust*, et al.*, 1997) and the C-termini of Gβ and Gγ (Taylor*, et al.*, 1996; Kisselev*, et al.*, 1994). Although these studies have outlined the receptor contact surface on the G protein, they provide little insight into the molecular mechanism of R*-catalyzed nucleotide exchange because GDP is bound nearly 30 Å away from this interaction surface (Bourne, 1997; Hamm, 1998). Thus, the receptor must induce some conformational change in the G protein to cause GDP release over this distance. The most apparent route from a receptor contact site to the nucleotide binding pocket is the α5 helix, which connects the Gα C-terminus to the β6/α5 loop at the nucleotide binding pocket (Fig. 19). Previous studies have provided indirect evidence that the α5 helix may play a role in R*-catalyzed nucleotide

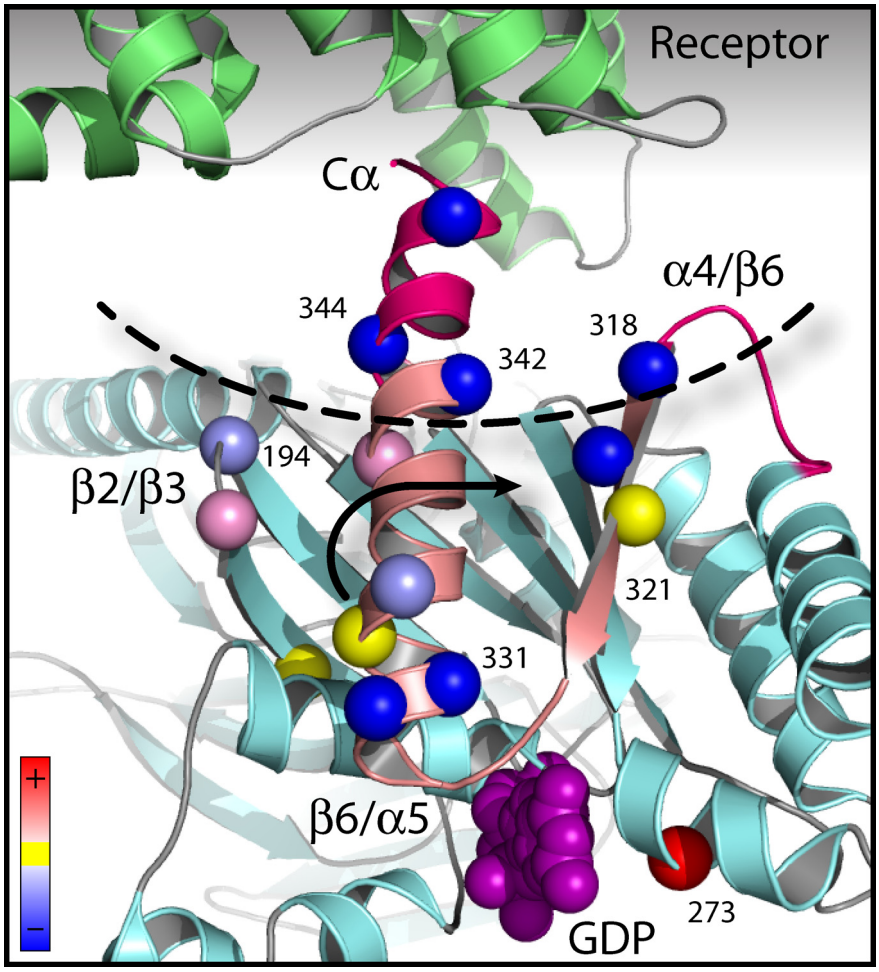

Figure 19 | Summary of mobility changes observed for sites near the α5 helix Ribbon model of the G_{i1} heterotrimer, showing the α subunit (*cyan*) with part of the C-terminal fragment of $G\alpha_t$ (corresponding to $G\alpha_{i1}$ residues 347-354) from the NMR structure (1AQG) attached, juxtaposed with the rhodopsin structure (1GZM) (*green*). The α5 helix and β6 strand (*salmon*) connect known receptor contact sites at the C-terminus and α4/β6 loop (*pink*) to the nucleotide binding pocket at the β6/α5 loop some 30 Å away. The residues selected for site-directed spin-labeling are represented by spheres at their α-carbon, and are colored according to their change in mobility following receptor activation (*inset*, lower left). Several sites undergo a dramatic immobilization upon binding to R*, thereby outlining the R*-interacting surface (*dashed line*). The pattern of mobility changes observed in labeled residues in the α5 helix suggest that R* induces a rotation and translation of the α5 helix toward the β6 strand (*arrow*), disrupting the nucleotide-binding pocket at the β6/α5 loop.

exchange. Many alanine and proline point mutations in this helix alter basal and/or receptor-catalyzed GTPγS binding (Marin*, et al.*, 2001b; Marin*, et al.*, 2002). Additionally, the insertion of a flexible five-glycine linker between the Gα C-terminus and the α5 helix severely reduces R*-catalyzed nucleotide exchange while only modestly decreasing receptor binding (Natochin*, et al.*, 2001).

In the present study, we used site-directed spin-labeling and electron paramagnetic resonance spectroscopy to directly examine the structural changes in the α5 helix during R*-mediated GDP release. Since this technique monitors side chain and backbone dynamics, each labeled residue serves as a local reporter of conformational changes (Hubbell*, et al.*, 2000). When interpreted in terms of the G_{i1} crystal structure (Wall*, et al.*, 1995), the R*-dependent conformational changes observed in the α5 helix provide the first direct evidence for the structural mechanism of R*-catalyzed G protein activation.

Results

Characterization of spin-labeled mutants

Site-directed mutagenesis was performed on a cysteine-depleted $G\alpha_{i1}$ mutant (Medkova*, et al.*, 2002) to introduce cysteines, one at a time, at sites along the α5 helix (330, 331, 333, 334, 340, 342), on an adjacent loop between the β2 and β3 strands (191, 194), in the β2 strand (187), in the β6 strand (318, 320, 321), in the C-terminal tail (344, 349) and near the nucleotide-binding pocket (273) (Fig. 19). One double cysteine mutation, 187-333, was also constructed. These mutants were expressed in *E. coli*, purified and labeled with a thiol-selective paramagnetic probe to generate a nitroxide side chain designated R1. All of the spin-labeled mutants demonstrated R*-catalyzed increases in GTPγS binding and the ability to form stable R*-G protein complexes in the absence of nucleotide (Fig. 20). Interestingly, increased basal exchange rates were observed for labeled sites where the native side chain faces the contact surface between the α5 helix and the β2/β3 loop (191R1, 194R1, 333R1, 340R1, 344R1), while decreased basal exchange rates were observed for mutants facing the β6 strand (331R1,

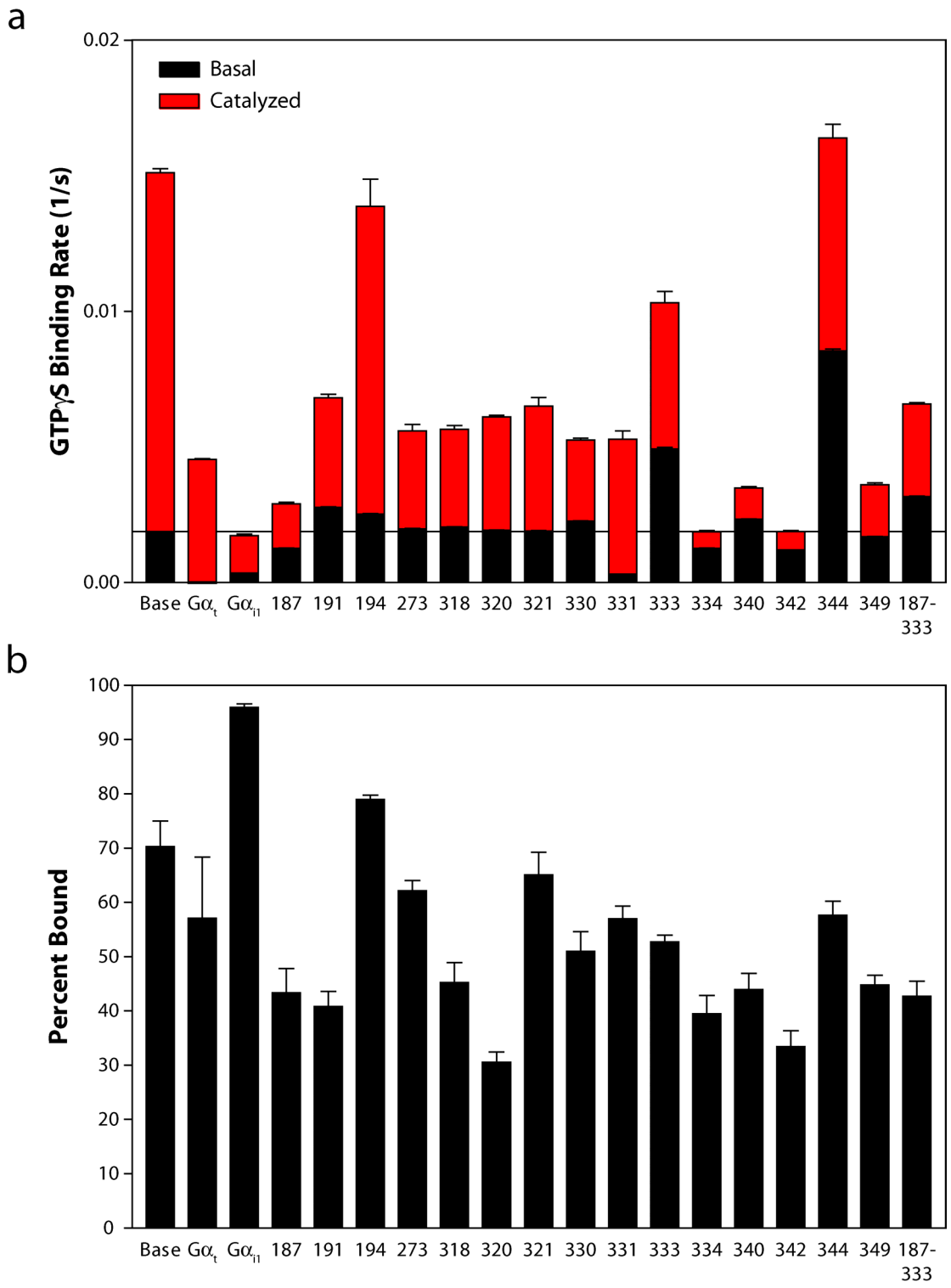

Figure 20 | Biochemical characterization of mutants near the α5 helix (**a**) Nucleotide exchange assay. Data represent the mean ± s.e.m. of 4-6 independent experiments. (**b**) Rhodopsin binding assay. Data represent the mean ± s.e.m. of 3 independent experiments.

334R1, 342R1). Overall, this pattern suggests that displacing the α5 helix away from the β2/β3 loop by disrupting stabilizing interactions between these structures can increase nucleotide exchange on Gα. Alternatively, placing a spin label on the opposite side of the helix may slow nucleotide exchange by sterically inhibiting this movement.

Conformational changes distant from receptor contacts

Following biochemical characterization, EPR spectra of the R1-labeled Gα mutants reconstituted with $G\beta_1\gamma_1$ and rhodopsin in native disc membranes were recorded before and after photoactivation of the receptor (Fig. 21). As shown in previous work, such spectra are fingerprints for local secondary and tertiary structure (Mchaourab*, et al.*, 1996; Langen*, et al.*, 2000), and changes in the spectra following receptor activation reflect alterations in the mobility of the R1 side chain due to structural differences between the heterotrimeric and R*-bound conformations of Gα. Indeed, the EPR spectrum of 273R1, which makes direct contact with GDP (Fig. 22c), reflects an increase in mobility following receptor activation, consistent with the formation of a nucleotide-free state of Gα and the concomitant loss of constraints on the motion of the R1 side chain at this position.

R*-mediated changes in EPR spectra are also found at sites near the N-terminus of the α5 helix. Prior to receptor activation, the spectra of 330R1, 331R1, 333R1 and 334R1 are characteristic of the nitroxide side chain at the solvent-exposed surface of an ordered α-helix, where the nitroxide has weak to zero interactions with the protein (Columbus & Hubbell, 2004) (Fig. 21, *black traces*), consistent with the location of these sites in the crystal structure and models of R1 (Fig. 22). Upon photoactivation and formation of the R*-G protein complex, a pattern of spectral changes occurs that suggests a structural rearrangement of the helix. For example, decreased mobility of R1 is reflected in the spectra of 330R1, 331R1 and 334R1, indicating that these residues establish new contact interactions absent in solution, while 333R1 in this helix shows no changes upon interaction with R* (Fig. 21, *red traces*). Importantly, the absence of changes for 333R1 strongly suggests a simple rigid-body movement that does not involve

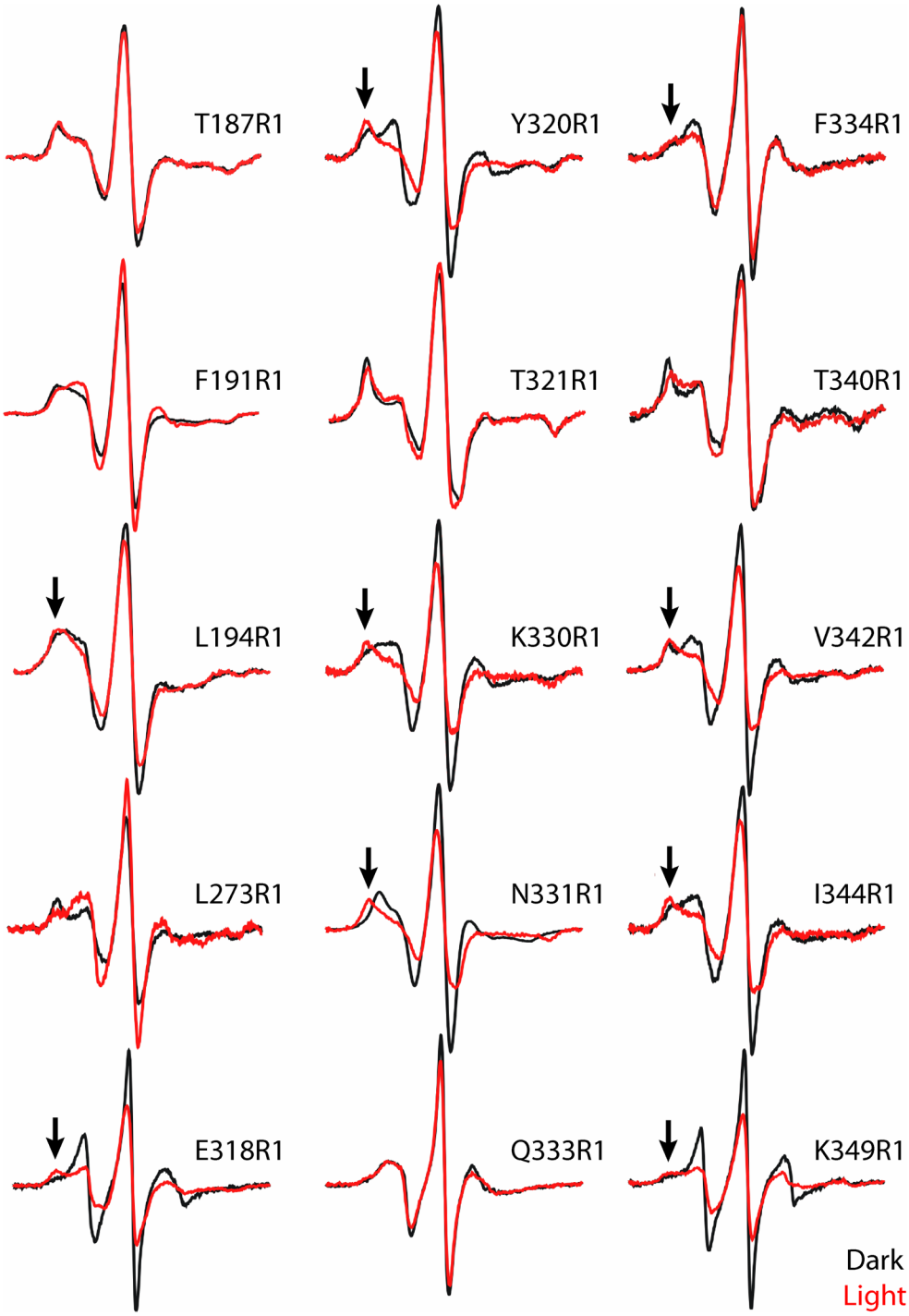

Figure 21 | Receptor activation-dependent conformational changes in the α5 helix Spectra for each of the spin-labeled mutants in solution with $G\beta_1\gamma_1$ and rhodopsin were recorded before (*black traces*) and after (*red traces*) photoactivation of the receptor. Differences in EPR lineshape reflect conformational changes observed at the individual sites. The *arrows* indicate the position of a spectral component corresponding to an immobile state of R1 that increases in several residues following receptor activation.

changes in the secondary structure of the α5 helix. Furthermore, the lack of change shows that residue 333R1 cannot participate in the R*-binding interface, indicating that the conformational changes observed at 330R1, 331R1 and 334R1 must be transmitted from a distant receptor contact site.

The extreme C-terminus of Gα (residues 344 to 354) is a known receptor contact site that undergoes an R*-mediated conformational change, wherein residues disordered or absent in crystal structures of the protein are induced to form an α_L-type C-cap motif upon R* binding (Coleman*, et al.*, 1994b; Coleman*, et al.*, 1994a; Wall*, et al.*, 1995; Dratz*, et al.*, 1993; Kisselev*, et al.*, 1998). The EPR spectra for residues 344R1 and 349R1 in this region reflect a moderate and high degree of mobility, respectively, prior to receptor activation. This result is consistent with the environment of these residues in the crystal structure of Gα; residue 344 is located at the C-terminus of the ordered α-helix, α5, while residue 349 is in the flexible C-terminal tail. Upon binding to R*, the changes in the spectra indicate an overall immobilization of R1 consistent with the expected interactions at the R*-G protein interface.

Similarly, decreases in R1 mobility were observed at nearby residues 194R1, 318R1 and 342R1, where the nitroxide side chains point toward the receptor, suggesting that these sites may also contribute to the R*-binding surface (Fig. 22a). Prior to receptor activation, the spectrum for 318R1 reflects a rapid isotropic motion characteristic of a disordered structure, a result anticipated from the high thermal factor for this residue at the N-terminus of the β6 strand (Fig. 22a) (Wall*, et al.*, 1995). Spectra for sites 194R1 and 342R1, however, reflect complex multi- component states characteristic of R1 at sites where the nitroxide interacts with nearby structures, giving rise to an immobilized component (Langen*, et al.*, 2000; Mchaourab*, et al.*, 1996). Following receptor activation, the spectra for 194R1, 318R1 and 342R1 exhibit an increase in the amplitude of the immobilized component, with a concomitant decrease in the intensity of the mobile component (Fig. 21).

By mapping these changes to models of the R1 side chain in the G_{i1} crystal structure, the apparent receptor contact surface on Gα can be delineated (Fig. 19, *dashed line*). Together with the absence of spectral change at 333R1, these data indicate that the contact interface does not extend further toward the

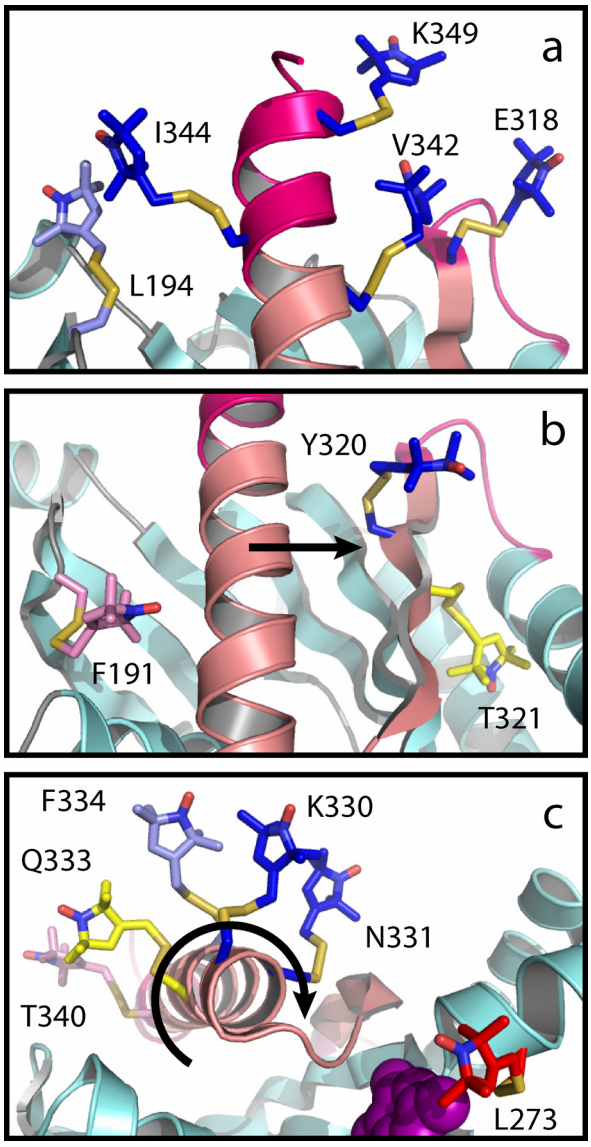

Figure 22 | Models of the R1 side chain at sites near the α5 helix Models of R1 are based on rotamer conformations observed in crystal structures. The side chains are color-coded according to the change in mobility observed upon receptor activation as in Figure 19. (**a**) The strong immobilization of residues 194R1, 318R1, 344R1 and 349R1, and possibly 320R1 and 342R1, are likely due to their proximity to known receptor contact sites. The gradient of mobility changes observed for residues 330R1, 331R1, 333R1 and 334R1 suggest a rotation of the α5 helix (**c**, *arrow*), while the differences at residues 191R1, 340R1, as well as 320R1, indicate an additional translational component of this motion by the helix toward the β6 strand (**b**, *arrow*).

nucleotide-binding pocket than a surface described by residues 194R1, 318R1 and 342R1 (Fig. 22). Thus, the mobility changes observed at the N-terminus of the α5 helix must arise from conformational changes in Gα transmitted from a distant R* contact site.

Conformational changes couple R binding to GDP release*

Although it is clear that binding to R* induces a structural change in the α5 helix, its role in GDP release is unclear. Several mutations in the Gα subunit that uncouple G protein activation from receptor activation have been described in the literature. The best characterized mutation is a flexible five-glycine linker inserted between the R*-binding C-terminus and the α5 helix, which results in a mutant Gα that still binds to photolyzed ROS membranes, but has a critical defect in R*-catalyzed nucleotide exchange (Natochin*, et al.*, 2001). A substitution in the C-terminus of $G\alpha_s$, R385H (K345H in $G\alpha_{i1}$), uncouples β-adrenergic receptor stimulation from adenylyl cyclase activation in patients with Albright's hereditary osteodystrophy (Schwindinger*, et al.*, 1994). Another famous mutation in $G\alpha_s$, R389P (K349P), was discovered in the *unc* clone of S49 murine lymphoma cells (Sullivan*, et al.*, 1987). Finally, two proline mutations in the α5 helix of $G\alpha_t$, V338P (V342P) and I339P (I343P), had impaired receptor-catalyzed nucleotide exchange (Marin*, et al.*, 2002). Although all of these mutations had decreased receptor-catalyzed GTPγS binding, the ability of the mutant to bind to the receptor had only been investigated for the 5G mutant.

These six mutations were created in the base mutant background to evaluate their ability to bind to activated rhodopsin without being activated. First, the basal and R*-catalyzed rates of nucleotide exchange were measured. In the cysteine-depleted background, the V342P and K345H mutations had little effect on the rate of R*-catalyzed nucleotide exchange, while catalyzed exchange was impaired in the remaining mutants. The ability of the remaining mutants to bind to activated rhodopsin in ROS membranes was evaluated, and consistent with the previous study, the 5G mutant bound to R* very well, however, the other mutants did not. Together, these results indicate that the 5G mutation may uncouple

receptor binding from nucleotide exchange (Fig. 23), while the reduced receptor-catalyzed exchange rates for the other mutants are likely due to impaired receptor binding.

Using the uncoupling 5G mutation, we introduced spin labels into the C-terminus (5G-349R1) and the α5 helix (5G-330R1) of Gα (Fig. 23a). Interestingly, the five-glycine insertion increased the dynamics at both sites (compare Fig. 21 and Fig. 23c, *black traces*). While the increase in mobility of 5G-349R1 is expected based on the increased length of the C-terminal tail extending from the protein core, the increase observed for 5G-330R1 is surprising, and suggests that the N-terminus of the α5 helix is sensitive to perturbations made at the C-terminus of the helix. Additionally, the amplified dynamics of 5G-330R1 may explain the substantial increase in the basal nucleotide exchange rate for the five-glycine insertion (Natochin*, et al.*, 2001).

Upon receptor activation, 5G-349R1 exhibits a striking decrease in side chain mobility, similar to 349R1 in the coupled protein, consistent with its location at the R*-G protein interface. However, receptor activation-dependent conformational changes are no longer observed in 5G-330R1, despite normal binding (Fig. 23). Together with the biochemical phenotype of this mutation, these data indicate that the conformational change leading to GDP release is propagated along the α5 helix to the nucleotide-binding pocket, and without movement of the α5 helix, GDP is not released.

Modeling the structural change

To further characterize the conformational change in the α5 helix, R1 was also introduced at an interior site in the middle of the helix (340R1), and in structures flanking the α5 helix (191R1 in the β2/β3 loop, and 320R1, 321R1 in the β6 strand). Prior to receptor activation, all of these sites exhibited complex multicomponent spectra consistent with their locations at sites of tertiary contact (Fig. 22). Following receptor activation, the spectra of 191R1 and 340R1 reveal a general increase in R1 mobility, the spectrum of 320R1 shows a dramatic decrease in mobility, and that for 321R1 shows little change (Fig. 21).

Collectively, the results for all of the sites demonstrate direct contact interactions between Gα and R* and, most importantly, an allosteric change in the Gα subunit involving the α5 helix. In Figure 22, the R1 side chains are color-coded according to mobility changes induced by interaction with R*, revealing a distinctive pattern that suggests a model for the allosteric change. For example, there is an angular gradient of mobility change along the α5 helix (Fig. 22c), suggesting a rigid-body rotation of the α5 helix that would bring 330R1 and 331R1 into strong contact with the β6 strand and 334R1 into weaker contact with the same structure, resulting in a decrease in the mobility as observed at each site. At the same time, 340R1 on the opposite side of the helix would experience an increase in mobility as tertiary interactions with the β2/β3 loop are weakened, while 333R1 would experience no change as it has no tertiary interactions prior to receptor activation and it is too far to make contact with the β6 strand following receptor activation.

However, a simple rotation of the α5 helix cannot readily account for the increase and decrease in mobility observed for 191R1 and 320R1, respectively, a result that implies an additional translation of the α5 helix away from the β2/β3 loop toward the β6 strand (Fig. 22b). A translational component of the motion could also contribute to the decreased mobility of 342R1, in addition to direct interactions with R* (Fig. 22a). The lack of change for the buried 321R1 indicates that the β6 strand itself does not move away from the body of the protein.

The rigid-body rotation-translation model was tested using double electron-electron resonance EPR spectroscopy, a pulsed EPR technique capable of measuring distances between 15 and 80 Å (Pannier*, et al.*, 2000), to determine the distance distribution between spin labels at sites 187 and 333 before and after receptor activation (Fig. 24). Prior to receptor binding, the major population in the distribution is centered at 19 Å, which is consistent with modeling of these side chains into the G_{i1} crystal structure (Fig. 24a). The minor population centered on 30 Å can be accounted for by a second rotamer of R1 at site 187 since the multi-component continuous wave EPR spectrum of 187R1 supports the presence of two R1 rotamers at this site.

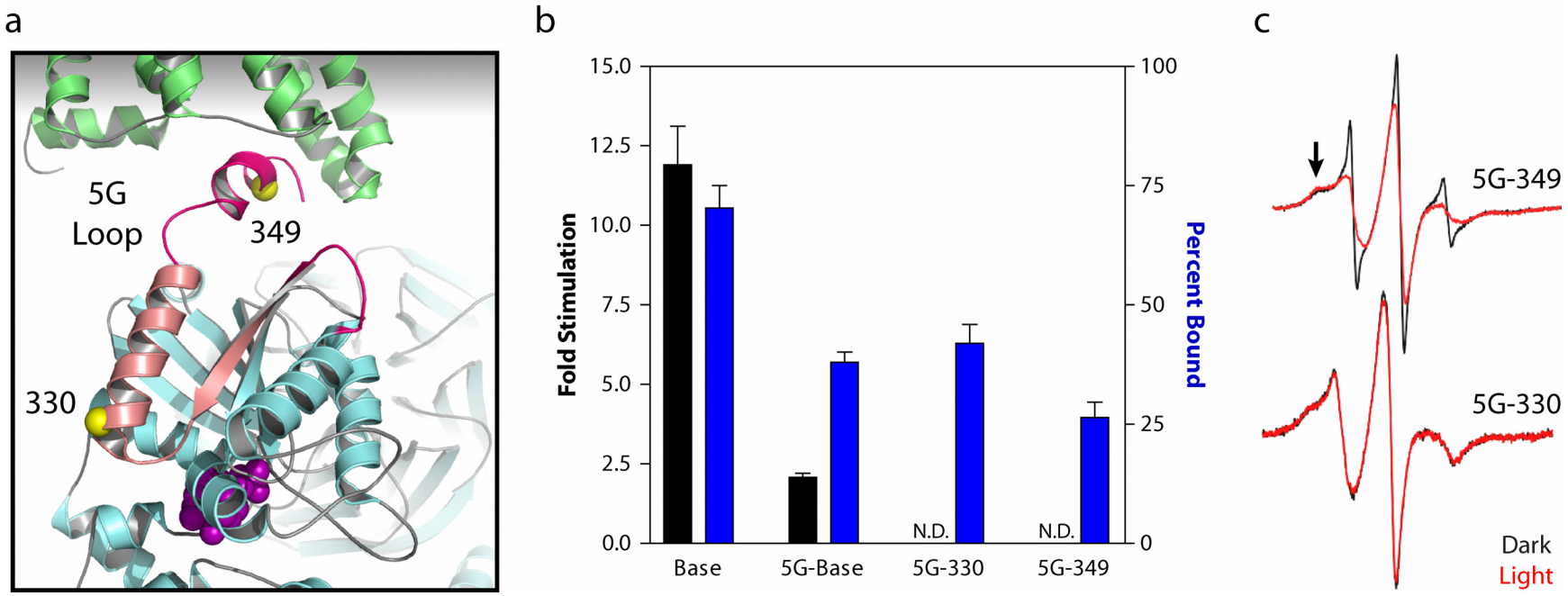

Figure 23 | Movement of the α5 helix is necessary for GDP release (**a**) We introduced spin labels at two sites within an uncoupled base mutant, one at the R*-binding surface (349) and the other at the end of the α5 helix (330) (*yellow spheres*). (**b**) This mutation uncouples receptor stimulation from receptor binding. Both of the 5G mutants bind to R*. (**c**) When EPR spectra were recorded for these mutants before (*black trace*) and after (*red trace*) receptor binding, 5G-349 still demonstrated a decrease in side chain mobility. However, no changes in the EPR spectrum were observed for 5G-330 following receptor activation, whereas in the coupled protein, residue 330 becomes less mobile. This exciting result indicates that the movement of the α5 helix couples R* binding to GDP release.

Upon receptor activation, the distance distribution is dramatically modified to a broad distribution centered at 24 Å. Interestingly, broadening of the distribution suggests increased dynamics of the region upon binding to R* (Fig. 24d). Importantly, the EPR spectra for 187R1 and 333R1 individually do not change upon R* binding (Fig. 21), indicating that the observed distance change is not due simply to rearrangements in R1 conformation, but must be due to movement of the α5 helix relative to 187R1. This distance measurement is entirely consistent with the motion of the α5 helix suggested by the pattern of mobility changes for spin-labeled side chains in this region.

With GTPγS addition, changes in the EPR spectra are observed that reflect the activating conformational change in Gα and destabilization of the R*-G protein complex. These EPR spectra are generally similar to spectra recorded for purified, labeled $G\alpha_{i1}$(GDP) alone in solution.

Discussion

Our results provide the first direct evidence of receptor activation-dependent structural changes in G proteins. The striking pattern of mobility changes observed for these sites in the C-terminal region of Gα demonstrates that binding to R* induces a structural change in the α5 helix. Furthermore, we show that this movement is coupled to GDP release, suggesting the exciting possibility that this conformational change is the trigger for G protein activation.

Movement of the α5 helix would disrupt the loop connecting it to the β6 strand, which contains the TCAT motif conserved throughout the G protein superfamily. This loop interacts with the guanine ring of the bound nucleotide, and mutations in this motif greatly enhance spontaneous GDP release (Thomas*, et al.*, 1993; Iiri*, et al.*, 1994; Posner*, et al.*, 1998). The cysteine-to-alanine mutation in $G\alpha_o$ decreases GDP affinity by 10-fold (Thomas*, et al.*, 1993), and this mutation in our cysteine-depleted base mutant explains its increased basal nucleotide exchange rate over the native $G\alpha_{i1}$ protein (Fig. 20). Additionally, the alanine-to-serine mutation in $G\alpha_s$, A366S, causes pseudohypoparathyroidism and

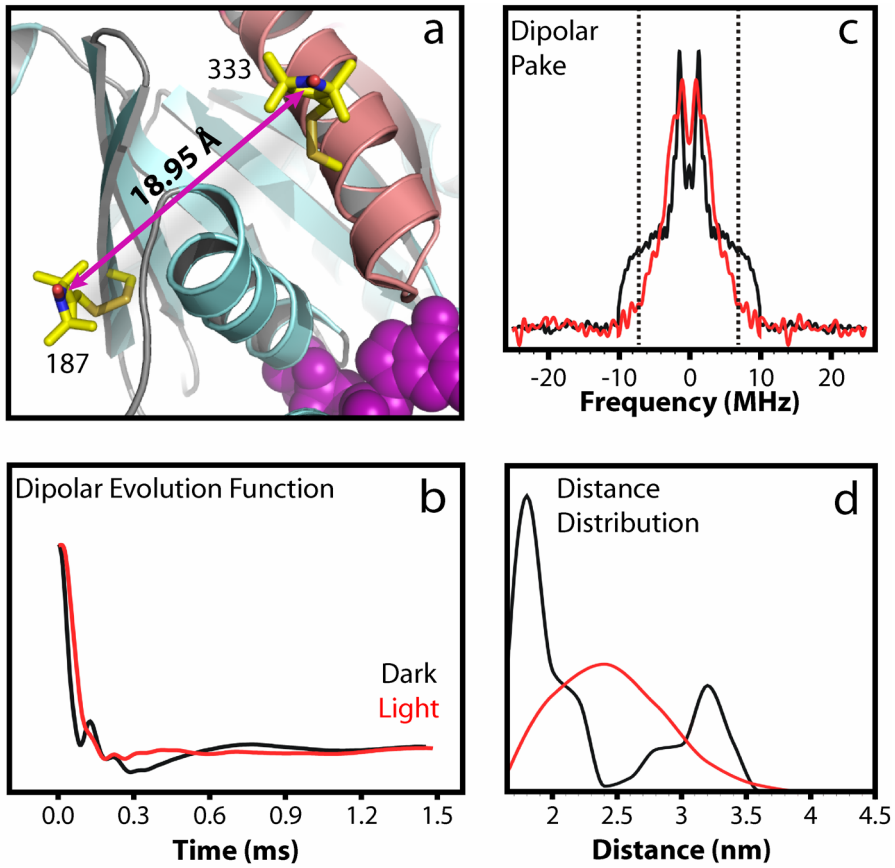

Figure 24 | Distance measurements support the proposed rotation-translation of the α5 helix (**a**) Molecular modeling of the R1 side chain at positions 187 and 333 suggests an internitroxide distance of approximately 19 Å. (**b**) Dipolar evolution functions after background subtraction using the Deer Analysis 2004 program (Jeschke*, et al.*, 2002; Weese, 1992). The data were recorded before (*black trace*) and after (*red trace*) receptor activation. (**c**) Dipolar pake spectrum generated from each evolution function. The dotted vertical lines highlight a frequency splitting corresponding to a 19 Å distance. (**d**) The distance distribution between nitroxide labels increases upon receptor binding. A broad distribution is observed in the receptor-bound state that is centered at 24 Å. This 5-6 Å increase is consistent with the 30° rotation predicted from the single site studies.

gonadotropin-independent precocious puberty in male patients due to constitutive G_s signaling (Iiri*, et al.*, 1994). A homologous mutation in $G\alpha_{i1}$ also greatly enhances GDP release (Posner*, et al.*, 1998). However, no significant structural differences were observed in the crystal structure of the $G\alpha_{i1}$-A326S heterotrimer compared to the wild type protein although the GDP-binding site was only partially occupied in the crystal (Posner*, et al.*, 1998). Taken together, these data support our model whereby the receptor-mediated movement of the α5 helix is sufficient to cause nucleotide release by perturbing the interaction between the TCAT motif in the β6/α5 loop and the guanine ring of GDP.

In addition to providing a direct connection between the Gα C-terminus and the β6/α5 loop, mutagenesis and computational studies have suggested that a receptor-induced movement of the α5 helix may be transmitted to the GDP-binding pocket *via* the α1 helix and β2 and β3 strands (Marin*, et al.*, 2001b; Ceruso*, et al.*, 2004). The absence of receptor activation-dependent changes in the EPR spectra for 187R1 indicates that this is a less likely model than a simple perturbation of the β6/α5 loop. Several other potential routes linking R*-binding sites on Gα to GDP release have also been proposed, mainly based on the effects of various mutations on basal and R*-catalyzed nucleotide exchange rates. These include the β6 strand connecting the α4/β6 loop to the β6/α5 loop (Onrust*, et al.*, 1997), the α3 helix connecting the α3/β5 loop to Switch III (Grishina & Berlot, 1998; Grishina & Berlot, 2000; Pereira & Cerione, 2005), and β strands 1-3 connecting the N-terminus to the phosphate-binding loop and Switches I and II (Thomas*, et al.*, 2001). Reorientation of the GTPase and helical domains has also been suggested in order to free the GDP buried between these domains (Warner*, et al.*, 1998; Grishina & Berlot, 1998; Warner & Weinstein, 1999; Ceruso*, et al.*, 2004; Majumdar*, et al.*, 2004), however the role of interdomain interactions in R*-catalyzed GDP release remains unclear (Marin*, et al.*, 2001a). Although additional studies will be necessary to characterize any potential receptor activation-dependent conformational changes in these regions, our data show that an R*-mediated translocation of the α5 helix is required for GDP release.

In addition to structural changes in Gα, two models have been proposed whereby the receptor uses Gβγ as a nucleotide exchange factor to disrupt the nucleotide binding pocket through its interactions with Switch II. In the lever-arm hypothesis, the receptor uses the interactions between the N-terminal helix of Gα and Gβγ to pry open the nucleotide binding pocket at the Gβ/Switch II interface (Iiri*, et al.*, 1998). An alternative gear-shift model proposes that the receptor uses the N-terminal helix to cause close-packing of Gβ to Switch II, allowing the N-terminus of Gγ to engage the helical domain, thereby opening the cleft between the helical and GTPase domains to allow GDP release (Cherfils & Chabre, 2003). Although sites at the N-terminus of Gα do not demonstrate any receptor activation-dependent differences in EPR spectra (Medkova*, et al.*, 2002), sites within Switch I show significant structural changes while sites in Switch II report only a minor change at the Gα-Gβ interface (Chapters IV and V). Further studies will be necessary to characterize these changes in Gα-Gβ contacts to test the models suggested by the lever-arm and gear-shift hypotheses.

Some knowledge about the nature of conformational changes in the α5 helix also enables speculation about the nature of the molecular interaction causing this change. Site-directed mutagenesis of residues on the side of the α5 helix opposite the β6 strand significantly increase the basal nucleotide exchange rate of Gα (Marin*, et al.*, 2001b), which is consistent with our own data (Fig. 20). Indeed, several studies have shown that interactions between the α5 helix and the N-terminal region of Gα are critical for preserving a low basal nucleotide exchange rate (Denker*, et al.*, 1995; Denker*, et al.*, 1992; Natochin*, et al.*, 2000). This mutagenesis data further supports the role of the conformational change described above, and suggests that binding to R* perturbs the stabilizing interactions with α5 helix, allowing it to relax into a conformation permissive for GDP release. One model of the molecular trigger suggests that there is a conserved binding site among Gα family members between the α5 helix and the adjacent β2/β3 loop for the conserved arginine in the D(E)RY motif of receptors, and that this interaction may underlie the mechanism for R*-mediated conformational changes in Gα (Oliveira*, et al.*, 1999).

Much work remains to be done, however, to refine our model of the nucleotide-free conformation of the G protein, identify the structural cause of the conformational change observed in the α5 helix and incorporate these data into improved models of the R*-G protein complex. Until such time as a high resolution crystal structure of the complex is solved, biophysical approaches, like the one described here, will be essential to study this crucial step in G protein activation.

CHAPTER IV

STRUCTURE AND DYNAMICS OF SWITCH II IN G PROTEIN ACTIVATION

Introduction

Heterotrimeric G proteins mediate signal transduction and amplification in a variety of cell signaling pathways (Chapter I). The affinity of Gα for Gβγ and effector proteins is controlled by the identity of the bound nucleotide. Crystal structures of $G\alpha_t$(GDP), $G\alpha_t$(GTPγS) and $G\alpha_{i1}$(GDP), $G\alpha_{i1}$(GTPγS) have been determined (Lambright, *et al.*, 1994; Noel, *et al.*, 1993; Mixon, *et al.*, 1995; Coleman, *et al.*, 1994a), and reveal that the nucleotide modulates the structure of three sequences, designated Switches I-III, two of these sequences (Switches I and II) are located at the interface of Gα with Gβ, effectors, and regulatory proteins, and both make direct contact with the bound nucleotide. In crystals of $G\alpha_t$, the α2 helix in Switch II is displaced approximately 8 Å to a position with increased packing in $G\alpha_t$(GTPγS) relative to $G\alpha_t$(GDP); in $G\alpha_{i1}$(GDP), Switch II is not resolved due to disorder, but within $G\alpha_{i1}$(GTP), an irregular helix is formed. Both results may be interpreted to reflect an increase in order of Switch II upon activation in these homologous proteins. The difference between the Switch II structure in $G\alpha_t$(GDP) and $G\alpha_{i1}$(GDP) may be due to crystal lattice contacts at Switch II in the former, which are absent in the latter. If this is the case, Switch II might be expected to be flexible on some time scale in the Gα(GDP) states in solution, a view supported by NMR studies of corresponding regions of the small G proteins Ras and Cdc42Hs (Loh, *et al.*, 1999; Feltham, *et al.*, 1997; Kraulis, *et al.*, 1994; Ito, *et al.*, 1997). Crystal lattice forces are sufficiently strong to distort flexible structures; indeed, crystal structures of Ras from different space groups have different structures within Switch II (Milburn, *et al.*, 1990). This raises the possibility that the structures of the Switch regions in the active Gα(GTP) states in

solution may differ from those in crystals as well, because they are located at lattice contacts in the crystals of $G\alpha_t$(GTPγS) and $G\alpha_{i1}$(GTPγS) (Noel*, et al.*, 1993; Coleman*, et al.*, 1994a).

The above considerations make it imperative to investigate the status of the Switch regions in solution. In the present work, SDSL is used to investigate the structure and dynamics of Switch II and the α4 helix of $G\alpha_{i1}$ through G protein activation. Seven sites were chosen for introduction of R1 in the Switch II sequence $G\alpha_{i1}$ (205, 206, 209, 211, 213, 214, 217), one within a putative effector binding domain in the α4 helix (300), and a control site in the helical domain (106) (Fig. 25) (Rarick*, et al.*, 1992). For each of these spin-labeled mutants, EPR spectra were recorded in five states: (1) Gα(GDP); (2) Gα(GDP)βγ; (3) the heterotrimer with dark ROS membranes; (4) the heterotrimer in complex with activated rhodopsin, and (5) Gα(GTPγS) formed by addition of GTPγS to the R*-bound complex. As described below, the EPR spectra report salient structural and dynamical features of Switch II in each state, providing a basis for comparison with crystal structure where available, and providing the first structural data on Switch II in the R*-G protein complex.

Results

Sites 205, 206, 209, 211, 213, 214, and 217 lie in Switch II, but not at conserved sites in the signature (DxGGQxxxRxxW) sequence, except W211; site 300 is in the α4 helix. All spin-labeled derivatives of $G\alpha_{i1}$ bind to R* and undergo R*-catalyzed nucleotide exchange (Fig. 26). To follow structural changes within Gα at these sites throughout the G protein cycle, a series of EPR spectra were collected after sequential sample additions to each R1 labeled $G\alpha_{i1}$ mutant. The results for each state of Gα are provided in the sections below.

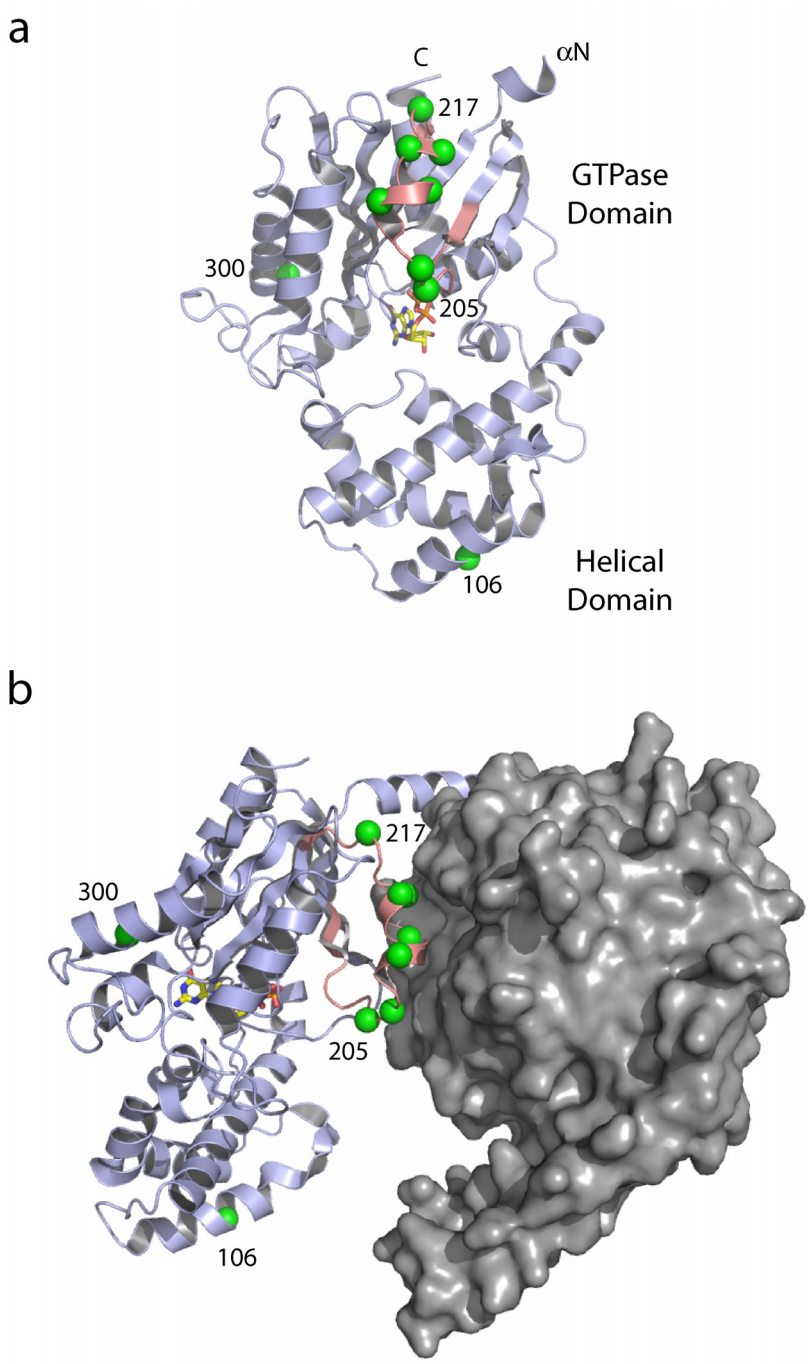

Figure 25 | Location of spin-labeled sites in Switch II (**a**) Ribbon model of $G\alpha_{i1}$(GDP) (from 1GP2), highlighting the sites chosen for SDSL studies in Switch II (205, 206, 209, 211, 213, 214, 217), the α4 helix (300), and the αB helix (106) (*green spheres*). (**b**) Several of these sites contribute to the Gβ-binding surface.

Gα(GDP)

The spectra of Gα(GDP) mutants 205R1, 206R1, 209R1, 211R1, 213R1, and 214R1 in Switch II and 300R1 in the α4 helix are very similar, each having partially resolved components reflecting populations of R1 with different mobility (Fig. 27). Similar spectra have been previously observed for R1 in a short helix in T4 lysozyme (Mchaourab*, et al.*, 1996). The spectra are reasonably well fit to a model with two components in slow exchange, one of which corresponds to an R1 population with weakly ordered and fast anisotropic motion ($S \approx 0.2$, τ_c = 2-3 ns) and the other with essentially isotropic slow motion ($\tau_c \approx 8.5$ ns) (Fig. 28). The weakly ordered population has little or no contact interaction in the structure, and thus serves to exclusively monitor internal side chain and backbone motions (Columbus & Hubbell, 2004; Columbus & Hubbell, 2002), while the more immobilized population arises from direct nitroxide interactions with nearby groups in the protein (Mchaourab*, et al.*, 1996; Hubbell*, et al.*, 2000). By contrast, the EPR spectrum for 106R1 is a typical single-component spectrum at a site in a rigid helix lacking contact interactions ($S = 0.45$, τ_c = 3 ns) (Fig. 28). The similar anisotropic motion, but low order, for the weakly ordered components of 205R1, 206R1, 209R1, 213R1, 214R1, and 300R1 is compatible with R1 on a helical structure in which the low order arises from either internal motions of R1 or a relatively flexible backbone.

Site 217R1, in the α2/β4 loop is also fit with a two component model, but the more mobile R1 population (dominant) is disordered with motion of shorter correlation time (τ_c = 1.5 ns) than that for the other sites in Switch II, consistent with a highly flexible loop structure (Mchaourab*, et al.*, 1996). The more immobilized component is similar to the other sites.

Heterotrimer formation

The Switch II sequence makes direct contact with the Gα subunit upon heterotrimer formation (Fig. 25). Spin labels in Switch II facing the Gβ interface would thus be expected to become immobilized upon heterotrimer formation. This is indeed the case, as shown by the greatly increased intensity of a

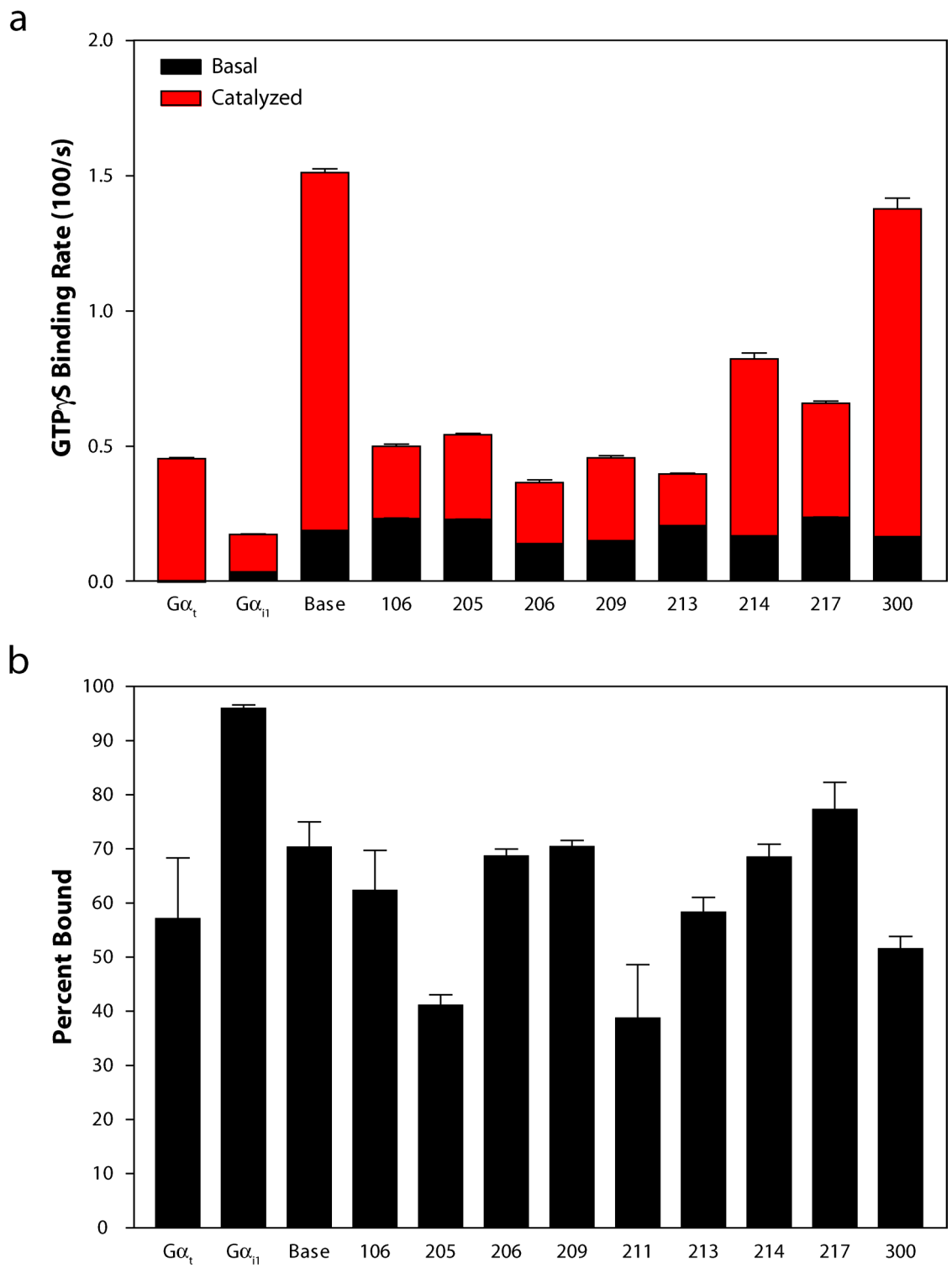

Figure 26 | Biochemical characterization of spin-labeled mutants in Switch II (**a**) Nucleotide exchange assay. Data represent the mean ± s.e.m. of 4-6 independent experiments. Site 211R1 is the source of the intrinsic fluorescence changes, so it cannot be measured with this assay. (**b**) Rhodopsin binding assay. Data represent the mean ± s.e.m. of 3 independent experiments.

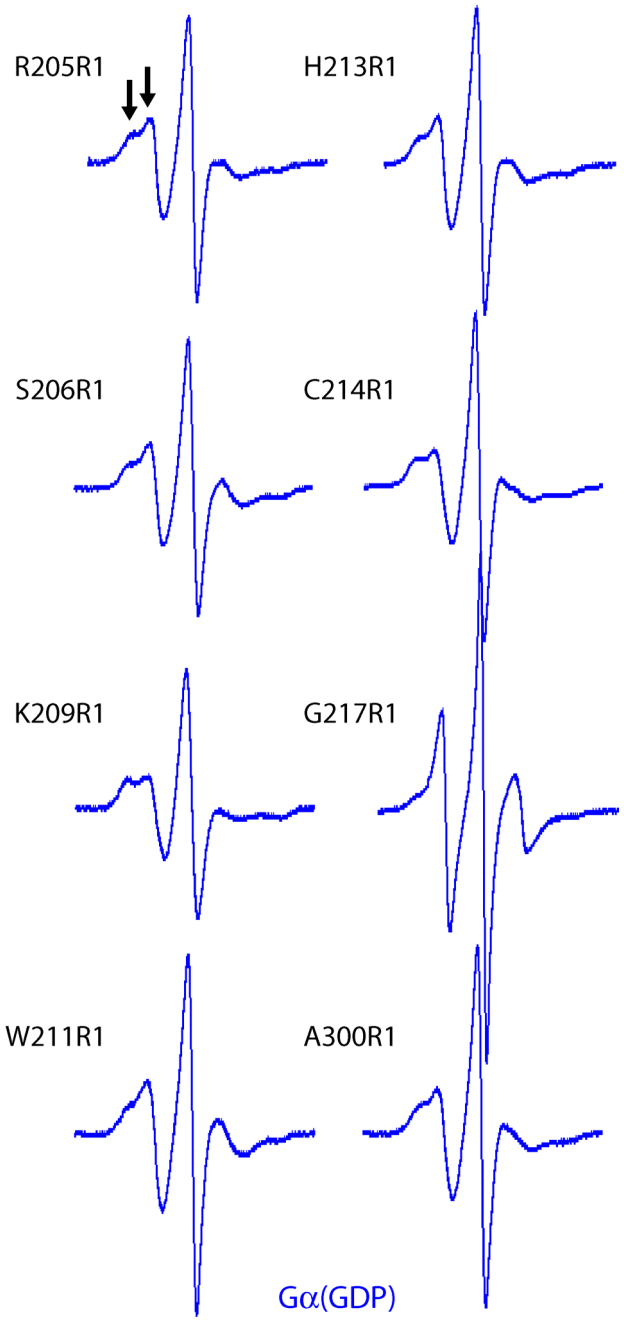

Figure 27 | EPR spectra of GDP-bound Switch II mutants These spectra were recorded from purified, labeled Gα(GDP) alone in solution. *Arrows* highlight the two components that comprise these spectra.

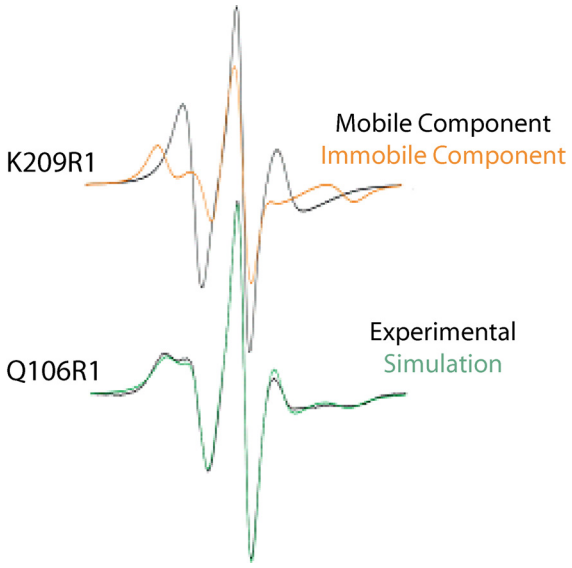

Figure 28 | Switch II mutants report two spectral components in Gα(GDP) Two components were required to simulate the experimental EPR lineshape of K209R1 (*black* and *orange traces*). The individual component lineshapes were compared to an additional helix surface site spectrum within $G\alpha_{i1}$ (Q106R1). A simulation of this spectrum reports the backbone dynamics at this site, as it makes no tertiary contact interactions (*green trace*).

spectral component corresponding to a strongly immobilized state of R1 upon addition of Gβγ at sites 206R1, 209R1, 211R1, 214R1, and 217R1 (Fig. 29). No changes are observed for 205R1 and 213R1. In the G_{i1} crystal structure, R205 is in a flexible loop and does not interact with Gβ, unlike the other residues that contribute directly to the interface. However, 213R1 is located at the Gβ interface, suggesting that a change upon binding should be observed. Although labeling at this site may perturb heterotrimer formation, this mutant does form stable R*-G protein complexes and undergoes R*-catalyzed nucleotide exchange. Modeling of the R1 side chain at this position suggests that the nitroxide can adopt a side chain conformation that points into the space between Gα and Gβ, which may account for the absence of spectral changes.

The presence of a more mobile component in the spectra of 206R1 and 217R1 (Fig. 29), located in loops preceding and following the α2 helix, respectively, is also compatible with the crystal structure of the heterotrimer. At these sites, some rotamers of the R1 side chain can project away from the interface, removing constraints on the motion. Interestingly, the spectrum of 300R1, distant from the binding interface, shows significant immobilization, indicating allosteric changes in Gα upon heterotrimer formation.

Although heterotrimer formation increases the rotational correlation time of $G\alpha_{i1}$ by approximately two-fold, this does not account for the changes in the EPR spectra. Increasing the viscosity of the sample by a factor of two with ficoll similarly increases the rotational correlation time of $G\alpha_{i1}$, but has little effect on the EPR spectrum of 214R1 (data not shown). This demonstrates that the immobilized component, the most sensitive to overall rotational diffusion and similar in all cases, is insensitive to increases in rotational correlation time.

To evaluate the level of perturbation caused by introduction of R1 at the subunit interface, Gβγ was titrated into solutions containing a fixed concentration of the individual spin-labeled $G\alpha_{i1}$ subunits. In these experiments, changes in normalized EPR spectral intensity at a particular magnetic field strength serve as an indicator of heterotrimer formation. The fractional change in the intensity of the low-field

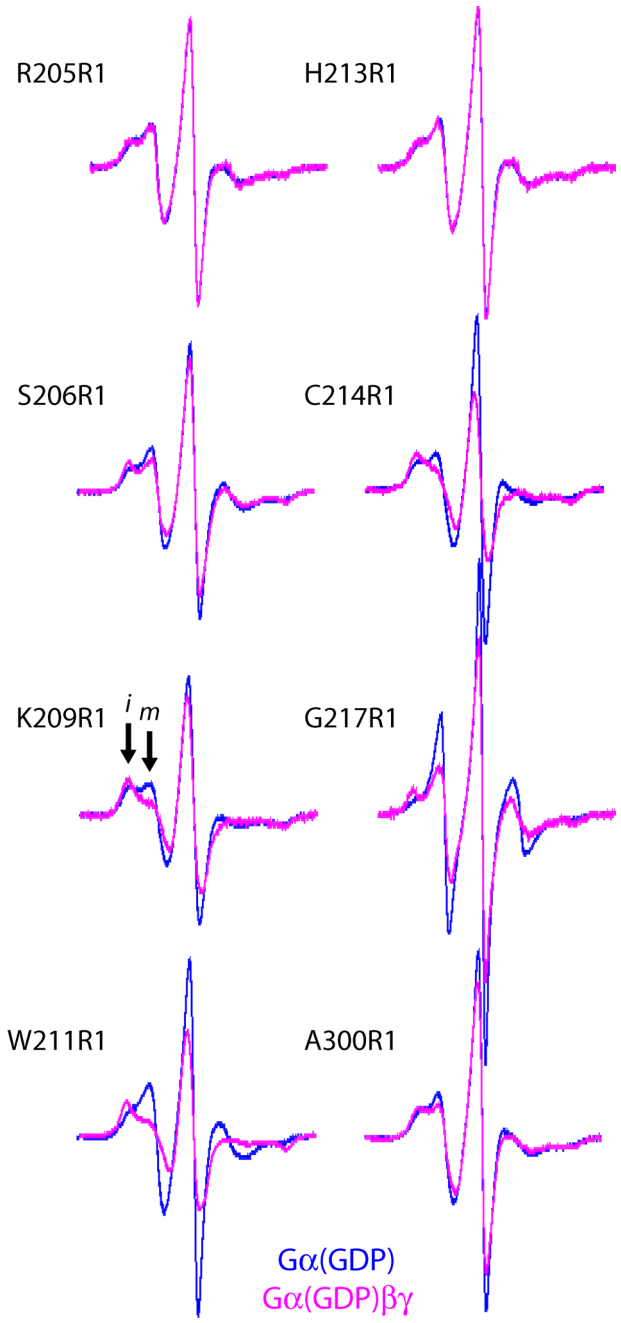

Figure 29 | Structural changes in Switch II upon heterotrimer formation Overlay of the EPR spectra recorded before (*blue traces*) and after (*pink traces*) the addition of an equimolar concentration of Gβγ. *Arrows* indicate the mobile (*m*) and immobile (*i*) components of the EPR spectra.

nitroxide line plotted against the concentration of Gβγ provides a measure of the affinity of heterotrimer formation (Fig. 30). As is evident, the presence of R1 at the interaction interface apparently has remarkably little effect on the binding for the mutants examined.

Receptor activation-dependent conformational changes

Binding of the heterotrimer to R* in the absence of GTP results in the release of GDP from Gα resulting in a nucleotide-free R*-G protein complex (Rodbell, *et al.*, 1971b; Emeis, *et al.*, 1982; Bornancin, *et al.*, 1989). Under the conditions of the experiments, each spin-labeled heterotrimer shows wild-type levels of binding to R* (40-75% bound; Fig. 26). The EPR spectra for the heterotrimer show little change upon addition of ROS membranes in the dark. Upon photoactivation, there is a large decrease in the mobility of 217R1, which is likely due to its location near the R*-binding surface of Gα (Fig. 31). No other sites in Switch II exhibit receptor activation-dependent conformational changes. Interestingly, the spectrum of 300R1, distant from both the Gα-Gβ interface and the receptor contact surface, shows a slight decrease in mobility upon binding to R*.

Activated Gα(GTPγS)

Addition of GTPγS to the R*-G protein complex results in dissociation of activated Gα(GTPγS) from Gβγ and the receptor (Bornancin, *et al.*, 1989), with concomitant changes in the corresponding EPR spectra (Fig. 32). For all except 217R1, the EPR spectra of activated Gα are dramatically different from those of Gα(GDP), and signal changes in the structure and dynamics of Switch II and the α4 helix that are directly coupled to the change in nucleotide. The qualitative change is most readily recognized in the unusual lineshapes of 214R1 and 300R1. Fitting these spectra reveals a single dynamic mode with high ordering about the nitroxide x-axis ($S \approx 0.6$), as compared to the z-axis ordering typical of R1 at most helical sites, including the mobile components in Gα(GDP) discussed above. In addition to the change in ordering, correlation times in Gα(GTPγS) have decreased to $\tau_c \approx 0.6$ ns compared to $\tau_c \approx 2$ ns in

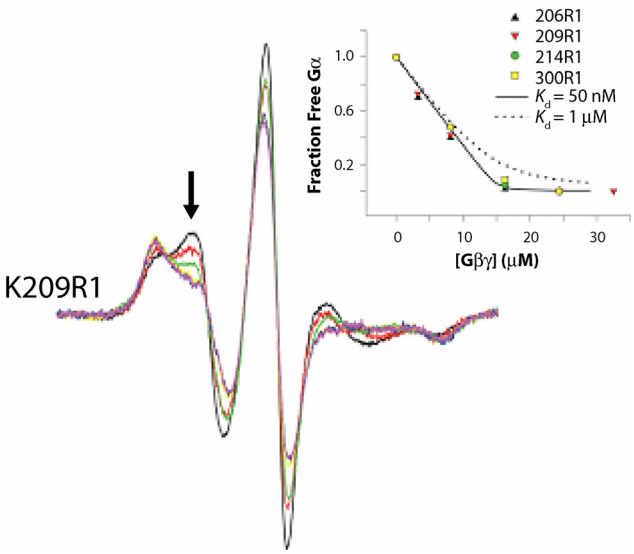

Figure 30 | Spin-labeled sites within Gα are sensors of heterotrimer formation Overlaid spectra show an EPR titration experiment following heterotrimer formation with K209R1. Gβγ was added to the spin-labeled mutants (206, 209, 214, 300) and spectral lineshape changes were recorded upon titration. The fractional change in intensity of the low-field nitroxide line was plotted *versus* Gβγ concentration (*inset*). The data are consistent with a 50 nM dissociation constant (*solid line*) reported for the cysteine-depleted $G\alpha_{i1}$ mutant (Medkova*, et al.*, 2002). A K_d of 1 μM is shown (*dotted line*), illustrating the sensitivity of this assay.

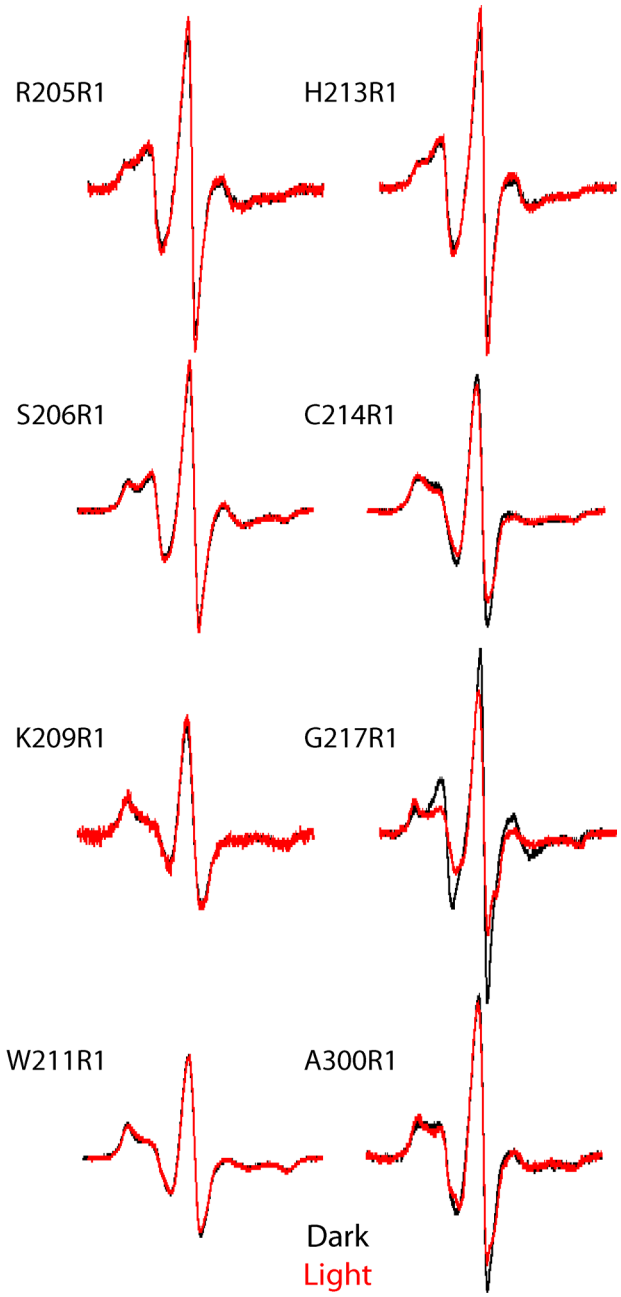

Figure 31 | Probing the structure of Switch II in the R*-G protein complex Overlay of the EPR spectra recorded before (*black traces*) and after (*red traces*) receptor activation and the formation of the R*-G protein complex.

Gα(GDP). Although distinction of x- and y- axis anisotropy is ambiguous from fitting of spectra from a single frequency, global fits of 214R1 and 300R1 to S-band (3 GHz), X-band (9.5 GHz) and Q band (35 GHz) spectra confirm x-axis anisotropy (Fig. 33). Spectra of nearby sites 206R1, 209R1, and 213R1 are also reasonably well fit to a single component with x-axis anisotropy, but with reduced ordering ($S \approx 0.2$) and decreased rates ($\tau_c \approx 1.5$). By contrast, the EPR spectra for 205R1 and 211R1 correspond to a decrease in the mobility of these side chains in the activated conformation. Collectively, these data reveal a single highly dynamic, but ordered state of Switch II in the activated subunit.

Discussion

The objective of the present study was to explore salient structural features of Switch II of $G\alpha_{i1}$ along the activation pathway to complement static crystallographic data, add a dimension of dynamic information, and to obtain the first direct structural data for this region in the R*-G protein complex. The sections below provide an interpretation of the SDSL data in relation to the crystal structures and current models of the empty complex.

Solution structure and dynamics in Gα(GDP)

In the crystal structure of $G\alpha_{i1}$(GDP), the entire Switch II sequence from 204-217 is unresolved, presumably due to static disorder (Coleman & Sprang, 1998); in the heterotrimer, residues 206-215 form an irregular helix, with 217 in a connecting loop (Fig. 25) (Wall*, et al.*, 1995). In $G\alpha_t$(GDP), residues corresponding to 206-214 in $G\alpha_{i1}$ are irregularly helical, but the structure may be stabilized by contacts with symmetry related molecules in the lattice (Lambright*, et al.*, 1994). In all structures, residues 296-309 form a regular helix, α4.

In solution, the EPR spectra of R1 at 205, 206, 209, 211, 213, and 214 are similar to each other and similar to spectra of R1 along the solvent exposed surface of helix B in T4 lysozyme. Thus, the data

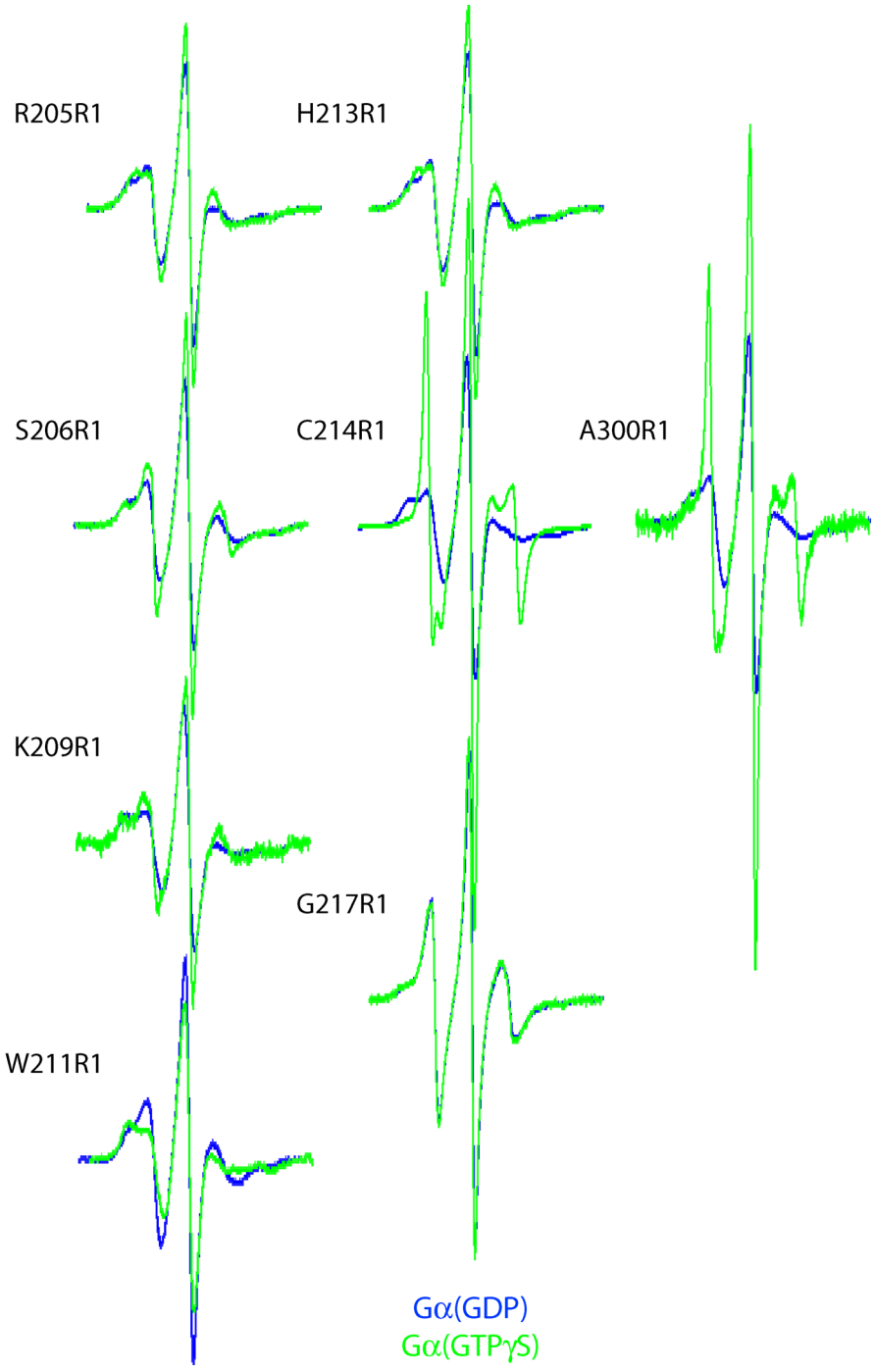

Figure 32 | Sites in Switch II sense the identity of the bound nucleotide Overlay of the GDP-bound (*blue traces*) and GTPγS-bound (*green traces*) Gα spectra.

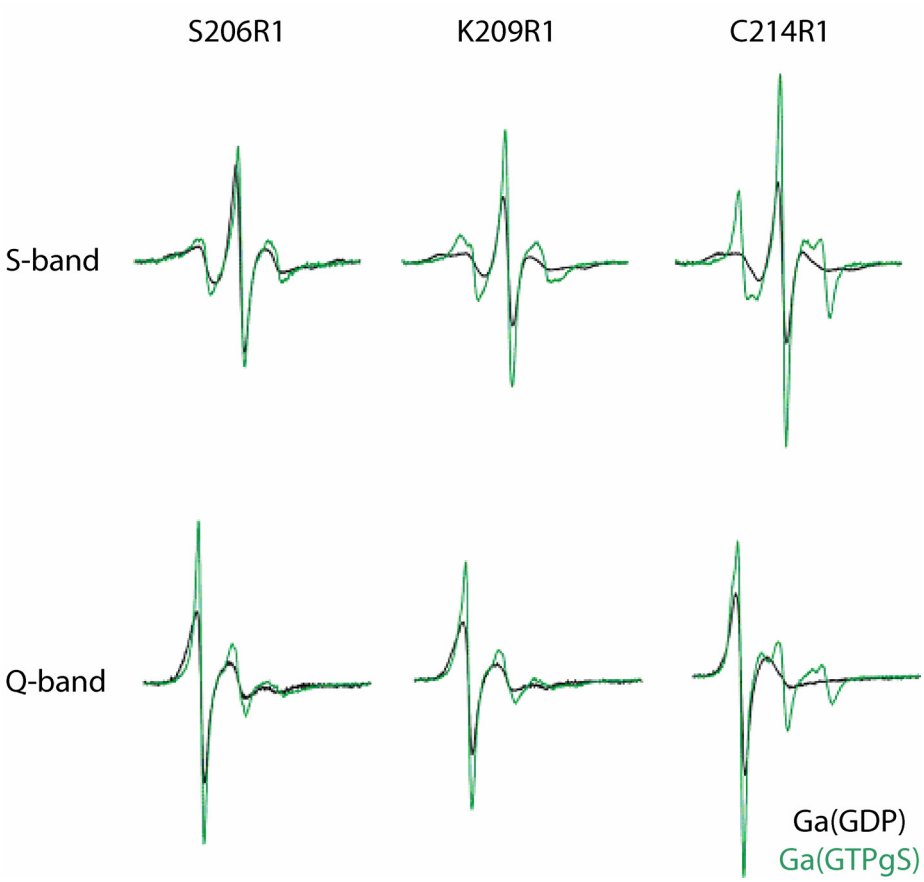

Figure 33 | S- and Q-band spectra of Switch II mutants Upon nucleotide exchange, a clear increase in side chain dynamics is observed at each site. Q-band EPR spectra were collected using a Bruker, ER5106QTW, resonator, while S-band measurements were recorded with a SB-1111 microwave bridge (Jagmar, Poland) equipped with a loop gap resonator. Incident microwave power was set to 10 mW (Q-band) and 2 mW (S-band). Field modulation amplitudes were adjusted to give maximal signal with no lineshape distortion.

are consistent with a helical-like structure for 206-214, which may even extend to 205 based on the EPR spectra for this residue. The two components in such spectra arise either from two rotamers of R1 or two conformations of the helix in solution in slow exchange on the EPR time scale (μs – ms). Given the facts that Switch II is helical in some structures, statically disordered in the structure of $G\alpha_{i1}$(GDP), and that slow conformational exchange (ms) is observed in Switch II in solution structures of small G proteins by NMR, the most attractive interpretation of the EPR data is that a helix in Switch II in $G\alpha_{i1}$(GDP) is also in slow conformational exchange between at least two states in solution.

The crystal structure of G_{i1} provides a basis for speculation on the nature of the putative states. In that structure, 206, 209, 211, 213, and 214 in the α2 helix all face the Gβγ interface, and would lay on the solvent-exposed surface of the helix in the isolated $G\alpha_{i1}$(GDP) subunit if the structures were similar. At such sites, R1 is has relatively high mobility with a characteristic anisotropic motion modulated by backbone motions (Columbus & Hubbell, 2004). Indeed, one component of each spectrum has such a lineshape (Fig. 28) reflecting a comparatively large amplitude backbone fluctuation on the nanosecond time scale. The other component corresponds to an immobilized state that could arise from a partially unfolded structure or a rotated state of the helix where R1 can make contacts with other parts of the protein. In this model, the α2 helix would fluctuate between these states.

Although the spectrum of 300R1 resembles those in Switch II, a similar conclusion cannot be extended to the α4 helix based on data from a single site. Site 217 is located in the α2/β4 loop and the dominance of a highly mobile component of the spectrum is consistent with a flexible backbone. Collectively, these considerations suggest that Switch II exists as a helix, flexible on the nanosecond time scale in exchange on a much slower time scale with another conformation.

Sites in Switch II and the α4 helix sense heterotrimer formation

Spin-labeled mutants in Switch II of Gα(GDP) form heterotrimers with Gβγ with a K_d similar to that for the wild-type subunits (Medkova*, et al.*, 2002), despite the presence of R1 directly at the Gα-Gβ

interface (Fig. 25). This remarkable result is in line with earlier observations that R1 at contact surfaces has little effect on arrestin-rhodopsin interactions (Hanson*, et al.*, 2006) or SecA-SecB interactions (Crane*, et al.*, 2005). This result will not likely be general, but as long as highly specific polar interactions are not perturbed, the non-polar and flexible nature of the R1 side chain will allow labeling with minimum perturbation of the protein-protein interface.

The strong immobilization of 209R1, 211R1, and 214R1 upon heterotrimer formation is expected due to intimate contact of these side chains with the Gβ subunit (Fig. 25). By contrast, the side chains of 205R1, 206R1, and 217R1, can adopt conformations that allow the nitroxide to project into cavities in the structure. Accordingly, the EPR spectra of these sites have a relatively increased proportion of a more mobile component. As this mobile component is also observed for residue 213R1, the nitroxide side chain at this position must also be oriented away from the subunit interface despite its proximity to 211R1 and 214R1, both of which show substantial changes. This possibility is consistent with models of the R1 side chain at site 213. Thus, the EPR spectra of sites in Switch II in the heterotrimer in solution reflect the crystal structure.

By contrast, a comparison of the crystal structures of $G\alpha_{i1}$(GDP) and the G_{i1} heterotrimer reveals little difference in the structure of the α4 helix. Thus, the allosteric change at 300R1, detected as decreased mobility of the nitroxide, is an unexpected result of heterotrimer formation, and suggests that long range structural changes are propagated though Gα upon heterotrimer formation. The spectral change could be accounted for by a slight reorientation of the α4 helix, a motion that could be masked by crystal lattice forces.

Absence of R-mediated structural changes in Switch II*

Complex formation between the G protein heterotrimer and the activated receptor results in dissociation of GDP to form a nucleotide-free complex. The structural changes in the complex that liberate the nucleotide are unknown, but current models for the complex require changes propagated

through the heterotrimer, triggered by receptor binding, because the nucleotide binding site is some 30 Å from the receptor binding interface. Detailed mechanisms for the allosteric switch have been proposed. In the lever-arm model, both the N- and C-termini of Gα interact with the receptor in such a way as to rotate Gβγ away from Gα, pulling Switches I and II with it, thereby opening a door for GDP to escape (Iiri*, et al.*, 1998; Rondard*, et al.*, 2001). Thus, overall packing at the Gα-Gβ interface is decreased. Conversely, the gearshift model proposes that a motion occurs in the opposite direction, rotating Gβγ into Gα, increasing packing at the interface (Cherfils & Chabre, 2003). The R1 side chains in Switch II, located at this interface, are positioned to sense such changes.

However, 217R1 is the only site in this region that reports significant R*-dependent conformational changes (Fig. 31). The EPR spectral changes indicate that the mobility of this side chain decreases upon binding R*, which is likely due to direct contact interactions with the receptor. Residue 217 is adjacent to the extreme C-terminus of Gα, a well established R* contact site. Additionally, the α2/β4 loop has been identified as a specificity determinant in the R*-G protein interaction (Lee*, et al.*, 1995b). Although the absence of R*-mediated changes in Switch II does not disprove the lever-arm or gear-shift models, it does strongly suggest that significant structural rearrangements are not occurring at the Switch II-Gβ interface.

Switch II structure and dynamics in Gα(GDP), Gαβγ, and Gα(GTPγS)

The EPR spectra of R1 clearly reveal that the Switch II sequence in $G\alpha_{i1}$(GDP) is uniquely different in both structure and dynamics from that in $G\alpha_{i1}$(GTPγS). To the extent that they can be compared, the solution SDSL and crystal structure data for Switch II in the two states provide compatible views, but SDSL adds a dimension of dynamic information. In particular, the absence of electron density for Switch II in the crystal structure of $G\alpha_{i1}$(GDP) indicates static disorder, but SDSL data are compatible with a helical state ordered on the EPR time scale (> 100 ns), but in conformational exchange on a longer time scale (> μs). In the heterotrimer, no specific structural information is available from SDSL, but here

the crystal structure is definitive, and the strong immobilization of R1 in Switch II confirms a rigid state. In the activated $G\alpha_{i1}$(GTPγS), the crystal structure reveals an irregular helix located at a crystal contact site with average thermal factors for the structure in which 205, 206, 209, 213, and 217 are solvent-exposed, 214 is partially buried, and 211R1 is fully buried. In solution, SDSL data is consistent in detail with this structure, but shows Switch II to be in a highly flexible state on the nanosecond time scale. Thus, R1 for 206, 209, and 217 exhibits rapid and weakly-ordered anisotropic motion characteristic of the side chain at solvent exposed sites in flexible helices (Mchaourab*, et al.*, 1996). The striking x-axis anisotropic motion of 214R1 can be accounted for by its partially buried location. Modeling 214R1 in the $G\alpha_{i1}$(GTP) crystal structure reveals that the entire side chain up to the nitroxide is highly constrained by the steric interactions, allowing free rotation only about the terminal bond. This motion is approximately along the molecular x-axis of the nitroxide, and rotational diffusion about this bond has been previously shown to be rapid (Liang*, et al.*, 2004). The constraints imposed by the structure, together with rapid motions of the backbone indicated by the other sites, account for the unusual lineshape, as revealed by the spectral simulations.

Summary

This study illustrates the capability of SDSL to map structural and dynamical changes stepwise along the entire activation pathway of a Gα subunit, and provides the first direct structural and dynamical data on changes in Switch II along that pathway. From the standpoint of SDSL technology, it is interesting that the presence of the R1 side chain at a direct subunit contact interface has little effect on the interaction. Thus, SDSL will find use in mapping protein-protein interaction sites and their modulation related to function. Regarding this point, a most interesting result reported here is the identification of allosteric changes propagated from the Gα-Gβ interface to the α4 helix. For Gα, catalysis of nucleotide exchange from GDP to GTP by the receptor releases Gα(GTP) into solution and transforms Switch II from the rigid, partially helical structure observed in crystals to a unique structure

entirely consistent with the crystal conformation (spatially ordered), but with a highly flexible backbone. This feature is not apparent from the crystal structure. This is in striking contrast to the conformational exchange in Switch II inferred from the dynamics of R1 in the isolated $G\alpha_{i1}$(GDP) subunit (spatially disordered). The flexible backbone in Switch II of the activated subunit is consistent with the emerging view that flexible sequences are involved in protein-protein interaction.

CHAPTER V

DYNAMICS OF SWITCH I IN G PROTEIN ACTIVATION

Introduction

In addition to Switch II, which forms an important effector-binding site on Gα (Chen, *et al.*, 2005b; Tesmer, *et al.*, 1997b; Tesmer, *et al.*, 2005; Slep, *et al.*, 2001), Switch I plays a more critical role in binding RGS proteins (Slep, *et al.*, 2001; Tesmer, *et al.*, 1997a). Switch I is composed of a loop connecting the αF helix to the β2 strand (Fig. 34). In crystals of $G\alpha_t$, GTP binding draws Switch I toward to the nucleotide as it forms stabilizing interactions with Mg^{2+} and the γ-phosphate (Lambright, *et al.*, 1994); a similar structural transition is observed in $G\alpha_{i1}$ (Mixon, *et al.*, 1995). These results suggest that G protein activation orders Switch I through interactions with GTP. Compared to $G\alpha_t$(GDP), Switch I in $G\alpha_{i1}$(GDP) is in a more compact conformation, closer to the nucleotide-binding pocket, which is likely due to quaternary contacts with the N-terminal microdomain of an adjacent molecule in the crystal (Mixon, *et al.*, 1995). Switch I is also located at sites of crystal contact in the GTPγS-bound structures of these proteins (Noel, *et al.*, 1993; Coleman, *et al.*, 1994a), suggesting the possibility that the conformation and dynamics of this region is different than would be predicted based on the crystal structures.

Due to the crucial role this flexible region plays in the structural switch leading to G protein activation, it is important to investigate the native structure and dynamics of Switch I in solution. Toward this end, conformational changes in the region were directly monitored with SDSL through each transition leading to G protein activation. For each spin-labeled mutant, EPR spectra were recorded for each of five conformations: Gα(GDP), Gα(GDP)βγ, the heterotrimer in the presence of dark ROS membranes, R*·Gα(O)βγ, and Gα(GTPγS). These spectra are characteristic of the local secondary and tertiary structure of the spin-labeled region (Mchaourab, *et al.*, 1996; Langen, *et al.*, 2000).

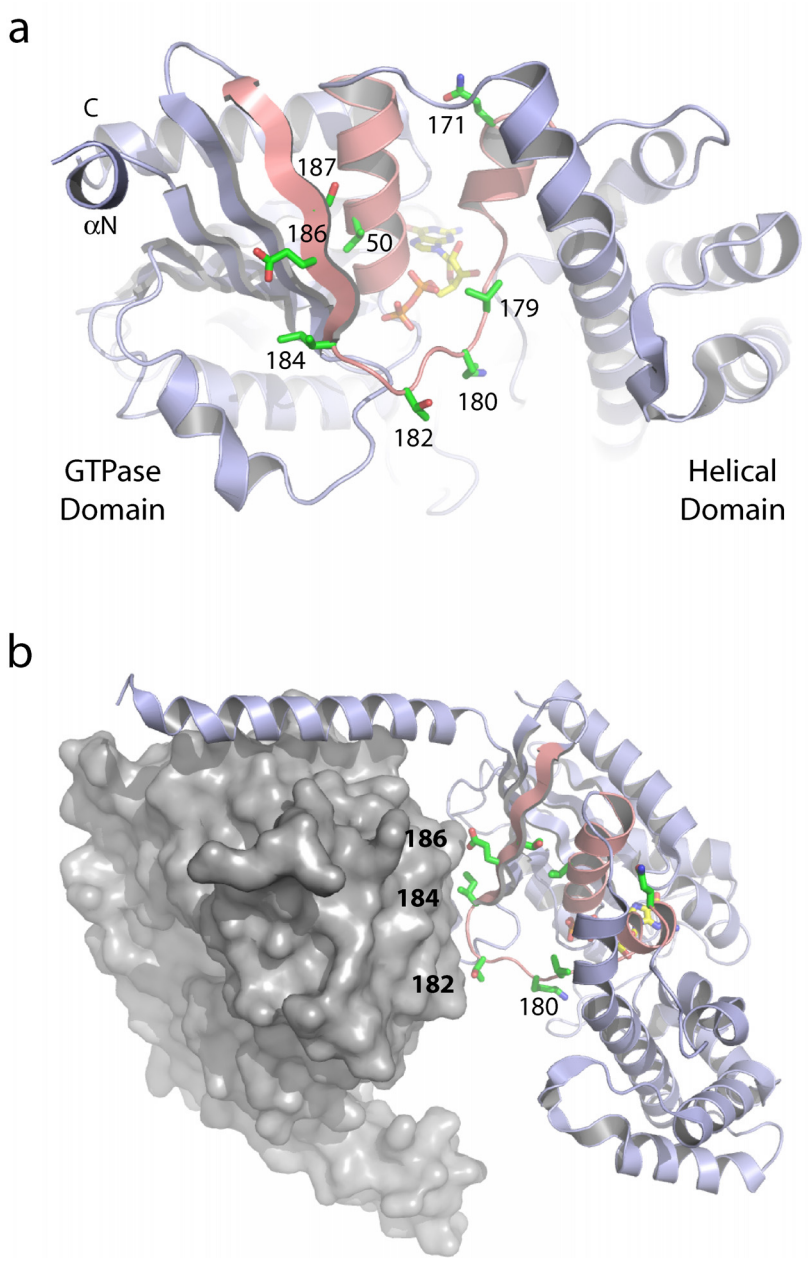

Figure 34 | Location of spin-labeled sites in the Switch I region (**a**) Ribbon model of $G\alpha_{i1}$(GDP) (from 1GP2), highlighting the sites chosen for SDSL studies in the αF helix (171), Switch I (179, 180, 182, 184, 186, 187), and the α1 helix (50) (*green side chains*). (**b**) Several of these sites contribute to the Gβ-binding surface.

In this work, the EPR spectra presented describe the native structure and dynamics of the Switch I region at each point in G protein activation, enable comparison with the crystal structures when available, and provide the first structural insight into the conformation of Switch I in the R*-bound, nucleotide-free conformation of Gα.

Results

Characterization of spin-labeled mutants

Several sites were chosen for the introduction of the nitroxide side chain, R1, into the Switch I sequence (179, 180, 182, 184, 186, 187), one site in a contiguous sequence of the helical domain on the αF helix (171), and one site on the adjacent α1 helix (50) (Fig. 34). Each of these sites is on the surface of Gα, although 50 and 187 are slightly more buried. Importantly, none of the side chains mutated in the Switch I loop contribute directly to nucleotide binding. All of the spin-labeled mutants demonstrate R*-catalyzed increases in GTPγS binding, except for 184R1, and all had the ability to form stable R*-G protein complexes in the absence of nucleotide (Fig. 35). Three of the spin-labeled mutants (171, 182, 184) demonstrated substantially faster rates of basal nucleotide exchange compared to the cysteine-depleted $G\alpha_{i1}$ base mutant, while the basal exchange rate for 187R1 was slightly slower. Site 184R1 was the only mutant that did not have a further increase in the GTPγS binding rate in the presence of R*. However, this mutant is clearly able to bind to Gβγ and R* in a GTPγS-dependent manner, as shown both by the rhodopsin binding assay and EPR measurements. Following biochemical characterization, a series of EPR spectra were recorded for these mutants at each step in the G protein cycle from Gα(GDP) to Gα(GTPγS).

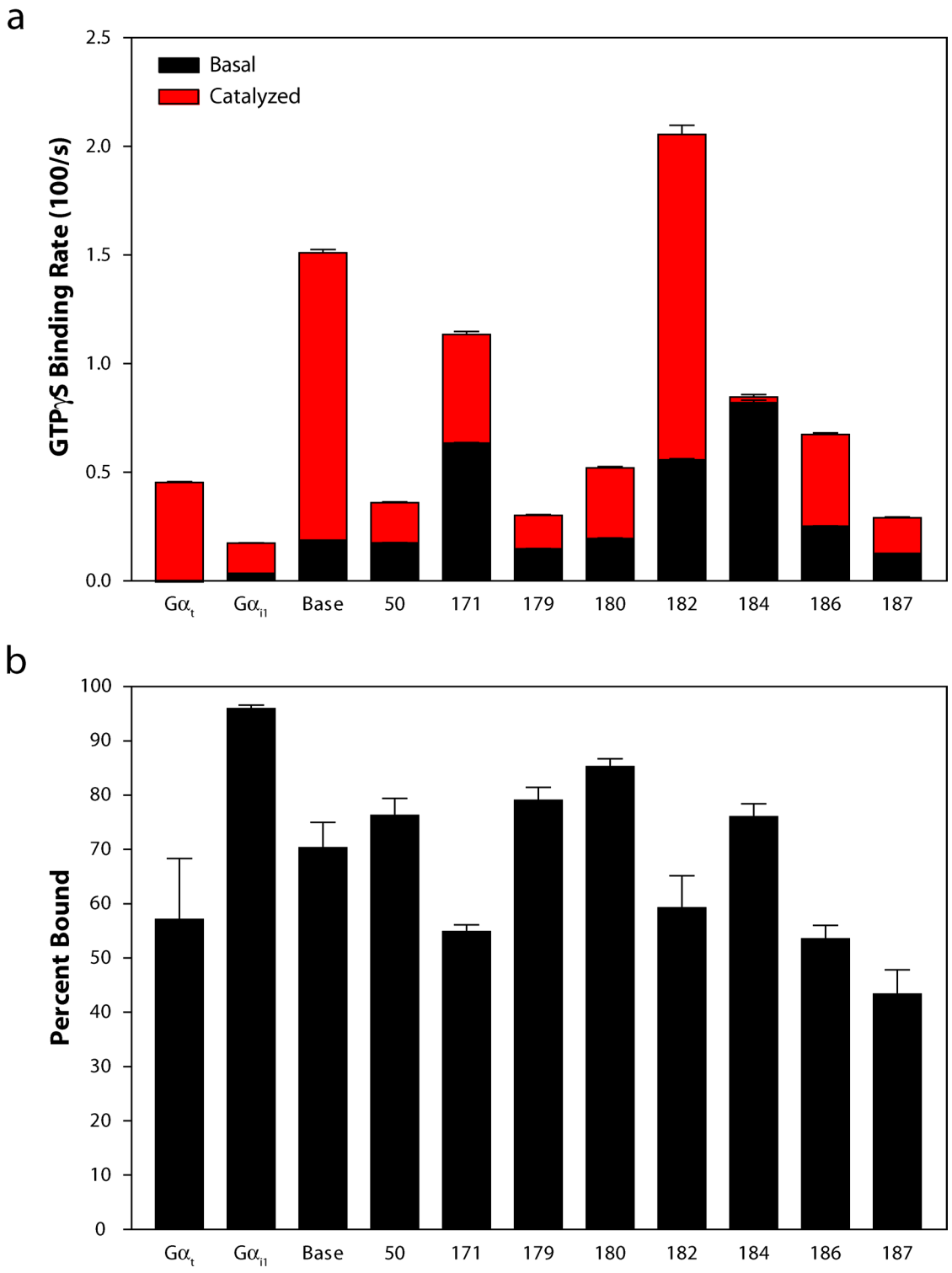

Figure 35 | Biochemical characterization of spin-labeled mutants near Switch I (**a**) Nucleotide exchange assay. Data represent the mean ± s.e.m. of 5-6 independent experiments. (**b**) Rhodopsin binding assay. Data represent the mean ± s.e.m. of 3 independent experiments.

Gα(GDP)

The EPR spectra for Gα(GDP) mutants 179R1, 180R1, 182R1, 184R1, and 186R1 in Switch I are very similar, each reflecting a high degree of side chain mobility where the nitroxide has little or no contact interaction in the structure (Fig. 36, *blue traces*) (Columbus & Hubbell, 2002; Columbus & Hubbell, 2004). As expected, the dynamics of this region increase near the center of the Switch I loop. This is consistent with the location of these side chains in the $G\alpha_{i1}$(GDP) crystal structure (Mixon*, et al.*, 1995; Coleman & Sprang, 1998). Additionally, the spectra for 179R1, 180R1 and 182R1 indicate a small, less mobile population where the nitroxide makes direct contact with nearby groups in the protein.

The remaining sites, 50R1, 171R1, and 187R1, exhibit complex, multi-component spectra suggesting that the nitroxide makes tertiary contacts with adjacent chemical groups in the protein (Fig. 36, *blue traces*) (Langen*, et al.*, 2000; Mchaourab*, et al.*, 1996). While the mobile component of the spectrum for 171R1 is predominant, the spectra for sites 50R1 and 187R1 reflect much lower nitroxide mobility. Again, this is consistent with the location of these sites in the structure, where 187R1 is on the internal face of the β2 strand, which overlays the α1 helix where residue 50 is located, while 171R1 is the most surface-exposed of these three residues, but still forms interactions across the interdomain cleft.

Heterotrimer formation

Switch I contributes to the Gβ-binding surface on Gα, and several interesting changes are observed in the EPR spectra for these residues upon heterotrimer formation. Sites 182R1, 184R1, and 186R1 are located in the Gα-Gβ interface, and each reports a decrease in side chain mobility with Gβγ binding (Fig. 36, *pink traces*). This is most clearly observed at residue 184R1, which reports a new spectral component corresponding to a strongly immobilized R1 conformation. The spectral changes at 182R1 and 186R1 are more subtle, where the spectra are still dominated by the mobile component. These two sites are at the edges of the Gβ interface with Switch I, and some rotamers of the R1 side chain can escape the steric constraints associated with complex formation.

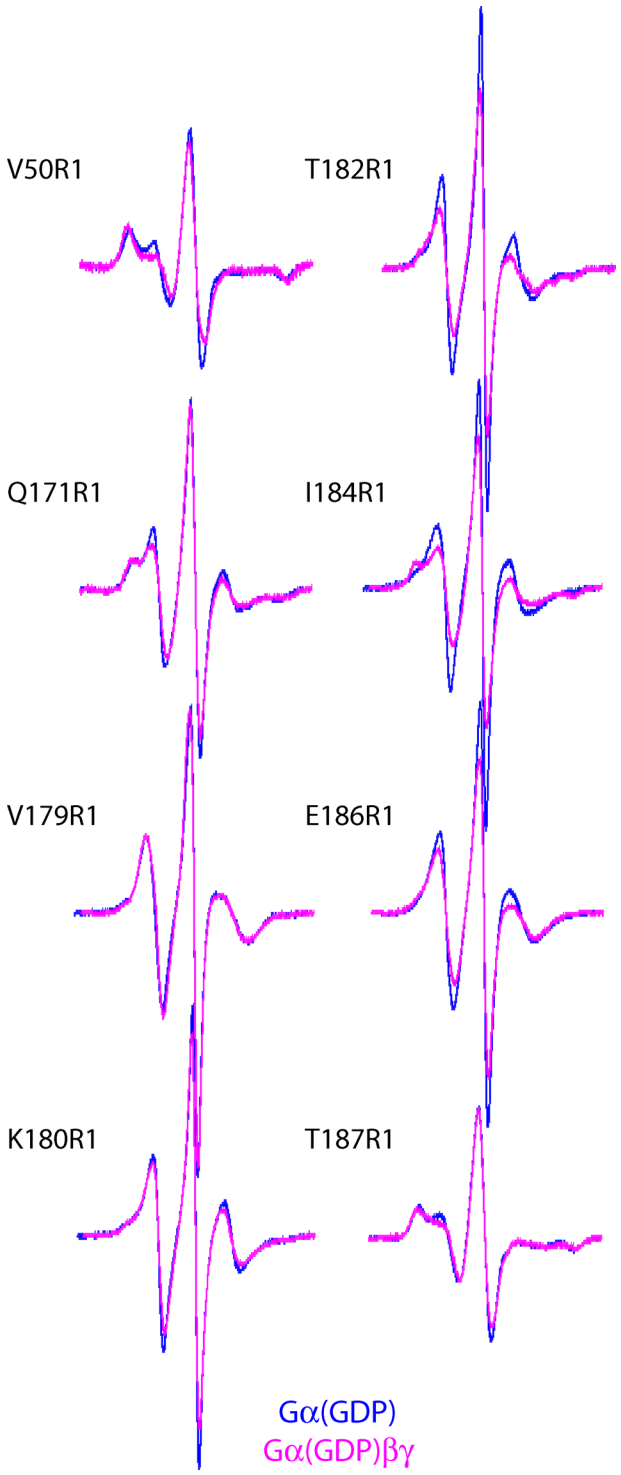

Figure 36 | Structural changes in Switch I upon heterotrimer formation Overlay of the EPR spectra recorded before (*blue traces*) and after (*pink traces*) the addition of an equimolar concentration of Gβγ.

Residues 179R1 and 180R1 are further from the Gβ-binding site, and while 180R1 reports a slight decrease in mobility, no changes are observed for 179R1 (Fig. 36, *pink traces*). By contrast, each of the three remaining sites, 50R1, 171R1, and 187R1 all demonstrate a striking increase in the intensity of the immobile component following Gβγ binding (Fig. 36, *pink traces*). Inspection of the G_{i1} heterotrimer crystal structure suggests that binding to Gβγ moves the β2 strand with residue 187R1 approximately 1 Å closer to the α1 helix and residue 50R1, which may account for the decrease in the mobility observed at these sites. However, there are no obvious differences in the crystal structures around residue 171R1.

Receptor activation-dependent conformational changes

Upon the addition of ROS membranes in the dark, spectral changes are observed for residues 50R1, 180R1, 182R1, and 184R1, which may be due to heterotrimer association with the membrane or some interaction with inactive rhodopsin (Fig. 37, *black traces*). While there is a small increase in the mobility of 50R1 and small decreases in that of 180R1 and 182R1, there is a significant increase in the mobility of 184R1. Although the dark spectra for 50R1, 180R1, and 182R1 represent an intermediate shift in the dynamics between the free heterotrimeric conformation and the R*-bound, nucleotide-free conformation, the difference in the mobility of 184R1 is the opposite of that observed upon receptor activation, suggesting that these changes are not simply due to a small amount of activated rhodopsin in the membrane preparations. No changes following the addition of dark ROS membranes were observed at the other sites.

Photoactivation of rhodopsin results in G protein binding and GDP release. This nucleotide-free conformation of the G protein is stable in the absence of nucleotides, and each of the mutants shows wild-type levels of binding under the conditions of these experiments (Fig. 35b). A very interesting pattern of spectral changes emerges upon formation of the R*-G protein complex (Fig. 37, *red traces*). Beginning from the β2 strand of Switch I, a slight decrease in the mobility of 187R1 is observed, while 184R1 and

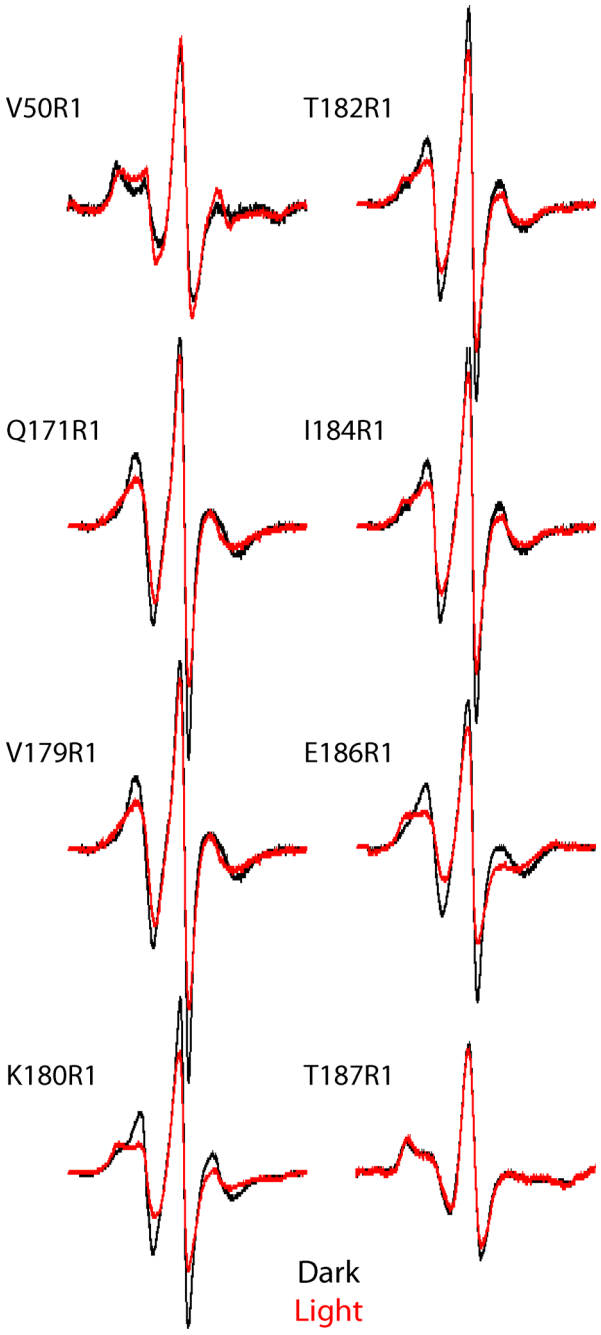

Figure 37 | Receptor activation-dependent conformational changes in Switch I Overlay of the EPR spectra recorded before (*black traces*) and after (*red traces*) receptor activation and the formation of the R*-G protein complex.

186R1 at the Gβ interface become immobilized. There are no differences in the EPR spectra for 182R1. These data suggest some structural rearrangement of the Gα-Gβ interface upon binding to R*.

At the empty nucleotide-binding pocket, there is a decrease in the mobility of 179R1, and a substantial decrease in the mobility of 180R1, which is immobilized by new tertiary contact interactions in the nucleotide-free conformation of Gα. Interestingly, residue 171R1 at the interdomain hinge also becomes immobilized upon binding R*.

Activated Gα(GTPγS)

Addition of GTPγS to the R*-bound, nucleotide-free G protein causes a conformational change leading to dissociation of the activated Gα(GTPγS) subunit from Gβγ and the receptor. As a result of these conformational changes, the EPR spectra for all sites, except 50R1, indicate a reversal of the immobilization observed upon formation of the R*-bound complex (Fig. 38, *green traces*). The mobility of 50R1 does not change with the addition of GTPγS.

A comparison of the GDP-bound and GTPγS-bound conformations of Gα illustrates the dependence of the Switch I conformation on the identity of the bound nucleotide (Fig. 38). The EPR spectra for three sites, 171R1, 182R1 and 187R1, are similar in both conformations. However, the remaining five sites reflect conformational differences between these two states. The dynamics of sites 184R1 and 186R1 decrease and increase, respectively, in the GTPγS-bound conformation relative to the GDP-bound subunit. Residue 180R1 is immobilized while the mobility of 179R1 increases in the activated conformation. Similarly, the mobility of 50R1 is increased relative to the GDP-bound conformation.

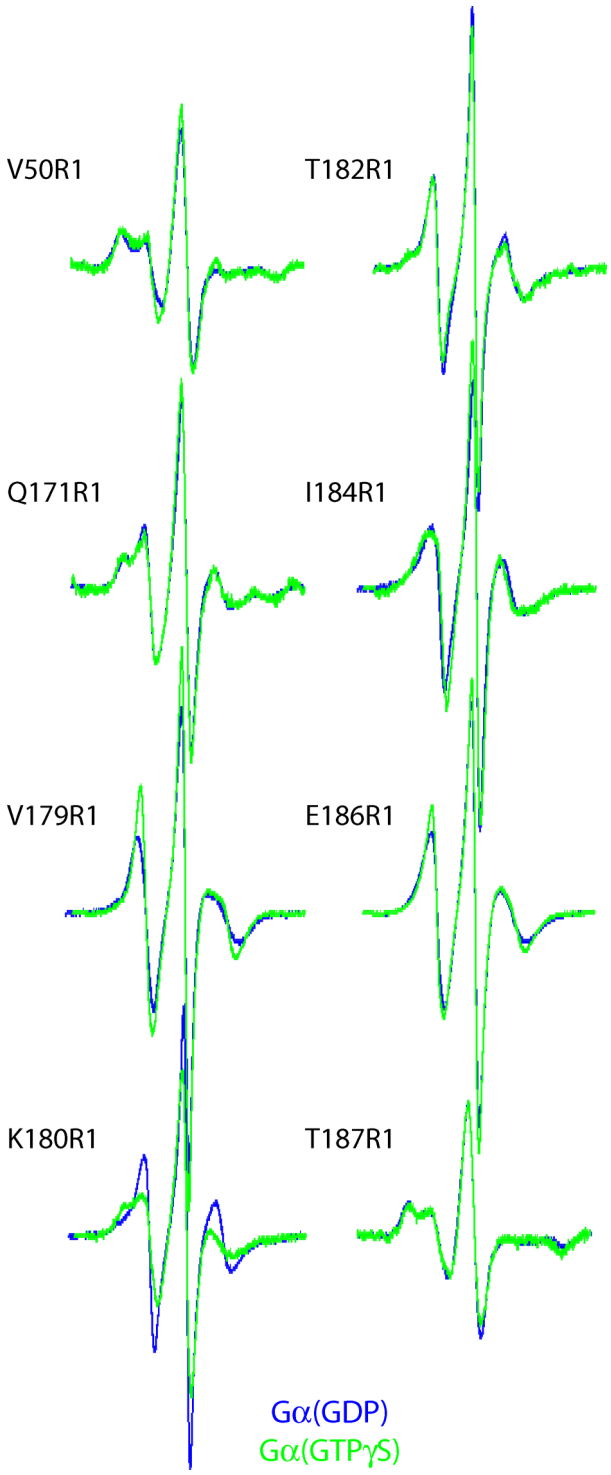

Figure 38 | Comparison of Switch I dynamics in GTPγS- and GDP-bound Gα Overlay of the GDP-bound (*blue traces*) and GTPγS-bound (*green traces*) Gα spectra.

Discussion

Crystallographic studies have identified conformational changes in the Switch I region as an important feature of the activating conformational change in Gα subunits. The goals of this study were to explore the dynamics of Switch I in solution and to obtain structural information about the R*-bound, nucleotide-free conformation of the G protein.

Switch I structure and dynamics in Gα(GDP), Gαβγ, and Gα(GTPγS)

Although located in or near the Switch I sequence, all of the sites examined in this study have significantly different local environments based on the G protein crystal structures. Three sites, 182, 184, and 186 face the solvent and form direct interactions with Gβ. As expected, the mobility of these residues decreases upon heterotrimer formation, however, the spectrum for 184R1 is the only one that shows a strongly immobilized component upon Gβγ binding. Modeling the R1 side chain at these sites indicates that 182R1 and 186R1 can adopt conformations that move the nitroxide into gaps between Gα and Gβ, while 184R1 remains buried at the interface. As the subunits dissociate following GTPγS binding, the spectrum of 182R1 reflects a high degree of side chain mobility, similar to the spectrum recorded in the Gα(GDP) conformation. By contrast, 184R1 and 186R1 are less mobile in the Gα(GTPγS) conformation. This observation is consistent with the interpretation of the changes seen in Switch I in the G protein crystal structures, where activation induces close-packing of the Switch I loop onto the β3 strand.

Residues 179R1 and 180R1 are on the flexible Switch I loop much closer to the nucleotide-binding pocket. In the GDP-bound conformation, both residues exhibit a very high degree of side chain mobility that is relatively unaffected by heterotrimer formation. There is a slight decrease in the mobility of residue 180R1 and no detectable change at 179R1. The local environment of these residues does not change much as a result of Gβγ binding, in line with crystallographic observation. Upon G protein activation, 179R1 becomes more mobile while 180R1 becomes less mobile. Based on the orientation of

the 180R1 side chain, the decrease in mobility is likely due to direct contact interactions with the γ-phosphate. The 179R1 side chain points toward the helical domain, and upon GTPγS binding, Switch I translates away from the helical domain, toward the nucleotide. This would account for the increase in dynamics at 179R1 compared to the Gα(GDP) conformation.

At the other end of the Switch I loop, sites 50R1 and 186R1 report significantly less mobile EPR spectra due to their more buried location in the protein. Heterotrimer formation significantly decreases the mobility of these sites. Since the mobility at both sites decreases, it seems likely that the β2 strand is moving closer to the α1 helix, which is supported by the crystal structures of the G protein heterotrimers. Although GTPγS binding induces a side chain conformation at 187R1 that is similar to the Gα(GDP) structure, the spectra of 50R1 indicates a more mobile side chain conformation. Modeling suggests that 50R1 may make some contact with the Switch I loop in the GDP-bound state, but the GTP-induced conformational change moves Switch I away from 50R1, possibly accounting for the observed increase in mobility.

Residue 171R1 is located near the interdomain hinge on the αF helix. A model of R1 at this position suggests that the nitroxide makes interactions across the interdomain cleft that account for the immobile component of the spectra. The intensity of the immobile component increases when Gβγ binds, which may be due to structural changes in Linker 1, the α1 helix, or even the α5 helix, although a precise structural explanation is not obvious from the crystal structures. GTPγS binding reverses the changes observed with heterotrimer formation.

Receptor activation-dependent conformational changes near Switch I

Excitingly, nearly every site examined in this region demonstrated receptor activation-dependent conformational changes, and this study is the first to implicate Switch I in the mechanism of GDP release. Three mutants, 171R1, 182R1, and 184R1, had much faster rates of basal nucleotide exchange than the base mutant did. This result is particularly surprising since mutations of 179R1 and 180R1, two residues

much closer to the nucleotide, had no effect on the exchange rate. Although no structural explanation is obvious for the effects of 182R1 and 184R1, as these residues point away from the binding pocket into solution, the R1 side chain at 171 is long enough to perturb the β6/α5 loop, which can have a significant impact on nucleotide exchange (Thomas*, et al.*, 1993; Iiri*, et al.*, 1994; Posner*, et al.*, 1998).

Comparing the dark and light EPR spectra for the Gβ-binding residues, 182R1, 184R1 and 186R1, suggests some structural rearrangement of the Gα-Gβ interface. No differences are seen at 182R1, while there is a decrease in the mobility at 184R1, with a greater decrease in mobility at 186R1. The location of 186R1 in the structure suggests that the new contact interactions formed are with Gβ, indicating a reorientation of the subunits compared to the heterotrimeric conformation. Two models have previously suggested that the activated receptor uses Gβγ to open the nucleotide-binding pocket for GDP release. In the lever-arm model, R* rotates Gβγ away from Gα, pulling Switches I and II along with it, thereby causing GDP release (Iiri*, et al.*, 1998; Rondard*, et al.*, 2001). The gear-shift model proposes a rotation in the opposite direction that causes close-packing of Switches I and II with the core of Gα (Cherfils & Chabre, 2003). In light of the lever-arm hypothesis, the observation that the mobility of residue 50R1 increases upon receptor activation is very interesting. The spectra suggest that the nucleotide-free and GTPγS-bound conformations of the 50R1 side chain are similar, and the GTPγS crystal structure shows that Switch I has translated away from the α1 helix. Although the spectral changes at these four sites do not uniquely describe the motion, they generally do support a role for intersubunit structural rearrangements in the formation of the R*-bound, nucleotide-free G protein complex.

In addition to conformational changes at the Gα-Gβ interface, GDP release causes a decrease in the mobility of 179R1 and 180R1 near the nucleotide-binding pocket. Indeed, residue 180R1 establishes new contact interactions in the absence of nucleotide. Based on the orientation of the R1 side chain, the most likely interaction is with the α1 helix across the binding pocket. If Switch I closes onto the empty pocket, then perhaps this is evidence that the nucleotide is released through the opposite side of the

protein. The decrease in the mobility of 179R1 is likely secondary to immobilization of the backbone due to the new contact interactions formed by K180.

Site 171R1 also demonstrates receptor activation-dependent conformational changes. The EPR spectra for this site report a decrease in mobility upon formation of the empty complex. Based on the location of this residue at the interdomain hinge, one exciting possibility is that 171R1 is reporting an interdomain reorientation. The location of GDP buried deeply between the GTPase and helical domains seems to demand some sort of opening in the interdomain cleft to allow GDP release. If there was an opening in the cleft, the mobility of residue 171R1 at the hinge would be predicted to decrease. Alternatively, this side chain may be sensing conformational changes in the α5 helix (Chapter III) or a more localized structural change in the αF helix.

Summary

This study demonstrates the utility of combining low resolution dynamic information provided by SDSL with high resolution crystal structures to explore protein function in solution. Unlike the Switch II region (Chapter IV), the structure and dynamics of Switch I agree well with each of the corresponding crystal structures. Importantly, this approach has provided the first structural information for Switch I in the receptor-G protein complex, revealing convincing evidence of structural changes at the Gα-Gβ interface as well as the nucleotide-binding pocket, and interdomain hinge. Additional studies will be necessary to characterize these conformational changes further, using additional single-site mutants and interspin distance measurements. Future studies using this series of spin-labeled mutants will explore how the dynamics of this region influence GTP hydrolysis and interaction with RGS proteins to provide greater insight into the mechanisms of G protein inactivation.

CHAPTER VI

ADDITIONAL SDSL STUDIES OF G PROTEIN STRUCTURAL CHANGES

Introduction

Receptor activation-dependent conformational changes in the α5 helix play a prominent role in the mechanism of receptor-catalyzed GDP release (Chapter III). In addition to exploring this region for changes associated with the formation of the R*-bound, nucleotide-free complex, the dynamics of the other G protein conformations were also recorded. This chapter provides a more quantitative analysis of the EPR spectra at each point in the activation pathway, and presents data for sites that have not been discussed previously.

Results and Discussion

Location and characterization of spin-labeled mutants

The structure and dynamics of several regions in $G\alpha_{i1}$ have been explored with SDSL, including the α5 helix (330, 331, 333, 334, 340, 342), the C-terminal tail (344, 345, 349, 351), the β6 strand (318, 320, 321), the β2/β3 loop (191, 192, 194), and miscellaneous sites in α-helices 1 (56), 4 (305), B (106), and G (273) (Fig. 39). Each of these spin-labeled mutants undergoes R*-catalyzed nucleotide exchange and forms stable R*-G protein complexes with rhodopsin in ROS membranes (Fig. 40 for data not reported elsewhere). Similar to other residues located between the α5 helix and β strands 2 and 3, 192R1 has a much faster basal exchange rate than the base mutant does. Biochemical characterization of 305R1 has not yet been completed. For each spin-labeled mutant, EPR spectra were recorded for each of five

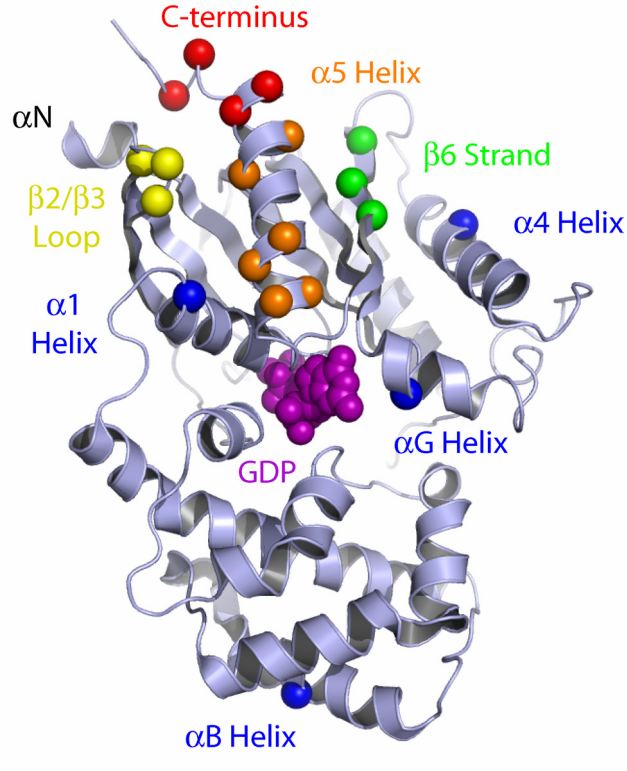

Figure 39 | Location of spin-labeled mutants Ribbon diagram of the $G\alpha_{i1}$ subunit from the structure of the G_{i1} heterotrimer (1GP2). The N-terminus is truncated, and the extreme C-terminus was modeled as a flexible loop. Sites chosen for spin-labeling are identified as spheres on the α-carbons and color-coded according to their location in the structure.

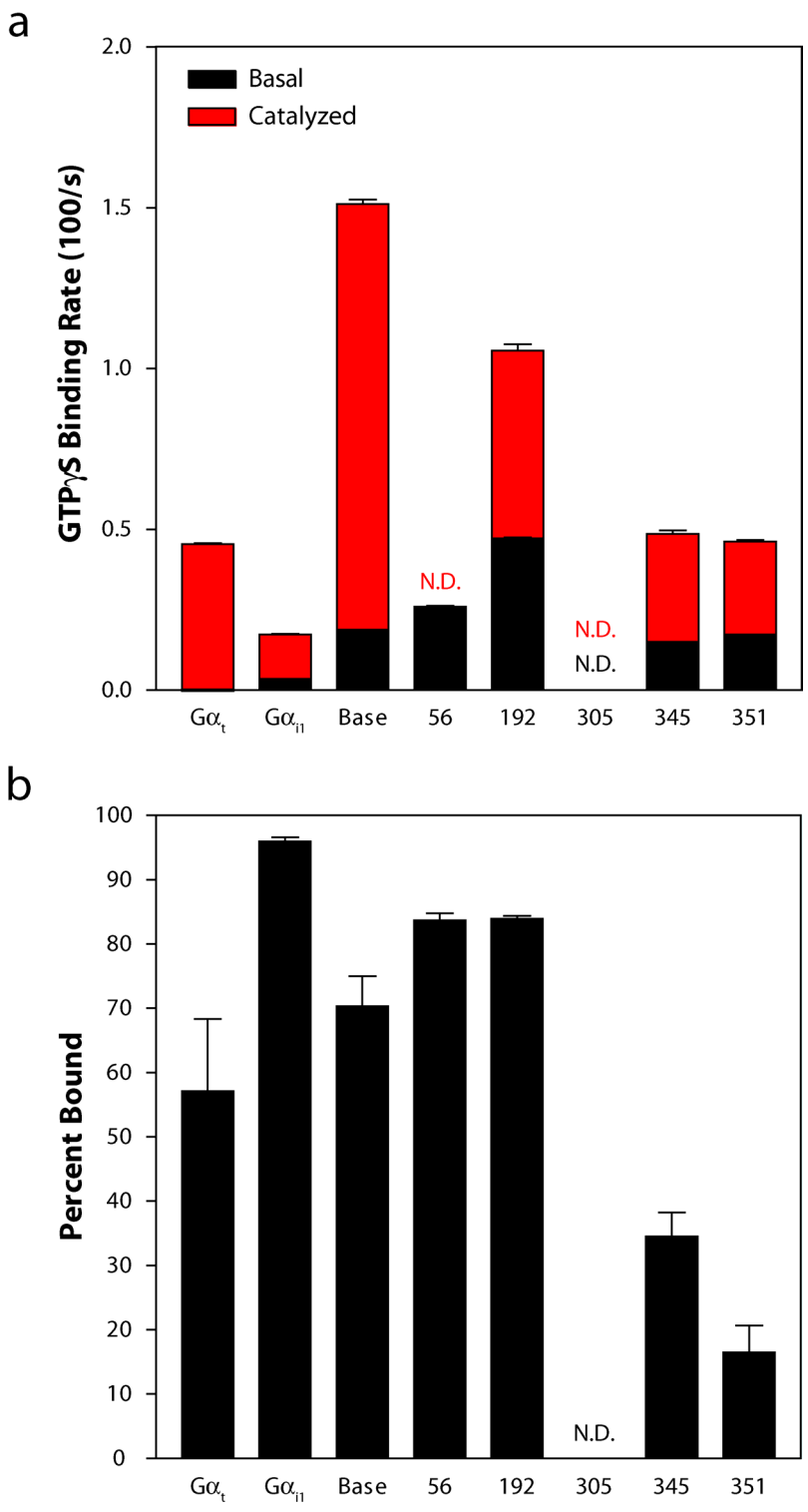

Figure 40 | Biochemical characterization of spin-labeled mutants (**a**) Nucleotide exchange assay. Data represent the mean ± s.e.m. of 4-6 independent experiments. (**b**) Rhodopsin binding assay. Data represent the mean ± s.e.m. of 3 independent experiments.

conformations: Gα(GDP), Gα(GDP)βγ, the heterotrimer in the presence of dark ROS membranes, R*·Gα(O)βγ, and Gα(GTPγS).

Comparison of Gα(GDP) and Gα(GDP)βγ

The EPR spectra of R1 residues at sites 106, 331, 333, 334, 344, and 345 in Gα(GDP) reveal an anisotropic motion characteristic of R1 at the solvent-exposed surface of an α-helix (Fig. 41, *blue traces*), where the nitroxide has no interactions with other residues or main chain atoms (Columbus*, et al.*, 2001). Models of R1 at these sites based on the crystal structure are consistent with this result. The EPR spectra of 349R1 and 351R1 are characteristic of dynamically disordered sequences (Columbus & Hubbell, 2004), and these residues are in the statically disordered C-terminal sequence not resolved in the crystal structure. For non-interacting helix surface sites, site-dependent variations of the correlation time and order parameter are due to backbone motions (Columbus & Hubbell, 2004). Using sites 331, 333, 344, 345, 349, and 351 as monitors of backbone motion, a clear gradient in fast backbone dynamics (measured by τ_c^{-1}) is resolved along α5 helix into the C-terminal sequence (Fig. 42b). This result is in agreement with the crystallographic B-factors in the structure, which also reveal a gradient (Fig. 42c). Residue 106R1 also has a spectral lineshape reflecting highly ordered anisotropic motion, in agreement with the helix surface location of this site in the crystal structure.

The EPR spectrum of 318R1 reflects a surprisingly high mobility, again compatible with the crystallographic data, which show residues in the α4/β6 loop to have high B-factors (Fig. 42c). The EPR spectra of R1 at other sites in Gα(GDP) are multicomponent, suggesting tertiary contact interactions of the nitroxide (Mchaourab*, et al.*, 1996), generally consistent with expectations from the crystal structure.

When Gβγ is added to Gα(GDP) to form the heterotrimer, significant spectral changes are detected for 191R1 and 194R1 in the β2/β3 loop, 320R1 in the β6 strand, and 340R1 in the α5 helix (Fig. 41, *pink traces*). In each case, except 194R1, the change is a reduction in spectral intensity in a region corresponding to more mobile components (Fig. 41). These residues, except for 320R1, are located in

Figure 41 | Conformational changes upon heterotrimer formation Spectra for each of the spin-labeled mutants before (*blue traces*) and after (*pink traces*) addition of an equimolar amount of $G\beta_1\gamma_1$. The spectral intensity for sites 349R1 and 351R1 has been reduced by half as compared to the intensity of the other spectra.

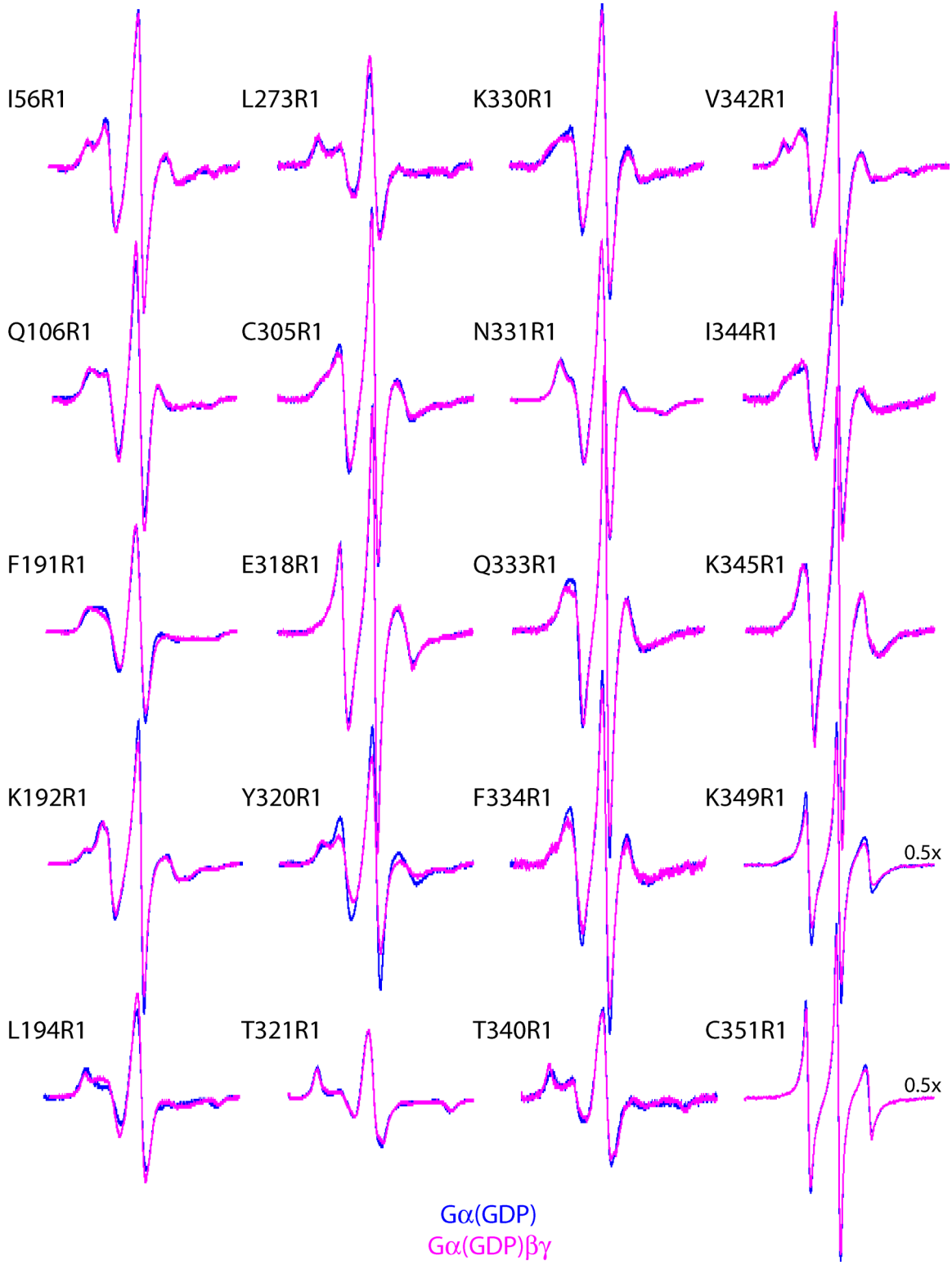
I56R1
L273R1
K330R1
V342R1
Q106R1
C305R1
N331R1
I344R1
F191R1
E318R1
Q333R1
K345R1
K192R1
Y320R1
F334R1
K349R1
0.5x
L194R1
T321R1
T340R1
C351R1
0.5x
Gα(GDP)
Gα(GDP)βγ

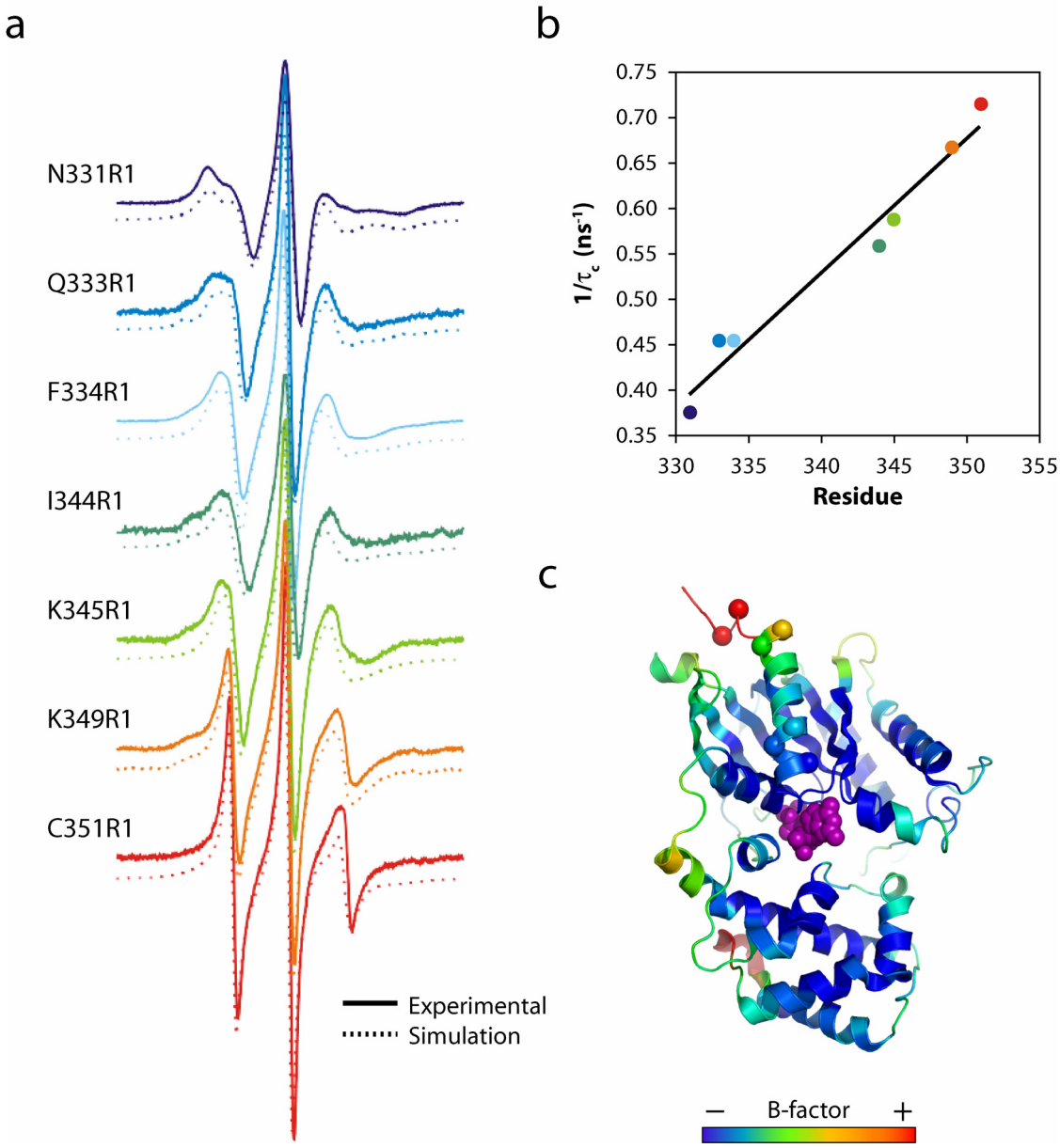

Figure 42 | Gradient of backbone mobility within the α5 helix (**a**) MOMD simulations (*dashed lines*) of the experimental spectra (*solid lines*) corresponding to labeled sites on the surface of the α5 helix when bound to Gβγ. The spectra are colored by B-factor values observed at each site in the crystal structure. (**b**) The rotational correlation time (τ_c) was determined from spectral simulation, and τ_c^{-1} was plotted against sequence position. For multi-component spectra, the fastest τ_c was used. A linear gradient is observed, in agreement with the crystallographic B-factors. (**c**) Ribbon diagram of the $G\alpha_{i1}$ subunit from the structure of the G_{i1} heterotrimer (1GP2). The backbone is colored according to crystallographic B-factor, and spheres within the α5 helix represent sites where R1 was introduced to measure backbone dynamics. Residues beyond 348 where not observed in the structure and have been modeled in as a flexible loop.

structures that face the binding surface of the Gβ subunit, and the spectral changes are likely due to changes in internal structure; components of such high mobility would not be affected by the reduction in the rotational diffusion of Gα subunit due to heterotrimer formation. The origin of such changes is not obvious in a comparison of the crystal structures of $G\alpha_{i1}$(GDP) (Mixon*, et al.*, 1995) and G_{i1} (Wall*, et al.*, 1995), which are essentially identical at these sites, but may be due to damping of backbone motions. Although residue 194R1 is adjacent to sites that become less mobile in the heterotrimer, it reports an increase in the intensity of the mobile component of the spectrum. A comparison of the crystal structures suggests that this residue may be uniquely positioned to monitor the structural change in the αN helix as it stretches out to bind Gβ, accounting for the increase in mobility at this site. Addition of the heterotrimer to dark ROS membranes produces essentially no change in the EPR spectra at any site.

Structural changes upon formation of the R-G protein complex*

Upon photoactivation of rhodopsin to form R*, the heterotrimer undergoes dramatic changes throughout the nucleotide binding domain (Figs. 21, 43a). Only 20-70% of the labeled protein binds to the activated receptor (Figs. 20, 40), so the spectral changes shown represent the lower limit of the mobility changes within the actual complex. As shown in Chapter III, R1 side chains near the α5 helix support a rotation and translation of this helix upon binding to R*. The spectral changes observed for 56R1 in the α1 helix and 192R1 in the β2/β3 loop may also support this movement, although the interpretation of these differences is less clear. Residue 56R1 undergoes a striking decrease in side chain mobility upon binding to R*. This is a surprising result, as the predicted result based on our model is that the mobility of this residue would increase as the α5 helix moved away from the α1 helix. One possibility that may account for this change is that the R1 side chain at this position is repacking into a pocket formed following the rotation-translation of the α5 helix, thereby accounting for the decreased mobility observed. Similarly, new contacts may be formed upon rotation of the helix that immobilize 56R1. The spectral change at 192R1 is more complicated in that the order or anisotropy of the side chain

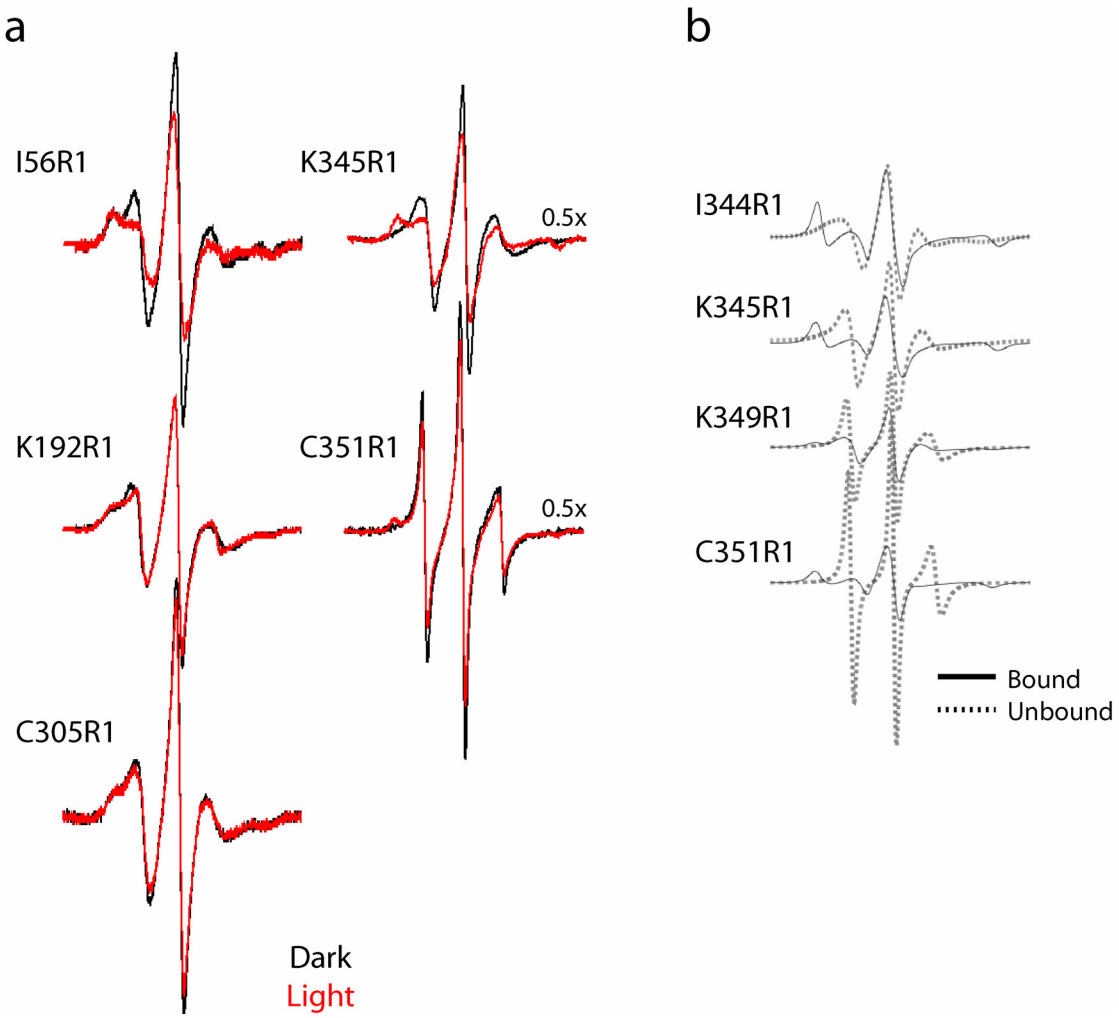

Figure 43 | Receptor activation-dependent conformational changes (**a**) Spectra for each of the spin-labeled mutants in solution with $G\beta_1\gamma_1$ and rhodopsin were recorded before (*black traces*) and after (*red traces*) photoactivation of the receptor. (**b**) Spectra from the extreme C-terminal mutants represent a mixture of bound and unbound G protein components. To extract the individual spectral components, MOMD simulations were used. The bound (*solid lines*) and unbound (*dashed lines*) lineshape components are shown for each site.

is different, making a definitive interpretation regarding any changes in mobility difficult. Based on the decreases in side chain mobility observed at adjacent receptor contact sites (Chapter III), residue 192R1 may be at the edge of this interface.

Nitroxides at residues 344, 345, 349, and 351 in the C-terminal tail of Gα show the appearance of a strongly immobilized state in the presence of R*. Only about 30% of the labeled protein is bound to R* for 345, 349 and 351 (Figs. 20, 40). In the spectrum of 351R1, the relative intensity of the immobilized component is quite low, partly due to the presence of the very narrow lineshape corresponding to the unbound state (60%) which dominates the first-derivative display. In each case, "spectral titration" by subtraction of the unbound component yields the EPR spectrum of the bound state (Fig. 43b). The titration suggests that about 30% of the protein is bound to the receptor to give the immobilized conformation, which is consistent with the result from the rhodopsin binding assay. Except in the case of 349R1, the spectrum of the bound component is essentially a powder pattern, characteristic of a completely immobilized state. A number of studies have shown that a synthetic undecapeptide corresponding to the C-terminal segment of Gα binds to R*, implying that this sequence is involved in direct receptor-G protein interaction (Dratz*, et al.*, 1993; Kisselev*, et al.*, 1998; Koenig*, et al.*, 2002; Janz & Farrens, 2004). The present study is the first direct demonstration that this sequence in the intact G protein is involved in R* binding, and demonstrates the utility of the SDSL method for identifying protein-protein interaction sites.

Changes do not occur everywhere in the structure; in particular residues 106R1 and 305R1, which are located at some distance from the nucleotide-binding pocket.

Structural changes upon activation with GTPγS

When GTP or GTPγS binds to the empty nucleotide-binding site of the complex, the Gα subunit is switched to a new, active, conformation. In general, the spectra return to a state more closely resembling the Gα(GDP) form (Fig. 44). However, in the case of 191R1, 330R1, 331R1, and 344R1, the

nitroxide is significantly more immobilized in Gα(GTPγS) compared to Gα(GDP). This suggests that the disposition of the helix is different in the two forms, although this is not apparent from a comparison of the crystal structures of these two conformers. Additionally, sites 56R1 and 305R1 are much less mobile in the activated conformation. While the difference at 56R1 may be associated with differences observed in the α5 helix, more sites will be required to define the structural rearrangement at the α4 helix. As expected, the strongly immobilized components of 345R1, 349R1 and 351R1 disappear as the G protein dissociates from the receptor.

Figure 44 | Comparison between the GTPγS- and GDP-bound conformations Spectra for each of the spin-labeled mutants in the GDP-bound (*blue traces*) and GTPγS-bound (*green traces*) conformations highlight sites that are sensitive to the identity of the bound nucleotide. The spectral intensity for sites 349R1 and 351R1 has been reduced by half compared to the intensity of the other spectra.

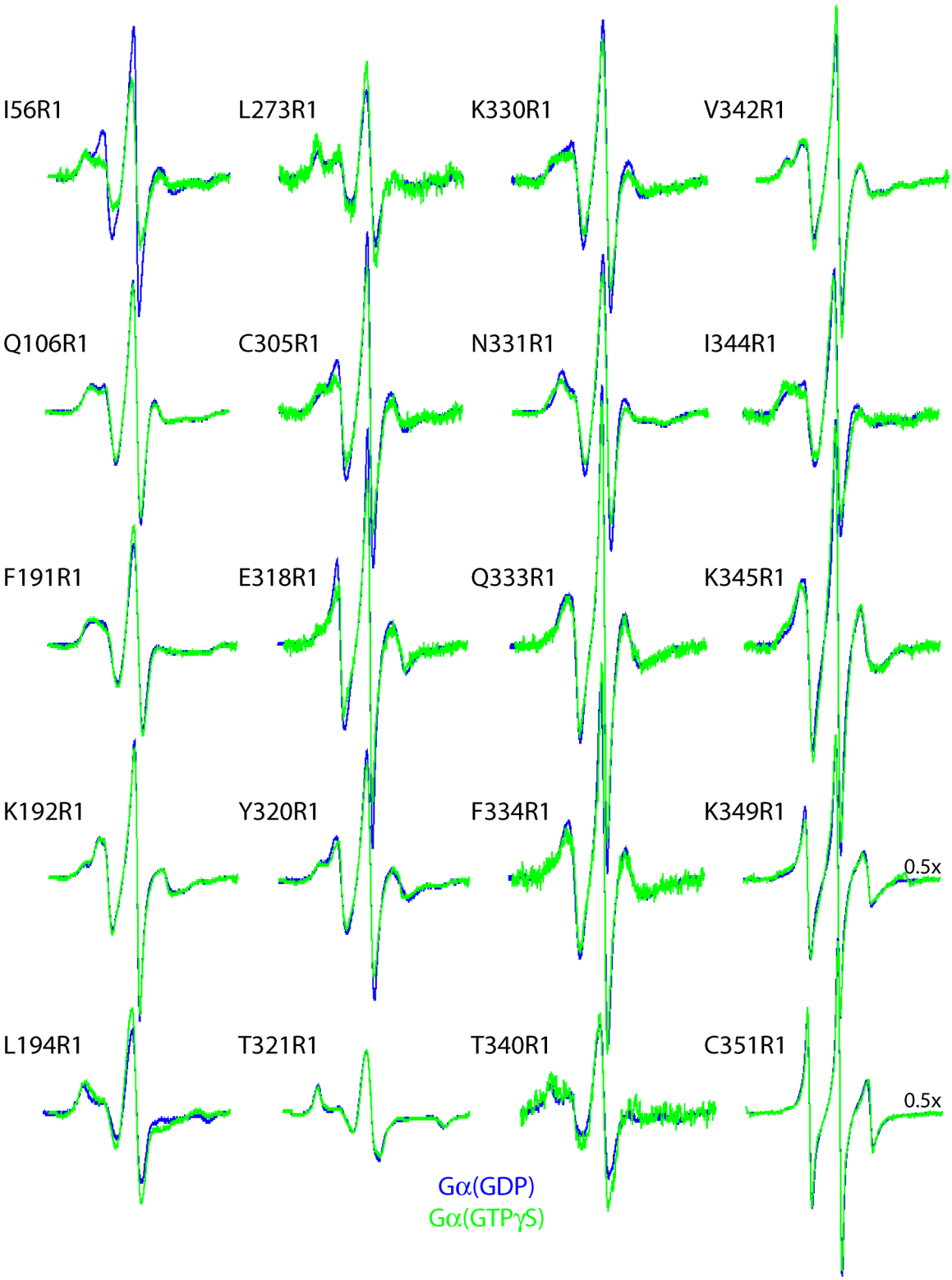
I56R1
L273R1
K330R1
V342R1
Q106R1
C305R1
N331R1
I344R1
F191R1
E318R1
Q333R1
K345R1
K192R1
Y320R1
F334R1
K349R1
0.5x
L194R1
T321R1
T340R1
C351R1
0.5x
Gα(GDP)
Gα(GTPγS)

CHAPTER VII

COMPLEMENTARY APPROACHES TO STUDY G PROTEIN STRUCTURE

Each of the preceding four chapters has described results from site-directed spin-labeling studies of the G protein α subunit, which have revealed exciting new insights into the mechanism of receptor-catalyzed nucleotide exchange and provided important information on the dynamics of each conformational state in G protein activation. To complement the conclusions from SDSL, several alternative approaches were undertaken with varying degrees of success, including site-directed mutagenesis, cross-linking experiments, x-ray crystallography, and computational approaches. This chapter will serve to discuss these as works-in-progress.

Mutagenesis of Evolutionarily Conserved Residues in the α5 Helix

Introduction

Activated receptors catalyze GDP release from Gα by inducing a rotation and translation in the α5 helix (Chapter III). Although we have developed a reasonably good model of this conformational change, less is known about the specific point-to-point contacts between the receptor and G protein that cause this movement. One hypothesis that is consistent with our model is based on evolutionary sequence analysis of receptors and G proteins, which identifies groups of amino acids that are either conserved or mutated together using a large multiple sequence alignment. This analysis identified set of conserved residues that cluster around a conserved negative charge in the α5 helix (Fig. 45) (Oliveira*, et al.*, 1999). The authors propose that these residues form a binding site for the conserved, positively charged arginine of the D(E)RY motif in receptors. Upon G protein binding, this arginine would disrupt interactions with the α5 helix, leading to GDP release. In support of this hypothesis, several mutations in this region have

been shown to increase the spontaneous nucleotide exchange rate of Gα (Denker, *et al.*, 1992; Marin, *et al.*, 2001b; Woon, *et al.*, 1989).

In $G\alpha_{i1}$, the conserved residues form a salt bridge between K192 in the β2/β3 loop and D341 in the α5 helix (Fig. 45a), which may serve as an ionic buckle to maintain the α5 helix in the proper orientation for high-affinity GDP binding. When this restraint is removed, the α5 helix could rotate, thereby altering the geometry of the nucleotide binding pocket and reducing its affinity for GDP. To investigate this hypothesis, several mutants have been made where charges on the salt bridge were reversed, paired or eliminated and the basal nucleotide exchange rates were measured.

Results and Discussion

Several of the mutations had no effect on the basal nucleotide exchange rate of $G\alpha_{i1}$ (Fig. 46a). Compared to the wild-type sequence (KD), the KA and AA mutations have the same affinity for GDP. Since alanine mutations effectively eliminate the side chains beyond the β-carbon, these two mutants suggest the presence of additional interactions that stabilize the α5 helix. Although the AD mutant would be important to examine for completeness, this mutation would likely not be predicted to affect the exchange rate. Similar to the KA mutant, the RA mutant had no effect on the exchange rate. Surprisingly, the RR mutant also had no effect on exchange. The close proximity of two positive charges would be expected to force the α5 helix and β2/β3 loop apart, thereby increasing GDP release. This result suggests that the two arginine residues can adopt a side chain conformation that places the charges far apart from each other (Fig. 46b).

Other single mutations at site D341 had more significant effects on GTPγS-binding than the D341A (KA) mutant (Fig. 46c). Interestingly, the D341N (KN) mutation increased the basal exchange rate. Since asparagine is structurally similar to aspartate, but without the negative charge, this mutant seems to indicate that there is a charge interaction between K192 and D341 in the wild-type protein. A similar effect on the exchange rate was also observed in the D341K (KK) mutant. Although two positive

Figure 45 | Alignments of evolutionarily conserved residues in Gα subunits (**a**) Ribbon models of representatives of the four Gα subfamilies highlighting amino acids conserved or mutated as a group surrounding the highly conserved aspartate residue (D341 in $G\alpha_{i1}$) on the α5 helix. Interestingly, each of the Gα family members has devised different ways to balance the charges present in this region. (**b**) Sequence alignments of all human Gα subunit genes from the β2 strand to the β3 strand (*left*) and the α5 helix to the C-terminus (*right*) highlighting the similarities and differences in this region.

a

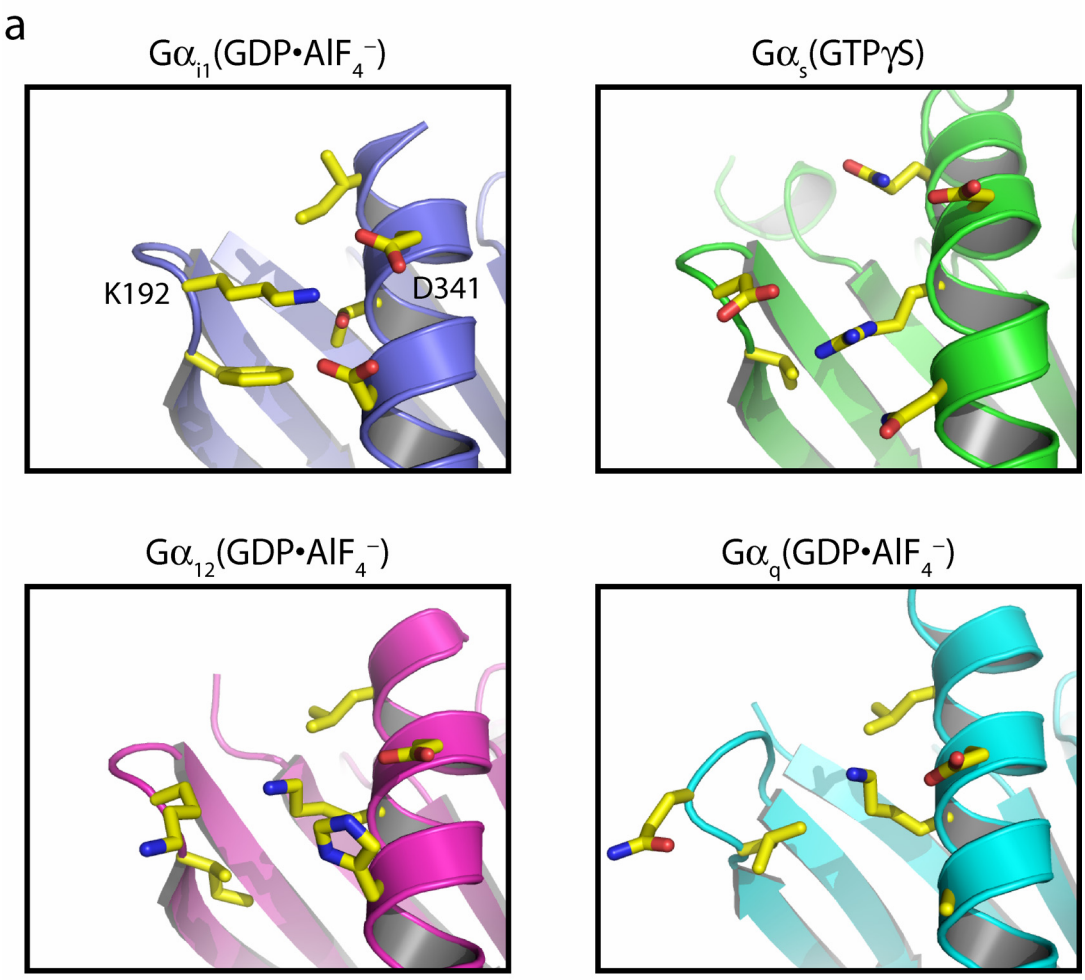
Gα$_{i1}$(GDP•AlF$_4^-$)
K192
D341
Gα$_s$(GTPγS)
Gα$_{12}$(GDP•AlF$_4^-$)
Gα$_q$(GDP•AlF$_4^-$)

b

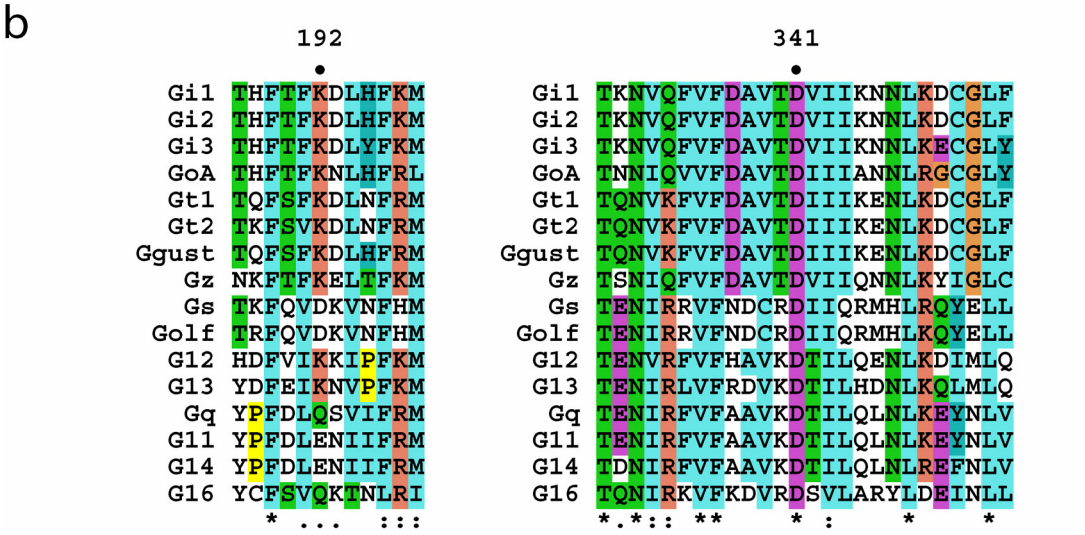
192
341
Gi1 THFTFKDLHFKM
Gi2 THFTFKDLHFKM
Gi3 THFTFKDLYFKM
GoA THFTFKNLHFRL
Gt1 TQFSFKDLNFRM
Gt2 TKFSVKDLNFRM
Ggust TQFSFKDLHFRM
Gz NKFTFKELTFKM
Gs TKFQVDKVNFHM
Golf TRFQVDKVNFHM
G12 HDFVIKKIPFKM
G13 YDFEIKNVPFKM
Gq YPFDLQSVIFRM
G11 YPFDLENIIFRM
G14 YPFDLENIIFRM
G16 YCFSVQKTNLRI
Gi1 TKNVQFVFDAVTDVIIKNNLKDCGLF
Gi2 TKNVQFVFDAVTDVIIKNNLKDCGLF
Gi3 TKNVQFVFDAVTDVIIKNNLKECGLY
GoA TNNIQVVFDAVTDIIIANNLRGCGLY
Gt1 TQNVKFVFDAVTDIIIKENLKDCGLF
Gt2 TQNVKFVFDAVTDIIIKENLKDCGLF
Ggust TQNVKFVFDAVTDIIIKENLKDCGLF
Gz TSNIQFVFDAVTDVIIQNNLKYIGLC
Gs TENIRRVFNDCRDIIQRMHLRQYELL
Golf TENIRRVFNDCRDIIQRMHLKQYELL
G12 TENVRFVFHAVKDTILQENLKDIMLQ
G13 TENIRLVFRDVKDTILHDNLKQLMLQ
Gq TENIRFVFAAVKDTILQLNLKEYNLV
G11 TENIRFVFAAVKDTILQLNLKEYNLV
G14 TDNIRFVFAAVKDTILQLNLREFNLV
G16 TQNIRKVFKDVRDSVLARYLDEINLL

charges might have had a more profound effect, rotamer analysis indicates that all of the favored side chain conformations for these residues would direct the positively charged amino group on K341 away from the α5 helix and the β2/β3 loop. Interestingly, the D341E (KE) mutant had a reduced exchange rate, which may be due to an increased ability of K192 to interact with an α5 helix containing a long, negatively charged side chain at site 341. Similar reasoning may apply to the reduced exchange rate observed for the RD mutant. The larger arginine side chain might make a better salt bridge with D341, as well as additional interactions with the gaunidino group to stabilize these two structural elements. This group of mutations indicates that a charge interaction between the α5 helix and the β2/β3 loop may play some role in stabilizing the GDP-binding pocket.

One approach to prove the importance of a charge interaction is to reverse the charges on the two structural elements to recapitulate the salt bridge in reverse (Fig. 46d). When the wild-type residues were swapped (DK), an increase in the basal exchange rate was observed similar to the increase with the KN and KK mutants, which supports the hypothesis that a lysine mutation at residue 341 has a minor impact on the structure of this region, but it does not have the appropriate geometry to recapitulate the interaction with the β2/β3 loop. Although a flexible arginine residue at site 341 might be expected to interact with an aspartate at site 192, the DR mutation actually had a much faster exchange rate than the wild-type (KD) and even the DK mutation. The structural basis for this effect is unclear, although one possibility is that there is, indeed, some interaction between D192 and K341 in the DK mutant. This is supported by the observation that the EK and ER mutants have approximately the same exchange rate as the DK mutant (*i.e.* the ER exchange rate is not significantly faster than the EK exchange rate, unlike the situation observed for the DR and DK mutants), which may indicate that the increased tether on the negative charge at E192 is more capable of forming a productive salt bridge with a positively charged amino acid at 341 than is the shorter side chain, D192. Further reinforcing this model is the fact that the QR exchange rate, which eliminates the negative charge at site 192, has a much faster exchange rate than the ER mutant. Several additional mutants would help to clarify these results, including DA, QK, NK, and

NR. For example, the QK, NK, and NR mutants would help dissect the role of a charge interaction with K341 and R341, and the DA mutation would test for the effects due to an arginine at position 341.

The interpretation of the final group of double mutants is the most clear. When two negatively charged residues are placed at positions 192 and 341 (DD, EE, and ED), substantial increases in nucleotide exchange are observed (Fig. 46e). Interestingly, these three mutations exhibit a range of effects, with ED having the fastest rate, EE the slowest, and DD intermediate between the two. Modeling suggests that the DD and ED mutants are the most conformationally constrained, and the additional length of the glutamate residue brings these two negatively charged residues into closer proximity than in the DD mutant (Fig. 46f). The EE mutant is most capable of moving these charges away from each other, although its rate is still faster than the EK and ER mutants. Since position 341 is less enclosed, the DE mutation should have an exchange rate intermediate between the DD and EE mutants.

In the context of the model for receptor-catalyzed nucleotide exchange described in Chapter III, the rapid exchange rates of the DD and ED mutations are even more exciting. These mutations support our model for the R*-mediated movements of the α5 helix, where the helix rotates and translates away from the β2/β3 loop toward the β6 strand. Indeed, the R*-catalyzed nucleotide exchange rate for the wild-type $G\alpha_{i1}$ is 0.0017 s^{-1}, which is only slightly faster than the basal exchange rate for the DD mutant, 0.0015 s^{-1} (Fig. 46e).

In summary, this particular salt bridge does not appear to be critical for maintaining the protein's affinity for GDP as indicated by the alanine substitutions, however, charge interactions play some role in defining the structure of the region, and perturbations in this region can have a substantial impact on GDP release. Besides the additional mutations described above, the effects of these mutations on the R*-catalyzed nucleotide exchange rate may shed more light on the mechanism of receptor-G protein coupling. Furthermore, although this particular salt bridge is unique to the $G\alpha_i$ family, the structures and the sequences of the other Gα family members may provide useful insight to guide future mutagenesis in this region (Fig. 45).

Figure 46 | Basal exchange rates of salt bridge mutants (**a**) Several mutations had little effect on the basal exchange rate, suggesting that this connection is not critical for the stability of the region. (**b**) Surprisingly, the RR mutation did not have a fast exchange rate, but this could be due to the flexibility of these side chains allowing the positive charges to move away from each other. (**c**) Single mutations at D341 resulted in relatively mild changes in GTPγS binding, particularly compared to DR and QR (**d**) and the double-negative mutants (**e**). The DD and ED mutants have basal exchange rates similar to or greater than the R*-catalyzed rate for the wild-type (KD) protein (*red bar*). (**f**) Modeling the ED mutant with the most common rotamer of glutamate clearly demonstrates the electrostatic repulsion between the α5 helix and β2/β3 loop. Positively charged amino acids are labeled in *blue*, negatively charged amino acids are labeled in *red*, and uncharged amino acids are labeled in *black*. Data are the mean ± s.e.m. of 6 independent experiments. (See Appendix C to compare the exchange rates for all of the mutants.)

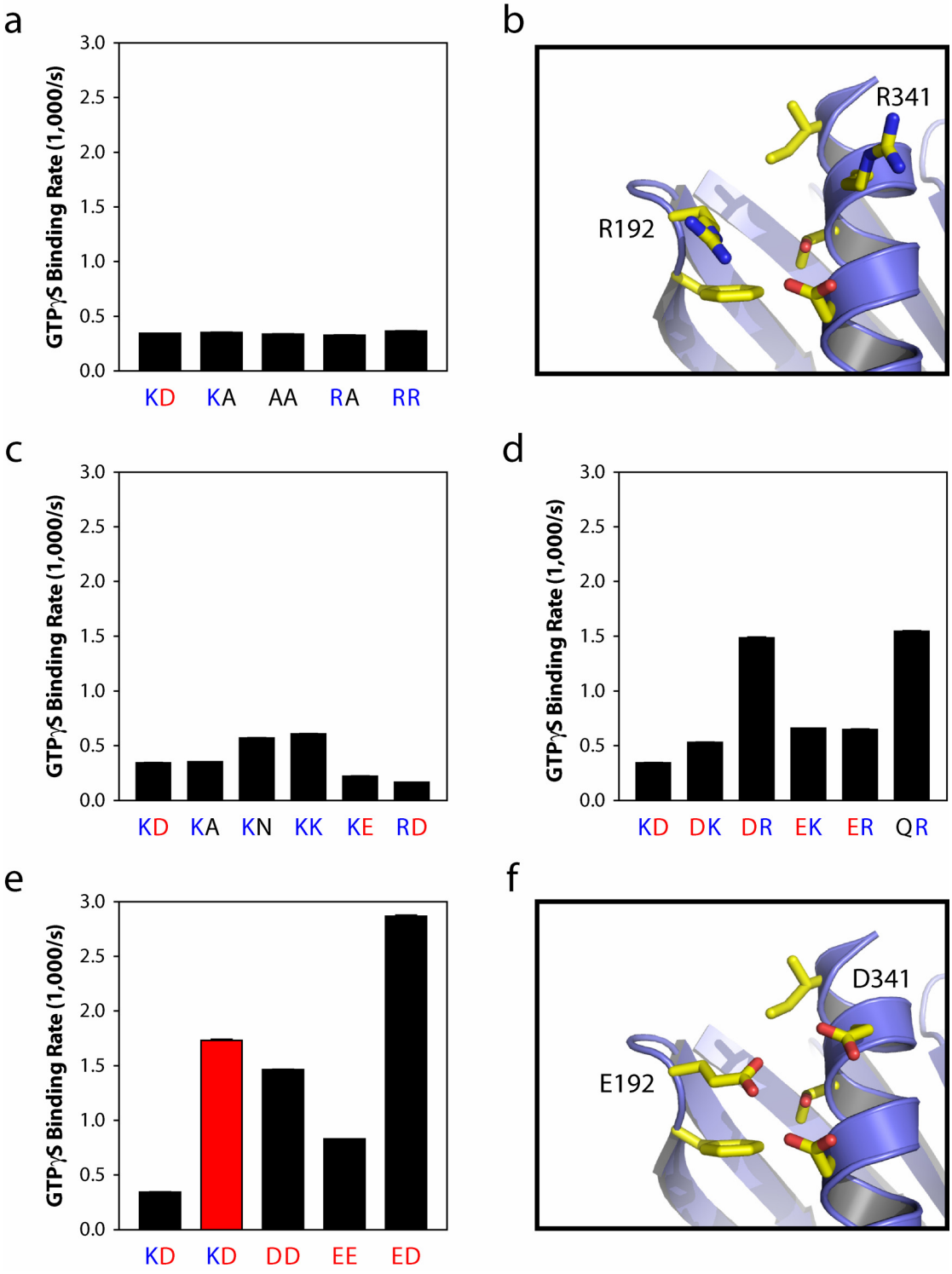
a
GTPγS Binding Rate (1,000/s)
3.0
2.5
2.0
1.5
1.0
0.5
0.0
KD KA AA RA RR
b
R341
R192
c
GTPγS Binding Rate (1,000/s)
KD KA KN KK KE RD
d
GTPγS Binding Rate (1,000/s)
KD DK DR EK ER QR
e
GTPγS Binding Rate (1,000/s)
KD KD DD EE ED
f
D341
E192

Double Cysteine Mutagenesis in $G\alpha_{i1}$

Preliminary cross-linking experiments

After SDSL studies identified a major conformational change in the α5 helix associated with GPCR activation, cross-linking studies were designed to either prevent the conformational change or to lock the helix in the receptor-bound conformation. Toward this end, six double cysteine mutations have been introduced into $G\alpha_{i1}$ in order to restrict the movement of the α5 helix with disulfide cross-links. The double cysteine mutants 56-333, 192-340, 192-341, and 194-344 were introduced to prevent the rotation-translation of the α5 helix, while 320-342 and 324-335 were intended to freeze the post-movement, R*-bound conformation of the α5 helix (Fig. 47).

When the $G\alpha_{i1}$(GDP) crystal structure (Mixon*, et al.*, 1995) was analyzed with Disulfide by Design (Dombkowski, 2003), no good opportunities for disulfide bond formation between the α5 helix and adjacent structures were identified. In order to encourage disulfide bond formation, these proteins were treated with the oxidizing agent copper phenanthroline. Treatment of 50 μM of wild-type $G\alpha_{i1}$, 56-333, and 192-341 with 50 μM CuPh (6.25 μL each of 12 mM 1,10-phenanthroline in 2% glycerol and 4 mM $CuSO_4$) for 1 h at room temperature precipitated much of the protein. The oxidized samples were subsequently washed with buffer B containing 10% glycerol and 50 μM GDP and the precipitant was separated by centrifugation. The protein concentration and activity for all three were reduced compared to a control aliquot containing 1 mM DTT. Disulfide bond formation was assessed by SDS-PAGE (Fig. 48). Proteins that have formed disulfide bonds will have a lower apparent molecular weight and high molecular weight aggregates will be apparent. When compared to untreated $G\alpha_{i1}$, the bands for both 56-333 and 192-341 were smeared toward faster-running species, consistent with the possibility that these proteins form disulfide bonds without oxidant treatment. This smearing was eliminated in the DTT-treated samples, and potentiated in the CuPh-treated samples. Similarly, the addition of reducing loading buffer reduced the amount of smearing in the CuPh-treated samples.

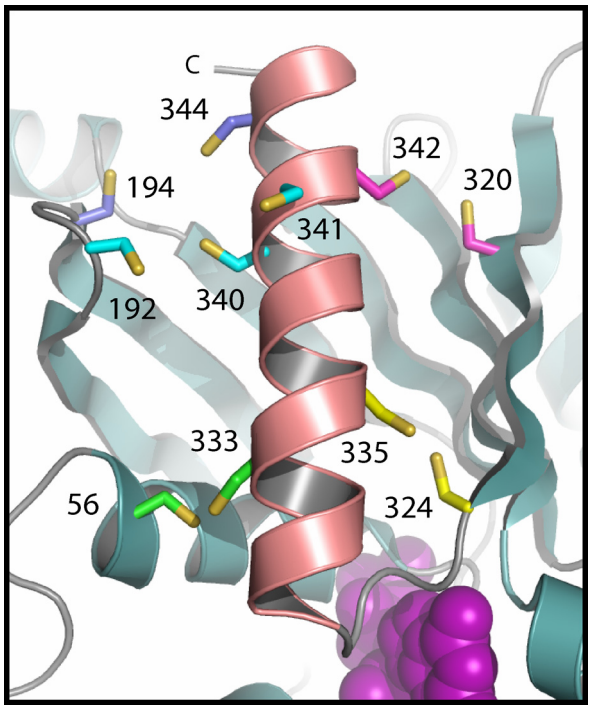

Figure 47 | Locations of double cysteine mutations in $G\alpha_{i1}$ Six pairs of cysteine mutants were constructed in $G\alpha_{i1}$, 56-333, 191-340, 191-341, 194-344, 320-342, and 324-335. These mutations were designed to allow disulfide bond formation to restrict the movement of the α5 helix in the GDP-bound (*blue*, *cyan*, and *green* side chains) or nucleotide-free (*pink* and *yellow* side chains) conformation based on the model developed from SDSL studies of receptor-catalyzed GDP release.

Overall, this study indicates that increased disulfide bonds are forming in the 56-333 and 192-341 mutants, even without CuPh treatment. Since spontaneous disulfide bond formation is not predicted from the crystal structure, this may suggest that the α5 helix is an inherently flexible and dynamic element of the protein, supporting our model of G protein activation. However, once the protein is denatured in SDS, any pair of cysteines may form a disulfide bond. This experiment needs to be repeated using a thiol-reactive reagent prior to denaturation, which will protect all of the free thiol groups and more clearly demonstrate whether a disulfide bond is formed between the two mutant cysteine residues. Furthermore, the oxidizing conditions using CuPh need to be optimized to prevent aggregation and precipitation. This chemical is a catalytic oxygen generator, and a much smaller concentration at a much lower temperature would still be effective. Glutathione may also be useful as a milder oxidizing agent.

As an alternative to disulfide bond formation, homo bi-functional sulfhydryl-reactive reagents may be used to cross-link two cysteine residues. The length of the linkers ranges from 8 Å with bis-maleimidoethane to greater than 15 Å for other compounds. Since the distance between the cysteines in the double mutants was approximately 8 Å, these proteins were treated with BMOE. Wild-type $G\alpha_{i1}$, 56-333, 192-341, 320-342, and 324-335 (25 μM in degassed buffer B, pH 6.0, containing 10 mM EDTA and 75 μM GDP) were treated with a 10 molar excess of BMOE for 1 h at room temperature. Degassing and EDTA were employed to reduce the extensive oxidation caused by the initial labeling reaction. The reaction was stopped with 10 molar excess over BMOE of βME. No obvious cross-linking was observed when the samples were analyzed by SDS-PAGE. However, treatment with the cross-linking reagent increased the basal rates of GTPγS binding for all of the treated mutants (Fig. 49). Since this effect was observed for each mutant, the effect may be either a non-specific consequence of protein oxidation or a result of labeling one of the other ten cysteines in the protein. Treatment with BMOE did not have the predicted effects on the catalyzed exchange rates, and the untreated exchange rates have not yet been measured for comparison.

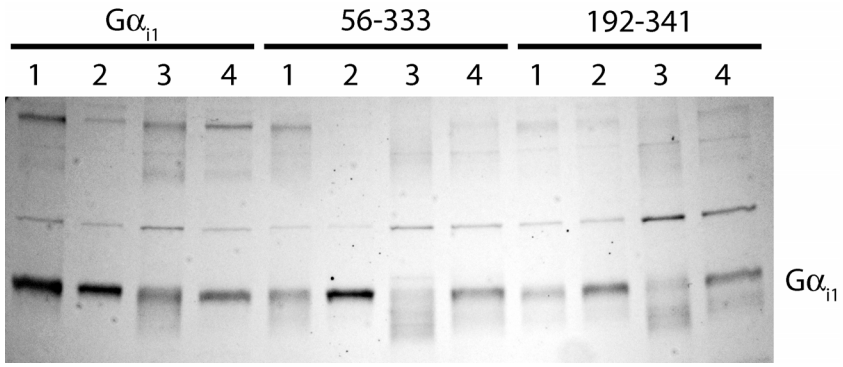

Figure 48 | SDS-PAGE analysis of CuPh-treated double cysteine mutants Samples of wild-type $G\alpha_{i1}$, 56-333, and 192-341 treated under oxidizing or reducing conditions were analyzed by SDS-PAGE. Lane 1 contains purified protein. Lane 2 contains purified protein treated with 1 mM DTT. Lane 3 contains CuPh-treated protein. Lane 4 contains CuPh-treated protein with loading buffer containing βME. The loading buffer used in Lanes 1-3 did not contain βME. This gel indicates that additional disulfide bonds are formed in the 56-333 and 192-341 mutants.

Although the consequences of BMOE modification are unclear from this preliminary experiment, this may prove to be a very useful technique to study conformational changes in G proteins. Some work remains to be completed to optimize the cross-linking conditions to prevent protein oxidation. Additionally, these double cysteine mutants should be introduced into our cysteine depleted base mutant, so that each pair of cysteines could be specifically labeled, thereby avoiding modification of the receptor-binding C-terminus and intermolecular cross-link formation. This would also allow a smaller excess of cross-linking reagent to be used. Once the appropriate system is in place, reagents of different linker lengths may be employed to more closely examine the conformational dynamics of this, or any, region of Gα.

Crystallographic study of a fast exchanging mutant $G\alpha_{i1}$

A serendipitous consequence of the double cysteine mutagenesis in $G\alpha_{i1}$ was the discovery of a fast-exchanging mutant, 56-333. This mutant has a 34-fold faster basal GTPγS-binding rate than the wild-type protein, which is 6.8-fold faster than even the R*-catalyzed rate of $G\alpha_{i1}$! (Fig. 50). Since this mutant has such a low affinity for GDP, it may structurally resemble the receptor-bound, nucleotide-free conformation of Gα. Moreover, a structure might provide insight into the mechanism of R*-catalyzed GDP release if the structural basis of the fast exchange rate could be identified. Although the structure of another fast exchanging mutant, A326S in $G\alpha_{i1}$, has been solved, it did not reveal any clues as to the mechanism of GDP release (Posner*, et al.*, 1998). Thus, in collaboration with Tina Iverson, Ph.D. and Michael Funk, crystallization trials of the 56-333 mutant were begun.

In addition to the purification steps described in Chapter II, the 56-333 eluent from anion exchange chromatography was further purified with gel filtration chromatography on a HiPrep™ 16/60 Sephacryl™ S-200 HR column (Amersham Biosciences, Piscataway, NJ) in buffer B containing 20 μM GDP and 10 mM βME. The purified protein was then buffer-exchanged into a low salt, AlF_4^--containing buffer (20 mM HEPES, pH 8.0, 1 mM EDTA, 2 mM DTT, 10 mM $MgCl_2$, 5 μM GDP, 16 μM $AlCl_3$, and

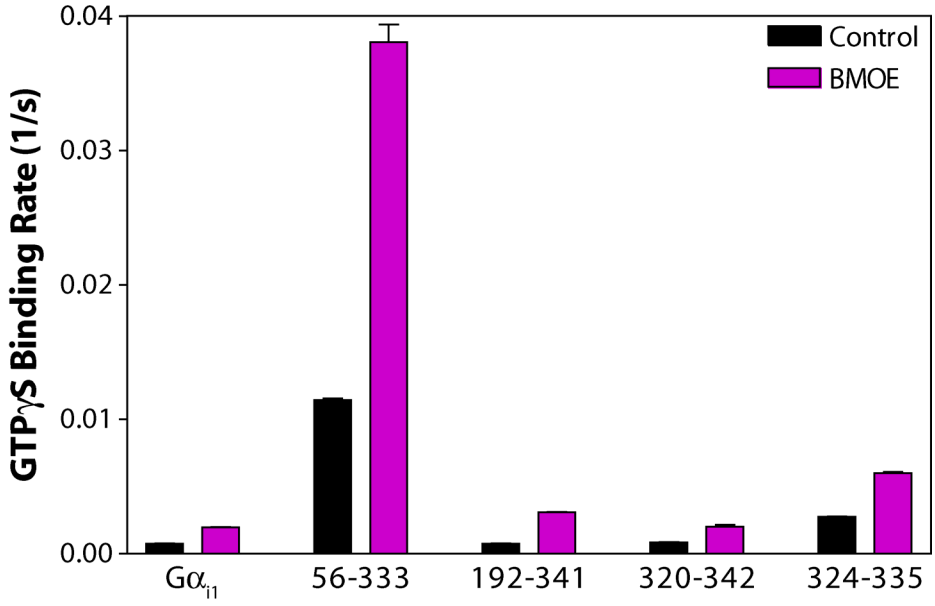

Figure 49 | Basal exchange rates of BMOE-treated double cysteine mutants BMOE treatment non-specifically increased the basal exchange rates of the double cysteine mutants examined.

40 μM NaF) prior to crystallization, which was performed using the hanging drop method. Protein drops (2-3 μL at 250-375 μM) were added to an equal volume of well solution containing 100 mM Bis-Tris, pH 5.5, 16% PEG 3350, 240 mM Li(CH_3COO), and 10 mM $SrCl_2$ or 100 mM guanidine-HCl and allowed to equilibrate for 4-5 days at 18 °C, although small bipyramidal crystals formed overnight (Fig. 51a). Crystals used for data collection were generally 50 μm × 50 μm × 25 μm or smaller and belonged to the spacegroup $P4_32_12$. Cryoprotection was performed by briefly equilibrating in well solution containing increasing concentrations of ethylene glycol, with a final concentration of 25%. Crystals were collected and flash cooled by plunging in liquid nitrogen.

In total, five data sets were collected from four crystals with a maximum resolution of 3.2 Å (Fig. 51b). All data were collected at the IMCA-CAT beamline at the Advanced Photon Source (Argonne National Laboratory, Chicago, IL). A wavelength of 1.0000 Å was used for screening and native collections on each of the four crystals, and an additional data set from a crystal diffracting to 3.5 Å was collected at 1.7712 Å for the purpose of single wavelength anomalous diffraction phasing from sulfur atoms. Native and sulfur data were indexed, integrated, and scaled using the programs DENZO and Scalepack (Otwinowski & Minor, 1997). Statistics for data collection and processing are provided in Table 3.

An initial molecular replacement solution was calculated from the data at 3.2 Å resolution using coordinates from the $G\alpha_{i1}$(GDP·AlF_4^-) crystal structure (1GFI) (Coleman*, et al.*, 1994a) in order to obtain the approximate location of the 17 endogenous sulfur atoms. These coordinates were read into SHARP (de La Fortelle & Bricogne, 1997) for determination of the sulfur anomalous intensities from which phases were calculated. Refinement of these initial phases was performed at 3.5 Å using MLPHARE and DM for solvent flattening (1994). At this resolution, sulfur phases alone proved insufficient to successfully interpret the data; phase combination with SIGMAA (Bailey, 1994) using coordinates from 1GFI as the starting model produced density maps ready for refinement. These coordinates were again used as a starting model for refinement and model building, which was carried out in the program O

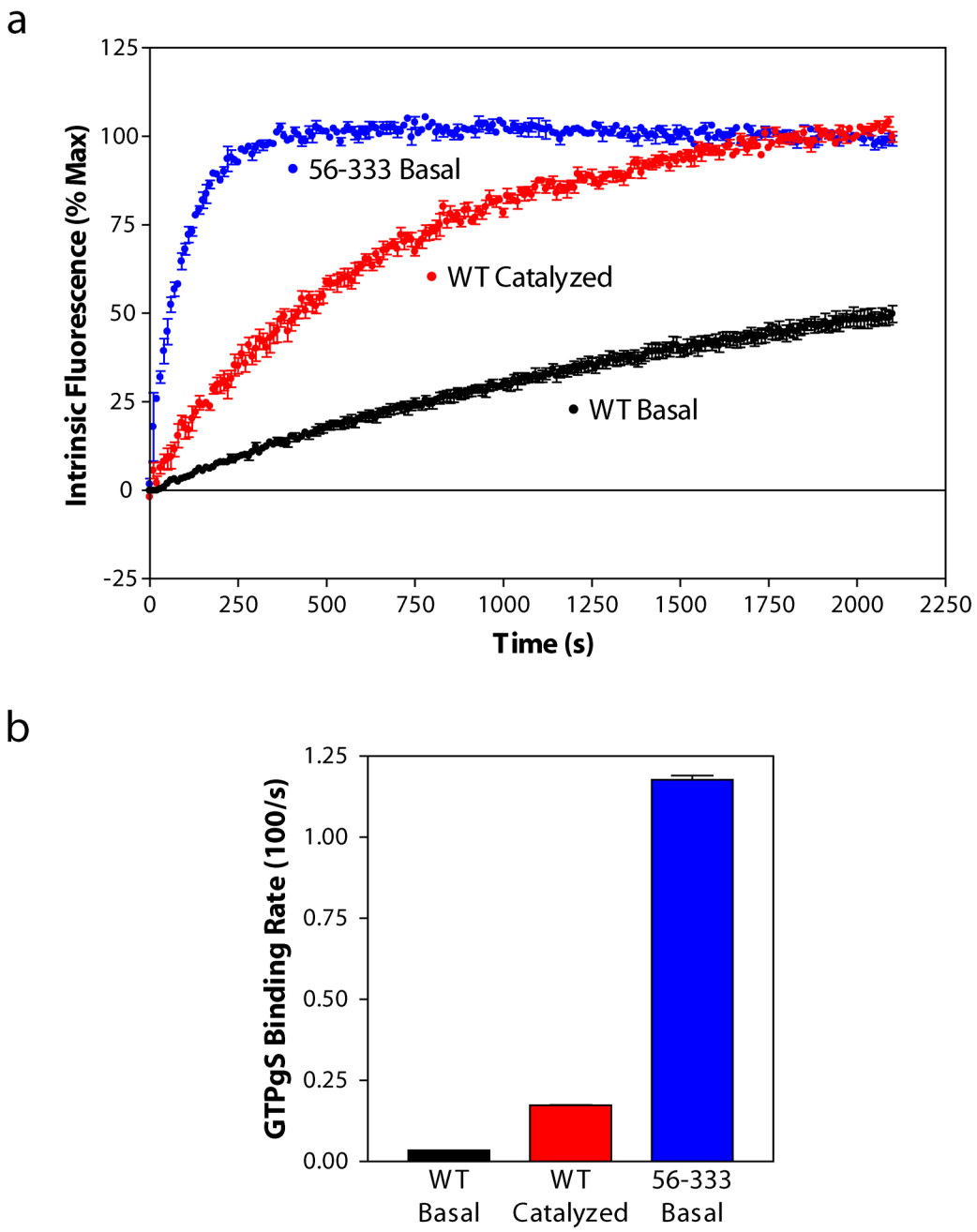

Figure 50 | Basal nucleotide exchange rate of the double cysteine mutant 56-333 (**a**) The 56-333 mutant (●) demonstrated a rapid increase in intrinsic fluorescence upon the addition of GTPγS, particularly as compared to the basal (●) and catalyzed (●) exchange rates of the wild-type protein. (**b**) Comparison of the exchange rates determined by nonlinear regression analysis of the curves in (**a**).

(Jones, *et al.*, 1991). Subsequent computational refinement was carried out in CNS (Brunger, *et al.*, 1998) and the CCP4 program REFMAC (Fig. 51c) (Bailey, 1994). Refinement statistics for the as yet uncompleted model are listed in Table 3.

In addition to refining the structure, several important biochemical studies must be completed to fully characterize this mutant. Although this mutant has a very fast exchange rate, the affinity of this protein for GDP and GTPγS must be measured directly with radionucleotide binding assays to determine how the mutation impacts the binding of these nucleotides. The effects of Gβγ on GDP dissociation and the stability of Gα will also be important to examine, as Gβγ inhibits GDP release and stabilizes the wild-type protein against irreversible inactivation at 37 °C. While Gβγ was able to stabilize the A326S mutant, it was unable to slow the release of GDP (Posner, *et al.*, 1998). Additionally, the interaction between this mutant and the receptor needs to be assessed in terms of catalyzed GTPγS binding and stabilization of a receptor-G protein complex in the absence of nucleotides. This mutation could also affect the GTPase activity and the ability of Gα to interact with RGS proteins. Each of these will be tested with GTP hydrolysis assays.

In light of the results described above, this double cysteine mutation may also be particularly sensitive to the redox potential of its environment, and the effects of oxidizing and reducing agents on its biochemical properties will be important to test. Similarly, single mutants or alanine mutants at these positions will help dissect the role of a putative disulfide bond in determining the phenotype of this mutant. Certainly the refined structure may suggest additional experiments, and crystallization screens for the GDP- and GTPγS-bound conformations of the 56-333 mutant are currently underway.

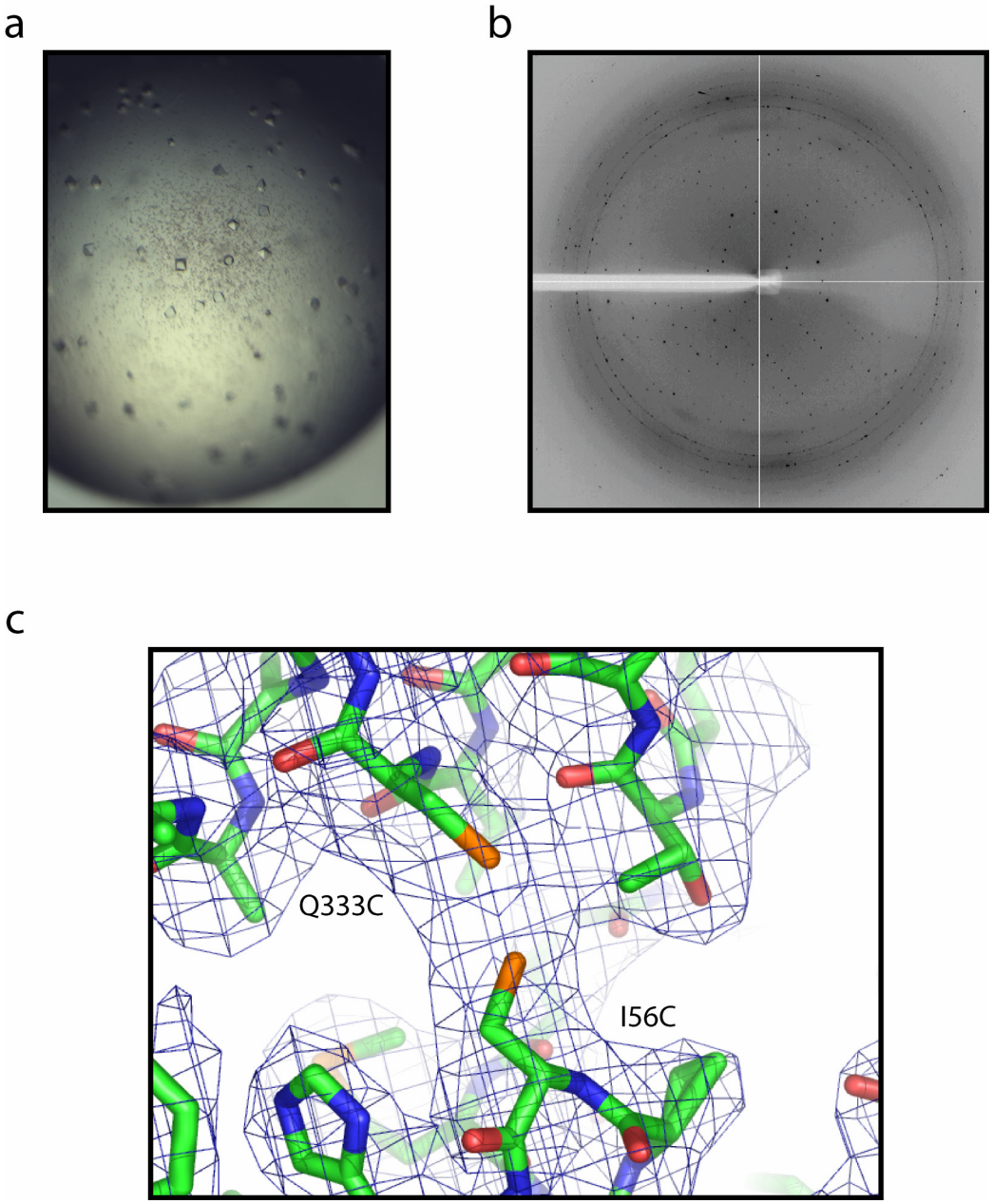

Figure 51 | Crystallographic data from the 56-333(GDP·AlF_4^-) double cysteine mutant (**a**) 56-333 crystals formed in well solution containing 100 mM Bis-Tris, pH 5.5, 16% PEG 3350, 240 mM $Li(CH_3COO)$, and 10 mM $SrCl_2$. (**b**) Diffraction pattern of the double mutant crystals to 2.9 Å collected with the IMCA-CAT beamline at APS at 1.0000 Å. (**c**) The F_o-F_c electron density map (*blue mesh*) was calculated using model structure factors and phases from a partially refined $G\alpha_{i1}$ structure (1GFI) (*green*). Preliminary refinement shows density that indicates a possible disulfide bond between 56C in the α1 helix and 333C in the α5 helix.

Table 3 | Data collection and refinement statistics for 56-333(GDP·AlF_4^-) crystals

Crystallographic Statistics		
	S Anomalous	Native
Wavelength (Å)	1.7712	1.0000
Maximum res.	3.50	3.20
Completeness	100% (100%)	99.3% (100%)
Reflections (Unique)	65,909 (5,060)	34,009 (6,498)
Redundancy	13.0	5.2
I/σ	62.9 (18.2)	30.14 (5.56)
R_{sym}	0.090	0.054

Sulfur Phasing Statistics	
No. of sites	17
R_{cullis}	0.937
Phasing power for bins:	
35-13.52	1.209
7.19	0.992
5.14	1.121
4.40	0.812
3.91	0.548
3.66	0.229
3.45	0.289
35-3.45 Å	0.495
Figure of merit	0.323

Refinement Statistics	
Res.	35-3.5 Å
R_{work}	0.3418
R_{free}	0.3831
RMS length deviation	0.0094 Å
RMS angle deviation	1.8186°

In Meso Crystallization Trials of Rhodopsin Complexes

Introduction

Despite extensive effort on the part of a number of investigators, no high resolution structures are currently available for an activated GPCR, let alone the R*-G protein complex. Indeed, the nucleotide-free conformation of Gα remains the only major G protein conformation for which atomic scale resolution remains unavailable. Membrane proteins are notoriously difficult to crystallize, and the crystallization of a membrane-bound protein-protein complex adds another layer of complexity. The cubic lipidic phase offers promise as a new technique for the crystallization of membrane proteins (Caffrey, 2003). In this method, detergent-solubilized protein is dispersed with lipid, typically monoolein, resulting in self-assembly of the cubic phase. A precipitant is added to trigger crystal nucleation and growth. Structures have been solved for multiple seven transmembrane-spanning proteins using this technique, including bacteriorhodopsin (1.55 Å) (Luecke*, et al.*, 1999), sensory rhodopsin II (2.1 Å) with (Edman*, et al.*, 1999) and without (1.93 Å) (Gordeliy*, et al.*, 2002) its transducer domain, and halorhodopsin (1.8 Å) (Kolbe*, et al.*, 2000). Using this approach, we screened for rhodopsin complexes with transducin and a high-affinity C-terminal peptide (Aris*, et al.*, 2001) in collaboration with Martin Caffrey, Ph.D. and Vadim Cherezov, Ph.D. in the Department of Chemistry at Ohio State University.

Materials

Urea-washed bovine ROS membranes (100 μM rhodopsin) and bovine transducin (70 μM in 20 mM Tris, pH 8.0, 10 mM $MgSO_4$, 10 μM GDP, 200 mM NaCl, 5mM βME, and 10% glycerol) were prepared as described in Chapter II. The high-affinity C-terminal peptide, Ac-MLRNLRDCGMF (1,397 g/mol; EC_{50} for Meta II stabilization = 9.9 μM) was synthesized as previously described (Aris*, et al.*, 2001). n-Heptyl-β-D-thioglucopyranoside (294.4 g/mol) was received from Anatrace, Inc. (Maumee, OH). All-*trans*-retinal (284.4 g/mol) was from Sigma-Aldrich, Inc. (St. Louis, MO). 9.9 MAG (356.5

g/mol) was obtained from Nu-Chek Prep, Inc. (Elysian, MN) and 7.7 MAG (300.5 g/mol) was synthesized by the David Hart, Ph.D. laboratory at OSU. The crystallization screens used were: Crystal Screen™ HT, Index™ HT, SaltRx™ HT, and MembFac™ screens from Hampton Research Corp. (Aliso Viejo, CA); JBScreen Membrane from Jena Bioscience GmbH (Jena, Germany); and MemStart™ from Molecular Dimensions, Inc. (Apopka, FL).

Rhodopsin solubilization

Rhodopsin was solubilized from ROS following Okada's selective extraction procedure (Okada, *et al.*, 2004). Briefly, 250 μL of ROS were centrifuged at 12,000 rpm at 15 °C for 15 min. The supernatant (~150 μL) was removed. The pellet was mixed with 41.5 μL of buffer containing 84 mM MES, pH 6.5, 7.95% HTG, and 386 mM $Zn(CH_3COO)_2$ for 1 min and centrifuged at 6,400 rpm at 15 °C for 1 min. There was not a clear separation of pellet and supernatant, and the detergent concentration was adjusted by the addition of 1 μL of 15% HTG. The sample was mixed for 1 min and left at 20 °C in the dark for 3 h. After incubation, the tube was centrifuged at 12,000 rpm at 15 °C for 5 min, and the resulting supernatant containing solubilized rhodopsin was collected. The rhodopsin concentration was determined to be 200 μM. All subsequent manipulations of solubilized rhodopsin were performed at room temperature in dim red light. Solubilized rhodopsin was stored on ice in the dark for three days prior to use in crystallization trials. Immediately before use, the rhodopsin solution was centrifuged at 12,000 rpm for 5 min to remove insoluble aggregates.

*Addition of all-*trans*-retinal to MAG*

All-*trans*-retinal was added to 7.7 MAG and 9.9 MAG lipids at a concentration of 1 mol% to increase the stability of rhodopsin complexes in the lipidic cubic phase. To this end, all-*trans*-retinal powder and lipid were combined in a small centrifuge tube. The tube containing 9.9 MAG was heated to 40 °C to melt the lipid, while the tube containing 7.7 MAG was manipulated at room temperature as the

lipid is liquid at this temperature. Both tubes were vigorously mixed until the lipid appeared transparent and uniform in color. All subsequent manipulations with all-*trans*-retinal were performed under dim light and the centrifuge tubes were covered in aluminum foil during mixing.

Crystallization screens

Solubilized rhodopsin (200 μM) was mixed with either transducin (70 μM) or peptide (7.15 mM) in 1:1 mol ratio and gently mixed. The rhodopsin/transducin solution became cloudy while the rhodopsin/peptide solution remained clear. Both solutions were mixed with either 7.7 MAG/all-*trans*-retinal (at 50% w/w lipid) or 9.9 MAG/all-*trans*-retinal (at 60% w/w lipid) using a lipid mixing device. Three types of samples were made, (1) rhodopsin/G_t in 9.9 MAG/all-*trans*-retinal, (2) rhodopsin/G_t in 7.7 MAG/all-*trans*-retinal, and (3) rhodopsin/peptide in 9.9 MAG/all-*trans*-retinal. Each solution formed transparent cubic phase upon mixing. Approximately 60-70 mg of each protein/lipid mixture was prepared. To activate rhodopsin, the syringe containing the lipid/protein cubic phase was illuminated by a 150 W white spectrum lamp for 2 min. After activation, the lipid/protein cubic phase was used directly in crystallization. Crystallization set-up was performed by the in meso robot using 50 nL cubic phase and 1 μL precipitant solution per drop. The commercial screen kits described above were applied to each protein/lipid combination in duplicate. In the case of rhodopsin/peptide in 9.9 MAG/all-*trans*-retinal only Crystal Screen™ HT and Index™ HT screens were duplicated due to a shortage of lipid/protein dispersion. Dim red light was used while the trays were prepared. Immediately after set-up, the plates were covered in aluminum foil and stored at 20 °C. In total, 32 plates, each containing 96 conditions, were made. Screening was performed manually four times during a period of 35 days using a microscope, and the results were recorded into spreadsheets using a 10-point scoring scheme. Photographs were taken with a Nikon CoolPix 995 digital camera attached to the microscope.

Results

Many screens containing phosphates (regardless of protein/lipid mixture) produced small crystallites (Fig. 52a) or needle clusters (Fig. 52b). Crystallites were colorless, either non-birefringent or had low birefringency, and formed predominantly in the lipidic cubic phase. However, in some cases, they were found in the bathing solution outside the cubic phase droplet. These crystallites are most likely formed by insoluble $Zn_3(PO_4)_2$ (Zinc was used to extract rhodopsin from ROS membranes and would be present in the rhodopsin solution). These crystallites were the only type of hits observed with rhodopsin/G_t in 9.9 MAG/all-*trans*-retinal.

More hits were identified with 7.7 MAG/all-*trans*-retinal trials. The most interesting was the formation of rod or plate-like crystals in the lipidic cubic phase in the presence of imidazole (10% w/v PEG-8000, 0.1 M imidazole, pH 8.0 with rhodopsin/G_t and 10% v/v 2-propanol, 0.1 M imidazole, pH 8.0 with rhodopsin/peptide) (Fig. 52c). These crystals were highly birefringent and most likely colorless, although it is hard to judge the color of crystals in the cubic phase due to the bright yellow-green background from the all-*trans*-retinal. Although it is possible that these crystals are due to the combination of zinc and imidazole (see Fernandez-Patron*, et al.*, 1995), no crystals were observed in these or similar solutions with rhodopsin/G_t in 9.9 MAG/all-*trans*-retinal.

The next group of hits is associated with high molecular weight PEGs. Crystals here typically look like bunches of fine, colorless plates (Fig. 52d). These were more frequently observed with the rhodopsin/peptide in 9.9 MAG/all-*trans*-retinal system. The last group of hits that formed in the lipidic cubic phase was observed in the presence of Li_2SO_4. These colorless and birefringent crystals were either plates or needles and were found both in the cubic phase and in the precipitant solution.

Discussion

Many crystalline hits were identified in this trial, however, many of them are likely zinc salts and all of them are colorless. Therefore, it is unlikely that any of them represent crystals of rhodopsin complexes. Although it is possible that some of the hits are crystals of G_t, peptide, or bleached rhodopsin,

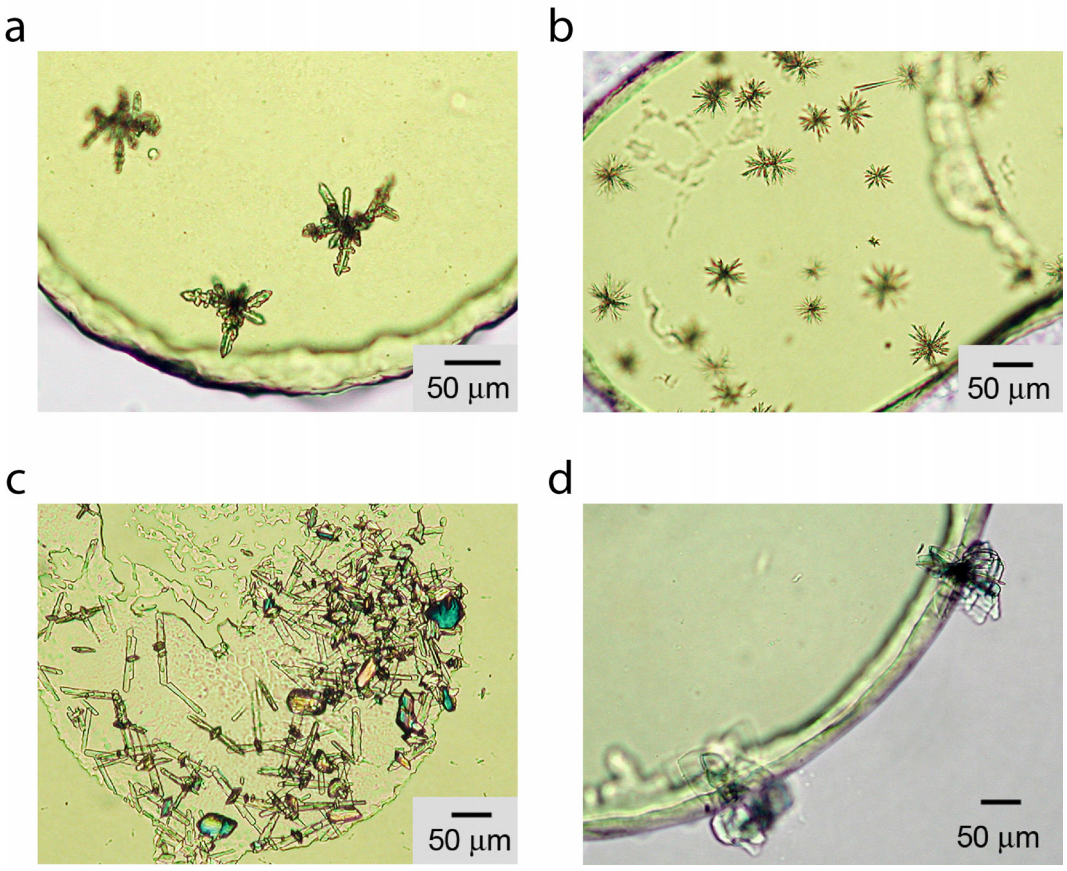

Figure 52 | Hits from an in meso crystallization trial (**a**) Rhodopsin/G_t in 7.7 MAG/all-*trans*-retinal + 100 mM NaH_2PO_4, pH 6.8, 15% PEG 2000, and 500 mM NaCl. (**b**) Rhodopsin/G_t in 9.9 MAG/all-*trans*-retinal + 100 mM Tris/HCl, pH 8.50, 100 mM NH_4HPO_4, and 12% w/v PEG 6000. (**c**) Rhodopsin/peptide in 9.9 MAG/all-*trans*-retinal + 100 mM imidazole, pH 7.8 and 10% v/v 2-propanol. Photograph was taken using polarized light. (**d**) Rhodopsin/peptide in 9.9 MAG/all-*trans*-retinal + 100 mM Tris, pH 6.9 and 20% w/v PEG 1000.

protein-free controls need to be done to test this possibility. The approach to this first screening attempt was to mix the proteins and hope for the best. Much more work remains to be done in order to characterize the rhodopsin-transducin complex in the lipidic cubic phase. A previous report demonstrated rhodopsin-dependent G_t activation in meso (Navarro*, et al.*, 2002), and fluorescence and UV-visible spectrophotometry may be used to study the stability of this complexes and identify the optimal ratios of the proteins. A similar approach may be used with the rhodopsin-peptide complex. Additionally, a higher affinity peptide sequence may be more suitable to use in these experiments. In addition to the proteins used in the study, the cubic lipidic phase may be modified with different lipids, detergents and additives. Recent work has identified a lipid that forms the cubic phase at low temperatures (Misquitta*, et al.*, 2004), which may be more suitable for these trials. Based on the optimized experimental conditions, new crystallization screens may be more successful in forming crystals of rhodopsin complexes.

BEST Analysis of G Protein Structures

Introduction

Structural and kinetic studies have provided extensive information about the molecular mechanisms of G protein function, however, much less is known about how changes in protein dynamics regulate the interactions between G proteins, nucleotides, and binding proteins. One experimental strategy to study the conformational flexibility of proteins is monitoring amide backbone hydrogen/deuterium exchange using NMR or mass spectrometry. Since the rate of exchange is proportional to the solvent-accessibility of the backbone amide, this technique can provide a wealth of information about protein structure and dynamics as well as changes due to ligand binding, covalent modification, and protein-protein interactions (reviewed in Hoofnagle*, et al.*, 2003). In 1996, Hilser and Freire developed a statistical thermodynamic formalism that could describe the hydrogen exchange behavior that is observed in proteins under native conditions reasonably well (Hilser & Freire, 1996). Since the current version of this algorithm, Biology using Ensemble-based Structural Thermodynamics,

or BEST, is freely accessible online (Vertrees*, et al.*, 2005), several of the numerous G protein crystal structures were subjected to this analysis in the hopes that this approach would provide some insight into the variations in G protein dynamics throughout the G protein cycle.

Theory

The unique approach adopted by the BEST algorithm is that, rather than treating a protein as a static structure, the algorithm generates an ensemble of conformational states. The protein ensemble is generated through the combinatorial unfolding of a set of predefined folding units, the boundaries of which are incrementally shifted to provide an exhaustive enumeration of that protein's partially folded states (Fig. 53) (Hilser & Freire, 1996). The Gibbs energy for each partially folded state is calculated based on changes in heat capacity, enthalpy, solvation entropy, and conformational entropy compared to the fully folded structure. These differences are determined based on the change in the solvent-accessible surface area of a region in the native conformation (based on the high-resolution structure) and the region in the unfolded state of the protein, except for the change in conformational entropy, which has been determined empirically for each amino acid. The Boltzmann weight of each partially folded state is determined from the calculated Gibbs energy, which provides the probability of each state in the ensemble. A more stable state will have a smaller Gibbs energy and a higher energetic contribution to the ensemble. Therefore, the more stable states will have a higher probability of being in the ensemble. From these probabilities, a residue-specific stability constant may be calculated that indicates the relative probability that a residue is folded *versus* unfolded in the states in the ensemble (*i.e.* a high stability constant indicates a higher folded probability) (Hilser & Freire, 1996). These residue-specific stability constants correlate to experimentally determined hydrogen exchange protection factors (Hilser & Freire, 1996; Hilser & Freire, 1997). Of course, residues with a higher probability of being folded are likely the more stable residues in the protein.

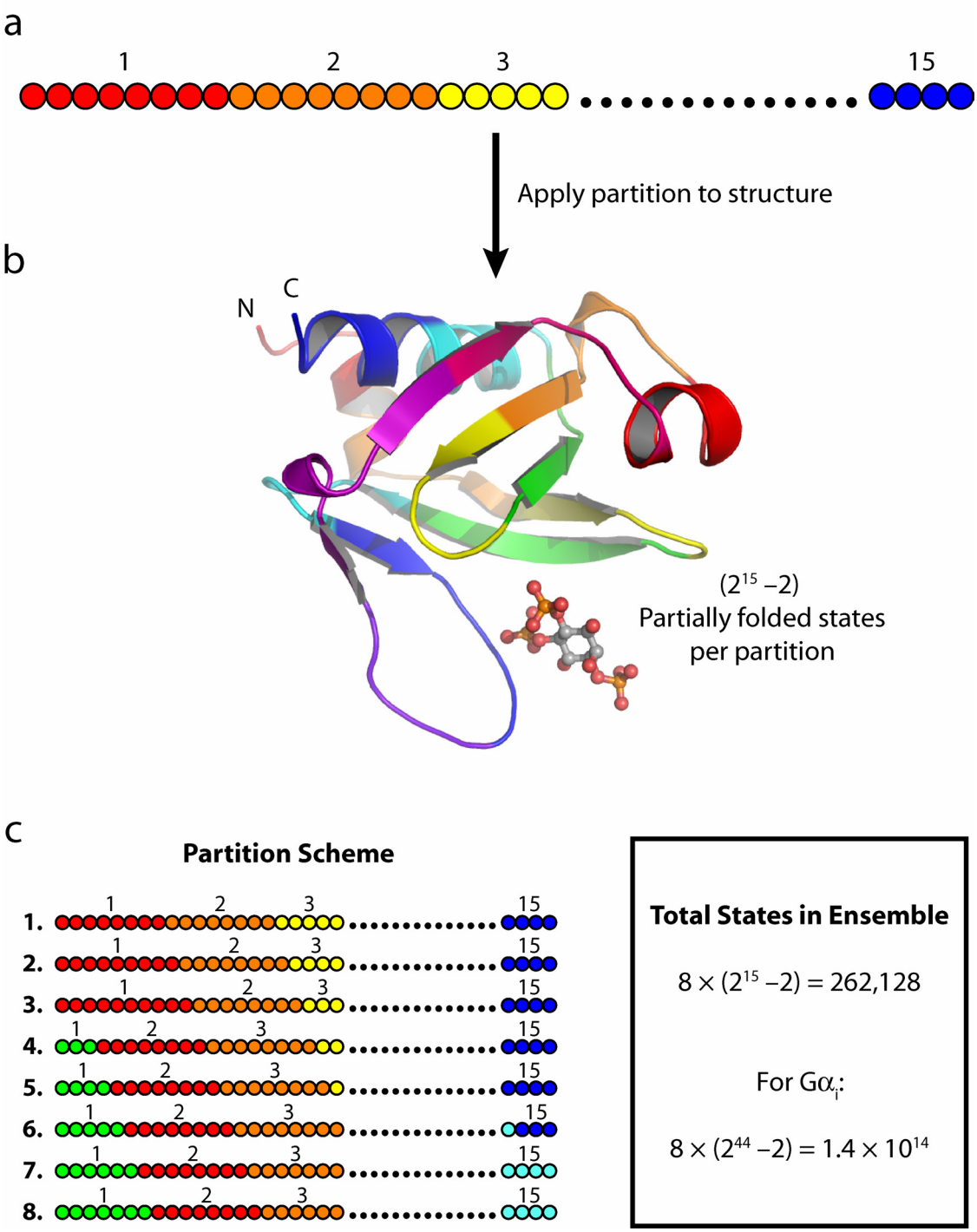

Figure 53 | Enumeration of the protein ensemble (**a**) The linear sequence of the protein is partitioned into folding units. (**b**) The folding units are applied to the three dimensional structure and all possible combinations of 'unfolded' and 'folded' states of each folding unit are created to define the ensemble. (**c**) The boundaries of the folding units are shifted to completely enumerate the possible folding states. Each unit must have a minimum of three amino acids; otherwise the ends are included with the adjacent unit.

Results

The residue-specific stability constants for the Gα subunit in several G protein crystal structures were calculated using the web-based portal for the BEST algorithm (Vertrees, *et al.*, 2005). Unfortunately, an exhaustive enumeration of the ensemble is computationally impossible for a protein as large as Gα. A 350-residue protein divided into 8-residue folding units equals 1.4×10^{14} partially folded states (Fig. 53). To account for this, a Monte Carlo simulation was employed to generate 150,000 partially folded states per partition, for a total of 1.2×10^{6} states in the ensemble. Using this method, the residue-specific stability constant for several different conformations of Gα were determined.

The first group of structures explored were $G\alpha_{i1}$(GDP), $G\alpha_{i1}$(GDP)βγ, and $G\alpha_{i1}$(GTPγS) (Fig. 54). In order to decrease the number of folding units in the heterotrimer, the atoms in PDB file for Gβγ were treated as heteroatoms, similar to GDP, so they would not be considered in the partitioning scheme, but they would still impact the solvent-accessible surface area of the atoms in Gα. Generally, the heterotrimer had higher stability overall, followed by the GDP-bound conformation, and the pattern of changes in the stability constant is similar for each structure. The least stable regions are found at the N- and C-termini and the helical domain. In the absence of Gβγ, there is less stability observed in the β2 and β3 strands as well. As expected, the most stable residues are located at the core of the protein near the nucleotide-binding pocket. Interestingly, Gβγ binding has a global stabilizing effect on the structure, which is consistent with the results from SDSL experiments that show a decrease in side chain mobility at residue 300 in the α4 helix upon heterotrimer formation (Chapter IV).

A similar comparison was made between the three conformations of $G\alpha_t$ (Fig. 55). Unlike the $G\alpha_{i1}$ structures, there were no global differences in the stability of one conformation *versus* another, although the most stable regions of the protein were more so in the presence of Gβγ. Surprisingly, one of the least stable regions of the G_t heterotrimer is Switch II (residues 199-219) according to this analysis.

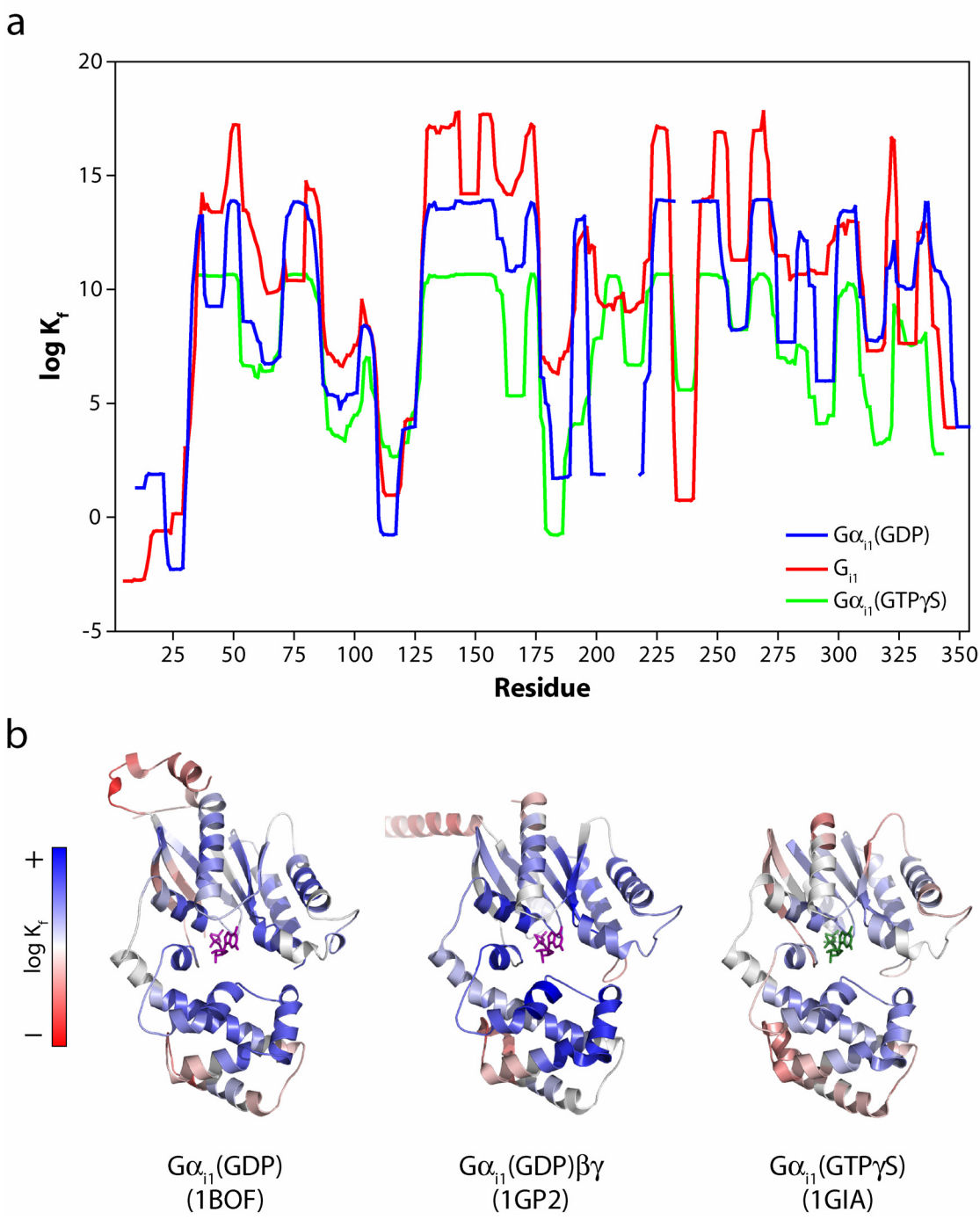

Figure 54 | Residue-specific stability constants for $G\alpha_{i1}$ structures (**a**) The log of the residue-specific stability constants are plotted as a function of primary sequence. (**b**) The stability constants have been mapped onto the appropriate $G\alpha_{i1}$ structure, where *red* indicates low stability and *blue* indicates high stability.

A similar pattern of stability constants was also recorded for the $G\alpha_t(GDP{\cdot}AlF_4^-)$ structure alone and in complex with RGS9 and RGS9 with PDEγ. The transition-state conformation generally had lower stability than the GTPγS-bound conformation, but the stability values were similar to the activation conformation in the presence of RGS9. However, PDEγ binding reversed these effects.

In addition to comparing different crystal structures, the stability constants in the presence or absence of nucleotide or Gβγ can also be calculated. These determinations were performed on the G_{i1} heterotrimer with the C-terminal tail of $G\alpha_t$ attached. Although some differences were observed between the four states, Gα(O), Gα(GDP), Gα(O)βγ, and Gα(GDP)βγ, the overall pattern was nearly identical.

Discussion

Clearly this is a less intensive approach to gaining insights into protein stability than measuring hydrogen exchange rates experimentally. However, there are some questions that remain about the interpretation of these results. One concern is that stability constants cannot be compared between two different crystal structures, as described above. The effects of the resolution, thermal factors, and other features of a crystal structure on the stability constants returned from this analysis are unclear, and may confound direct comparisons between different structures. Perhaps this concern can be alleviated by normalizing each pattern to the most and least stable structural regions in any given model prior to comparing the differences. Along similar lines, it is unclear how large a difference in the stability constant is significant. Within one structure it is very easy to see the relative differences in stability; however, this issue complicates the direct comparison of several structures. Finally, since all of the ensembles were generated using a Monte Carlo sampling protocol, although the same number of states was calculated for each conformation, multiple ensembles may have to be generated to obtain an accurate pattern of stability constants for comparison between structures. Indeed, these ensembles contain 1×10^{-6} % of the possible states in an exhaustively enumerated ensemble for Gα. Several iterations of ensemble

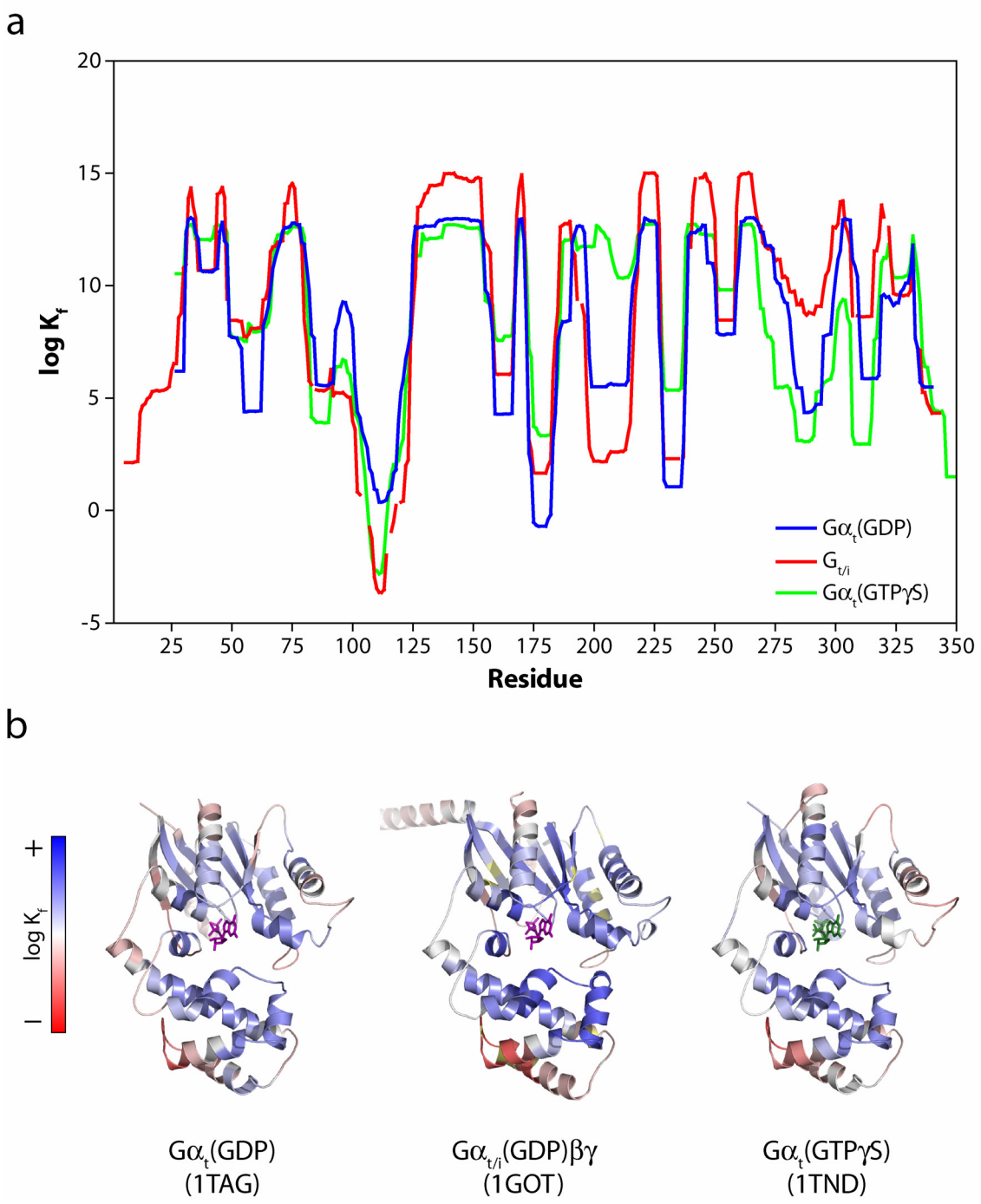

Figure 55 | Residue-specific stability constants for $G\alpha_t$ structures (**a**) The log of the residue-specific stability constants are plotted as a function of primary sequence. (**b**) The stability constants have been mapped onto the appropriate $G\alpha_{i1}$ structure, where *red* indicates low stability and *blue* indicates high stability. In the 1GOT structure, *yellow* sites are selenomethionine heteroatoms that were not considered in the analysis.

generation will need to be run for each conformation to accurately assess the fidelity of the Monte Carlo protocol.

Perhaps a more interesting use of the BEST algorithm is to explore the effects of ligand or protein binding on the stability of the protein. Connectivity between residues can be identified by exploring the ensemble to see if the folded status of a given residue impacts the folded status of another residue (Pan*, et al.*, 2000). This analysis can be extended to look at how the folded probability of any given residue correlates to the probability of a group of residues, like a ligand-binding site, being folded (Pan*, et al.*, 2000). Unfortunately, the ensembles themselves are not available from the web site, so it is impossible to examine each state in the ensemble to compare the folded status of two residues in this manner. However, this information may provide some important insight into the intramolecular connections between the nucleotide-binding pocket and protein-interaction surfaces on Gα. Until that data is assembled, this technique provides another simple method to explore changes in G protein dynamics, and, in its current form, may be most useful as a tool to guide future SDSL studies of the protein.

CHAPTER VIII

FUTURE DIRECTIONS

Assembling the Receptor-G Protein Complex

Perhaps the most important unanswered question regarding G protein function is how these proteins are activated by heptahelical receptors. Although there is experimental evidence supporting a variety of conformational changes that may lead to GDP release, these models are based primarily on the indirect evidence that mutagenesis can provide. Direct structural observation of R*-mediated conformational changes in G proteins is needed to identify how receptors are actually causing GDP release. Unfortunately, crystallographic approaches are hampered by the size and membrane-bound location of the receptor-G protein complex. Until such time as these technical challenges are solved, biophysical approaches, like SDSL, will be invaluable to test specific hypotheses and explore the nucleotide-free conformation of the G protein. From the work described here, the most important next steps are to complete the survey of Gα for receptor activation-dependent conformational changes, model the observed structural changes, and measure intermolecular distances between the receptor and G protein to assemble a model of the complex based on these experimental constraints.

Additional targets for SDSL in Gα

Our lab has already completed an extensive SDSL study of Gα, but has primarily focused on a few structural regions, the N-terminus (Medkova*, et al.*, 2002; Preininger*, et al.*, 2003), the α5 helix (Chapters III and VI), and Switches I and II (Chapters IV and V). Several other interesting structural elements remain to be explored. The α3 helix connects the R*-binding α3/β5 loop to the nucleotide-binding pocket at Switch III (Grishina & Berlot, 2000), and a point mutation in Switch III has recently

been shown to stabilize the nucleotide-free G protein (Pereira & Cerione, 2005). In addition to potential R*-mediated conformational changes, this region plays an important role in G protein activation and interaction with effector proteins. Interdomain interactions between Switch III and the αD/αE loop have also been shown to regulate basal nucleotide exchange in $G\alpha_s$ (Grishina & Berlot, 1998). Similarly, several mutations at the interdomain interface affect basal and receptor-catalyzed nucleotide exchange rates (Marsh*, et al.*, 1998; Warner*, et al.*, 1998; Grishina & Berlot, 1998; Warner & Weinstein, 1999), although there is some controversy as to the role these interactions play in G protein activation (Marin*, et al.*, 2001a). Interestingly, 171R1 in Linker 2 at the interdomain hinge becomes immobilized upon binding R*, and mutagenesis of the linker regions has significant effects on nucleotide exchange (Heydorn*, et al.*, 2004; Majumdar*, et al.*, 2004; Kostenis*, et al.*, 2005). These regions, the α3 helix, Switch III, and the interdomain cleft, will be the most important future targets of SDSL studies of Gα to test for receptor activation-dependent conformational changes. In addition, these sites have already been shown to undergo interesting structural changes crystallographically. Switch III undergoes a significant structural rearrangement upon binding GTP and subtle differences in the relative orientation of the GTPase and helical domains have been observed in different G protein conformations (activated conformations adopt a more closed orientation). Thus, the exploration of these regions with SDSL will surely provide fascinating insight into G protein dynamics.

Another relatively straightforward, but important, experimental question is whether myristoylation of Gα has an impact on the conformational changes observed with EPR. All of the studies described here were completed with non-myristoylated proteins, as these are much easier to express and give greater yields than the myristoylated proteins. However, myristoylation certainly affects the structure of the N-terminus of Gα (Preininger*, et al.*, 2003), and plays an important role in membrane localization. At minimum, myristoylation should increase the percentage of G protein bound to the receptor by increasing the concentration on the membrane, providing a clearer picture of the spectral changes observed upon formation of the R*-G protein complex. A more exciting possibility is that

myristoylation will influence the conformational changes observed in the G protein upon GDP release. At first, several of the most interesting single sites should be explored as myristoylated proteins, followed by a systematic examination if interesting results are found. Although it is difficult to speculate about the effects of myristoylation on R*-mediated conformational changes, this lipid modification would provide an additional anchoring point for the protein, which may facilitate certain conformational changes. Interestingly, the effects of myristoylation on the basal and receptor-catalyzed nucleotide exchange rates seem to be unknown, so the influence of this moiety on receptor-G protein interactions remains relatively uncharacterized.

Modeling the R-bound, nucleotide-free conformation of Gα*

Once receptor activation-dependent conformational changes have been identified, additional studies are required to characterize the nature of the conformational change in any given region. Part of this analysis includes a systematic SDSL study of the region, from which a detailed model of the conformational change may be developed. Another part relies on interspin distance measurements to quantify the magnitude of the structural changes. These distance constraints can be combined with computational approaches to develop a sophisticated model of the R*-bound G protein conformation.

Careful analysis of the mobility changes observed for spin-labeled side chains in and around the α5 helix suggests a 30° rotation and translation of the helix. Preliminary distance measurements between 187R1 and 333R1 before and after receptor activation are exactly consistent with this model; however, this single distance measurement is not sufficient to constrain a precise conformational change. Several additional double cysteine mutants have been constructed, but the distances between the spin-labeled side chains have been measured with varying degrees of success (Table 4). While some of these measurements may improve with repetition, it is likely that additional mutants must be made to measure enough experimental distances to define the nucleotide-free orientation of the α5 helix. Furthermore, myristoylation may increase the number of R*-G protein complexes formed, thereby improving the

resolution between the signal from the free and bound G proteins, enabling a more accurate distance determination. Once an adequate set of interspin distances has been collected, it can be used to constrain steered molecular dynamics simulations to generate models of the R*-bound conformation of the α5 helix (Israelewitz*, et al.*, 2001).

Care must be taken in the interpretation of interspin distances. While an increase in the distance between two nitroxides may be due to a separation of their structural elements, it may also be due to changes in the rotamer conformation of the R1 side chain. Ideally, distances should be measured between two sites where the single-site EPR spectra are the same before and after the conformational change. Where this is not possible, sites at the solvent-exposed surface of α-helices have predictable rotamer conformations (Mchaourab*, et al.*, 1999; Langen*, et al.*, 2000; Altenbach*, et al.*, 2001), which can be accounted for in the modeling process. Additionally, the use of multiple, overlapping pairs of labeled sites can help define the position of the R1 side chain. This is particularly important when the EPR spectrum indicates tertiary interactions that may affect the side chain conformation. Fortunately, the development of DEER EPR allows R1 pairs to be introduced at greater distances, increasing the options for spin-label placement and reducing concerns that closely-placed spin labels will alter the conformation of R1 relative to the singly-labeled mutant.

Improving models of the R-G protein complex*

Although enough data has been accumulated to begin to develop rudimentary models of the receptor-G protein complex that meet some of the important experimentally-derived structural constraints (Slusarz & Ciarkowski, 2004; Fotiadis*, et al.*, 2004; Ciarkowski*, et al.*, 2005), the currently available information about point-to-point interactions between the proteins remains sparse and the structural resolution of these models remains too low to answer questions about determinants of receptor-G protein specificity or the mechanism of activation. Many experiments remain to be done in order to refine our current models of this complex.

Table 4 | Summary of double cysteine mutants for distance measurements Each of the following double mutants has been constructed in the cysteine-depleted base mutant. Experimental results are indicated by the following: (●) unsuccessful, (●) successful, and (●) undetermined.

		CW	DEER	Notes
Double mutants to examine the R-mediated movement of the α5 helix*				
187	333	●	●	6 Å increase
191	320	●	●	Poor signal:noise
191	330	●	●	Too far for CW; DEER candidate
191	333	●		Too close for distance measurement
191	334	●		No change with R activation; binding?
320	330	●	●	Poor signal:noise
320	333	●	●	2 Å decrease
320	334	●	●	
321	333	●	●	Distances not consistent with modeling
300	333			Made construct
305	330		●	Surprising 6 Å increase
305	333			No expression
Additional double mutants				
21	333			Made construct
29	330			Expresses
106	273			No expression
106	330		●	45 Å distance in HT

Particularly important information will come from intermolecular distance measurements between the receptor and G protein. Two large libraries of single cysteine mutants have been generated in rhodopsin (Hubbell*, et al.*, 2003) and $G\alpha_{i1}$. Initially, relatively few long-range distance measurements would be necessary to define the relative orientation of the receptor and G protein, which is a fundamental but unanswered question about the complex. Once the proper orientation has been established experimentally, the model will suggest additional distance measurements that will be necessary to "pin down" intracellular loops onto the surface of the G protein. Proceeding in such an iterative fashion should provide the experimental evidence that is critically important in refining the current models of the receptor-G protein complex.

Any improvements in the models of the components of the complex will enhance our model of the complex itself. The current R*-G protein models were assembled from an R* model based on the inactive crystal structure of rhodopsin and biophysical constraints, a crystal structure of the GDP-bound G protein heterotrimer, and NMR structures of C-terminal peptides of Gα and Gγ. While the current models do not account for the conformational changes in the G protein that cause GDP release, the biophysical studies described in this work will provide the foundation for incorporating this information. Similarly, the crystal structure of the fast-exchanging 56-333 mutant may provide a better approximation for the R*-bound G protein than the currently available structures. Success in developing a SDSL system to study G protein dynamics, and the insight to use rhodopsin as the receptor, affords a unique opportunity to provide critical structural information on the R*-G protein complex. By far, the most exciting future direction of this work is modeling the interaction based on experimentally-derived distance constraints from DEER EPR.

Mapping Conformational Changes Along the Inactivation Pathway

The major focus of the SDSL studies of Gα has been the conformational changes leading to G protein activation. Future work should use these same cysteine mutants to explore the structure and dynamics of Gα through GTP hydrolysis and reassociation of the heterotrimer. Initially, EPR spectra for the Gα(GDP·AlF_4^-) and Gα(GDP·AlF_4^-)·RGS conformations should be compared to the GDP- and GTPγS-bound conformations that have already been recorded. Although the crystal structures of activated Gα are virtually the same as the transition state, differences in the dynamics, particularly near the nucleotide-binding pocket, may be observed with EPR. Presumably the transition state conformation would have decreased dynamics compared to the GTPγS-bound conformation, however, there may not be any differences at all based on the observation from the crystal structures. While the effects of AlF_4^--binding are not necessarily obvious, RGS binding should certainly immobilize the Switch regions as it interacts with them to stabilize the transition state for GTP hydrolysis. RGS binding may have a similar effect of dampening backbone motions throughout Gα as Gβγ binding does (300R1 and 320R1). The reagents have been developed to perform these simple characterizations, and excitingly, unexpected structural changes may pop up in this analysis that would not have been identified otherwise.

Following these relatively straightforward measurements, more complicated studies could be performed. Using time-resolved EPR measurements, it would be possible to follow changes in the dynamics of the protein during GTP hydrolysis. The spin-labeled proteins could be loaded with GTP in the absence of Mg^{2+}, and after recording a baseline spectra, the GTPase could be activated by the addition of Mg^{2+} through a stop-flow apparatus in the presence or absence of an RGS protein. One advantage of these studies is that it is much easier to obtain high concentrations of a more homogeneous population of Gα conformers than the activation studies described in this work, enabling kinetic measurements where signal quality is sacrificed for rapid acquisition.

Several mutations in Gα have been described that affect the GTPase activity of the protein, including G42V and G203A that stabilize a Gα(GDP·P_i) complex that has been characterized crystallographically (Berghuis*, et al.*, 1996; Raw*, et al.*, 1997). These structures reveal a large conformational change in Switch II and less striking changes in Switch I. Since these two different mutations stabilize a similar Gα conformation, it seems likely that this is a transient intermediate state of the wild-type protein during GTP hydrolysis. A K180P mutation in Switch I seems to accelerate a conformational change in the Switch regions, but decreases the rate of GTP hydrolysis, suggesting that this transition is an obligatory step leading to bond breakage (Thomas*, et al.*, 2004). These mutations can be engineered into the cysteine mutants used in SDSL studies to test the hypotheses suggested by the crystal structures. This biophysical approach will yield much more insight into the role of Switch dynamics in GTP hydrolysis than crystallography can. Moreover, EPR is perfectly suited to address the impact of these mutations on Switch dynamics. Certainly, the structural changes associated with G protein inactivation are not yet completely understood, and these should be one of the next targets of SDSL studies.

Alternate Approaches to Study G Protein Dynamics

Site-directed labeling

In a similar approach to SDSL, fluorescent labels may be incorporated into proteins to probe conformational dynamics. For example, steady-state fluorescence measurements can monitor changes in environmental polarity, fluorescence anisotropy is related to the mobility of the fluorophore, and quenching reagents may be used to determine the solvent accessibility of the fluorophore (Mansoor*, et al.*, 1999). A little surprisingly, this light-based technique has been used successfully to study the activating conformational changes in the photoreceptor, rhodopsin (Dunham & Farrens, 1999; Janz & Farrens, 2004). Recently, the interaction between arrestin and rhodopsin has been examined with site-directed

fluorescent-labeling (Sommer*, et al.*, 2005), which provides encouragement for adopting this approach to study receptor-G protein interactions. A SDFL approach may provide complementary information to the SDSL data that has been accumulated. Additionally, the fluorescence of the bimane probe used in these studies is quenched by tryptophan residues, which suggests an additional means to test conformational changes within the protein by using cysteine-tryptophan double mutants.

As an alternative to using labels to monitor conformational changes in Gα, it should be possible to map protein-protein interaction surfaces by measuring the effects of complex formation on the accessibility of the cysteine residue to thiol-reactive molecules. For example, cysteines that are buried in the R*-G protein interface would be protected from modification by thiol-reactive reagents upon R* binding. Determining the extent that binding to R* protects residues from labeling would complement our results from SDSL studies. Although the striking decreases in the mobility of spin-labeled side chains at the C-terminus of Gα is most likely due to direct contact interactions with R*, this experiment would offer additional evidence to support that conclusion. Using reagents with different sizes and chemical properties would also help define a particular interface (*i.e.* a site that is accessible to small molecules, but not bulky reagents is more buried than a site accessible to both) (Hofmann & Reichert, 1985). Certainly, this extensive library of $G\alpha_{i1}$ cysteine mutants combined with the vast number of sulfhydryl-modifying reagents available opens nearly every region of Gα for exploration with a variety of creative experimental approaches.

Hydrogen-deuterium exchange mass spectrometry

As mentioned previously, one experimental strategy to study the conformational flexibility of proteins is monitoring amide backbone hydrogen/deuterium exchange using mass spectrometry. As a protein incubates in the presence of the heavy isotope of hydrogen, deuterium, hydrogen atoms in the protein exchange for deuterium atoms in the solvent, thereby increasing the mass of the protein. Since hydrogens covalently bound to carbon atoms do not exchange and hydrogen atoms on side chains

exchange very quickly, only the increase in the mass due to the exchange of amide hydrogens is detected by mass spectrometry. As a consequence of this chemistry, there is only one site available for labeling on each amino acid, except for proline. Therefore, the hydrogen exchange rates can be measured for each amino acid over the length of the entire protein. The labeling reaction is quenched by reducing the pH to 2.5 and placing the reaction on ice. The protein can be cleaved with pepsin, and the peptides are separated by reverse phase chromatography prior to injection on the mass spectrometer.

Since the rate of exchange is proportional to the solvent-accessibility of the backbone amide, this technique can provide a wealth of information about protein structure and dynamics as well as changes due to ligand binding, covalent modification, and protein-protein interactions. Moreover, there is no limitation on the size of the protein, small amounts of protein are required, and membrane proteins are accessible to this technique (reviewed in Hoofnagle*, et al.*, 2003).

Surprisingly, HXMS experiments have not been performed on heterotrimeric G proteins or complexes that contain them and a wealth of information on G protein dynamics would be available from very simple preliminary experiments. As a first step, exchange rates can be compared between the GDP- and GTPγS-bound conformations of the Gα subunit alone. These data could be compared to our own SDSL results, as well as the G protein crystal structures and the output from BEST analysis of them (Chapter VII). Once the experimental conditions have been optimized with Gα alone, increasingly complex conformations can be studied as Gα binds Gβγ and the activated receptor. These studies should define the interaction surfaces on all partners and identify regions where the dynamics are altered due to complex formation. The clear advantages of this technique are the use of native proteins and the ability to study all proteins involved in the complex simultaneously. When interpreted in terms of the rhodopsin and G protein crystal structures, these data should provide important information on the structure of the R*-G protein complex and might hint at structural changes leading to GDP release.

Mapping allosteric connectivity with computational approaches

Collectively, the group of G protein crystal structures provides a rich data set for computational studies of G protein biophysics. Moreover, the Gα subunit is particularly interesting in that it cycles through at least six limit conformations, Gα(GDP), Gα(GDP)βγ, R*·Gα(O)βγ, Gα(GTP), Gα(GDP·AlF_4^-), Gα(GDP·P_i), in addition to its interactions with a variety of regulatory proteins, including receptors, effectors, GAPs and GDIs, each of which specifically interacts with different surfaces of Gα or different conformations of the protein. One of the fundamental problems in understanding the complex interplay between the occupants of the nucleotide-binding pocket and various regulatory proteins is the identification of the allosteric or intramolecular signaling pathways in Gα subunits. Several elegant computational approaches have been developed to address these fundamental questions in signal transduction.

Two methods are based on the hypothesis that, over the course of evolution, functionally important amino acids in proteins will not be mutated, while unimportant amino acids will vary. In the evolutionary trace analysis (Lichtarge*, et al.*, 1996b), a multiple sequence alignment is generated for a given family of proteins and the individual members of the family are clustered together with their closest relatives based on their relative sequence identity. Then, a consensus sequence is generated for each cluster, and if an amino acid varies at a given position, it is left blank. The consensus sequences for all of the clusters are then aligned to provide the evolutionary trace. A residue is either conserved if it is the same in all of the consensus sequences, class-specific if it varies among the consensus sequences, or neutral if it is blank in any one of the consensus sequences. The conserved and class-specific amino acids can then be mapped onto the crystal structure, and will identify functionally important areas of the protein. When applied to heterotrimeric G proteins, the evolutionary trace identified subunit interfaces, receptor and effector interaction sites (Lichtarge*, et al.*, 1996a).

Statistical coupling analysis is an extension of the evolutionary trace (Lockless & Ranganathan, 1999). This method uses a very large multiple sequence alignment to identify statistical interactions

between any two amino acid positions in the protein, and is based on the additional hypothesis that functional coupling between any two sites in the protein should mutually constrain the evolution at those two sites. In this approach, conservation is defined as the deviance of amino acid frequencies at a given position from their average abundance in all proteins in nature. Statistical coupling is the extent to which an amino acid at one site changes in response to a perturbation at another site. This analysis predicted long-range interactions with the ligand-binding site in the PDZ domain family, which were subsequently verified by mutagenesis (Lockless & Ranganathan, 1999). When SCA was applied to the G protein superfamily, including the monomeric G proteins, a network of amino acids was identified that surrounds the nucleotide-binding pocket and links it to the effector-binding surface at the switch regions (Hatley*, et al.*, 2003). Interestingly, this connectivity is only observed in the GTP-bound conformation of the G proteins, but not in the GDP-bound conformation. Since mutations in this allosteric network significantly affected the nucleotide sensitivity of the interactions between $G\alpha_s$ and $G\beta\gamma$ or AC, these residues likely form a core allosteric network conferring nucleotide-dependent switching in G proteins (Hatley*, et al.*, 2003).

Unfortunately, the SCA approach is limited by the large sequence alignment that must be assembled for statistical analysis in order to identify coupling energetics, and it is unable to provide a physical explanation for the coupling between two residues, whether it be ligand specificity, structural stability, folding or intramolecular signaling. An alternative method that follows anisotropic thermal diffusion through proteins has recently been described to identify intramolecular signaling pathways (Ota & Agard, 2005). In the ATD method, a protein is energy minimized and equilibrated to 10 K with molecular dynamics, which essentially "freezes" each atom. Then, a particular region of interest is "heated" to 300 K, and the propagation of the kinetic energy is followed by the deviation of atoms from their positions in the minimized structure in subsequent dynamics simulations. Interestingly, the energy propagates along defined pathways that highlight the physical connectivity of intramolecular signaling pathways. When this approach was applied to a PDZ domain family member, the results were consistent with the SCA pathway, but provided a more direct physical connection between the binding pocket and

distant residues (Lockless & Ranganathan, 1999; Ota & Agard, 2005). This method would be very useful to trace the connectivity between bound nucleotides and protein-protein interaction surfaces in G proteins, particularly the receptor-binding surface. Since the monomeric G proteins were included in the SCA analysis (Hatley*, et al.*, 2003), connectivity to the receptor-binding site could not be addressed by this method. The ATD technique provides an interesting new way to explore the current models of the receptor-G protein complex, and the interface between these proteins.

Certainly the G protein system is an excellent example of how the allosteric connectivity between proteins is as important as the connections within a protein. Since this intermolecular communication must occur through the sites of contact, it becomes an important theoretical question to ask if protein-protein interaction surfaces can be identified based on other structural information. One method is to analyze the surface of a protein in search of areas with favorable energy exchange when buried in a protein-protein interaction (Fernandez-Recio*, et al.*, 2005). This approach identifies optimal docking areas by finding the area with the lowest docking surface energy centered on each of a series of randomly assigned surface points (Fig. 56). When the structure of $G\alpha_{i1}$ from the heterotrimer crystal structure was examined with this algorithm, two potential protein-protein interaction surfaces were identified, the region around the $\alpha 5$ helix and the helical domain (Fig. 56). Surprisingly, the $G\beta$-binding interface was not identified even despite the use of the heterotrimeric conformation of $G\alpha$ as the input for the analysis.

Computational tools for analyzing protein structure are becoming increasingly sophisticated. Although these tools cannot replace hard experimental data, they can be invaluable as "pre-experiments" that provide a glimpse of what to expect or "post-experiments" that aid in the analysis and interpretation of the experimental data. Furthermore, a computational approach may provide data that would not be immediately accessible experimentally, and as these algorithms are increasingly used, the correspondence between the *in silico* result and the experimental result should continue to increase. Heterotrimeric G proteins are an excellent proving ground for these applications as they help to address many of the issues

of interest to theoretical structural biologists, such as the role of protein dynamics in function, tracing allosteric connectivity in proteins, and the regulation of protein-protein interactions, among others.

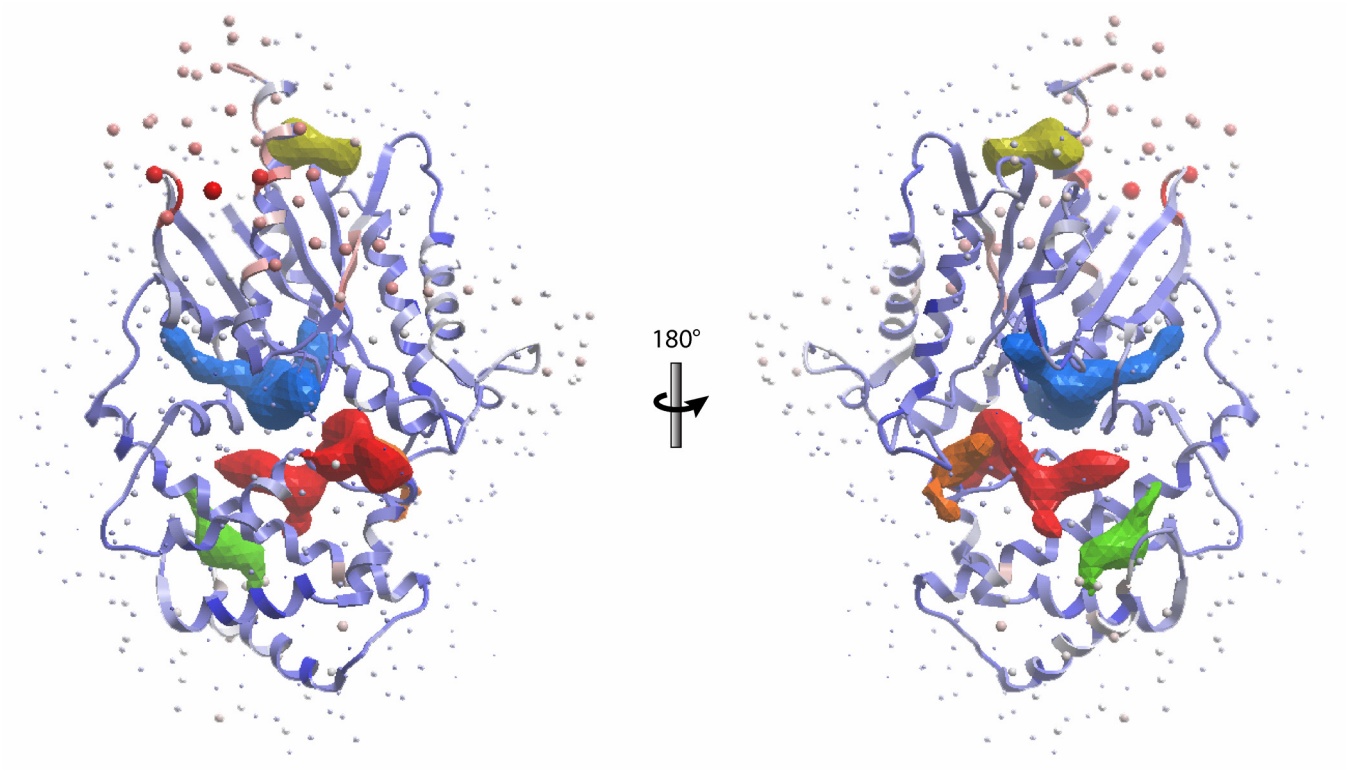

Figure 56 | Optimal docking areas in $G\alpha_{i1}$ In order to identify ODA, a network of points is assigned to the surface of the protein (*colored spheres*). For each sphere, the lowest energy docking surface is chosen from a series of surfaces centered on each surface point. The size and color of the surface points identifies the ODA (*large red spheres*) in this N-terminally truncated $G\alpha_{i1}$ subunit from the G_{i1} heterotrimer (1GP2). The colored meshes describe potential ligand-binding pockets in the G protein (An*, et al.*, 2005). Indeed, this analysis identified the nucleotide-binding pocket (*blue mesh*).

CHAPTER IX

PERSPECTIVE AND CONCLUSIONS

As seems only fitting, the unanswered questions about the structural basis for function in heterotrimeric G proteins are framed in terms of what is not known from the many crystal structures of these proteins in a variety of conformations and complexes. For example, the amino and carboxyl termini of Gα play key functional roles in mediating its interaction with regulatory proteins, yet limited structural information for these regions is available from crystallography. Furthermore, answers to some of the most important questions in G protein signaling await a better understanding of the structure of the receptor-G protein complex, including agonist-mediated conformational changes in receptors, point-to-point interactions between the receptor and G protein, the transition leading to GDP release, the structural determinants of R*-G protein specificity, and the functional role of receptor dimerization in G protein activation. Although low resolution models have been described that address all of these issues, the strongest evidence in favor of any structural hypothesis comes once it has been captured on film.

In the meantime, the biophysical approaches described in this work offer an excellent alternative approach to addressing issues relating to G protein function. By far, the most exciting result of the SDSL of Gα is the identification and characterization of receptor activation-dependent conformational changes in the α5 helix that couple receptor binding to GDP release. Previously, exploration of the R*-G protein complex was not technically possible and models of R*-catalyzed GDP release were based on the results of mutagenesis studies. Even though a given mutation can alter the nucleotide exchange rate, the receptor does not necessarily use a similar mechanism. For this reason, the importance of testing specific conformational changes with direct observation cannot be overstated.

In addition to providing structural information for unknown protein conformations, SDSL reports dynamic information that is not necessarily evident from crystallographic analysis. For example, a

comparison of the GDP- and GTPγS-bound crystal structures of Gα suggests that G protein activation immobilizes the Switch regions, while SDSL reports amplified backbone dynamics of Switch II in that conformation. Similarly, the striking decreases in the mobility of residues 300 and 320 upon binding to Gβγ could never have been predicted from examination of the structures. As more and more sites are selected for spin-labeling, equally interesting results will likely be identified relating to interdomain movements, effector binding, and GTP hydrolysis. Unfortunately, SDSL is not adequate on its own to follow these allosteric connections through the protein, and computational approaches may help to explain these interesting experimental results.

The overall success of this approach is due, in large part, to the amount of detailed structural information available for G proteins. The ability to model the R1 side chain into these crystal structures allows rather detailed mechanisms to be described based on relatively low resolution structural information. As this study continues forward, results from biophysical approaches will be used to assemble detailed models of the R*-G protein complex. Current models of the complex are based on the relatively few experimental constraints that are available, and are therefore dominated by the computational approaches that produced them. Only a few intermolecular distance measurements would go a long way toward refining these models, and SDSL combined with DEER EPR is perfectly poised to provide that data.

In conclusion, the methodology and results presented here form a strong foundation for continued studies of the biomechanics of G protein signaling. The most productive approach toward answering questions in this field relies on integrating all of the structural and dynamical information obtained from these varied experimental sources into a cohesive model of the allosterism that underlies the G protein molecular switch.

APPENDIX A

$G\alpha_{i1}$ MUTANT CONSTRUCTS

The first table summarizes the progress made in the SDSL project. Prior to my joining the lab, the cysteine-depleted construct had been constructed and characterized, and 60% of the single cysteine mutant constructs listed had been created. While in the lab, I made the remaining mutants, and at one time or another, attempted to express each of the mutants listed. Thus, this table represents, to the best of my knowledge, the current status of the SDSL project.

The second table summarizes the constructs I generated to test a variety of hypotheses. Most groups will be familiar to the reader based on the preceding chapters (uncoupling, cross-linking, salt bridge, distance measurements, and 5G). However, several mutations were made in an attempt to improve the cysteine-less background used in the SDSL studies by removing additional cysteine residues and by substituting different residues at C325 to slow the very fast basal exchange rate in the Hexa I mutant. One of the cysteines that remains in Hexa I contributes to a reasonable degree of background labeling, which can be avoided by labeling for short times with low concentrations of MTSSL. Despite my best efforts, I was unable to convincingly identify the source of the background labeling. Moreover, none of the subsequent constructs (Hepta I, Octa I, Nona I, or Deca I) express nearly as well as the Hexa I protein, and thus, we continued using this background for SDSL.

Table 5 | Single-site mutant constructs for SDSL studies of $G\alpha_{i1}$ Sites 3, 214, 305, 325, and 351 (*bold italic*) are cysteines in the wild-type protein, but have been mutated in the cysteine-depleted background (along with 66). The status of each mutant is indicated as follows: (●) successful, (●) unsuccessful or incomplete, and (●) not determined.

Site	aa	Region	Expression	Activity	Labeled	Basal	Catalyzed	Binding	EPR Files	Notes
3	S	αN	●	●	●	●	●	●	●	
10	K	αN	●	●	●	●	●	●	●	Incomplete biochemical characterization. Missing data files for EPR spectra. Repeat measurements of R*-bound conformation. Published in (Medkova, *et al.*, 2002; Preininger, *et al.*, 2003).
13	V	αN	●	●	●	●	●	●	●	
14	E	αN	●	●	●	●	●	●	●	
15	R	αN	●	●	●	●	●	●	●	
16	S	αN	●	●	●	●	●	●	●	
17	K	αN	●	●	●	●	●	●	●	
21	R	αN	●	●	●	●	●	●	●	
29	K	αN	●	●	●	●	●	●	●	
50	V	α1	●	●	●	●	●	●	●	
56	I	α1	●	●	●	●	●	●	●	Dark spectrum
106	Q	αB	●	●	●	●	●	●	●	
154	Y	αE	●							
171	Q	αF	●	●	●	●	●	●	●	
172	Q	αF	●							
175	Q	αF	●	●						
179	V	L2 (SwI)	●	●	●	●	●	●	●	
180	K	L2 (SwI)	●	●	●	●	●	●	●	
182	T	L2 (SwI)	●	●	●	●	●	●	●	
184	R	β2 (SwI)	●	●	●	●	●	●	●	No increase in exchange
186	E	β2 (SwI)	●	●	●	●	●	●	●	
187	T	β2 (SwI)	●	●	●	●	●	●	●	
191	F	β2/β3	●	●	●	●	●	●	●	
192	K	β2/β3	●	●	●	●	●	●	●	
194	L	β2/β3	●	●	●	●	●	●	●	
205	R	β3/α2 (SwII)	●	●	●	●	●	●	●	
206	S	β3/α2 (SwII)	●	●	●	●	●	●	●	
209	G	α2 (SwII)	●	●	●	●	●	●	●	
210	K	α2 (SwII)								
211	W	α2 (SwII)	●		●			●	●	
213	H	α2 (SwII)	●	●	●	●	●	●	●	
214	S	α2 (SwII)	●	●	●	●	●	●	●	
217	G	α2/β4 (SwII)	●	●	●	●	●	●	●	
251	D	α3								
273	L	αG	●	●	●	●	●	●	●	
300	A	α4	●	●	●	●	●	●	●	
305	S	α4	●	●	●	●	●	●	●	

Table 5 | Continued

Site	aa	Region	Expression	Activity	Labeled	Basal	Catalyzed	Binding	EPR Files	Notes
312	K	α4/β6	●							
314	K	α4/β6	●							
318	E	α4/β6	●	●	●	●	●	●	●	
320	Y	β6	●	●	●	●	●	●	●	
321	T	β6	●	●	●	●	●	●	●	Dark and GTPγS spectra
322	H	β6	●							
323	F	β6	●							
325	A	β6/α5	●	●	●					
329	T	β6/α5	●							
330	K	α5	●	●	●	●	●	●	●	
331	N	α5	●	●	●	●	●	●	●	
333	Q	α5	●	●	●	●	●	●	●	
334	F	α5	●	●	●	●	●	●	●	
335	V	α5	●	●	●					
337	D	α5	●							
338	A	α5	●							
339	V	α5	●	●	●					
340	T	α5	●	●	●	●	●	●	●	Dark spectrum
341	D	α5	●							
342	V	α5	●	●	●	●	●	●	●	
344	I	α5	●	●	●	●	●	●	●	
345	K	α5	●	●	●	●	●	●	●	
349	K	C	●	●	●	●	●	●	●	
351	I	C	●	●	●	●	●	●	●	

Table 6 | Miscellaneous constructs

Construct	Mutant	Notes
Improve cysteine-depleted background		
Hepta I	C139V	
Hepta I	C224V	Four independent C mutations in Hexa I
Hepta I	C254A	
Hepta I	C286A	
Hepta I	Q333C	C224V Hepta I
Hepta I	K345C	
Octa I	C254A, C286A	
Nona I	C254	
Hexa I	C325M	Slow basal exchange
Hexa I	C325V	
Uncoupling mutations		
Hexa I	V342P	
Hexa I	I343P	
Hexa I	K345H	
Hexa I	K345S	
Hexa I	K349P	
Hexa I	i348A	
Double cysteines for cross-linking experiments		
$G\alpha_{i1}$	I56C Q333C	
$G\alpha_{i1}$	K192C T340C	
$G\alpha_{i1}$	K192C D341C	
$G\alpha_{i1}$	L194C I344C	
$G\alpha_{i1}$	Y320C V342C	
$G\alpha_{i1}$	T324C V335C	
Hexa I	K192C D341C	
$G\alpha_{i1}$	L194C I344C	With C351I mutation
$G\alpha_{i1}$	K192C	
$G\alpha_{i1}$	L194C	
$G\alpha_{i1}$	Q333C	
$G\alpha_{i1}$	V335C	
$G\alpha_{i1}$	V342C	
$G\alpha_{i1}$	I344C	With C351I mutation
Salt bridge mutants (K192, D341)		
$G\alpha_{i1}$	A, A	
$G\alpha_{i1}$	D, D	
$G\alpha_{i1}$	D, E	
$G\alpha_{i1}$	D, K	
$G\alpha_{i1}$	D, R	
$G\alpha_{i1}$	E, D	
$G\alpha_{i1}$	E, E	

Table 6 | Continued

Construct	Mutant		Notes
Salt bridge mutants (K192, D341)			
$G\alpha_{i1}$	E, K		
$G\alpha_{i1}$	E, R		
$G\alpha_{i1}$	K, A		
$G\alpha_{i1}$	K, E		
$G\alpha_{i1}$	K, K		
$G\alpha_{i1}$	K, N		
$G\alpha_{i1}$	Q, R		
$G\alpha_{i1}$	R, A		
$G\alpha_{i1}$	R, D		
$G\alpha_{i1}$	R, R		
Double cysteine mutants for distance measurements			
Hexa I	R21C	Q333C	
Hexa I	K29C	K330C	
Hexa I	Q106C	L273C	
Hexa I	Q106C	K330C	
Hexa I	T187C	Q333C	
Hexa I	F191C	K330C	
Hexa I	F191C	Q333C	
Hexa I	F191C	F334C	
Hexa I	F191C	Y320C	
Hexa I	A300C	Q333C	
Hexa I	C305	K330C	
Hexa I	C305	Q333C	
Hexa I	Y320C	K330C	
Hexa I	Y320C	Q333C	
Hexa I	Y320C	F334C	
Hexa I	T321C	Q333C	
Mutations in the cysteine-less $G\alpha_{i1}$ construct			
Deca I	Q106C		
Deca I	S206C		
Deca I	C214		
Deca I	C325		
Deca I	N331C		
Deca I	Q333C		
Deca I	F334C		
Deca I	C351		
Deca I	C325, I344C		
Deca I	C325, F334C		Slow basal exchange
Deca I	C325, Q333C		

Table 6 | Continued

Construct	Mutant	Notes
Five-glycine loop insertion mutants		
5G	L273C	
5G	K330C	
5G	F334C	
5G	K349C	

APPENDIX B

BIOCHEMICAL CHARACTERIZATION OF SPIN-LABELED MUTANTS

Each new spin-labeled mutant Gα is characterized by measuring its basal and receptor-catalyzed nucleotide exchange rates as well as its ability to form stable R*-G protein complexes in ROS membranes. Although the primary goal of this work is to explore G protein structure and dynamics with EPR spectroscopy, a secondary result has been the generation of a large number of Gα mutants with a correspondingly large amount of biochemical data (Figs. 57, 58). Interesting patterns emerge when these data are mapped onto the $G\alpha_{i1}$ crystal structure (Fig. 59). Perhaps surprisingly, there is no correlation between the absolute or fold increase in the rates of R*-catalyzed nucleotide exchange and the extent of rhodopsin binding. However, this may not be expected in a system where the two events, R* binding and GDP release, can be uncoupled from each other, as in the 5G mutant.

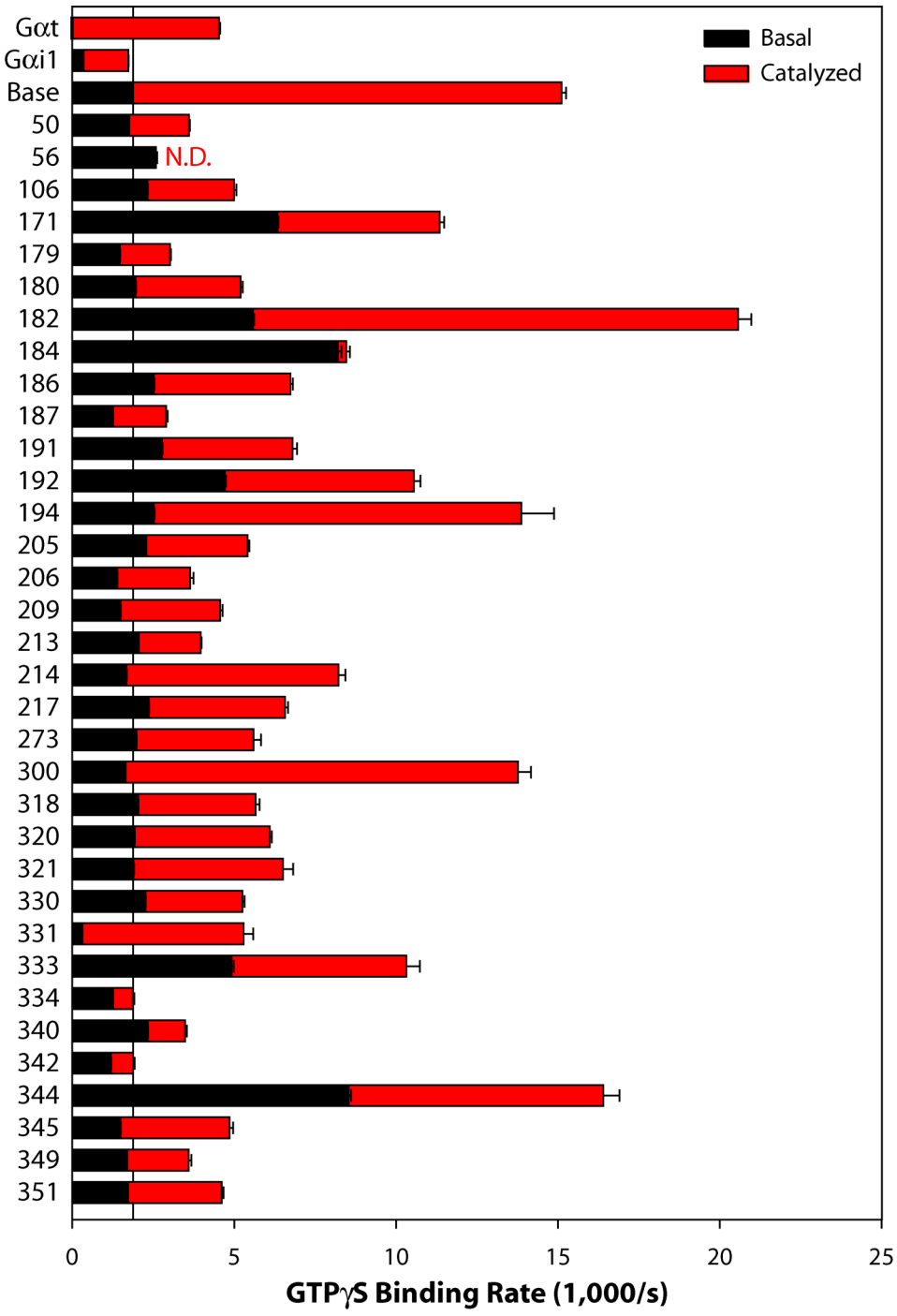

Figure 57 | Nucleotide exchange rates for spin-labeled mutants Data represent the mean ± s.e.m. of 4-6 independent experiments.

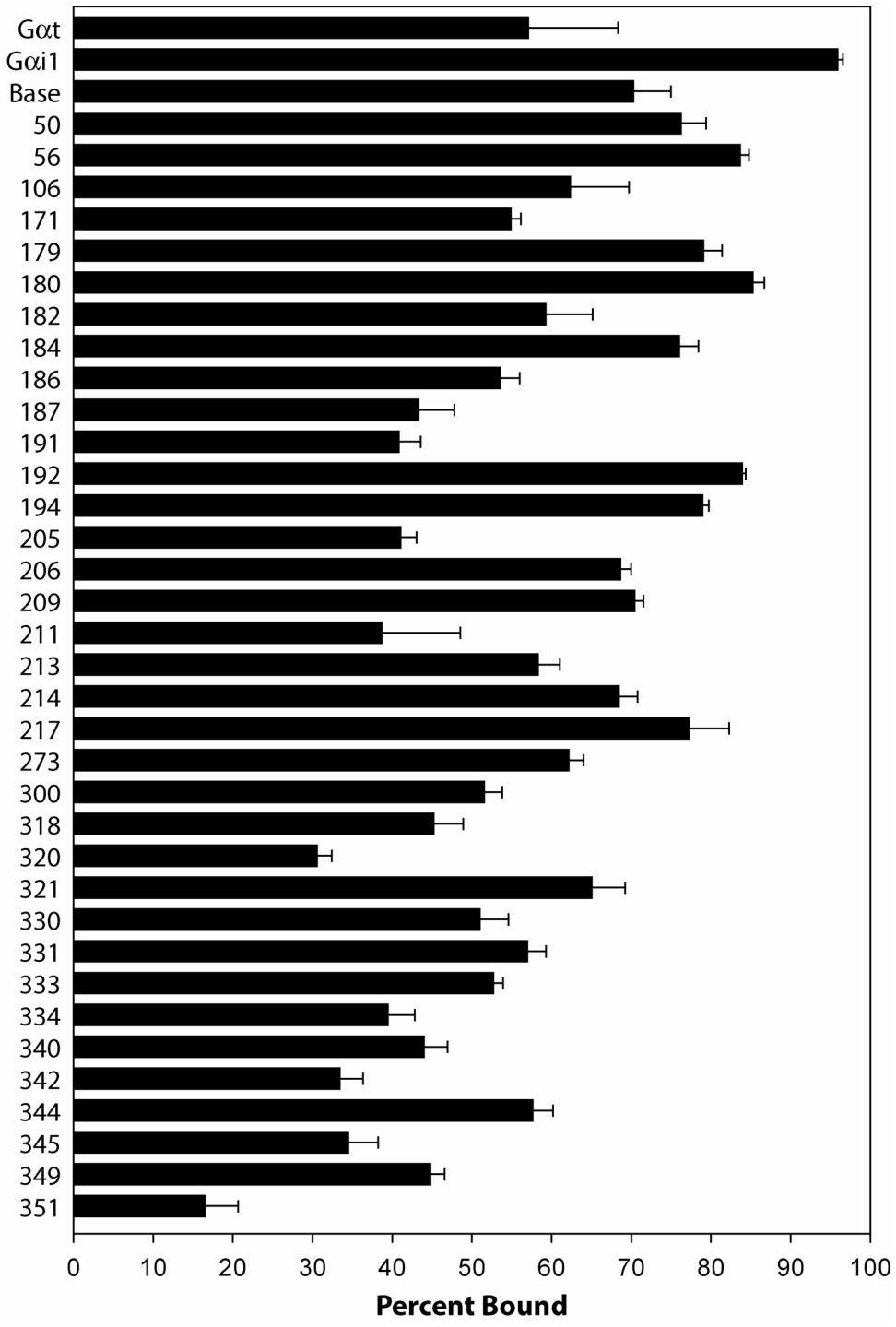

Figure 58 | Rhodopsin binding data for spin-labeled mutants Data represent the mean ± s.e.m. of 3 independent experiments.

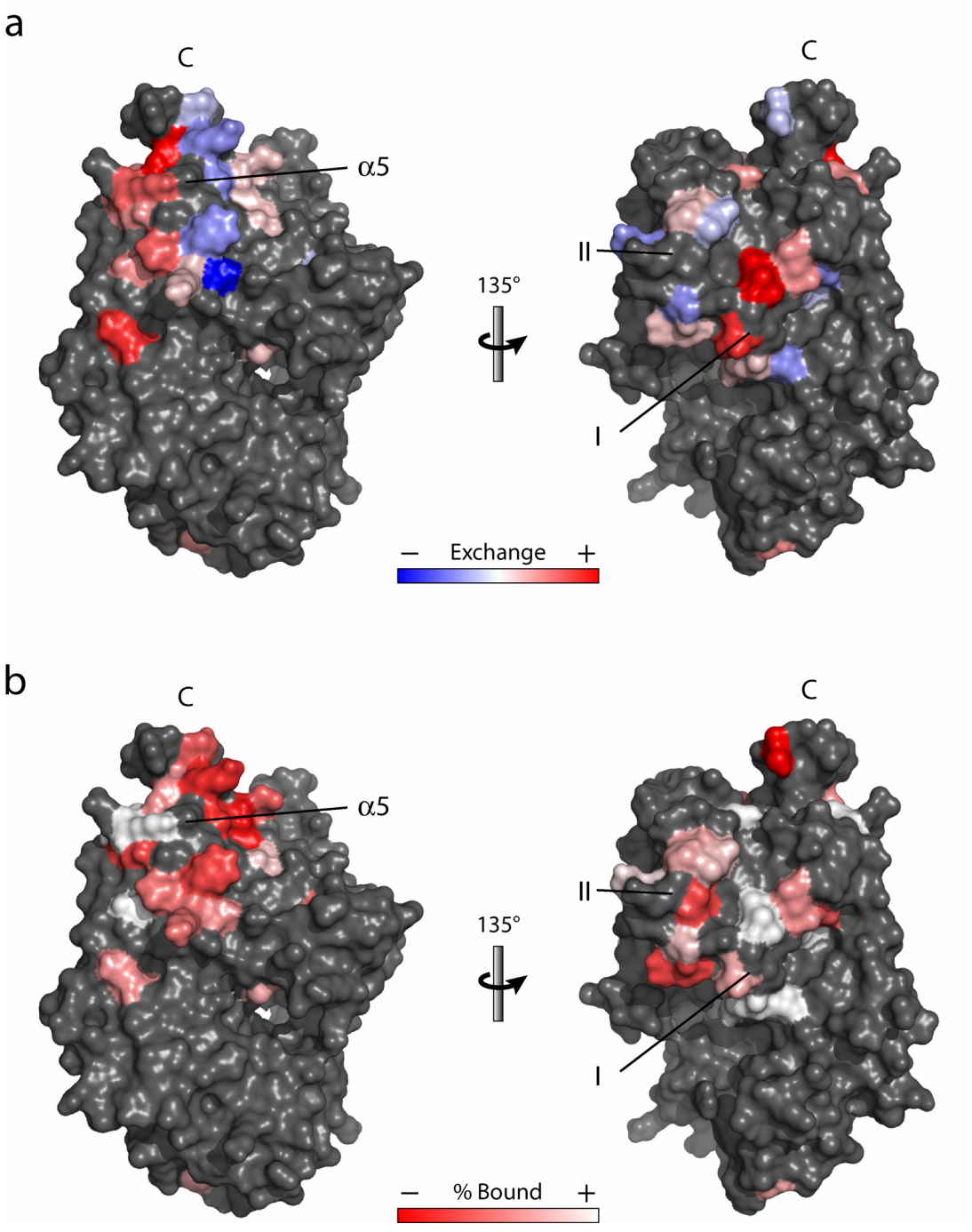

Figure 59 | Mapping biochemical data onto the $G\alpha_{i1}$ crystal structure (**a**) The fold difference in basal nucleotide exchange compared to the cysteine-depleted base mutant are mapped onto the surface of $G\alpha_{i1}$ from the G_{i1} structure (scale ± 4.5-fold). A clear pattern is observed on the α5 helix. (**b**) The effects of mutagenesis and spin-labeling at various sites have been mapped onto the surface of $G\alpha_{i1}$ (scale 20-80% bound). Compare this result with the ODA identified in Figure 56.

APPENDIX C

COMPARISON OF SALT BRIDGE MUTANT EXCHANGE RATES

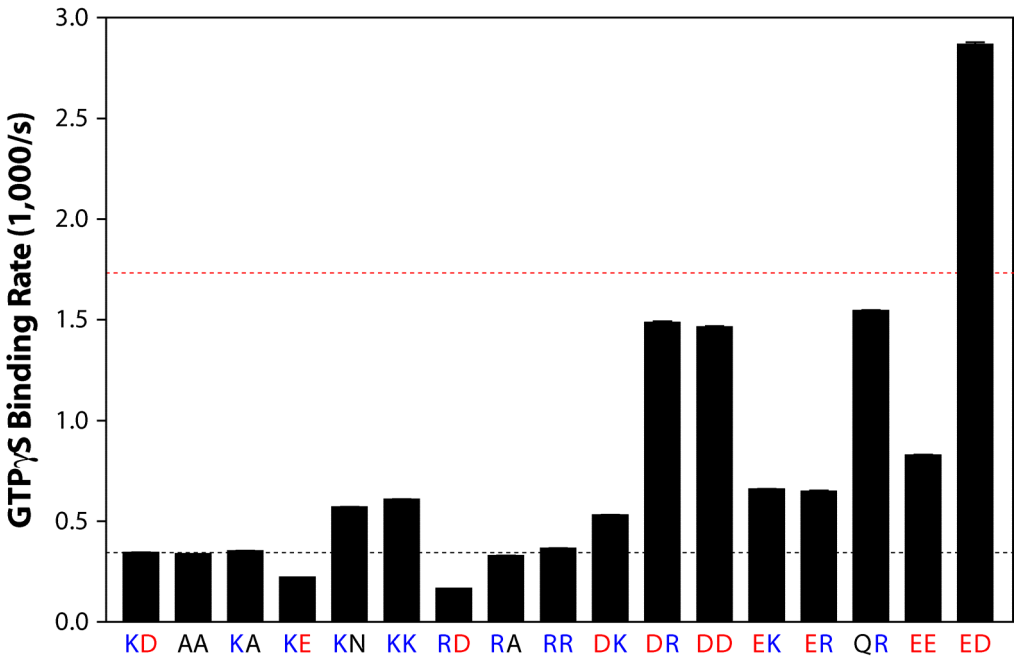

Figure 60 | Summary of salt bridge mutant exchange rates The basal and receptor-catalyzed exchange rates for wild-type $G\alpha_{i1}$ are marked (*black* and *red dashed lines*, respectively). Positively, negatively, and uncharged amino acids are colored *blue*, *red*, and *black*, respectively. Data represent the mean ± s.e.m. of six independent experiments.

REFERENCES

Abdulaev, N.G., Ngo, T., Chen, R., Lu, Z. and Ridge, K.D. (2000) Functionally Discrete Mimics of Light-activated Rhodopsin Identified through Expression of Soluble Cytoplasmic Domains. *J. Biol. Chem.*, **275**, 39354-39363.

Abdulaev, N.G., Ngo, T., Zhang, C., Dinh, A., Brabazon, D.M., Ridge, K.D. and Marino, J.P. (2005a) Heterotrimeric G-protein α-Subunit Adopts a "Preactivated" Conformation When Associated with βγ-Subunits. *J. Biol. Chem.*, **280**, 38071-38080.

Abdulaev, N.G., Zhang, C., Dinh, A., Ngo, T., Bryan, P.N., Brabazon, D.M., Marino, J.P. and Ridge, K.D. (2005b) Bacterial expression and one-step purification of an isotope-labeled heterotrimeric G-protein α-subunit. *J. Biomol. NMR*, **32**, 31-40.

Akgoz, M., Azpiazu, I., Kalyanaraman, V. and Gautam, N. (2002) Role of the G Protein γ Subunit in βγ Complex Modulation of Phospholipase Cβ Function. *J. Biol. Chem.*, **277**, 19573-19578.

Altenbach, C., Oh, K.J., Trabanino, R.J., Hideg, K. and Hubbell, W.L. (2001) Estimation of Inter-Residue Distances in Spin Labeled Proteins at Physiological Temperatures: Experimental Strategies and Practical Limitations. *Biochemistry*, **40**, 15471-15482.

Alves, I.D., Salamon, Z., Varga, E., Yamamura, H.I., Tollin, G. and Hruby, V.J. (2003) Direct Observation of G-protein Binding to the Human δ-Opioid Receptor Using Plasmon-Waveguide Resonance Spectroscopy. *J. Biol. Chem.*, **278**, 48890-48897.

Alves, I.D., Salgado, G.F., Salamon, Z., Brown, M.F., Tollin, G. and Hruby, V.J. (2005) Phosphatidylethanolamine Enhances Rhodopsin Photoactivation and Transducin Binding in a Solid Supported Lipid Bilayer as Determined Using Plasmon-Waveguide Resonance Spectroscopy. *Biophys. J.*, **88**, 198-210.

An, J., Totrov, M. and Abagyan, R. (2005) Pocketome via Comprehensive Identification and Classification of Ligand Binding Envelopes. *Mol. Cell. Proteomics*, **4**, 752-761.

Aris, L., Gilchrist, A., Rens-Domiano, S., Meyer, C., Schatz, P.J., Dratz, E.A. and Hamm, H.E. (2001) Structural Requirements for the Stabilization of Metarhodopsin II by the C Terminus of the α subunit of Transducin. *J. Biol. Chem.*, **276**, 2333-2339.

Arshavsky, V. and Bownds, M.D. (1992) Regulation of deactivation of photoreceptor G protein by its target enzyme and cGMP. *Nature*, **357**, 416-417.

Azpiazu, I., Cruzblanca, H., Li, P., Linder, M., Zhuo, M. and Gautam, N. (1999) A G protein γ Subunit-specific Peptide Inhibits Muscarinic Receptor Signaling. *J. Biol. Chem.*, **274**, 35305-35308.

Azpiazu, I. and Gautam, N. (2001) G Protein γ Subunit Interaction with a Receptor Regulates Receptor-stimulated Nucleotide Exchange. *J. Biol. Chem.*, **276**, 41742-41747.

Bae, H., Anderson, K., Flood, L.A., Skiba, N.P., Hamm, H.E. and Graber, S.G. (1997) Molecular Determinants of Selectivity in 5-Hydroxytryptamine$_{1B}$ Receptor-G Protein Interactions. *J. Biol. Chem.*, **272**, 32071-32077.

Bae, H., Cabrera-Vera, T.M., Depree, K.M., Graber, S.G. and Hamm, H.E. (1999) Two Amino Acids Within the α4 Helix of $G\alpha_{i1}$ Mediate Coupling with 5-Hydroxytryptamine$_{1B}$ Receptors. *J. Biol. Chem.*, **274**, 14963-14971.

Bailey, S. (1994) The CCP4 Suite: Programs for Protein Crystallography. *Acta Crystallogr. D. Biol. Crystallogr.*, **50**, 760-763.

Baneres, J.L. and Parello, J. (2003) Structure-based Analysis of GPCR Function: Evidence for a Novel Pentameric Assembly between the Dimeric Leukotriene B_4 Receptor BLT1 and the G-protein. *J. Mol. Biol.*, **329**, 815-829.

Bayewitch, M.L., Avidor-Reiss, T., Levy, R., Pfeuffer, T., Nevo, I., Simonds, W.F. and Vogel, Z. (1998a) Inhibition of adenylyl cyclase isoforms V and VI by various $G_{\beta\gamma}$ subunits. *FASEB J.*, **12**, 1019-1025.

Bayewitch, M.L., Avidor-Reiss, T., Levy, R., Pfeuffer, T., Nevo, I., Simonds, W.F. and Vogel, Z. (1998b) Differential Modulation of Adenylyl Cyclases I and II by Various G_{β} Subunits. *J. Biol. Chem.*, **273**, 2273-2276.

Beavo, J.A. and Brunton, L.L. (2002) Cyclic nucleotide research - still expanding after half a century. *Nat. Rev. Mol. Cell Biol.*, **3**, 710-718.

Bennett, N. and Dupont, Y. (1985) The G-protein of Retinal Rod Outer Segments (Transducin). Mechanism of Interaction with Rhodopsin and Nucleotides. *J. Biol. Chem.*, **260**, 4156-4168.

Berghuis, A.M., Lee, E., Raw, A.S., Gilman, A.G. and Sprang, S.R. (1996) Structure of the GDP-Pi complex of Gly203→Ala $G_{i\alpha1}$: a mimic of the ternary product complex of Gα-catalyzed GTP hydrolysis. *Structure*, **4**, 1277-1290.

Berlot, C.H. and Bourne, H.R. (1992) Identification of effector-activating residues of $G_{s\alpha}$. *Cell*, **68**, 911-922.

Berstein, G., Blank, J.L., Jhon, D.Y., Exton, J.H., Rhee, S.G. and Ross, E.M. (1992) Phospholipase C-β1 is a GTPase-activating protein for $G_{q/11}$, its physiologic regulator. *Cell*, **70**, 411-418.

Berthet, J., Rall, T.W. and Sutherland, E.W. (1957) The Relationship of Epinephrine and Glucagon to Liver Phosphorylase. IV. Effect of Epinephrine and Glucagon on the Reactivation of Phosphorylase in Liver Homogenates. *J. Biol. Chem.*, **224**, 463-475.

Bhattacharyya, R. and Wedegaertner, P.B. (2000) $G\alpha_{13}$ Requires Palmitoylation for Plasma Membrane Localization, Rho-dependent Signaling, and Promotion of p115-RhoGEF Membrane Binding. *J. Biol. Chem.*, **275**, 14992-14999.

Bigay, J., Faurobert, E., Franco, M. and Chabre, M. (1994) Roles of Lipid Modifications of Transducin Subunits in Their GDP-Dependent Association and Membrane Binding. *Biochemistry*, **33**, 14081-14090.

Birnbaumer, L. and Rodbell, M. (1969) Adenyl Cyclase in Fat Cells. II. Hormone Receptors. *J. Biol. Chem.*, **244**, 3477-3482.

Birnbaumer, L., Pohl, S.L., Rodbell, M. and Sundby, F. (1972) The Glucagon-sensitive Adenylate Cyclase System in Plasma Membranes of Rat Liver. VII. Hormonal Stimulation: Reversibility and Dependence on Concentration of Free Hormone. *J. Biol. Chem.*, **247**, 2038-2043.

Blackmer, T., Larsen, E.C., Takahashi, M., Martin, T.F., Alford, S. and Hamm, H.E. (2001) G Protein βγ Subunit-Mediated Presynaptic Inhibition: Regulation of Exocytotic Fusion Downstream of Ca^{2+} Entry. *Science*, **292**, 293-297.

Blackmer, T., Larsen, E.C., Bartleson, C., Kowalchyk, J.A., Yoon, E.J., Preininger, A.M., Alford, S., Hamm, H.E. and Martin, T.F. (2005) G protein βγ directly regulates SNARE protein fusion machinery for secretory granule exocytosis. *Nat. Neurosci.*, **8**, 421-425.

Blahos, J., Fischer, T., Brabet, I., Stauffer, D., Rovelli, G., Bockaert, J. and Pin, J.P. (2001) A Novel Site on the Gα-protein That Recognizes Heptahelical Receptors. *J. Biol. Chem.*, **276**, 3262-3269.

Blahos, J., II, Mary, S., Perroy, J., de Colle, C., Brabet, I., Bockaert, J. and Pin, J.P. (1998) Extreme C Terminus of G Protein α-Subunits Contains a Site that Discriminates between G_i-coupled Metabotropic Glutamate Receptors. *J. Biol. Chem.*, **273**, 25765-25769.

Bokoch, G.M., Katada, T., Northup, J.K., Ui, M. and Gilman, A.G. (1984) Purification and Properties of the Inhibitory Guanine Nucleotide-binding Regulatory Component of Adenylate Cyclase. *J. Biol. Chem.*, **259**, 3560-3567.

Bornancin, F., Pfister, C. and Chabre, M. (1989) The transitory complex between photoexcited rhodopsin and transducin. Reciprocal interaction between the retinal site in rhodopsin and the nucleotide site in transducin. *Eur. J. Biochem.*, **184**, 687-698.

Bourne, H.R., Coffino, P. and Tomkins, G.M. (1975) Selection of a Variant Lymphoma Cell Deficient in Adenylate Cyclase. *Science*, **187**, 750-752.

Bourne, H.R. (1997) How receptors talk to trimeric G proteins. *Curr. Opin. Cell Biol.*, **9**, 134-142.

Brunger, A.T., Adams, P.D., Clore, G.M., DeLano, W.L., Gros, P., Grosse-Kunstleve, R.W., Jiang, J.S., Kuszewski, J., Nilges, M., Pannu, N.S., Read, R.J., Rice, L.M., Simonson, T. and Warren, G.L. (1998) Crystallography & NMR System: A New Software Suite for Macromolecular Structure Determination. *Acta Crystallogr. D. Biol. Crystallogr.*, **54**, 905-921.

Budil, D.E., Lee, S., Saxena, S. and Freed, J.H. (1996) Nonlinear-Least-Squares Analysis of Slow-Motion EPR Spectra in One and Two Dimensions Using a Modified Levenberg-Marquardt Algorithm *J. Magn. Reson. A*, **120**, 155-189.

Bunemann, M., Frank, M. and Lohse, M.J. (2003) Gi protein activation in intact cells involves subunit rearrangement rather than dissociation. *Proc. Natl. Acad. Sci. U. S. A.*, **100**, 16077-16082.

Butkerait, P., Zheng, Y., Hallak, H., Graham, T.E., Miller, H.A., Burris, K.D., Molinoff, P.B. and Manning, D.R. (1995) Expression of the Human 5-Hydroxytryptamine$_{1A}$ Receptor in Sf9 Cells. Reconstitution of a Coupled Phenotype by Co-expression of Mammalian G Protein Subunits. *J. Biol. Chem.*, **270**, 18691-18699.

Cabrera-Vera, T.M., Vanhauwe, J., Thomas, T.O., Medkova, M., Preininger, A., Mazzoni, M.R. and Hamm, H.E. (2003) Insights into G Protein Structure, Function, and Regulation. *Endocr. Rev.*, **24**, 765-781.

Cabrera, J.L., de Freitas, F., Satpaev, D.K. and Slepak, V.Z. (1998) Identification of the Gβ5-RGS7 Protein Complex in the Retina. *Biochem. Biophys. Res. Commun.*, **249**, 898-902.

Caffrey, M. (2003) Membrane protein crystallization. *J. Struct. Biol.*, **142**, 108-132.

Cai, K., Itoh, Y. and Khorana, H.G. (2001) Mapping of contact sites in complex formation between transducin and light-activated rhodopsin by covalent crosslinking: Use of a photoactivatable reagent. *Proc. Natl. Acad. Sci. U. S. A.*, **98**, 4877-4882.

Cassel, D. and Selinger, Z. (1976) Catecholamine-stimulated GTPase activity in turkey erythrocyte membranes. *Biochim. Biophys. Acta*, **452**, 538-551.

Cassel, D. and Selinger, Z. (1978) Mechanism of adenylate cyclase activation through the beta-adrenergic receptor: Catecholamine-induced displacement of bound GDP by GTP. *Proc. Natl. Acad. Sci. U. S. A.*, **75**, 4155-4159.

Cerione, R.A., Regan, J.W., Nakata, H., Codina, J., Benovic, J.L., Gierschik, P., Somers, R.L., Spiegel, A.M., Birnbaumer, L., Lefkowitz, R.J. and Caron, M.G. (1986) Functional Reconstitution of the α_2-Adrenergic Receptor with Guanine Nucleotide Regulatory Proteins in Phospholipid Vesicles. *J. Biol. Chem.*, **261**, 3901-3909.

Ceruso, M.A., Periole, X. and Weinstein, H. (2004) Molecular Dynamics Simulations of Transducin: Interdomain and Front to Back Communication in Activation and Nucleotide Exchange. *J. Mol. Biol.*, **338**, 469-481.

Chabre, M. and le Maire, M. (2005) Monomeric G-Protein-Coupled Receptor as a Functional Unit. *Biochemistry*, **44**, 9395-9403.

Chen, C.A. and Manning, D.R. (2001) Regulation of G proteins by covalent modification. *Oncogene*, **20**, 1643-1652.

Chen, C.K., Burns, M.E., He, W., Wensel, T.G., Baylor, D.A. and Simon, M.I. (2000) Slowed recovery of rod photoresponse in mice lacking the GTPase accelerating protein RGS9-1. *Nature*, **403**, 557-560.

Chen, C.K., Eversole-Cire, P., Zhang, H., Mancino, V., Chen, Y.J., He, W., Wensel, T.G. and Simon, M.I. (2003) Instability of GGL domain-containing RGS proteins in mice lacking the G protein β-subunit Gβ5. *Proc. Natl. Acad. Sci. U. S. A.*, **100**, 6604-6609.

Chen, S., Lin, F. and Hamm, H.E. (2005a) RACK1 Binds to a Signal Transfer Region of Gβγ and Inhibits Phospholipase C β2 Activation. *J. Biol. Chem.*, **280**, 33445-33452.

Chen, Z., Singer, W.D., Sternweis, P.C. and Sprang, S.R. (2005b) Structure of the p115RhoGEF rgRGS domain-Gα13/i1 chimera complex suggests convergent evolution of a GTPase activator. *Nat. Struct. Mol. Biol.*, **12**, 191-197.

Cherfils, J. and Chabre, M. (2003) Activation of G-protein Gα subunits by receptors through Gα–Gβ and Gα–Gγ interactions. *Trends Biochem. Sci.*, **28**, 13-17.

Chidiac, P. and Ross, E.M. (1999) Phospholipase C-β1 Directly Accelerates GTP Hydrolysis by $G\alpha_q$ and Acceleration Is Inhibited by Gβγ Subunits. *J. Biol. Chem.*, **274**, 19639-19643.

Ciarkowski, J., Witt, M. and Slusarz, R. (2005) A hypothesis for GPCR activation. *J. Mol. Model.*, **11**, 407-415.

Clapham, D.E. and Neer, E.J. (1997) G Protein βγ Subunits. *Annu. Rev. Pharmacol. Toxicol.*, **37**, 167-203.

Coleman, D.E., Berghuis, A.M., Lee, E., Linder, M.E., Gilman, A.G. and Sprang, S.R. (1994a) Structures of Active Conformations of $G_{i\alpha1}$ and the Mechanism of GTP Hydrolysis. *Science*, **265**, 1405-1412.

Coleman, D.E., Lee, E., Mixon, M.B., Linder, M.E., Berghuis, A.M., Gilman, A.G. and Sprang, S.R. (1994b) Crystallization and Preliminary Crystallographic Studies of Giα1 and Mutants of Giα1 in the GTP and GDP-Bound States. *J. Mol. Biol.*, **238**, 630-634.

Coleman, D.E. and Sprang, S.R. (1998) Crystal Structures of the G Protein $G_{i\alpha1}$ Complexed with GDP and Mg^{2+}: A Crystallographic Titration Experiment. *Biochemistry*, **37**, 14376-14385.

Coleman, D.E. and Sprang, S.R. (1999) Structure of $G_{i\alpha1}$•GppNHp, Autoinhibition in a G_α Protein-Substrate Complex. *J. Biol. Chem.*, **274**, 16669-16672.

Columbus, L., Kalai, T., Jeko, J., Hideg, K. and Hubbell, W.L. (2001) Molecular Motion of Spin Labeled Side Chains in α-Helices: Analysis by Variation of Side Chain Structure. *Biochemistry*, **40**, 3828-3846.

Columbus, L. and Hubbell, W.L. (2002) A new spin on protein dynamics. *Trends Biochem. Sci.*, **27**, 288-295.

Columbus, L. and Hubbell, W.L. (2004) Mapping Backbone Dynamics in Solution with Site-Directed Spin Labeling: GCN4-58 bZip Free and Bound to DNA. *Biochemistry*, **43**, 7273-7287.

Conklin, B.R., Farfel, Z., Lustig, K.D., Julius, D. and Bourne, H.R. (1993) Substitution of three amino acids switches receptor specificity of $G_q\alpha$ to that of $G_i\alpha$. *Nature*, **363**, 274-276.

Conklin, B.R., Herzmark, P., Ishida, S., Voyno-Yasenetskaya, T.A., Sun, Y., Farfel, Z. and Bourne, H.R. (1996) Carboxyl-Terminal Mutations of $G_{q\alpha}$ and $G_{s\alpha}$ That Alter the Fidelity of Receptor Activation. *Mol. Pharmacol.*, **50**, 885-890.

Crane, J.M., Mao, C., Lilly, A.A., Smith, V.F., Suo, Y., Hubbell, W.L. and Randall, L.L. (2005) Mapping of the Docking of SecA onto the Chaperone SecB by Site-directed Spin Labeling: Insight into the Mechanism of Ligand Transfer During Protein Export. *J. Mol. Biol.*, **353**, 295-307.

Daaka, Y., Pitcher, J.A., Richardson, M., Stoffel, R.H., Robishaw, J.D. and Lefkowitz, R.J. (1997) Receptor and Gβγ isoform-specific interactions with G protein-coupled receptor kinases. *Proc. Natl. Acad. Sci. U. S. A.*, **94**, 2180-2185.

Daniel, V., Litwack, G. and Tomkins, G.M. (1973) Induction of Cytolysis of Cultured Lymphoma Cells by Adenosine 3':5'-Cyclic Monophosphate and the Isolation of Resistant Variants. *Proc. Natl. Acad. Sci. U. S. A.*, **70**, 76-79.

Davis, T.L., Bonacci, T.M., Sprang, S.R. and Smrcka, A.V. (2005) Structural and Molecular Characterization of a Preferred Protein Interaction Surface on G Protein βγ Subunits. *Biochemistry*, **44**, 10593-10604.

de La Fortelle, E. and Bricogne, G. (1997). Maximum Likelihood Heavy Atom Parameter Refinement for Multiple Isomorphous Replacement and Multiwavelength Analomous Diffraction Methods. In *Macromolecular Crystallography Part A*, (J. C. W. Carter and R. M. Sweet, eds.), **276**, 472-494. New York: Academic Press.

Degtyarev, M.Y., Spiegel, A.M. and Jones, T.L. (1993) The G Protein α_s Subunit Incorporates [^{3}H]Palmitic Acid and Mutation of Cysteine-3 Prevents This Modification. *Biochemistry*, **32**, 8057-8061.

Degtyarev, M.Y., Spiegel, A.M. and Jones, T.L. (1994) Palmitoylation of a G Protein α_i Subunit Requires Membrane Localization Not Myristoylation. *J. Biol. Chem.*, **269**, 30898-30903.

Dell, E.J., Connor, J., Chen, S., Stebbins, E.G., Skiba, N.P., Mochly-Rosen, D. and Hamm, H.E. (2002) The βγ Subunit of Heterotrimeric G Proteins Interacts with RACK1 and Two Other WD Repeat Proteins. *J. Biol. Chem.*, **277**, 49888-49895.

Denker, B.M., Schmidt, C.J. and Neer, E.J. (1992) Promotion of the GTP-liganded State of the $G_{o\alpha}$ Protein by Deletion of the C Terminus. *J. Biol. Chem.*, **267**, 9998-10002.

Denker, B.M., Boutin, P.M. and Neer, E.J. (1995) Interactions between the Amino- and Carboxyl-Terminal Regions of Gα Subunits: Analysis of Mutated $G\alpha_o$/$G\alpha_{i2}$ Chimeras. *Biochemistry*, **34**, 5544-5553.

Dessauer, C.W., Tesmer, J.J., Sprang, S.R. and Gilman, A.G. (1998) Identification of a $G_{i\alpha}$ Binding Site on Type V Adenylyl Cyclase. *J. Biol. Chem.*, **273**, 25831-25839.

Dombkowski, A.A. (2003) Disulfide by Design: A Computational Method for the Rational Design of Disulfide Bonds in Proteins. *Bioinformatics*, **19**, 1852-1853.

Downes, G.B. and Gautam, N. (1999) The G Protein Subunit Gene Families. *Genomics*, **62**, 544-552.

Dratz, E.A., Furstenau, J.E., Lambert, C.G., Thireault, D.L., Rarick, H., Schepers, T., Pakhlevaniants, S. and Hamm, H.E. (1993) NMR structure of a receptor-bound G-protein peptide. *Nature*, **363**, 276-281.

Dunham, T.D. and Farrens, D.L. (1999) Conformational Changes in Rhodopsin. Movement of Helix F Detected by Site-Specific Chemical Labeling and Fluorescence Spectroscopy. *J. Biol. Chem.*, **274**, 1683-1690.

Edman, K., Nollert, P., Royant, A., Belrhali, H., Pebay-Peyroula, E., Hajdu, J., Neutze, R. and Landau, E.M. (1999) High-resolution X-ray structure of an early intermediate in the bacteriorhodopsin photocycle. *Nature*, **401**, 822-826.

Emeis, D., Kuhn, H., Reichert, J. and Hofmann, K.P. (1982) Complex formation between metarhodopsin II and GTP-binding protein in bovine photoreceptor membranes leads to a shift of the photoproduct equilibrium. *FEBS Lett.*, **143**, 29-34.

Ernst, O.P., Meyer, C.K., Marin, E.P., Henklein, P., Fu, W.Y., Sakmar, T.P. and Hofmann, K.P. (2000) Mutation of the Fourth Cytoplasmic Loop of Rhodopsin Affects Binding of Transducin and Peptides Derived from the Carboxyl-terminal Sequences of Transducin α and γ Subunits. *J. Biol. Chem.*, **275**, 1937-1943.

Evanko, D.S., Thiyagarajan, M.M. and Wedegaertner, P.B. (2000) Interaction with Gβγ Is Required for Membrane Targeting and Palmitoylation of $G\alpha_s$ and $G\alpha_q$. *J. Biol. Chem.*, **275**, 1327-1336.

Evanko, D.S., Thiyagarajan, M.M., Siderovski, D.P. and Wedegaertner, P.B. (2001) Gβγ Isoforms Selectively Rescue Plasma Membrane Localization and Palmitoylation of Mutant $G\alpha_s$ and $G\alpha_q$. *J. Biol. Chem.*, **276**, 23945-23953.

Fanelli, F. and Dell'Orco, D. (2005) Rhodopsin Activation Follows Precoupling with Transducin: Inferences from Computational Analysis. *Biochemistry*, **44**, 14695-14700.

Farrens, D.L., Altenbach, C., Yang, K., Hubbell, W.L. and Khorana, H.G. (1996) Requirement of Rigid-Body Motion of Transmembrane Helices for Light Activation of Rhodopsin. *Science*, **274**, 768-770.

Feltham, J.L., Dotsch, V., Raza, S., Manor, D., Cerione, R.A., Sutcliffe, M.J., Wagner, G. and Oswald, R.E. (1997) Definition of the Switch Surface in the Solution Structure of Cdc42Hs. *Biochemistry*, **36**, 8755-8766.

Fernandez-Patron, C., Hardy, E., Sosa, A., Seoane, J. and Castellanos, L. (1995) Double Staining of Coomassie Blue-Stained Polyacrylamide Gels by Imidazole-Sodium Dodecyl Sulfate-Zinc Reverse Staining: Sensitive Detection of Coomassie Blue-Undetected Proteins. *Anal. Biochem.*, **224**, 263-269.

Fernandez-Recio, J., Totrov, M., Skorodumov, C. and Abagyan, R. (2005) Optimal docking area: A new method for predicting protein-protein interaction sites. *Proteins*, **58**, 134-143.

Fields, T.A. and Casey, P.J. (1997) Signalling functions and biochemical properties of pertussis toxin-resistant G-proteins. *Biochem. J.*, **321 (Pt 3)**, 561-571.

Figler, R.A., Graber, S.G., Lindorfer, M.A., Yasuda, H., Linden, J. and Garrison, J.C. (1996) Reconstitution of Recombinant Bovine A_1 Adenosine Receptors in Sf9 Cell Membranes with Recombinant G Proteins of Defined Composition. *Mol. Pharmacol.*, **50**, 1587-1595.

Figler, R.A., Lindorfer, M.A., Graber, S.G., Garrison, J.C. and Linden, J. (1997) Reconstitution of Bovine A_1 Adenosine Receptors and G Proteins in Phospholipid Vesicles: bg-Subunit Composition Influences Guanine Nucleotide Exchange and Agonist Binding. *Biochemistry*, **36**, 16288-16299.

Fishburn, C.S., Pollitt, S.K. and Bourne, H.R. (2000) Localization of a Peripheral Membrane Protein: Gβγ Targets $G\alpha_Z$. *Proc. Natl. Acad. Sci. U. S. A.*, **97**, 1085-1090.

Fletcher, J.E., Lindorfer, M.A., DeFilippo, J.M., Yasuda, H., Guilmard, M. and Garrison, J.C. (1998) The G Protein β5 Subunit Interacts Selectively with the $G_q\alpha$ Subunit. *J. Biol. Chem.*, **273**, 636-644.

Ford, C.E., Skiba, N.P., Bae, H., Daaka, Y., Reuveny, E., Shekter, L.R., Rosal, R., Weng, G., Yang, C.S., Iyengar, R., Miller, R.J., Jan, L.Y., Lefkowitz, R.J. and Hamm, H.E. (1998) Molecular Basis for Interactions of G Protein βγ Subunits with Effectors *Science*, **280**, 1271-1274.

Fotiadis, D., Liang, Y., Filipek, S., Saperstein, D.A., Engel, A. and Palczewski, K. (2003) Atomic-force microscopy: Rhodopsin dimers in native disc membranes. *Nature*, **421**, 127-128.

Fotiadis, D., Liang, Y., Filipek, S., Saperstein, D.A., Engel, A. and Palczewski, K. (2004) The G protein-coupled receptor rhodopsin in the native membrane. *FEBS Lett.*, **564**, 281-288.

Frank, M., Thumer, L., Lohse, M.J. and Bunemann, M. (2005) G Protein Activation without Subunit Dissociation Depends on a $G\alpha_i$-specific Region. *J. Biol. Chem.*, **280**, 24584-24590.

Fredriksson, R. and Schiöth, H.B. (2005) The Repertoire of G-Protein-Coupled Receptors in Fully Sequenced Genomes. *Mol. Pharmacol.*, **67**, 1414-1425.

Freissmuth, M. and Gilman, A.G. (1989) Mutations of $G_{S\alpha}$ Designed to Alter the Reactivity of the Protein with Bacterial Toxins. Substitutions at ARG^{187} Result in Loss of GTPase Activity. *J. Biol. Chem.*, **264**, 21907-21914.

Fukada, Y., Matsuda, T., Kokame, K., Takao, T., Shimonishi, Y., Akino, T. and Yoshizawa, T. (1994) Effects of Carboxyl Methylation of Photoreceptor G Protein γ-subunit in Visual Transduction. *J. Biol. Chem.*, **269**, 5163-5170.

Fung, B.K., Hurley, J.B. and Stryer, L. (1981) Flow of information in the light-triggered cyclic nucleotide cascade of vision. *Proc. Natl. Acad. Sci. U. S. A.*, **78**, 152-156.

Fung, B.K. (1983) Characterization of Transducin from Bovine Retinal Rod Outer Segments. I. Separation and Reconstitution of the Subunits. *J. Biol. Chem.*, **258**, 10495-10502.

Galbiati, F., Guzzi, F., Magee, A.I., Milligan, G. and Parenti, M. (1994) N-terminal fatty acylation of the α-subunit of the G-protein G_i1: Only the myristoylated protein is a substrate for palmitoylation. *Biochem. J.*, **303 (Pt 3)**, 697-700.

Gales, C., Rebois, R.V., Hogue, M., Trieu, P., Breit, A., Hebert, T.E. and Bouvier, M. (2005) Real-time monitoring of receptor and G-protein interactions in living cells. *Nat. Methods*, **2**, 177-184.

Gallego, C., Gupta, S.K., Winitz, S., Eisfelder, B.J. and Johnson, G.L. (1992) Myristoylation of the $G\alpha_{i2}$ polypeptide, a G protein α subunit, is required for its signaling and transformation functions. *Proc. Natl. Acad. Sci. U. S. A.*, **89**, 9695-9699.

Garritsen, A., van Galen, P.J. and Simonds, W.F. (1993) The N-terminal coiled-coil domain of β is essential for γ association: A model for G-protein βγ subunit interaction. *Proc. Natl. Acad. Sci. U. S. A.*, **90**, 7706-7710.

Garritsen, A. and Simonds, W.F. (1994) Multiple Domains of G Protein β Confer Subunit Specificity in βγ Interaction. *J. Biol. Chem.*, **269**, 24418-24423.

Gaudet, R., Bohm, A. and Sigler, P.B. (1996) Crystal Structure at 2.4 Å Resolution of the Complex of Transducin βγ and Its Regulator, Phosducin. *Cell*, **87**, 577-588.

Gaudet, R., Savage, J.R., McLaughlin, J.N., Willardson, B.M. and Sigler, P.B. (1999) A Molecular Mechanism for the Phosphorylation-Dependent Regulation of Heterotrimeric G Proteins by Phosducin. *Mol. Cell*, **3**, 649-660.

Gerachshenko, T., Blackmer, T., Yoon, E.J., Bartleson, C., Hamm, H.E. and Alford, S. (2005) Gβγ acts at the C terminus of SNAP-25 to mediate presynaptic inhibition. *Nat. Neurosci.*, **8**, 597-605.

Gether, U. (2000) Uncovering Molecular Mechanisms Involved in Activation of G Protein-Coupled Receptors. *Endocr. Rev.*, **21**, 90-113.

Gether, U., Asmar, F., Meinild, A.K. and Rasmussen, S.G. (2002) Structural Basis for Activation of G-Protein-Coupled Receptors. *Pharmacol. Toxicol.*, **91**, 304-312.

Ghahremani, M.H., Cheng, P., Lembo, P.M. and Albert, P.R. (1999) Distinct Roles for $G\alpha_i2$, $G\alpha_i3$, and Gβγ in Modulation of Forskolin- or G_s-Mediated cAMP Accumulation and Calcium Mobilization by Dopamine D2S Receptors. *J. Biol. Chem.*, **274**, 9238-9245.

Gilchrist, R.L., Ryu, K.S., Ji, I. and Ji, T.H. (1996) The Luteinizing Hormone/Chorionic Gonadotropin Receptor Has Distinct Transmembrane Conductors for cAMP and Inositol Phosphate Signals. *J. Biol. Chem.*, **271**, 19283-19287.

Gilman, A.G. (1987) G proteins: transducers of receptor-generated signals. *Annu. Rev. Biochem.*, **56**, 615-649.

Glick, J.L., Meigs, T.E., Miron, A. and Casey, P.J. (1998) RGSZ1, a G_z-selective Regulator of G Protein Signaling Whose Action Is Sensitive to the Phosphorylation State of $G_z\alpha$. *J. Biol. Chem.*, **273**, 26008-26013.

Godchaux, W., 3rd and Zimmerman, W.F. (1979) Membrane-dependent Guanine Nucleotide Binding and GTPase Activities of Soluble Protein from Bovine Rod Cell Outer Segments. *J. Biol. Chem.*, **254**, 7874-7884.

Goldberg, J. (1998) Structural Basis for Activation of ARF GTPase: Mechanisms of Guanine Nucleotide Exchange and GTP-Myristoyl Switching. *Cell*, **95**, 237-248.

Gordeliy, V.I., Labahn, J., Moukhametzianov, R., Efremov, R., Granzin, J., Schlesinger, R., Buldt, G., Savopol, T., Scheidig, A.J., Klare, J.P. and Engelhard, M. (2002) Molecular basis of transmembrane signalling by sensory rhodopsin II-transducer complex. *Nature*, **419**, 484-487.

Graf, R., Mattera, R., Codina, J., Evans, T., Ho, Y.K., Estes, M.K. and Birnbaumer, L. (1992) Studies on the interaction of α subunits of GTP-binding proteins with βγ dimers. *Eur. J. Biochem.*, **210**, 609-619.

Grishina, G. and Berlot, C.H. (1998) Mutations at the Domain Interface of G_{sa} Impair Receptor-mediated Activation by Altering Receptor and Guanine Nucleotide Binding. *J. Biol. Chem.*, **273**, 15053-15060.

Grishina, G. and Berlot, C.H. (2000) A Surface-Exposed Region of $G_{s\alpha}$ in Which Substitutions Decrease Receptor-Mediated Activation and Increase Receptor Affinity. *Mol. Pharmacol.*, **57**, 1081-1092.

Hallak, H., Brass, L.F. and Manning, D.R. (1994) Failure to Myristoylate the α Subunit of G_z Is Correlated with an Inhibition of Palmitoylation and Membrane Attachment, but Has No Affect on Phosphorylation by Protein Kinase C. *J. Biol. Chem.*, **269**, 4571-4576.

Hamm, H.E. and Bownds, M.D. (1986) Protein Complement of Rod Outer Segments of Frog Retina. *Biochemistry*, **25**, 4512-4523.

Hamm, H.E., Deretic, D., Hofmann, K.P., Schleicher, A. and Kohl, B. (1987) Mechanism of Action of Monoclonal Antibodies That Block the Light Activation of the Guanyl Nucleotide-binding Protein, Transducin. *J. Biol. Chem.*, **262**, 10831-10838.

Hamm, H.E., Deretic, D., Arendt, A., Hargrave, P.A., Koenig, B. and Hofmann, K.P. (1988) Site of G Protein Binding to Rhodopsin Mapped with Synthetic Peptides from the α Subunit. *Science*, **241**, 832-835.

Hamm, H.E. (1998) The Many Faces of G protein Signaling. *J. Biol. Chem.*, **273**, 669-672.

Hanson, S.M., Francis, D.J., Vishnivetskiy, S.A., Kolobova, E.A., Hubbell, W.L., Klug, C.S. and Gurevich, V.V. (2006) Differential interaction of spin-labeled arrestin with inactive and active phosphorhodopsin. *Proc. Natl. Acad. Sci. U. S. A.*, **103**, 4900-4905.

Hatley, M.E., Lockless, S.W., Gibson, S.K., Gilman, A.G. and Ranganathan, R. (2003) Allosteric determinants in guanine nucleotide-binding proteins. *Proc. Natl. Acad. Sci. U. S. A.*, **100**, 14445-14450.

Hebert, T.E., Gales, C. and Rebois, R.V. (2006) Detecting and Imaging Protein-Protein Interactions During G Protein-Mediated Signal Transduction *In Vivo* and *In Situ* by Using Fluorescence-Based Techniques. *Cell Biochem. Biophys.*, **45**, 85-109.

Heck, M. and Hofmann, K.P. (2001) Maximal Rate and Nucleotide Dependence of Rhodopsin-catalyzed Transducin Activation. Initial Rate Analysis Based on a Double Displacement Mechanism. *J. Biol. Chem.*, **276**, 10000-10009.

Hedin, K.E., Duerson, K. and Clapham, D.E. (1993) Specificity of Receptor-G Protein Interactions: Searching for the Structure Behind the Signal. *Cell. Signal.*, **5**, 505-518.

Hepler, J.R., Biddlecome, G.H., Kleuss, C., Camp, L.A., Hofmann, S.L., Ross, E.M. and Gilman, A.G. (1996) Functional Importance of the Amino Terminus of $G_{q\alpha}$. *J. Biol. Chem.*, **271**, 496-504.

Herlitze, S., Garcia, D.E., Mackie, K., Hille, B., Scheuer, T. and Catterall, W.A. (1996) Modulation of Ca^{2+} channels by G-protein βγ subunits. *Nature*, **380**, 258-262.

Herrmann, R., Heck, M., Henklein, P., Kleuss, C., Hofmann, K.P. and Ernst, O.P. (2004) Sequence of Interactions in Receptor-G Protein Coupling. *J. Biol. Chem.*, **279**, 24283-24290.

Heydorn, A., Ward, R.J., Jorgensen, R., Rosenkilde, M.M., Frimurer, T.M., Milligan, G. and Kostenis, E. (2004) Identification of a Novel Site within G Protein α Subunits Important for Specificity of Receptor-G Protein Interaction. *Mol. Pharmacol.*, **66**, 250-259.

Higashijima, T., Ferguson, K.M., Smigel, M.D. and Gilman, A.G. (1987a) The Effect of GTP and Mg^{2+} on the GTPase Activity and the Fluorescent Properties of G_o. *J. Biol. Chem.*, **262**, 757-761.

Higashijima, T., Ferguson, K.M., Sternweis, P.C., Smigel, M.D. and Gilman, A.G. (1987b) Effects of Mg^{2+} and the bg-Subunit Complex on the Interactions of Guanine Nucleotides with G proteins. *J. Biol. Chem.*, **262**, 762-766.

Higgins, J.B. and Casey, P.J. (1996) The Role of Prenylation in G-Protein Assembly and Function. *Cell. Signal.*, **8**, 433-437.

Hildebrandt, J.D., Codina, J., Risinger, R. and Birnbaumer, L. (1984) Identification of a γ Subunit Associated with the Adenylyl Cyclase Regulatory Proteins N_s and N_i. *J. Biol. Chem.*, **259**, 2039-2042.

Hilser, V.J. and Freire, E. (1996) Structure-based Calculation of the Equilibrium Folding Pathway of Proteins. Correlation with Hydrogen Exchange Protection Factors *J. Mol. Biol.*, **262**, 756-772.

Hilser, V.J. and Freire, E. (1997) Predicting the Equilibrium Protein Folding Pathway: Structure-Based Analysis of Staphylococcal Nuclease. *Proteins*, **27**, 171-183.

Ho, M.K. and Wong, Y.H. (2000) The Amino Terminus of $G\alpha_z$ Is Required for Receptor Recognition, Whereas its α4/β6 Loop Is Essential for Inhibition of Adenylyl Cyclase. *Mol. Pharmacol.*, **58**, 993-1000.

Hoffmann, C., Gaietta, G., Bunemann, M., Adams, S.R., Oberdorff-Maass, S., Behr, B., Vilardaga, J.P., Tsien, R.Y., Ellisman, M.H. and Lohse, M.J. (2005) A FlAsH-based FRET approach to determine G protein-coupled receptor activation in living cells. *Nat. Methods*, **2**, 171-176.

Hofmann, K.P. and Reichert, J. (1985) Chemical Probing of the Light-induced Interaction between Rhodopsin and G-protein. Near-infrared Light-scattering and Sulfhydryl Modifications. *J. Biol. Chem.*, **260**, 7990-7995.

Hoofnagle, A.N., Resing, K.A. and Ahn, N.G. (2003) Protein Analysis by Hydrogen Exchange Mass Spectrometry. *Annu. Rev. Biophys. Biomol. Struct.*, **32**, 1-25.

Hou, Y., Azpiazu, I., Smrcka, A. and Gautam, N. (2000) Selective Role of G Protein γ Subunits in Receptor Interaction. *J. Biol. Chem.*, **275**, 38961-38964.

Hou, Y., Chang, V., Capper, A.B., Taussig, R. and Gautam, N. (2001) G Protein β Subunit Types Differentially Interact with a Muscarinic Receptor but Not Adenylyl Cyclase Type II or Phospholipase C-β2/3. *J. Biol. Chem.*, **276**, 19982-19988.

Hubbell, W.L., Cafiso, D.S. and Altenbach, C. (2000) Identifying conformational changes with site-directed spin labeling. *Nat. Struct. Biol.*, **7**, 735-739.

Hubbell, W.L., Altenbach, C., Hubbell, C.M. and Khorana, H.G. (2003) Rhodopsin Structure, Dynamics, and Activation: A Perspective from Crystallography, Site-Directed Spin Labeling, Sulfhydryl Reactivity, and Disulfide Cross-Linking. *Adv. Protein Chem.*, **63**, 243-290.

Iiri, T., Herzmark, P., Nakamoto, J.M., van Dop, C. and Bourne, H.R. (1994) Rapid GDP release from G_{sa} in patients with gain and loss of endocrine function. *Nature*, **371**, 164-168.

Iiri, T., Backlund, P.S., Jr., Jones, T.L., Wedegaertner, P.B. and Bourne, H.R. (1996) Reciprocal regulation of $G_{s\alpha}$ by palmitate and the βγ subunit. *Proc. Natl. Acad. Sci. U. S. A.*, **93**, 14592-14597.

Iiri, T., Farfel, Z. and Bourne, H.R. (1998) G-protein diseases furnish a model for the turn-on switch. *Nature*, **394**, 35-38.

Ikeda, S.R. (1996) Voltage-dependent modulation of N-type calcium channels by G-protein βγ subunits. *Nature*, **380**, 255-258.

Inglese, J., Koch, W.J., Touhara, K. and Lefkowitz, R.J. (1995) $G_{\beta\gamma}$ interactions with PH domains and Ras-MAPK signaling pathways. *Trends Biochem. Sci.*, **20**, 151-156.

Iniguez-Lluhi, J.A., Simon, M.I., Robishaw, J.D. and Gilman, A.G. (1992) G Protein βγ Subunits Synthesized in Sf9 Cells. Functional Characterization and the Significance of Prenylation of γ. *J. Biol. Chem.*, **267**, 23409-23417.

Insel, P.A., Maguire, M.E., Gilman, A.G., Bourne, H.R., Coffino, P. and Melmon, K.L. (1976) β Adrenergic Receptors and Adenylate Cyclase: Products of Separate Genes? *Mol. Pharmacol.*, **12**, 1062-1069.

Israelewitz, B., Gao, M. and Schulten, K. (2001) Steered molecular dynamics and mechanical functions of proteins. *Curr. Opin. Struct. Biol.*, **11**, 224-230.

Ito, Y., Yamasaki, K., Iwahara, J., Terada, T., Kamiya, A., Shirouzu, M., Muto, Y., Kawai, G., Yokoyama, S., Laue, E.D., Walchli, M., Shibata, T., Nishimura, S. and Miyazawa, T. (1997) Regional Polysterism in the GTP-Bound Form of the Human c-Ha-Ras Protein. *Biochemistry*, **36**, 9109-9119.

Itoh, Y., Cai, K. and Khorana, H.G. (2001) Mapping of contact sites in complex formation between light-activated rhodopsin and transducin by covalent crosslinking: Use of a chemically preactivated reagent. *Proc. Natl. Acad. Sci. U. S. A.*, **98**, 4883-4887.

Janetopoulos, C., Jin, T. and Devreotes, P. (2001) Receptor-Mediated Activation of Heterotrimeric G-Proteins in Living Cells. *Science*, **291**, 2408-2411.

Janz, J.M. and Farrens, D.L. (2004) Rhodopsin Activation Exposes a Key Hydrophobic Binding Site for the Transducin α-Subunit C Terminus. *J. Biol. Chem.*, **279**, 29767-29773.

Javitch, J.A. (2004) The Ants Go Marching Two by Two: Oligomeric Structure of G-Protein-Coupled Receptors. *Mol. Pharmacol.*, **66**, 1077-1082.

Jeschke, G., Koch, A., Jonas, U. and Godt, A. (2002) Direct Conversion of EPR Dipolar Time Evolution Data to Distance Distributions. *J. Magn. Reson.*, **155**, 72-82.

Jian, X., Sainz, E., Clark, W.A., Jensen, R.T., Battey, J.F. and Northup, J.K. (1999) The Bombesin Receptor Subtypes Have Distinct G Protein Specificities. *J. Biol. Chem.*, **274**, 11573-11581.

Jian, X., Clark, W.A., Kowalak, J., Markey, S.P., Simonds, W.F. and Northup, J.K. (2001) Gβγ Affinity for Bovine Rhodopsin Is Determined by the Carboxyl-terminal Sequences of the γ Subunit. *J. Biol. Chem.*, **276**, 48518-48525.

Jiang, Y., Ma, W., Wan, Y., Kozasa, T., Hattori, S. and Huang, X.Y. (1998) The G protein Gα12 stimulates Bruton's tyrosine kinase and a rasGAP through a conserved PH/BM domain. *Nature*, **395**, 808-813.

Johnston, C.A., Willard, F.S., Jezyk, M.R., Fredericks, Z., Bodor, E.T., Jones, M.B., Blaesius, R., Watts, V.J., Harden, T.K., Sondek, J., Ramer, J.K. and Siderovski, D.P. (2005) Structure of $G\alpha_{i1}$ Bound to a GDP-Selective Peptide Provides Insight into Guanine Nucleotide Exchange. *Structure*, **13**, 1069-1080.

Jones, M.B., Siderovski, D.P. and Hooks, S.B. (2004) The Gβγ Dimer as a Novel Source of Selectivity in G-Protein Signaling: GGL-ing at Convention. *Molecular Interventions*, **4**, 200-214.

Jones, T.A., Zou, J.Y., Cowan, S.W. and Kjeldgaard (1991) Improved Methods for Building Protein Models in Electron Density Maps and the Location of Errors in These Models. *Acta Crystallogr. A.*, **47** 110-119.

Katada, T. and Ui, M. (1982) Direct modification of the membrane adenylate cyclase system by islet-activating protein due to ADP-ribosylation of a membrane protein. *Proc. Natl. Acad. Sci. U. S. A.*, **79**, 3129-3133.

Katz, A., Wu, D. and Simon, M.I. (1992) Subunits βγ of heterotrimeric G protein activate β2 isoform of phospholipase C. *Nature*, **360**, 686-689.

Kenakin, T. (2003) Ligand-selective receptor conformations revisited: the promise and the problem. *Trends Pharmacol. Sci.*, **24**, 346-354.

Kimple, R.J., Kimple, M.E., Betts, L., Sondek, J. and Siderovski, D.P. (2002) Structural determinants for GoLoco-induced inhibition of nucleotide release by Gα subunits. *Nature*, **416**, 878-881.

Kisselev, O. and Gautam, N. (1993) Specific Interaction with Rhodopsin Is Dependent on the γ Subunit Type in a G protein. *J. Biol. Chem.*, **268**, 24519-24522.

Kisselev, O., Pronin, A., Ermolaeva, M. and Gautam, N. (1995) Receptor-G protein coupling is established by a potential conformational switch in the βγ complex. *Proc. Natl. Acad. Sci. U. S. A.*, **92**, 9102-9106.

Kisselev, O.G., Ermolaeva, M.V. and Gautam, N. (1994) A Farnesylated Domain in the G Protein γ Subunit Is a Specific Determinant of Receptor Coupling. *J. Biol. Chem.*, **269**, 21399-21402.

Kisselev, O.G., Kao, J., Ponder, J.W., Fann, Y.C., Gautam, N. and Marshall, G.R. (1998) Light-activated rhodopsin induces structural binding motif in G protein α subunit. *Proc. Natl. Acad. Sci. U. S. A.*, **95**, 4270-4275.

Kisselev, O.G., Meyer, C.K., Heck, M., Ernst, O.P. and Hofmann, K.P. (1999) Signal transfer from rhodopsin to the G-protein: Evidence for a two-site sequential fit mechanism. *Proc. Natl. Acad. Sci. U. S. A.*, **96**, 4898-4903.

Kisselev, O.G. and Downs, M.A. (2003) Rhodopsin Controls a Conformational Switch on the Transducin γ Subunit. *Structure*, **11**, 367-373.

Koenig, B.W., Kontaxis, G., Mitchell, D.C., Louis, J.M., Litman, B.J. and Bax, A. (2002) Structure and Orientation of a G protein Fragment in the Receptor Bound State from Residual Dipolar Couplings. *J. Mol. Biol.*, **322**, 441-461.

Kolbe, M., Besir, H., Essen, L.O. and Oesterhelt, D. (2000) Structure of the light-driven chloride pump halorhodopsin at 1.8 A resolution. *Science*, **288**, 1390-1396.

Konig, B., Arendt, A., McDowell, J.H., Kahlert, M., Hargrave, P.A. and Hofmann, K.P. (1989) Three cytoplasmic loops of rhodopsin interact with transducin. *Proc. Natl. Acad. Sci. U. S. A.*, **86**, 6878-6882.

Kostenis, E., Conklin, B.R. and Wess, J. (1997a) Molecular Basis of Receptor/G Protein Coupling Selectivity Studied by Coexpression of Wild Type and Mutant m2 Muscarinic Receptors with Mutant $G\alpha_q$ Subunits. *Biochemistry*, **36**, 1487-1495.

Kostenis, E., Degtyarev, M.Y., Conklin, B.R. and Wess, J. (1997b) The N-terminal Extension of $G\alpha_q$ Is Critical for Constraining the Selectivity of Receptor Coupling. *J. Biol. Chem.*, **272**, 19107-19110.

Kostenis, E., Gomeza, J., Lerche, C. and Wess, J. (1997c) Genetic Analysis of Receptor-$G\alpha_q$ Coupling Selectivity. *J. Biol. Chem.*, **272**, 23675-23681.

Kostenis, E., Zeng, F.Y. and Wess, J. (1998) Functional Characterization of a Series of Mutant G Protein α_q Subunits Displaying Promiscuous Receptor Coupling Properties. *J. Biol. Chem.*, **273**, 17886-17892.

Kostenis, E., Martini, L., Ellis, J., Waldhoer, M., Heydorn, A., Rosenkilde, M.M., Norregaard, P.K., Jorgensen, R., Whistler, J.L. and Milligan, G. (2005) A Highly Conserved Glycine within Linker I and the Extreme C Terminus of G Protein α Subunits Interact Cooperatively in Switching G Protein-Coupled Receptor-to-Effector Specificity. *J. Pharmacol. Exp. Ther.*, **313**, 78-87.

Kovoor, A., Chen, C.K., He, W., Wensel, T.G., Simon, M.I. and Lester, H.A. (2000) Co-expression of Gβ5 Enhances the Function of Two Gγ Subunit-like Domain-containing Regulators of G Protein Signaling Proteins. *J. Biol. Chem.*, **275**, 3397-3402.

Kraulis, P.J., Domaille, P.J., Campbell-Burk, S.L., Van Aken, T. and Laue, E.D. (1994) Solution Structure and Dynamics of Ras p21•GDP Determined by Heteronuclear Three- and Four-Dimensional NMR Spectroscopy. *Biochemistry*, **33**, 3515-3531.

Kreutz, B., Yau, D.M., Nance, M.R., Tanabe, S., Tesmer, J.J. and Kozasa, T. (2006) A New Approach to Producing Functional Gα Subunits Yields the Activated and Deactivated Structures of $G\alpha_{12/13}$ Proteins. *Biochemistry*, **45**, 167-174.

Kristiansen, K. (2004) Molecular mechanisms of ligand binding, signaling, and regulation within the superfamily of G-protein-coupled receptors: molecular modeling and mutagenesis approaches to receptor structure and function. *Pharmacol. Ther.*, **103**, 21-80.

Kuhn, H. (1980) Light- and GTP-regulated interaction of GTPase and other proteins with bovine photoreceptor membranes. *Nature*, **283**, 587-589.

Lambright, D.G., Noel, J.P., Hamm, H.E. and Sigler, P.B. (1994) Structural determinants for activation of the α-subunit of a heterotrimeric G protein. *Nature*, **369**, 621-628.

Lambright, D.G., Sondek, J., Bohm, A., Skiba, N.P., Hamm, H.E. and Sigler, P.B. (1996) The 2.0 Å crystal structure of a heterotrimeric G protein. *Nature*, **379**, 311-319.

Landis, C.A., Masters, S.B., Spada, A., Pace, A.M., Bourne, H.R. and Vallar, L. (1989) GTPase inhibiting mutations activate the α chain of G_s and stimulate adenylyl cyclase in human pituitary tumours. *Nature*, **340**, 692-696.

Langen, R., Oh, K.J., Cascio, D. and Hubbell, W.L. (2000) Crystal Structures of Spin Labeled T4 Lysozyme Mutants: Implications for the Interpretation of EPR Spectra in Terms of Structure. *Biochemistry*, **39**, 8396-8405.

Lee, C., Murakami, T. and Simonds, W.F. (1995a) Identification of a Discrete Region of the G Protein γ Subunit Conferring Selectivity in βγ Complex Formation. *J. Biol. Chem.*, **270**, 8779-8784.

Lee, C.H., Katz, A. and Simon, M.I. (1995b) Multiple Regions of $G_{\alpha 16}$ Contribute to the Specificity of Activation by the C5a Receptor. *Mol. Pharmacol.*, **47**, 218-223.

Levay, K., Cabrera, J.L., Satpaev, D.K. and Slepak, V.Z. (1999) Gβ5 prevents the RGS7-Gαo interaction through binding to a distinct Gγ-like domain found in RGS7 and other RGS proteins. *Proc. Natl. Acad. Sci. U. S. A.*, **96**, 2503-2507.

Li, J., Edwards, P.C., Burghammer, M., Villa, C. and Schertler, G.F. (2004) Structure of Bovine Rhodopsin in a Trigonal Crystal Form. *J. Mol. Biol.*, **343**, 1409-1438.

Li, Y., Sternweis, P.M., Charnecki, S., Smith, T.F., Gilman, A.G., Neer, E.J. and Kozasa, T. (1998) Sites for Gα Binding on the G protein β Subunit Overlap with Sites for Regulation of Phospholipase Cβ and Adenylyl Cyclase. *J. Biol. Chem.*, **273**, 16265-16272.

Liang, Y., Fotiadis, D., Filipek, S., Saperstein, D.A., Palczewski, K. and Engel, A. (2003) Organization of the G Protein-coupled Receptors Rhodopsin and Opsin in Native Membranes. *J. Biol. Chem.*, **278**, 21655-21662.

Liang, Z.C., Lou, Y., Freed, J.H., Columbus, L. and Hubbell, W.L. (2004) A Multifrequency Electron Spin Resonance Study of T4 Lysozyme Dynamics Using the Slowly Relaxing Local Structure Model. *Journal of Physical Chemistry B*, **108**, 17649-17659.

Lichtarge, O., Bourne, H.R. and Cohen, F.E. (1996a) Evolutionarily conserved $G_{\alpha\beta\gamma}$ binding surfaces support a model of the G protein-receptor complex. *Proc. Natl. Acad. Sci. U. S. A.*, **93**, 7507-7511.

Lichtarge, O., Bourne, H.R. and Cohen, F.E. (1996b) An Evolutionary Trace Method Defines Binding Surfaces Common to Protein Families. *J. Mol. Biol.*, **257**, 342-358.

Liebman, P.A. and Sitaramayya, A. (1984) Role of G-Protein-Receptor Interaction in Amplified Phosphodiesterase Activation of Retinal Rods. *Adv. Cyclic Nucleotide Protein Phosphorylation Res.*, **17**, 215-225.

Lim, W.K., Myung, C.S., Garrison, J.C. and Neubig, R.R. (2001) Receptor-G Protein γ Specificity: γ11 Shows Unique Potency for A_1 Adenosine and 5-HT_{1A} Receptors. *Biochemistry*, **40**, 10532-10541.

Limbird, L.E. and Lefkowitz, R.J. (1977) Resolution of β-Adrenergic Receptor Binding and Adenylate Cyclase Activity by Gel Exclusion Chromatography. *J. Biol. Chem.*, **252**, 799-802.

Linder, M.E., Pang, I.H., Duronio, R.J., Gordon, J.I., Sternweis, P.C. and Gilman, A.G. (1991) Lipid Modifications of G Protein Subunits. Myristoylation of $G_{o\alpha}$ Increases its Affinity for βγ. *J. Biol. Chem.*, **266**, 4654-4659.

Linder, M.E. and Gilman, A.G. (1992) G proteins. *Sci. Am.*, **267**, 56-61, 64-55.

Lindorfer, M.A., Myung, C.S., Savino, Y., Yasuda, H., Khazan, R. and Garrison, J.C. (1998) Differential Activity of the G Protein $\beta_5\gamma_2$ Subunit at Receptors and Effectors. *J. Biol. Chem.*, **273**, 34429-34436.

Liu, J., Conklin, B.R., Blin, N., Yun, J. and Wess, J. (1995) Identification of a receptor/G-protein contact site critical for signaling specificity and G-protein activation. *Proc. Natl. Acad. Sci. U. S. A.*, **92**, 11642-11646.

Liu, W., Clark, W.A., Sharma, P. and Northup, J.K. (1998) Mechanism of Allosteric Regulation of the Rod cGMP Phosphodiesterase Activity by the Helical Domain of Transducin α Subunit. *J. Biol. Chem.*, **273**, 34284-34292.

Liu, Y., Arshavsky, V.Y. and Ruoho, A.E. (1999) Interaction sites of the C-terminal region of the cGMP phosphodiesterase inhibitory subunit with the GDP-bound transducin α-subunit. *Biochem. J.*, **337 (Pt 2)**, 281-288.

Lockless, S.W. and Ranganathan, R. (1999) Evolutionarily Conserved Pathways of Energetic Connectivity in Protein Families. *Science*, **286**, 295-299.

Lodowski, D.T., Pitcher, J.A., Capel, W.D., Lefkowitz, R.J. and Tesmer, J.J. (2003) Keeping G Proteins at Bay: A Complex Between G Protein-Coupled Receptor Kinase 2 and Gβγ. *Science*, **300**, 1256-1262.

Loew, A., Ho, Y.K., Blundell, T. and Bax, B. (1998) Phosducin induces a structural change in transducin βγ. *Structure*, **6**, 1007-1019.

Logothetis, D.E., Kurachi, Y., Galper, J., Neer, E.J. and Clapham, D.E. (1987) The βγ subunits of GTP-binding proteins activate the muscarinic K^+ channel in heart. *Nature*, **325**, 321-326.

Loh, A.P., Guo, W., Nicholson, L.K. and Oswald, R.E. (1999) Backbone Dynamics of Inactive, Active, and Effector-Bound Cdc42Hs from Measurements of ^{15}N Relaxation Parameters at Multiple Field Strengths. *Biochemistry*, **38**, 12547-12557.

Londos, C., Salomon, Y., Lin, M.C., Harwood, J.P., Schramm, M., Wolff, J. and Rodbell, M. (1974) 5'-Guanylylimidodiphosphate, A Potent Activator of Adenylate Cyclase Systems in Eukaryotic Cells. *Proc. Natl. Acad. Sci. U. S. A.*, **71**, 3087-3090.

Luecke, H., Schobert, B., Richter, H.T., Cartailler, J.P. and Lanyi, J.K. (1999) Structure of bacteriorhodopsin at 1.55 Å resolution. *J. Mol. Biol.*, **291**, 899-911.

Lyons, J., Landis, C.A., Harsh, G., Vallar, L., Grunewald, K., Feichtinger, H., Duh, Q.Y., Clark, O.H., Kawasaki, E., Bourne, H.R. and McCormick, F. (1990) Two G Protein Oncogenes in Human Endocrine Tumors. *Science*, **249**, 655-659.

Macrez-Lepretre, N., Kalkbrenner, F., Schultz, G. and Mironneau, J. (1997) Distinct Functions of G_q and G_{11} Proteins in Coupling α_1-Adrenoreceptors to Ca^{2+} Release and Ca^{2+} Entry in Rat Portal Vein Myocytes. *J. Biol. Chem.*, **272**, 5261-5268.

Majumdar, S., Ramachandran, S. and Cerione, R.A. (2004) Perturbing the Linker Regions of the α-Subunit of Transducin: A New Class of Constitutively Active GTP-binding Proteins. *J. Biol. Chem.*, **279**, 40137-40145.

Makino, E.R., Handy, J.W., Li, T. and Arshavsky, V.Y. (1999) The GTPase activating factor for transducin in rod photoreceptors is the complex between RGS9 and type 5 G protein β subunit. *Proc. Natl. Acad. Sci. U. S. A.*, **96**, 1947-1952.

Manning, D.R. and Gilman, A.G. (1983) The Regulatory Components of Adenylate Cyclase and Transducin. A Family of Structurally Homologous Guanine Nucleotide-binding Proteins. *J. Biol. Chem.*, **258**, 7059-7063.

Mansoor, S.E., McHaourab, H.S. and Farrens, D.L. (1999) Determination of Protein Secondary Structure and Solvent Accessibility Using Site-Directed Fluorescence Labeling. Studies of T4 Lysozyme Using the Fluorescent Probe Monobromobimane. *Biochemistry*, **38**, 16383-16393.

Marin, E.P., Krishna, A.G., Zvyaga, T.A., Isele, J., Siebert, F. and Sakmar, T.P. (2000) The Amino Terminus of the Fourth Cytoplasmic Loop of Rhodopsin Modulates Rhodopsin-Transducin Interaction. *J. Biol. Chem.*, **275**, 1930-1936.

Marin, E.P., Krishna, A.G., Archambault, V., Simuni, E., Fu, W.Y. and Sakmar, T.P. (2001a) The Function of Interdomain Interactions in Controlling Nucleotide Exchange Rates in Transducin. *J. Biol. Chem.*, **276**, 23873-23880.

Marin, E.P., Krishna, A.G. and Sakmar, T.P. (2001b) Rapid Activation of Transducin by Mutations Distant from the Nucleotide-Binding Site. Evidence for a Mechanistic Model of Receptor-Catalyzed Nucleotide Exchange by G Proteins. *J. Biol. Chem.*, **276**, 27400-27405.

Marin, E.P., Krishna, A.G. and Sakmar, T.P. (2002) Disruption of the α5 Helix of Transducin Impairs Rhodopsin-Catalyzed Nucleotide Exchange. *Biochemistry*, **41**, 6988-6994.

Markby, D.W., Onrust, R. and Bourne, H.R. (1993) Separate GTP Binding and GTPase Activating Domains of a Gα Subunit. *Science*, **262**, 1895-1901.

Marsh, S.R., Grishina, G., Wilson, P.T. and Berlot, C.H. (1998) Receptor-Mediated Activation of $G_{s\alpha}$: Evidence for Intramolecular Signal Transduction. *Mol. Pharmacol.*, **53**, 981-990.

Martin, E.L., Rens-Domiano, S., Schatz, P.J. and Hamm, H.E. (1996) Potent Peptide Analogues of a G Protein Receptor-binding Region Obtained with a Combinatorial Library. *J. Biol. Chem.*, **271**, 361-366.

Mazzoni, M.R., Malinksi, J.A. and Hamm, H.E. (1991) Structural Analysis of Rod GTP-binding Protein, G_t. Limited Proteolytic Digestion Pattern of G_t with Four Proteases Defines Monoclonal Antibody Epitope. *J. Biol. Chem.*, **266**, 14072-14081.

Mazzoni, M.R. and Hamm, H.E. (1996) Interaction of Transducin with Light-Activated Rhodopsin Protects It from Proteolytic Digestion by Trypsin. *J. Biol. Chem.*, **271**, 30034-30040.

McCabe, J.B. and Berthiaume, L.G. (1999) Functional Roles for Fatty Acylated Amino-terminal Domains in Subcellular Localization. *Mol. Biol. Cell*, **10**, 3771-3786.

McCudden, C.R., Hains, M.D., Kimple, R.J., Siderovski, D.P. and Willard, F.S. (2005) G-protein signaling: back to the future. *Cell. Mol. Life Sci.*, **62**, 551-577.

Mchaourab, H.S., Lietzow, M.A., Hideg, K. and Hubbell, W.L. (1996) Motion of Spin-Labeled Side Chains in T4 Lysozyme. Correlation with Protein Structure and Dynamics. *Biochemistry*, **35**, 7692-7704.

Mchaourab, H.S., Kalai, T., Hideg, K. and Hubbell, W.L. (1999) Motion of spin-labeled side chains in T4 lysozyme: effect of side chain structure. *Biochemistry*, **38**, 2947-2955.

McIntire, W.E., MacCleery, G. and Garrison, J.C. (2001) The G Protein β Subunit Is a Determinant in the Coupling of G_s to the β_1-adrenergic and A2a Adenosine Receptors. *J. Biol. Chem.*, **276**, 15801-15809.

McLaughlin, J.N., Shen, L., Holinstat, M., Brooks, J.D., Dibenedetto, E. and Hamm, H.E. (2005) Functional Selectivity of G Protein Signaling by Agonist Peptides and Thrombin for the Protease-activated Receptor-1. *J. Biol. Chem.*, **280**, 25048-25059.

Medkova, M., Preininger, A.M., Yu, N.J., Hubbell, W.L. and Hamm, H.E. (2002) Conformational Changes in the Amino-Terminal Helix of the G Protein α_{i1} Following Dissociation from Gβγ Subunit and Activation. *Biochemistry*, **41**, 9962-9972.

Milburn, M.V., Tong, L., deVos, A.M., Brunger, A., Yamaizumi, Z., Nishimura, S. and Kim, S.H. (1990) Molecular Switch for Signal Transduction: Structural Differences Between Active and Inactive Forms of Protooncogenic *ras* Proteins. *Science*, **247**, 939-945.

Milligan, G. (2004) G Protein-Coupled Receptor Dimerization: Function and Ligand Pharmacology. *Mol. Pharmacol.*, **66**, 1-7.

Misquitta, Y., Cherezov, V., Havas, F., Patterson, S., Mohan, J.M., Wells, A.J., Hart, D.J. and Caffrey, M. (2004) Rational design of lipid for membrane protein crystallization. *J. Struct. Biol.*, **148**, 169-175.

Mixon, M.B., Lee, E., Coleman, D.E., Berghuis, A.M., Gilman, A.G. and Sprang, S.R. (1995) Tertiary and Quaternary Structural Changes in $G_{i\alpha1}$ Induced by GTP Hydrolysis. *Science*, **270**, 954-960.

Mochizuki, N., Ohba, Y., Kiyokawa, E., Kurata, T., Murakami, T., Ozaki, T., Kitabatake, A., Nagashima, K. and Matsuda, M. (1999) Activation of the ERK/MAPK pathway by an isoform of rap1GAP associated with $G\alpha_i$. *Nature*, **400**, 891-894.

Morales, J., Fishburn, C.S., Wilson, P.T. and Bourne, H.R. (1998) Plasma Membrane Localization of $G\alpha_z$ Requires Two Signals. *Mol. Biol. Cell*, **9**, 1-14.

Mukhopadhyay, S. and Ross, E.M. (1999) Rapid GTP binding and hydrolysis by G_q promoted by receptor and GTPase-activating proteins. *Proc. Natl. Acad. Sci. U. S. A.*, **96**, 9539-9544.

Mukhopadhyay, S. and Howlett, A.C. (2005) Chemically Distinct Ligands Promote Differential CB_1 Cannabinoid Receptor-Gi Protein Interactions. *Mol. Pharmacol.*, **67**, 2016-2024.

Mumby, S.M., Heukeroth, R.O., Gordon, J.I. and Gilman, A.G. (1990) G-protein α-subunit expression, myristoylation, and membrane association in COS cells. *Proc. Natl. Acad. Sci. U. S. A.*, **87**, 728-732.

Mumby, S.M., Kleuss, C. and Gilman, A.G. (1994) Receptor regulation of G-protein palmitoylation. *Proc. Natl. Acad. Sci. U. S. A.*, **91**, 2800-2804.

Muramatsu, T. and Suwa, M. (2006) Statistical analysis and prediction of functional residues effective for GPCR-G-protein coupling selectivity. *Prot. Eng. Des. Sel.*, **19**, 277-283.

Myung, C.S., Yasuda, H., Liu, W.W., Harden, T.K. and Garrison, J.C. (1999) Role of Isoprenoid Lipids on the Heterotrimeric G Protein γ Subunit in Determining Effector Activation. *J. Biol. Chem.*, **274**, 16595-16603.

Myung, C.S., Lim, W.K., Defilippo, J., Yasuda, H., Neubig, R. and Garrison, J.C. (2005) Regions in the G Protein γ Subunit Important for Interaction with Receptors and Effectors. *Mol. Pharmacol.*, **69**, 877-887.

Nanoff, C., Koppensteiner, R., Yang, Q., Fuerst, E., Ahorn, H. and Freissmuth, M. (2006) The Carboxyl Terminus of the Gα-Subunit Is the Latch for Triggered Activation of Heterotrimeric G Proteins. *Mol. Pharmacol.*, **69**, 397-405.

Natochin, M., Muradov, K.G., McEntaffer, R.L. and Artemyev, N.O. (2000) Rhodopsin Recognition by Mutant $G_s\alpha$ Containing C-terminal Residues of Transducin. *J. Biol. Chem.*, **275**, 2669-2675.

Natochin, M., Moussaif, M. and Artemyev, N.O. (2001) Probing the mechanism of rhodopsin-catalyzed transducin activation. *J. Neurochem.*, **77**, 202-210.

Natochin, M., Gasimov, K.G., Moussaif, M. and Artemyev, N.O. (2003) Rhodopsin Determinants for Transducin Activation: A Gain-of-Function Approach. *J. Biol. Chem.*, **278**, 37574-37581.

Navarro, J., Landau, E.M. and Fahmy, K. (2002) Receptor-dependent G-protein activation in lipidic cubic phase. *Biopolymers*, **67**, 167-177.

Neer, E.J. (1995) Heterotrimeric G Proteins: Organizers of Transmembrane Signals. *Cell*, **80**, 249-257.

Nikiforovich, G.V. and Marshall, G.R. (2003) Three-Dimensional Model for Meta-II Rhodopsin, an Activated G-Protein-Coupled Receptor. *Biochemistry*, **42**, 9110-9120.

Noel, J.P., Hamm, H.E. and Sigler, P.B. (1993) The 2.2 Å crystal structure of transducin-α complexed with GTPγS. *Nature*, **366**, 654-663.

Northup, J.K., Sternweis, P.C., Smigel, M.D., Schleifer, L.S., Ross, E.M. and Gilman, A.G. (1980) Purification of the regulatory component of adenylate cyclase. *Proc. Natl. Acad. Sci. U. S. A.*, **77**, 6516-6520.

Okada, T., Fujiyoshi, Y., Silow, M., Navarro, J., Landau, E.M. and Shichida, Y. (2002) Functional role of internal water molecules in rhodopsin revealed by X-ray crystallography. *Proc. Natl. Acad. Sci. U. S. A.*, **99**, 5982-5987.

Okada, T., Sugihara, M., Bondar, A.N., Elstner, M., Entel, P. and Buss, V. (2004) The Retinal Conformation and Its Environment in Rhodopsin in Light of a New 2.2 Å Crystal Structure. *J. Mol. Biol.*, **342**, 571-583.

Oliveira, L., Paiva, A.C. and Vriend, G. (1999) A low resolution model for the interaction of G proteins with G protein-coupled receptors. *Protein Eng.*, **12**, 1087-1095.

Onrust, R., Herzmark, P., Chi, P., Garcia, P.D., Lichtarge, O., Kingsley, C. and Bourne, H.R. (1997) Receptor and βγ Binding Sites in the α Subunit of the Retinal G Protein Transducin. *Science*, **275**, 381-384.

Osawa, S. and Weiss, E.R. (1995) The Effect of Carboxyl-terminal Mutagenesis of $G_t\alpha$ on Rhodopsin and Guanine Nucleotide Binding. *J. Biol. Chem.*, **270**, 31052-31058.

Ota, N. and Agard, D.A. (2005) Intramolecular Signaling Pathways Revealed by Modeling Anisotropic Thermal Diffusion. *J. Mol. Biol.*, **351**, 345-354.

Otwinowski, Z. and Minor, W. (1997). Processing of X-ray Diffraction Data Collected in Oscillation Mode. In *Macromolecular Crystallography Part A*, (C. W. Carter, Jr. and R. M. Sweet, eds.), **276**, 307-326. New York: Academic Press.

Palczewski, K., Kumasaka, T., Hori, T., Behnke, C.A., Motoshima, H., Fox, B.A., Le Trong, I., Teller, D.C., Okada, T., Stenkamp, R.E., Yamamoto, M. and Miyano, M. (2000) Crystal Structure of Rhodopsin: A G Protein-Coupled Receptor. *Science*, **289**, 739-745.

Pan, H., Lee, J.C. and Hilser, V.J. (2000) Binding sites in *Escherichia coli* dihydrofolate reductase communicate by modulating the conformational ensemble. *Proc. Natl. Acad. Sci. U. S. A.*, **97**, 12020-12025.

Panchenko, M.P., Saxena, K., Li, Y., Charnecki, S., Sternweis, P.M., Smith, T.F., Gilman, A.G., Kozasa, T. and Neer, E.J. (1998) Sites Important for PLCβ2 Activation by the G Protein βγ Subunit Map to the Sides of the β Propeller Structure. *J. Biol. Chem.*, **273**, 28298-28304.

Pannier, M., Veit, S., Godt, A., Jeschke, G. and Spiess, H.W. (2000) Dead-Time Free Measurement of Dipole-Dipole Interactions between Electron Spins. *J. Magn. Reson.*, **142**, 331-340.

Pereira, R. and Cerione, R.A. (2005) A Switch 3 Point Mutation in the α Subunit of Transducin Yields a Unique Dominant-negative Inhibitor. *J. Biol. Chem.*, **280**, 35696-35703.

Perez, D.M., Hwa, J., Gaivin, R., Mathur, M., Brown, F. and Graham, R.M. (1996) Constitutive Activation of a Single Effector Pathway: Evidence for Multiple Activation States of a G Protein-Coupled Receptor. *Mol. Pharmacol.*, **49**, 112-122.

Perez, D.M. and Karnik, S.S. (2005) Multiple Signaling States of G-Protein-Coupled Receptors. *Pharmacol. Rev.*, **57**, 147-161.

Phillips, W.J., Wong, S.C. and Cerione, R.A. (1992) Rhodopsin/Transducin Interactions. II. Influence of the Transducin-βγ Subunit Complex on the Coupling of the Transducin-α Subunit to Rhodopsin. *J. Biol. Chem.*, **267**, 17040-17046.

Pierce, K.L., Premont, R.T. and Lefkowitz, R.J. (2002) Seven-Transmembrane Receptors. *Nat. Rev. Mol. Cell Biol.*, **3**, 639-650.

Pitcher, J.A., Inglese, J., Higgins, J.B., Arriza, J.L., Casey, P.J., Kim, C., Benovic, J.L., Kwatra, M.M., Caron, M.G. and Lefkowitz, R.J. (1992) Role of βγ Subunits of G proteins in Targeting the β-Adrenergic Receptor Kinase to Membrane-Bound Receptors. *Science*, **257**, 1264-1267.

Posner, B.A., Mixon, M.B., Wall, M.A., Sprang, S.R. and Gilman, A.G. (1998) The A326S Mutant of $G_{i\alpha 1}$ as an Approximation of the Receptor-bound State. *J. Biol. Chem.*, **273**, 21752-21758.

Preininger, A.M., Van Eps, N., Yu, N.J., Medkova, M., Hubbell, W.L. and Hamm, H.E. (2003) The Myristoylated Amino Terminus of $G\alpha_{i1}$ Plays a Critical Role in the Structure and Function of $G\alpha_{i1}$ Subunits in Solution. *Biochemistry*, **42**, 7931-7941.

Preininger, A.M., Henage, L.G., Oldham, W.M., Yoon, E.J., Hamm, H.E. and Brown, H.A. (2006) Direct modulation of Phospholipase D activity by Gbg. *Mol. Pharmacol.*,

Pronin, A.N. and Gautam, N. (1992) Interaction between G-protein β and γ subunit types is selective. *Proc. Natl. Acad. Sci. U. S. A.*, **89**, 6220-6224.

Rabenstein, M.D. and Shin, Y.K. (1995) Determination of the distance between two spin labels attached to a macromolecule. *Proc. Natl. Acad. Sci. U. S. A.*, **92**, 8239-8243.

Rall, T.W., Sutherland, E.W. and Wosilait, W.D. (1956) The Relationship of Epinephrine and Glucagon to Liver Phosphorylase. III. Reactivation of Liver Phosphorylase in Slices and in Extracts. *J. Biol. Chem.*, **218**, 483-495.

Rarick, H.M., Artemyev, N.O. and Hamm, H.E. (1992) A Site on Rod G Protein α Subunit That Mediates Effector Activation. *Science*, **256**, 1031-1033.

Raw, A.S., Coleman, D.E., Gilman, A.G. and Sprang, S.R. (1997) Structural and Biochemical Characterization of the GTPγS-, GDP•Pi-, and GDP-bound Forms of a GTPase-Deficient $Gly^{42} \rightarrow Val$ mutant of $G_{i\alpha 1}$. *Biochemistry*, **36**, 15660-15669.

Remmers, A.E., Engel, C., Liu, M. and Neubig, R.R. (1999) Interdomain Interactions Regulate GDP Release from Heterotrimeric G Proteins. *Biochemistry*, **38**, 13795-13800.

Reuveny, E., Slesinger, P.A., Inglese, J., Morales, J.M., Iniguez-Lluhi, J.A., Lefkowitz, R.J., Bourne, H.R., Jan, Y.N. and Jan, L.Y. (1994) Activation of the cloned muscarinic potassium channel by G protein βγ subunits. *Nature*, **370**, 143-146.

Richardson, M. and Robishaw, J.D. (1999) The α_{2A}-Adrenergic Receptor Discriminates Between G_i Heterotrimers of Different βγ Subunit Composition in Sf9 Insect Cell Membranes. *J. Biol. Chem.*, **274**, 13525-13533.

Ridge, K.D., Abdulaev, N.G., Zhang, C., Ngo, T., Brabazon, D.M. and Marino, J.P. (2006) Conformational Changes Associated with Receptor Stimulated Guanine Nucleotide Exchange in a Heterotrimeric G-Protein α-subunit: NMR Analysis of GTPγS-Bound States. *J. Biol. Chem.*, **281**, 7635-7648.

Riobo, N.A. and Manning, D.R. (2005) Receptors coupled to heterotrimeric G proteins of the G_{12} family. *Trends Pharmacol. Sci.*, **26**, 146-154.

Robison, G.A., Butcher, R.W. and Sutherland, E.W. (1967) Adenyl cyclase as an adrenergic receptor. *Ann. N. Y. Acad. Sci.*, **139**, 703-723.

Rodbell, M., Birnbaumer, L., Pohl, S.L. and Krans, H.M. (1971a) The Glucagon-sensitive Adenyl Cyclase System in Plasma Membranes of Rat Liver. V. An Obligatory Role of Guanylnucleotides in Glucagon Action. *J. Biol. Chem.*, **246**, 1877-1882.

Rodbell, M., Krans, H.M., Pohl, S.L. and Birnbaumer, L. (1971b) The Glucagon-sensitive Adenyl Cyclase System in Plasma Membranes of Rat Liver. IV. Effects of Guanylnucleotides on Binding of ^{125}I-Glucagon. *J. Biol. Chem.*, **246**, 1872-1876.

Rondard, P., Iiri, T., Srinivasan, S., Meng, E., Fujita, T. and Bourne, H.R. (2001) Mutant G protein α subunit activated by Gβγ: A model for receptor activation? *Proc. Natl. Acad. Sci. U. S. A.*, **98**, 6150-6155.

Ross, E.M. and Gilman, A.G. (1977a) Resolution of Some Components of Adenylate Cyclase Necessary for Catalytic Activity. *J. Biol. Chem.*, **252**, 6966-6969.

Ross, E.M. and Gilman, A.G. (1977b) Reconstitution of catecholamine-sensitive adenylate cyclase activity: Interactions of solubilized components with receptor-replete membranes. *Proc. Natl. Acad. Sci. U. S. A.*, **74**, 3715-3719.

Ross, E.M., Howlett, A.C., Ferguson, K.M. and Gilman, A.G. (1978) Reconstitution of Hormone-sensitive Adenylate Cyclase Activity with Resolved Components of the Enzyme. *J. Biol. Chem.*, **253**, 6401-6412.

Ross, E.M. and Wilkie, T.M. (2000) GTPase-Activating Proteins for Heterotrimeric G Proteins: Regulators of G Protein Signaling (RGS) and RGS-Like Proteins. *Annu. Rev. Biochem.*, **69**, 795-827.

Ruiz-Velasco, V. and Ikeda, S.R. (2000) Multiple G-Protein βγ Combinations Produce Voltage-Dependent Inhibition of N-Type Calcium Channels in Rat Superior Cervical Ganglion Neurons. *J. Neurosci.*, **20**, 2183-2191.

Salamon, Z., Wang, Y., Soulages, J.L., Brown, M.F. and Tollin, G. (1996) Surface Plasmon Resonance Spectroscopy Studies of Membrane Proteins: Transducin Binding and Activation by Rhodopsin Monitored in Thin Membrane Films. *Biophys. J.*, **71**, 283-294.

Sato, M., Blumer, J.B., Simon, V. and Lanier, S.M. (2006) Accessory Proteins for G Proteins: Partners in Signaling. *Annu. Rev. Pharmacol. Toxicol.*, **46**, 151-187.

Schleicher, A. and Hofmann, K.P. (1987) Kinetic study on the equilibrium between membrane-bound and free photoreceptor G-protein. *J. Membr. Biol.*, **95**, 271-281.

Schmidt, C.J., Thomas, T.C., Levine, M.A. and Neer, E.J. (1992) Specificity of G Protein β and γ Subunit Interactions. *J. Biol. Chem.*, **267**, 13807-13810.

Scholich, K., Mullenix, J.B., Wittpoth, C., Poppleton, H.M., Pierre, S.C., Lindorfer, M.A., Garrison, J.C. and Patel, T.B. (1999) Facilitation of Signal Onset and Termination by Adenylyl Cyclase. *Science*, **283**, 1328-1331.

Schwindinger, W.F., Miric, A., Zimmerman, D. and Levine, M.A. (1994) A Novel $G_s\alpha$ Mutant in a Patient with Albright Hereditary Osteodystrophy Uncouples Cell Surface Receptors from Adenylyl Cyclase. *J. Biol. Chem.*, **269**, 25387-25391.

Seitz, H.R., Heck, M., Hofmann, K.P., Alt, T., Pellaud, J. and Seelig, A. (1999) Molecular Determinants of the Reversible Membrane Anchorage of the G-Protein Transducin. *Biochemistry*, **38**, 7950-7960.

Shahinian, S. and Silvius, J.R. (1995) Doubly-Lipid-Modified Protein Sequence Motifs Exhibit Long-Lived Anchorage to Lipid Bilayer Membranes. *Biochemistry*, **34**, 3813-3822.

Sheikh, S.P., Zvyaga, T.A., Lichtarge, O., Sakmar, T.P. and Bourne, H.R. (1996) Rhodopsin activation blocked by metal-ion-binding sites linking transmembrane helices C and F. *Nature*, **383**, 347-350.

Simon, M.I., Strathmann, M.P. and Gautam, N. (1991) Diversity of G Proteins in Signal Transduction. *Science*, **252**, 802-808.

Skiba, N.P., Bae, H. and Hamm, H.E. (1996) Mapping of Effector binding Sites of Transducin α-Subunit Using $G\alpha_t/G\alpha_{i1}$ Chimeras. *J. Biol. Chem.*, **271**, 413-424.

Skiba, N.P., Yang, C.S., Huang, T., Bae, H. and Hamm, H.E. (1999) The α-Helical Domain of $G\alpha_t$ Determines Specific Interaction with Regulator of G Protein Signaling 9. *J. Biol. Chem.*, **274**, 8770-8778.

Skiba, N.P., Hopp, J.A. and Arshavsky, V.Y. (2000) The Effector Enzyme Regulates the Duration of G Protein Signaling in Vertebrate Photoreceptors by Increasing the Affinity between Transducin and RGS Protein. *J. Biol. Chem.*, **275**, 32716-32720.

Slep, K.C., Kercher, M.A., He, W., Cowan, C.W., Wensel, T.G. and Sigler, P.B. (2001) Structural determinants for regulation of phosphodiesterase by a G protein at 2.0 Å. *Nature*, **409**, 1071-1077.

Slessareva, J.E., Ma, H., Depree, K.M., Flood, L.A., Bae, H., Cabrera-Vera, T.M., Hamm, H.E. and Graber, S.G. (2003) Closely Related G-protein-coupled Receptors Use Multiple and Distinct Domains on G-protein α-Subunits for Selective Coupling. *J. Biol. Chem.*, **278**, 50530-50536.

Slusarz, R. and Ciarkowski, J. (2004) Interaction of class A G protein-coupled receptors with G proteins. *Acta Biochim. Pol.*, **51**, 129-136.

Smotrys, J.E. and Linder, M.E. (2004) Palmitoylation of Intracellular Signaling Proteins: Regulation and Function. *Annu. Rev. Biochem.*, **73**, 559-587.

Snow, B.E., Krumins, A.M., Brothers, G.M., Lee, S.F., Wall, M.A., Chung, S., Mangion, J., Arya, S., Gilman, A.G. and Siderovski, D.P. (1998) A G protein γ subunit-like domain shared between

RGS11 and other RGS proteins specifies binding to $G_{\beta 5}$ subunits. *Proc. Natl. Acad. Sci. U. S. A.*, **95**, 13307-13312.

Sommer, M.E., Smith, W.C. and Farrens, D.L. (2005) Dynamics of Arrestin-Rhodopsin Interactions: Arrestin and Retinal Release Are Directly Linked Events. *J. Biol. Chem.*, **280**, 6861-6871.

Sondek, J., Lambright, D.G., Noel, J.P., Hamm, H.E. and Sigler, P.B. (1994) GTPase mechanism of Gproteins from the 1.7-Å crystal structure of transducin α•GDP•AlF_4^-. *Nature*, **372**, 276-279.

Sondek, J., Bohm, A., Lambright, D.G., Hamm, H.E. and Sigler, P.B. (1996) Crystal structure of a G-protein $\beta\gamma$ dimer at 2.1 Å resolution. *Nature*, **379**, 369-374.

Spiegelberg, B.D. and Hamm, H.E. (2005) G $\beta\gamma$ Binds Histone Deacetylase 5 (HDAC5) and Inhibits Its Transcriptional Co-repression Activity. *J. Biol. Chem.*, **280**, 41769-41776.

Sprang, S.R. (1997) G Protein Mechanisms: Insights from Structural Analysis. *Annu. Rev. Biochem.*, **66**, 639-678.

Stephens, L., Smrcka, A., Cooke, F.T., Jackson, T.R., Sternweis, P.C. and Hawkins, P.T. (1994) A novel phosphoinositide 3 kinase activity in myeloid-derived cells is activated by G protein $\beta\gamma$ subunits. *Cell*, **77**, 83-93.

Sullivan, K.A., Miller, R.T., Masters, S.B., Beiderman, B., Heideman, W. and Bourne, H.R. (1987) Identification of receptor contact site involved in receptor-G protein coupling. *Nature*, **330**, 758-760.

Sunahara, R.K., Dessauer, C.W., Whisnant, R.E., Kleuss, C. and Gilman, A.G. (1997a) Interaction of $G_{s\alpha}$ with the Cytosolic Domains of Mammalian Adenylyl Cyclase. *J. Biol. Chem.*, **272**, 22265-22271.

Sunahara, R.K., Tesmer, J.J., Gilman, A.G. and Sprang, S.R. (1997b) Crystal Structure of the Adenylyl Cyclase Activator $G_{s\alpha}$. *Science*, **278**, 1943-1947.

Takida, S. and Wedegaertner, P.B. (2003) Heterotrimer Formation, Together with Isoprenylation, Is Required for Plasma Membrane Targeting of G$\beta\gamma$. *J. Biol. Chem.*, **278**, 17284-17290.

Tall, G.G., Krumins, A.M. and Gilman, A.G. (2003) Mammalian Ric-8A (Synembryn) Is a Heterotrimeric Gα Protein Guanine Nucleotide Exchange Factor. *J. Biol. Chem.*, **278**, 8356-8362.

Tall, G.G. and Gilman, A.G. (2005) Resistance to inhibitors of cholinesterase 8A catalyzes release of Gαi-GTP and nuclear mitotic apparatus protein (NuMA) from NuMA/LGN/Gαi-GDP complexes. *Proc. Natl. Acad. Sci. U. S. A.*, **102**, 16584-16589.

Tang, W.J. and Gilman, A.G. (1991) Type-specific Regulation of Adenylyl Cyclase by G protein $\beta\gamma$ Subunits. *Science*, **254**, 1500-1503.

Taussig, R., Iniguez-Lluhi, J.A. and Gilman, A.G. (1993) Inhibition of Adenylyl Cyclase by $G_{i\alpha}$. *Science*, **261**, 218-221.

Taylor, J.M., Jacob-Mosier, G.G., Lawton, R.G., Remmers, A.E. and Neubig, R.R. (1994) Binding of an α_2 Adrenergic Receptor Third Intracellular Loop Peptide to Gβ and the Amino Terminus of Gα. *J. Biol. Chem.*, **269**, 27618-27624.

Taylor, J.M., Jacob-Mosier, G.G., Lawton, R.G., VanDort, M. and Neubig, R.R. (1996) Receptor and Membrane Interaction Sites on Gβ. A Receptor-Derived Peptide Binds to the Carboxyl Terminus. *J. Biol. Chem.*, **271**, 3336-3339.

Teller, D.C., Okada, T., Behnke, C.A., Palczewski, K. and Stenkamp, R.E. (2001) Advances in Determination of a High-Resolution Three-Dimensional Structure of Rhodopsin, a Model of G-Protein-Coupled Receptors (GPCRs). *Biochemistry*, **40**, 7761-7772.

Tesmer, J.J., Berman, D.M., Gilman, A.G. and Sprang, S.R. (1997a) Structure of RGS4 Bound to AlF_4^--activated $G_{i\alpha1}$: Stabilization of the Transition State for GTP Hydrolysis. *Cell*, **89**, 251-261.

Tesmer, J.J., Sunahara, R.K., Gilman, A.G. and Sprang, S.R. (1997b) Crystal Structure of the Catalytic Domains of Adenylyl Cyclase in a Complex with $G_{s\alpha}$·GTPγS. *Science*, **278**, 1907-1916.

Tesmer, J.J., Sunahara, R.K., Johnson, R.A., Gosselin, G., Gilman, A.G. and Sprang, S.R. (1999) Two-Metal-Ion Catalysis in Adenylyl Cyclase. *Science*, **285**, 756-760.

Tesmer, J.J., Dessauer, C.W., Sunahara, R.K., Murray, L.D., Johnson, R.A., Gilman, A.G. and Sprang, S.R. (2000) Molecular Basis for P-Site Inhibition of Adenylyl Cyclase. *Biochemistry*, **39**, 14464-14471.

Tesmer, V.M., Kawano, T., Shankaranarayanan, A., Kozasa, T. and Tesmer, J.J. (2005) Snapshot of Activated G Proteins at the Membrane: The $G\alpha_q$-GRK2-Gβγ Complex. *Science*, **310**, 1686-1690.

Thomas, C.J., Du, X., Li, P., Wang, Y., Ross, E.M. and Sprang, S.R. (2004) Uncoupling conformational change from GTP hydrolysis in a heterotrimeric G protein α-subunit. *Proc. Natl. Acad. Sci. U. S. A.*, **101**, 7560-7565.

Thomas, T.C., Schmidt, C.J. and Neer, E.J. (1993) G-protein α_o subunit: Mutation of conserved cysteines identifies a subunit contact surface and alters GDP affinity. *Proc. Natl. Acad. Sci. U. S. A.*, **90**, 10295-10298.

Thomas, T.O., Bae, H., Medkova, M. and Hamm, H.E. (2001) An Intramolecular Contact in Ga Transducin That Participates in Maintaining Its Intrinsic GDP Release Rate. *Mol. Cell Biol. Res. Comm.*, **4**, 282-291.

Tu, Y., Wang, J. and Ross, E.M. (1997) Inhibition of Brain G_z GAP and Other RGS Proteins by Palmitoylation of G Protein α Subunits. *Science*, **278**, 1132-1135.

Ueda, N., Iniguez-Lluhi, J.A., Lee, E., Smrcka, A.V., Robishaw, J.D. and Gilman, A.G. (1994) G Protein βγ Subunits. Simplified Purification and Properties of Novel Isoforms. *J. Biol. Chem.*, **269**, 4388-4395.

Van Dop, C., Tsubokawa, M., Bourne, H.R. and Ramachandran, J. (1984) Amino Acid Sequence of Retinal Transducin at the Site ADP-ribosylated by Cholera Toxin. *J. Biol. Chem.*, **259**, 696-698.

Vertrees, J., Barritt, P., Whitten, S. and Hilser, V.J. (2005) COREX/BEST server: a web browser-based program that calculates regional stability variations within protein structures. *Bioinformatics*, **21**, 3318-3319.

Wall, M.A., Coleman, D.E., Lee, E., Iniguez-Lluhi, J.A., Posner, B.A., Gilman, A.G. and Sprang, S.R. (1995) The Structure of the G Protein Heterotrimer $G_{i\alpha 1}\beta_1\gamma_2$. *Cell*, **83**, 1047-1058.

Wang, J., Ducret, A., Tu, Y., Kozasa, T., Aebersold, R. and Ross, E.M. (1998) RGSZ1, a G_z-selective RGS Protein in Brain. Structure, Membrane Association, Regulation by $G\alpha_z$ Phosphorylation, and Relationship to a G_z GTPase-activating Protein Subfamily. *J. Biol. Chem.*, **273**, 26014-26025.

Wang, J., Frost, J.A., Cobb, M.H. and Ross, E.M. (1999) Reciprocal Signaling between Heterotrimeric G Proteins and the p21-stimulated Protein Kinase. *J. Biol. Chem.*, **274**, 31641-31647.

Warner, D.R., Weng, G., Yu, S., Matalon, R. and Weinstein, L.S. (1998) A Novel Mutation in the Switch 3 Region of $G_s\alpha$ in a Patient with Albright Hereditary Osteodystrophy Impairs GDP Binding and Receptor Activation. *J. Biol. Chem.*, **273**, 23976-23983.

Warner, D.R. and Weinstein, L.S. (1999) A mutation in the heterotrimeric stimulatory guanine nucleotide binding protein α-subunit with impaired receptor-mediated activation because of elevated GTPase activity. *Proc. Natl. Acad. Sci. U. S. A.*, **96**, 4268-4272.

Watson, A.J., Katz, A. and Simon, M.I. (1994) A Fifth Member of the Mammalian G-Protein β-Subunit Family. Expression in Brain and Activation of the β2 Isotype of Phospholipase C. *J. Biol. Chem.*, **269**, 22150-22156.

Watson, A.J., Aragay, A.M., Slepak, V.Z. and Simon, M.I. (1996) A Novel Form of the G protein β Subunit $G\beta_5$ Is Specifically Expressed in the Vertebrate Retina. *J. Biol. Chem.*, **271**, 28154-28160.

Wedegaertner, P.B., Chu, D.H., Wilson, P.T., Levis, M.J. and Bourne, H.R. (1993) Palmitoylation Is Required for Signaling Functions and Membrane Attachment of $G_q\alpha$ and $G_s\alpha$. *J. Biol. Chem.*, **268**, 25001-25008.

Weese, J. (1992) A reliable and fast method for the solution of Fredholm integral equations of the first kind based on Tikhonov regularization. *Comput. Phys. Commun.*, **69**, 99-111.

Weinstein, L.S., Shenker, A., Gejman, P.V., Merino, M.J., Friedman, E. and Spiegel, A.M. (1991) Activating Mutations of the Stimulatory G Protein in the McCune-Albright Syndrome. *N. Engl. J. Med.*, **325**, 1688-1695.

Wess, J. (1997) G-protein-coupled receptors: molecular mechanisms involved in receptor activation and selectivity of G-protein recognition. *FASEB J.*, **11**, 346-354.

Wess, J. (1998) Molecular Basis of Receptor/G-Protein-Coupling Selectivity. *Pharmacol. Ther.*, **80**, 231-264.

West, R.E., Jr., Moss, J., Vaughan, M., Liu, T. and Liu, T.Y. (1985) Pertussis Toxin-catalyzed ADP-ribosylation of Transducin. Cysteine 347 is the ADP-ribose Acceptor Site. *J. Biol. Chem.*, **260**, 14428-14430.

Wheeler, G.L. and Bitensky, M.W. (1977) A light-activated GTPase in vertebrate photoreceptors: Regulation of light-activated cyclic GMP phosphodiesterase. *Proc. Natl. Acad. Sci. U. S. A.*, **74**, 4238-4242.

Willard, F.S., Kimple, R.J. and Siderovski, D.P. (2004) Return of the GDI: The GoLoco Motif in Cell Division. *Annu. Rev. Biochem.*, **73**, 925-951.

Willets, J.M., Challiss, R.A. and Nahorski, S.R. (2003) Non-visual GRKs: are we seeing the whole picture? *Trends Pharmacol. Sci.*, **24**, 626-633.

Wilson, P.T. and Bourne, H.R. (1995) Fatty Acylation of α_z. Effects of Palmitoylation and Myristoylation on α_z Signaling. *J. Biol. Chem.*, **270**, 9667-9675.

Wise, A., Grassie, M.A., Parenti, M., Lee, M., Rees, S. and Milligan, G. (1997a) A Cysteine-3 to Serine Mutation of the G-Protein $G_{i1}\alpha$ Abrogates Functional Activation by the α_{2A}-Adrenoceptor but Not Interactions with the $\beta\gamma$ Complex. *Biochemistry*, **36**, 10620-10629.

Wise, A., Parenti, M. and Milligan, G. (1997b) Interaction of the G-protein $G_{11}\alpha$ with receptors and phosphoinositidase C: The contribution of G-protein palmitoylation and membrane association. *FEBS Lett.*, **407**, 257-260.

Woon, C.W., Soparkar, S., Heasley, L. and Johnson, G.L. (1989) Expression of a $G_{\alpha s}/G_{\alpha i}$ Chimera that Constitutively Activates Cyclic AMP Synthesis. *J. Biol. Chem.*, **264**, 5687-5693.

Wosilait, W.D. and Sutherland, E.W. (1956) The Relationship of Epinephrine and Glucagon to Liver Phosphorylase. II. Enzymatic Inactivation of Liver Phosphorylase. *J. Biol. Chem.*, **218**, 469-481.

Yamanaka, G., Eckstein, F. and Stryer, L. (1985) Stereochemistry of the Guanyl Nucleotide Binding Site of Transducin Probed by Phosphorothioate Analogues of GTP and GDP. *Biochemistry*, **24**, 8094-8101.

Yasuda, H., Lindorfer, M.A., Woodfork, K.A., Fletcher, J.E. and Garrison, J.C. (1996) Role of the Prenyl Group on the G Protein γ Subunit in Coupling Trimeric G Proteins to A_1 Adenosine Receptors. *J. Biol. Chem.*, **271**, 18588-18595.

Yoshikawa, D.M., Hatwar, M. and Smrcka, A.V. (2000) G Protein β_5 Subunit Interactions with α Subunits and Effectors. *Biochemistry*, **39**, 11340-11347.

Zhang, F.L. and Casey, P.J. (1996) Protein Prenylation: Molecular Mechanisms and Functional Consequences. *Annu. Rev. Biochem.*, **65**, 241-269.

Zhang, S., Coso, O.A., Lee, C., Gutkind, J.S. and Simonds, W.F. (1996) Selective Activation of Effector Pathways by Brain-specific G Protein β_5. *J. Biol. Chem.*, **271**, 33575-33579.